2020

DEVELOPMENT OF METHODOLOGIES FOR RAMAN SPECTRAL ANALYSIS OF HUMAN SALIVA FOR DETECTION OF ORAL CANCER

Genecy Calado
Technological University Dublin

f

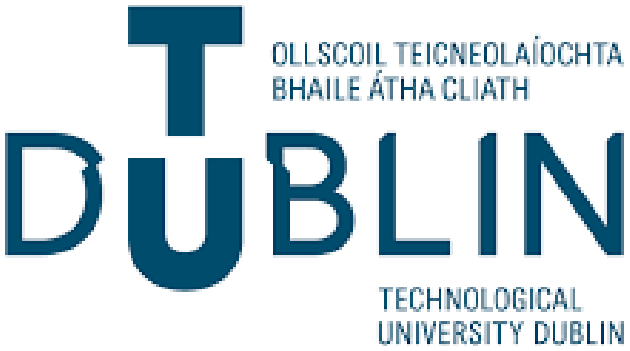

DEVELOPMENT OF METHODOLOGIES FOR RAMAN SPECTRAL ANALYSIS OF HUMAN SALIVA FOR DETECTION OF ORAL CANCER

Genecy Calado BDS MDS

Supervised by:

Prof. Fiona M. Lyng

Prof. Hugh J. Byrne

School of Physics and Clinical and Optometric Sciences
Radiation and Environmental Science Centre
FOCAS Research Institute
Technological University Dublin

Declaration

I certify that this thesis, which I now submit for the award of Doctor of Philosophy (PhD), is entirely my own work and has not been taken from the work of others, save and to the extent that such work has been cited and acknowledged within the text of my work.

This thesis was prepared according to the regulations for graduate study by research of the Technological University Dublin (TU Dublin) and has not been submitted in whole or in part for another award in any other third level institution.

The work reported on in this thesis conforms to the principles and requirements of the TU Dublin's guidelines for ethics in research.

Signature _____ Date _____

(Genecy Calado)

Acknowledgements

I would like to thank my supervisors Prof. Fiona M. Lyng and Prof. Hugh J. Byrne for their support, advice and patience throughout these 4 years – without their guidance and patience I don't know if any of this would be possible!

I would also to thank everybody in the RESC for their help particularly Ms. Isha Behl and Dr Ola Ibrahim not only for their help with the data analysis and sample collection but also for their friendship.

This work would not have been possible without our collaborators Prof. Stephen Flint, Dr Sheila Galvin, Dr Clare Hayley from Dublin Dental University Hospital. My sincerest thanks to all of them.

To my first supervisor (and almost a father) back in Brazil, Prof Dr Luis Ricardo de Alquerque Junior, and my dearest Dr Nely Pereira-Filho, who made me as a researcher: Thank you for everything!

Finally, I would like to thank my lovely mum, my dad (*in memorian*) and Adam for being the best that I had and still have in my life. Also, my Brazilian family and my Irish family for their incredible support and always keeping me grounded.

Abstract

Oral cancer is one of the most common malignancies worldwide, with over 350,000 to 400,000 new cases reported each year. Early detection, followed by appropriate treatment, can increase cure rates to 80 or 90%, and greatly improve the quality of life by minimising extensive, debilitating treatments.

Usually, the clinical diagnosis of most head and neck neoplasms, including oral cancer, is performed through time-consuming and invasive biopsies followed by histological examination of the excised tissue and may present psychological trauma and risk of infection to patients. In addition, histological grading can be subjective, as it is based on subtle morphological changes. In this context, saliva is gaining interest as a diagnostic fluid, since it represents a non-invasive, safe, cheap source of complex biomolecular information that can easily be obtained from the oral cavity. In parallel, increased effort is being devoted to developing less invasive early diagnostic modalities for oral cancer, of which novel optical systems, such as Raman spectroscopy, hold great promise.

The overall aim of this study is to develop methodologies for analysis of human saliva using Raman spectroscopy with a future applicability for oral cancer diagnosis. In order to optimise the measurement protocol, a number of different microscope configurations, source lasers, and substrates were trialled. Once the measurement protocol was optimised, it was validated using artificial saliva and real human saliva. The individual saliva constituent components as well as the artificial saliva itself were characterised and recorded. Following the standardisation protocol, real human whole saliva samples collected using two different collection methods were subjected to centrifugal filtration. The Raman signal from whole saliva was acquired and analysed through statistical tools, demonstrating the potential for diagnostic applications. Then, the Raman spectroscopic profiles of patients with saliva samples of different oral dysplastic pathologies, such as

epithelial oral dysplasia and oral cancer, were further analysed and spectroscopically assessed. To finalise, confounding factors, such as smoking habits and alcohol consumption, were also assessed in terms of their influence on the Raman classification of these pathologies.

This research showed that, Raman spectroscopy was able to successfully discriminate stimulated saliva samples from healthy volunteers and patients with oral cancer or potentially malignant lesions, highlighting the weak influence of confounding factors, such as gender, age, smoking and alcohol consumption. However further studies are still required to improve classification among the different dysplasia grades.

Glossary of Terms

ADH Alcohol dehydrogenase

AUC Area under the curve

BCA Bicinchoninic acid

CIS Carcinoma in situ

CCD Charge coupled device

CLS Classical least squares

COE Conventional oral exam

DLE Discoid Lupus Erythematoses

ELISA Enzyme-linked immunosorbent assay

FTIR Fourier Transform Infrared Spectroscopy

HIV Human immunodeficiency virus

HPV Human Papilloma Virus

LDA Linear Discriminant Analysis

LOH Loss of Heterozygosity

LOOCV Leave one out cross validation

LOPOCV Leave one patient out cross validation

LV Latent variable

MALDI-Q-TOF Matrix-assisted laser desorption ionization-quadrupole-time-of-flight

NNLS Non negatively Least Squares

OSCC Oral Squamous Cell Carcinoma

PC Principal Component

PCA Principal Component Analysis

PLS Partial Least squares

PLSDA Partial least squares-discriminant analysis

PLSR Partial least squares regression

ROC Receiver operating characteristic

SDS-PAGE Sodium dodecyl sulfate polyacrylamide gel electrophoresis

SERS Surface Enhanced Raman Spectroscopy

SLT Smokeless tobacco

SVM Support vector machine

TB Toludine Blue

TSNA Tobacco-specific nitrosamine

WHO World Health Organization

PMOL Potential malignant lesions

List of Figures

Chapter 1

Chapter 2a

Chapter 2b

Chapter 3

Chapter 4

Chapter 5

Chapter 6

List of Tables

Table of Contents

Chapter 1: Introduction - Thesis Outline, Oral Cancer and Saliva

1.1 Thesis Outline

This thesis describes the investigation of Raman spectroscopy as an alternative/adjuvant method for early detection of oral cancer on the basis of the biochemical fingerprint from saliva samples. The study entails initially establishing protocols for the routine measurement of human saliva samples, which was carried out using water and artificial saliva, before applying the protocol to human samples.

The broad objectives of the thesis were to:

1) develop and optimise the methodology for analysis of liquid whole human saliva using Raman spectroscopy, based on artificial saliva formulation;

2) discriminate qualitatively the nature of collection of saliva samples (e.g., Stimulated versus Non stimulated saliva) by Raman Spectroscopy;

3) develop models for classification of oral potentially malignant and malignant oral lesions using multivariate statistical methods;

4) evaluate the influence of confounding factors and clinical features from healthy volunteers and patients on the Raman spectra of saliva samples.

Healthy volunteers were consented and their samples collected at Technological University Dublin (TU Dublin) in order to form the control group. Patients with oral cancer/potentially malignant lesions were consented during their check-ups at the Dysplasia Clinic of Dublin Dental University Hospital (DDUH). All the saliva samples

were assessed with Raman spectroscopy and their individual biochemical profiles were analysed, taking into consideration the dysplastic profile of each sample.

The first chapter of this thesis is a general description of the background related to oral squamous cell carcinoma (OSCC) and potentially malignant lesions. It also details current methods for treatment and the importance of early detection of oral cancer. Chapter 2a describes the potential of Raman spectroscopy as a novel method for cancer detection and its current state of the art for oral medicine diagnostics. Chapter 2b of this thesis is a systematic review paper on the diagnosis of oral cancer through saliva samples by Raman spectroscopy, accepted for publication in Translational Biophotonics (DOI: 10.1002/tbio.201900001).

The subsequent chapters address the aims/objectives of this thesis. Chapters 3, 4, 5 and 6 specifically address objectives 1, 2, 3 and 4, respectively. Chapter 4 has been submitted for publication at Analyst.

Chapter 7 constitutes a summary of the work carried out, and furthermore considers the future perspectives and the potential clinical relevance of the current findings.

1.2 Oral Cancer

1.2.1 Definition and Epidemiology

Cancer is a general term for diseases in which abnormal cells divide without control and can invade nearby tissues. Cancer cells can also spread to other parts of the body through the blood and lymph systems[1].

Oral cancer is a malignant neoplasia which is manifest on the lip or in the oral cavity and, in 90% of the cases, and is histologically classified as Squamous Cell Carcinoma (OSCC)

due to an origin from oral squamous cells. This type of lesion is one of the most common malignancies worldwide, over 350,000 to 400,000 new cases being found each year, and was responsible for more than 170,000 deaths in 2018. Demographically, oral cancer has its highest incidence in South Central Asia, Eastern Europe and some regions in Asia (**Figure 1.1**)[1, 2].

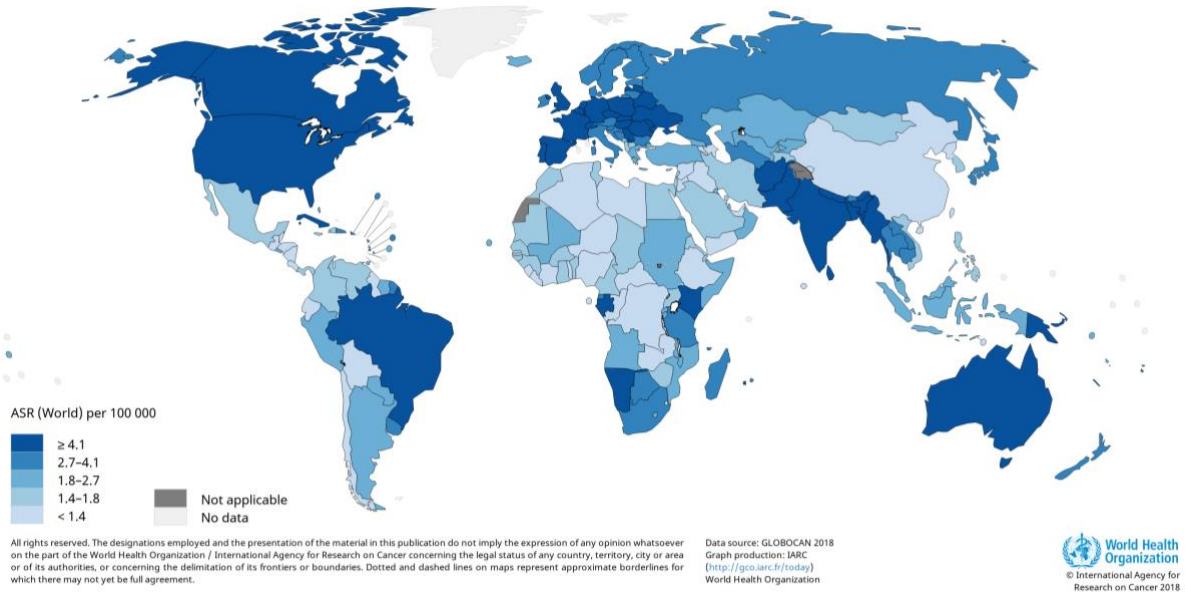

Figure 1.1: Map showing the incidence of oral cancer worldwide. Source: GLOBOCAN, 2018 (IARC)[1].

The risk of developing oral cancer increases with age and the majority of cases occur in people aged 50 or over. However, in high-incidence countries of the world, many cases are reported before the age of 40 and, for those cases, Human Papilloma Virus (HPV)-positive status seems to be a determinant. The reported sex differences are attributable to heavier indulgence in associated risk habits and exposure to sunlight (for lip cancer) as a

part of outdoor occupations, for men. The ratio of males to females diagnosed with oral cancer, however, has declined over the decades and is now about 1.5:1[3].

1.2.2 Aetiology and Major risk Factors

OSCC is considered a multifactorial entity. Several factors may contribute to the development and progress of this neoplasia, and the main and best understood ones in this carcinogenic process are described below.

Smoking

There is ample evidence suggesting that tobacco in various forms, including smoking, chewing and in betel quid etc., have carcinogenic impact in the oral cavity. The complexity of the mixture of carcinogens (over 60 in a cigarette, for example) in tobacco smoke means that, in different individuals, different carcinogens might cause different types of damage[4]. The different tobacco smoke compounds may exert carcinogenic, co-carcinogenic, or tumour promoting effects in an organ and tissue specific manner, depending on the rate of accumulation and metabolism at various sites in the body, coupled with the possibility that these compounds may damage the tumour suppressor gene P53[5].

Statistically, smoking is estimated to account for about 71% of deaths from oral cavity cancer (including pharynx) in high-income countries and 37% of deaths in low- and middle-income countries[6]. In terms of gender aspects, female smokers are more likely to develop oral cancer than male smokers when smoking is the only risk factor taken into consideration[7]. Also, the risk of carcinogenesis increases with increased tobacco consumption[7].

Alcohol

There is a certain degree of controversy concerning whether alcohol alone may have carcinogenic impact but, although through as yet uncertain mechanisms, alcohol is associated with 3.5% of all the cancer deaths worldwide[8]. Studies have shown that individuals consuming more than 170 g of whiskey daily have ten times higher risk of oral cancer than light drinkers[8,9]. Notably, anatomical sites in closest contact, on ingestion of alcohol, such as the mobile part of the tongue, present a high risk for developing this kind of neoplasm[10].

The most accepted theory regarding the carcinogenic capability of alcohol is the one correlated with the process of acetaldehyde production[11]. After alcohol intake, acetaldehyde is locally formed in the oral cavity by oral mucosal alcohol dehydrogenases (ADHs) and by the oral microflora and this chemical has been previously related to the carcinogenesis process *in vitro* [12]. Furthermore, alcohol is believed to act as a solvent for other carcinogens which would explain the synergistic relationship between its consumption and smoking in the development of oral cancer[13].

Smokeless tobacco (SLT)

Tobacco products which are used in a way other than smoking are called smokeless tobacco. The most common smokeless tobacco products are chewing tobacco, naswar, snuff, snus, gutka, and topical tobacco paste. There are more than twenty-five compounds in smokeless tobacco which have cancer causing activity[14]. The most harmful compounds in smokeless tobacco (SLT) are tobacco-specific nitrosamines (TSNAs) and their levels are directly related to the risk of cancer[14]. People using different forms of chewing SLT,

such as loose leaf, have an almost five times higher risk of developing oral cancer as compared to non-chewers[15].

Used in combination with SLT or on its own, betel quid, a substance, or mixture of substances, placed in the mouth, is usually wrapped in betel leaf (derived from the Piper Betel vine) with/without tobacco and sliced fresh or dried areca nut (*Areca catechu*)[15]. In contrast to the SLT by itself, the genotoxicity and mutagenicity seems to come from the areca nut extract along with areca alkaloids in betel quid[16,17].

Human Papilloma Virus (HPV)

The human papillomavirus (HPV), transmitted through conventional and oral sexual contact, is an important risk factor for certain types of oral cancer. In fact, HPV is now the major cause of oropharyngeal cancer in developed countries, detected in 45–90% of cases, but it has also been detected in a smaller subset of oral cavity cancers (23%)[18].

Among all the HPV subtypes (more than 100), the 16 and 18 subtypes are recognised as high-risk due to their relevance in a possible association with oral pre-cancer lesions and cancer itself[19]. Two proteins, in particular, of the early genomic region of high-risk HPVs are capable of forming specific complexes with vital cell-cycle regulators: E6, which binds to p53 and induces its degradation, and E7, which interacts with pRb and blocks its downstream activity. Functional deregulation of these key oncosuppressors results in uncontrolled DNA replication and apoptotic impairment and explains the increased tumorigenic ability of high-risk types[20].

1.2.3 Clinical features of Oral Cancer

The most common locations of occurrence of oral cancers are the tongue and the floor of the mouth, in over 50% of cases[1]. Other areas of involvement are the buccal mucosa,

retromolar area, gingiva, soft palate and, less frequently, the back of the tongue and hard palate[21]. These specific anatomic occurrences might be related to their own aetiology, as smoking could be associated with those malignant lesions in the retromolar area and floor of the mouth, while alcohol is mostly associated with the floor of the mouth only[21].

Clinically, OSCC has an extensive clinical variability, but very often it presents as an ulcer with fissuring or raised exophytic margins. It may also present as a lump, as a red lesion (erythroplakia), as a white or mixed white and red lesion, as a non-healing extraction socket or as a cervical lymph node enlargement, characterised by hardness or fixation[21,22].

Regarding symptomatology, usually, at the initial stages, oral cancer is painless but may develop a burning sensation or pain when it is advanced. This may be one of the principal reasons for diagnosis delay[23].

1.2.4 Diagnosis

Usually led by a doctor or a dentist, the process of diagnosis begins with a conventional oral examination followed by a scalpel/punch biopsy/histology. This procedure still remains the gold standard and most medical/dental schools worldwide have adopted and disseminated it as the protocol of management of suspicious oral lesions[24].

Histological stratification determines the risk, according to tissue abnormalities and cellular morphology of premalignant lesions and squamous cell carcinoma. The histopathological grading describes the invasiveness, biological nature and behaviour of the tumour[25].

Despite providing valuable morphological information, both methods have raised questions regarding their applicability and general capability in oral diagnostics. Not only

risky and invasive in surgical terms, the biopsy may also not be effective when incorrectly performed, or even processed during the histological treatment of the specimen[25].

Other complementary diagnostic methods currently available for oral cancer also include toluidine blue staining and oral brush biopsy.

Toluidine blue is a cationic metachromatic dye that may selectively bind to free anionic groups and it has been used for decades as an aid to the identification of mucosal abnormalities in the oral cavity. It has been valued by surgeons as a useful way of demarcating the extent of a lesion prior to excision, as toluidine blue stains deoxyribonucleic acid and/or may be retained in intracellular spaces of dysplastic epithelium. However, the high rate of false positives and the low specificity in staining dysplasia are very well known limitations of the technique[24,26].

Exfoliative cytology was first designed for early detection of cervical cancer and it has been primarily applied in oral medicine practice to detect early changes in oral mucosa related to malignancy. Exfoliative cytology is performed with cytobrushes, so as to obtain a good-quality smear that includes cells from deeper layers of the epithelium, especially of squamous intraepithelial lesions. However, this technique has been criticised for adding time and cost to the diagnosis of oral lesions without additional benefit to the patient once results must be confirmed with biopsy for a definitive diagnosis[24,27].

Concomitantly, or after the first diagnosis for oral cancer, a panoramic radiograph of the mandible, Computed tomography or Magnetic resonance imaging of the region may be done, each of which is useful in assessing the extent and stage of the cancer. Also, a chest radiograph and pre-treatment dental evaluation are recommended. For patients with advanced disease who will receive concurrent chemotherapy and radiation, blood counts and chemistries may be performed to assess critical organ function including renal and hepatic function[28].

1.2.5 Clinical Staging and Histopathological grading

Clinically, OSCC is often classified under the TNM system (T: Extent or size of the primary tumour, N: Absence or presence of regional lymph node involvement, M: Presence or absence of distant metastasis), widely applied by clinicians based on anatomical involvement[29].

Sub classifications of each factor previously cited into the TNM classification are also present and essential for further general staging. For T, TX, T0, Tis, T1, T2, T3, T4a and T4b are available as subclasses. TX characterises that the tumour could not be assessed. T0 represents tumour absence while Tis is used when a carcinoma *in situ* (CIS) is present. Tumours up to 2cm are clinically defined as T1. T2 and T3 tumours are primary tumours between 2-4cm or greater than 4cm, respectively. Furthermore, T4a and T4b designate nearby structures, such as cortical bone, muscles of the tongue and skin of the face, for T4a; and pterygoid plates, skull base or internal carotid artery, when T4b[29].

In the same way, NX, N0, N1, N2 and N3 are used for N classification. NX is the impossibility of assessment of the tumour. N0 is the tumour absence while N1 is the involvement of a single ipsilateral lymph node, no larger than 3cm. N2 is a single or multiple ipsilateral or contralateral lymph nodes, bigger than 3cm but less than 6cm. When bigger than 6 cm, the lymph node involvement can be classified as N3[29].

Regarding the distant metastasis assessment, M1 indicates the presence of distant metastasis, while M0 is the absence and MX refers to distant metastasis that cannot be assessed[29].

Finally, the TNM classification further determines the scores inherent to each one of the cancer stages, which are:

Stage 0: Tis N0 M0;

Stage I: T1 N0 M0;

Stage II: T2 N0 M0;

Stage III: Either T3 with N0 M0 or T1, T2, or T3 with N1;

Stage IV: Locally invasive neoplasm (T4a/T4b) with N0 M0 or any T with N2/N3 or any T with M1.

All these stages are extremely important for treatment strategy and to predict the survival probability. Furthermore, in 2018 other features were also added to the staging system in order to alter the clinical staging of these tumours, such as P16 positivity and the depth of invasion[29]. These guidelines were altered by the WHO, aiming for a better management of these different cases[29].

Complementary to the clinical staging, the histopathological grading for cancer in the oral cavity is also a determinant for the patient prognosis. Anneroth *et al.*[30] proposed the most common grading system adopted among Oral and Maxillofacial pathologists (**Table 1-1**) for oral tumours. It takes into consideration morphological patterns related to the tumour cell population and tumour-host relationship and translates these data to numbers (1 to 4) that have to be used for the final grade calculation[30].

Table 1-1: Anneroth *et al.* histological grading system for oral squamous cell carcinoma[30].

Histologic grading of malignancy of tumor cell population				
Morphologic Parameters	1	2	3	4
Degree of keratinization	Highly keratinized (>50% of the cells)	Moderately keratinized (5-20% of the cells)	Minimal keratinization (5-20% of the cells)	No keratinization (0-5%)
Nuclear polymorphisı	Little nuclear polymorphism (>75% mature cells)	Moderately abundant nuclear polymorphism (50-75% mature cells)	Abundant nuclear polymorphism (25-50% mature cells)	Extreme nuclear polymorphism (0-25% mature cells)
Number of mitoses/HPF*	0-1	2-3	4-5	>5
Histologic grading of malignancy of tumor-host relationship				
Morphologic parameters	1	2	3	4
Pattern of invasion	Pushing, well delineate infiltrating borders	Infiltrating, solid corc bands and or strands	Small groups or cords of infiltrating cells (n>15)	Marked and widespread cellular dissociation in small groups of cells (n<15) and/or in single cells
Stage of invasion (Depth)	Carcinoma in situ /or Questionable invasion	Distinct invasion, involving lamina propria only	Invasion below lamina propria adjacent to muscles salivary gland tissues and periosteum	Extensive and deep invasion replacing most of the stromal tissue and infiltrating jaw bone
Lympho-plasmacyti infiltrate	Marked	Moderate	Slight	None

* High power field

There are 4 grades in the histological classification and the total points scored by each patient are calculated by adding the points of each parameter[31]. The grades are:

Grade I: 5-10 points;

Grade II: 11-15 points;

Grade III: 16-20 points;

Grade IV: 21 or more.

1.2.6 Management and Treatment

Most oral cancers are treated with wide (radical) surgical excision, radiotherapy, or a combination of surgery and radiation therapy (multimodal treatment). Moreover, chemotherapy with platinum-containing compounds (e.g., cisplatin), 5-fluorouracil and texanes (e.g., paclitaxel) can integrate the range of therapy options[29,32].

The factors that influence the choice of initial treatment are those related to the characteristics of the primary tumour, those related to the patient and those related to the treatment team[33].

The tumour factors that affect the choice of initial treatment of oral cancer are primary site, size (T Stage), location (anterior versus posterior), proximity to bone (mandible or maxilla), status of cervical lymph nodes, previous treatment, and histology (type, grade and depth of invasion). When diagnosed early, only a single therapy is required; radiotherapy or surgical removal for small tumours and a surgical approach for larger neoplasms. On the other hand, advanced cases require a multimodal approach of surgery followed by radiation and/or chemotherapy[32,33].

Likewise, several factors relative to patient characteristics are crucial in the selection of initial treatment for oral cancer and the course of the treatment, such as the patient's age, general medical condition, tolerance of treatment, occupation of the patient, acceptance and compliance by the patient, lifestyle (smoking and drinking) and other socioeconomic considerations[32].

Also, the multidisciplinary approach is crucial in bringing about a successful outcome of the therapeutic program. Expertise in various disciplines including surgery, radiotherapy, chemotherapy, rehabilitation services, dental and prosthetic support, and psycho-social support are essential in making the individualised and correct selection of initial definitive treatment for oral cancer[32].

Follow up is mandatory for all oral cancer cases. The prognosis for survival from oral cancer depends on tumour stage. The great majority of deaths occur within the first 5 years after treatment. The 5-year relative survival rate for intraoral carcinoma is 53% to 68% if the tumour is relatively small and metastasis has not occurred by the time of

diagnosis. However, some patients die of their disease as many as 10 years after initial treatment[29,32,33].

1.3 Potentially malignant Oral lesions and disorders

1.3.1 Potentially malignant oral lesions

First used in 1875 by Romanian physician Victor Babeş, the term 'premalignant lesion', or potentially malignant lesions, is used to define *a morphologically altered tissue in which cancer is more likely to occur than its apparently normal counterpart*. Also, this sort of lesion– (disease, syndrome, or finding) is relatively common, appearing in about 2.5% of the general population[34,35].

Defined by the World Health Organisation (WHO) as "a white patch or plaque that cannot be characterised, clinically or pathologically, as any other disease", leukoplakia is by far the most common clinical presentation of premalignant oral lesions, representing around 80% from all pre-cancerous lesions in the anatomical region. This clinical term does not take into consideration any histopathologic tissue change but it is known that 60% of oral mucosa carcinomas are present as white, keratotic lesions[34,36].

Oral leukoplakia is also clinically classified in two main types: homogeneous type and non-homogeneous type. The homogeneous leukoplakia is a uniform, thin white area alternating or not with normal mucosa. Alternatively, non-homogeneous type includes also sub classifications: speckled, nodular and verrucous leukoplakia. A high risk of malignant transformation is associated with non-homogeneous lesions[37].

In contrast to leukoplakia, erythroplakia and/or erythroleukoplakia is a red or erythematous patch of the oral mucosa. This lesion is defined as a red patch that cannot

be clinically or pathologically diagnosed as any other lesion and is associated with significantly higher rates of dysplasia, CIS, and invasive carcinoma than leukoplakia[38].

1.3.2 Oral Dysplasia

While leukoplakia, erythroplakia and leukoerythroplakia are terms used to designate clinical features of potentially malignant lesions, dysplasia reflects histological changes which are followed by the loss of uniformity or of the architecture of the epithelial cells. Thus, the diagnosis and grading of oral epithelial dysplasia are based on a combination of architectural and cytological changes/atypia[39]:

- Mild dysplasia (grade I): Characterised as a proliferation or hyperplasia of cells of the basal and parabasal layers which does not extend beyond the lower third of the epithelium;
- Moderate dysplasia (grade II): Defined as a proliferation of atypical cells extending into the middle one-third of the epithelium;
- Severe dysplasia (grade III): Abnormal proliferation from the basal layer into the upper third of the epithelium with cytological and architectural changes usually very prominent. Carcinoma *in situ* (CIS), the most severe form of epithelial dysplasia, has been recently included in grade III along with severe dysplasia by recommendation of the WHO. CIS is characterised by full thickness cytological and architectural changes.

The presence and histopathological severity of dysplasia are often regarded as an indicator of the risk status of a precancerous lesion (some studies have shown as many as 36.4% of dysplasia cases transforming to cancer) and these histopathological determinants are present in 5-25% of oral leukoplakias[39]. Erythroplakia also carries a much higher transformation rate and is often associated with severe dysplasia, or even carcinoma *in situ*[39,40].

1.3.3 Potentially malignant oral conditions

Defined as generalised states associated with a significantly increased risk of cancer, the most common potentially malignant oral conditions are: oral submucous brosis, actinic cheilitis, lichen planus, sideropenic dysphagia (Plummer-Vinson syndrome), discoid lupus erythematosus, syphilis, and xeroderma pigmentosum. The fact that a "precancerous condition" can affect other parts of the body is of no concern to the increased risk of oral cancer, only the "precancerous lesions" that these conditions can produce in the oral cavity may occasionally undergo a malignant transformation[41].

1.3.4 Progression

Oral squamous carcinogenesis is a multistep process in which multiple genetic events occur that alter the normal functions of oncogenes and tumour suppressor genes. It is believed that OSCC follows a stepwise involvement of important cancer genes during the various stages of tumour progression, and thus, pre-malignant lesions, such as leukoplakia, erythroplakia, may precede malignancy[42]. The loss of chromosomal material, for example, is thought to result in changes leading to dysplasia (9p21, 3p21, 17p13), CIS (11g13, 13g21, 14g31) and invasive tumours (4q26-28, 6p, 8p, 8q). However, P53 and P16 expression levels and loss of heterozygosity (LOH) are considered very important predictors of progression in oral carcinogenesis[43].

Dysplastic changes are one of the signs of premalignant progression in oral lesions that can be observed in histopathology. However, although it is a strong determinant in the early diagnostic process of OSCC, the histological grade from premalignant lesions may not be the only factor or concern for determination of the progressive malignant nature of it; severe dysplastic changes might not develop further to a CIS, for example[44].

1.3.5 Diagnosis

The diagnostic procedure adopted as gold standard to detect premalignant lesions and/or conditions is the physical examination followed by a biopsy and histopathological examination. Similar to those designed for OSCC, other diagnostic systems are also available, such as Toluidine blue, cytology, etc. However, their specificity and sensitivity is not as reliable as biopsy and histology[45].

1.3.6 Management

All leukoplakic lesions should undergo biopsy if there is a strong suspicion of malignancy or when they do not respond to conservative therapy. For small areas of leukoplakia, excisional biopsy is usually appropriate. Erythroplakia is managed in much the same fashion as leukoplakia. Lesions characterised by dysplasia and CIS should be completely excised to clear margins when possible[46].

1.4 Saliva

1.4.1 Origin and Anatomy

Saliva is a clear, slightly acidic mucoserous exocrine biofluid produced in the oral cavity by three major (parotid, submandibular and sublingual) (**Figure 1.2**) and around 450-750 minor salivary glands (situated on the tongue, buccal mucosa and palate except the anterior part of the hard palate and gums)[47]. Saliva components have also a non-glandular origin, so oral fluid cannot be considered exclusively as the product of salivary glands, because it also contains fluids originating from oropharyngeal mucosae (oral mucosal transudate cells, bacteria, fungi, virus, upper airways secretions, gastrointestinal reflux) mucosal transudations, gingival crevicular fluid, serum and blood derivatives from oral

wounds, desquamated epithelial cells, expectorated bronchial and nasal secretions, bacteria and bacterial products, viruses and fungi, other cellular components, and food debris. It is a complex fluid containing an entire library of hormones, proteins, enzymes, antibodies, antimicrobial constituents, and cytokines[47,48].

Each salivary gland contributes differently to the final composition of whole saliva. Furthermore, stimulation, by for example mastication, can also change the performance of the group of salivary glands resulting in a unique composition.

The parotid glands are the largest of the salivary glands and lie wedged between the sternocleidomastoid muscle and the masseter, covering the ramus of the mandible and overflowing these structures behind and in front[49]. Hence, these glands are structurally associated with the peripheral branches of the facial nerve (seventh paired cranial nerve)[50]. Their ducts, also called Stensen's ducts, arise from the anterior aspect of these glands, run over the masseter and penetrate the buccinator to open in the mouth at the level of the second upper molars, where they primarily deliver a watery seromucous saliva type[49,51].

The submandibular gland, about half of the size of the parotid gland, occupies most of the submandibular triangle area which is delineated by the anterior and posterior bellies of the digastric muscle and the mandible. Anteriorly, the floor of the triangle is the mylohyoid muscle; posteriorly it is the hyoglossus muscle[39]. The submandibular duct, or ''Wharton's duct'', arises from the anterior portion of the gland and traverses the floor of mouth and opens at the base of the frenulum of the tongue, just posterior to the inferior incisors on the submandibular caruncle via one to three orifices where a mixture of mucous and serous fluids are liberated[52,53].

The sublingual gland is the smallest of the major salivary glands, about one fifth the size of the submandibular glands, and lies in the submucosal plane of the floor of the mouth

superior to the mylohyoid muscle and lateral to the genioglossus muscle. It is predominantly a mucous gland. The sublingual (Bartholin's) duct has several smaller tributaries, up to 20 salivary ducts, that subsequently open into Wharton's duct, the main duct of the submandibular gland. It is predominantly a mucous gland[54].

Finally, the minor salivary glands are distributed throughout the human oral cavity. These glands can be found on the lower and upper lips, the cheeks, much of the palate, and the salivary secretions from these glands are primarily mucous[55].

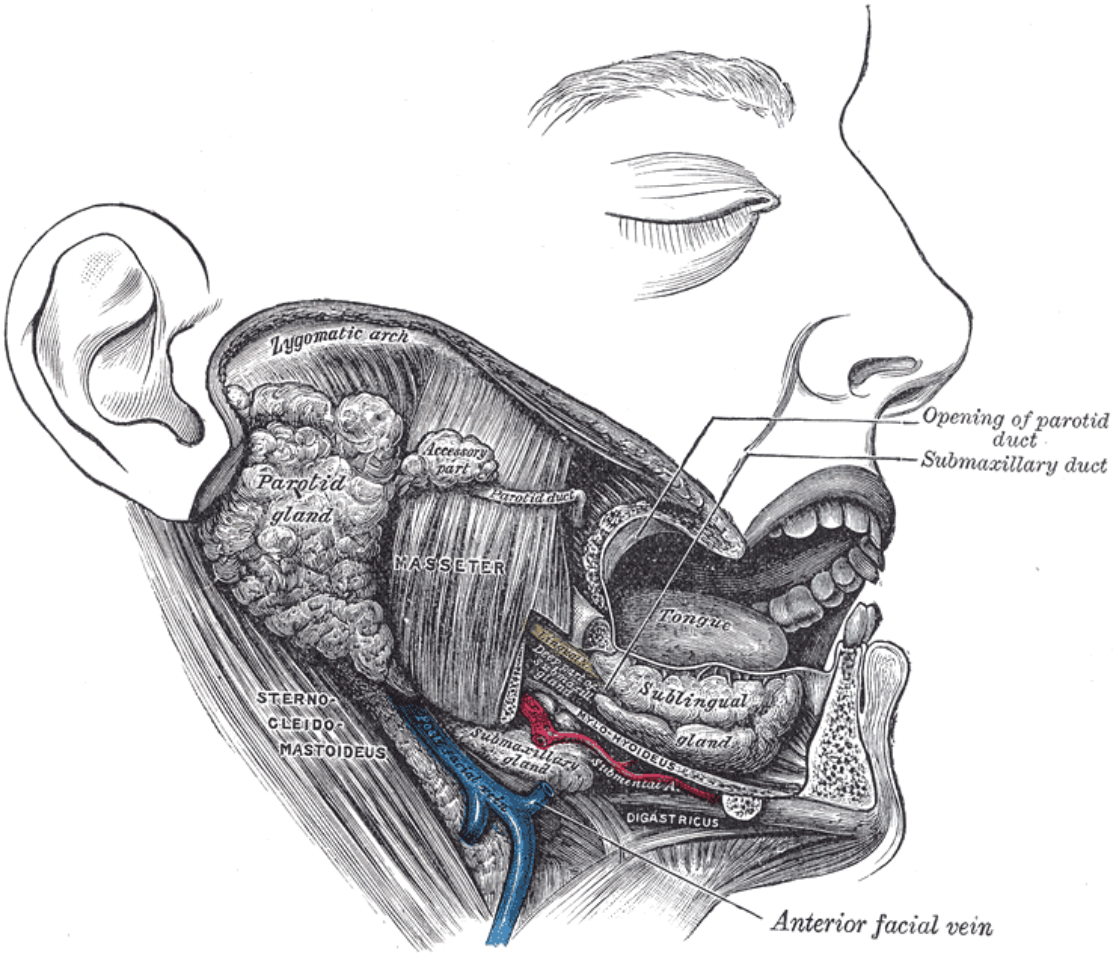

Figure 1.2: Dissection, showing salivary glands of right side. Note: "submaxillary" refers to present day submandibular gland. (Taken from the 20th U.S. edition of Gray's Anatomy of the Human Body, originally published in 1918)[56].

1.4.2 Histology of the Salivary Glands

Different types of cells constitute the salivary glandular tissue: acinar cells, various duct system cells, and myoepithelial cells (**Figure 1.3** and **Figure 1.4**). The secretory end pieces (or acini), in which saliva is first secreted, are formed by accinar cells arranged in a roughly spherical shape. Hence, this primary secretion can be classified as serous (mainly from parotid gland), mucous (from minor salivary glands), or mixed (from sublingual and submandibular glands)[51].

Regarding the salivary duct system, three types of duct are present in all salivary glands, according to cell type: intercalated, striated, and excretory ducts. Having low cuboidal epithelium and a narrow lumen, the intercalated ducts maintain the network connecting acinar secretions to the rest of the gland. The cells from the intercalated duct are not involved in the modification of electrolytes, as the remaining duct cells. Columnar cells with many mitochondria line the striated ducts, second in the network, and regulating electrolytes by resorbing sodium. Finally, the excretory ducts, constituted by cuboidal cells and the last part of the duct network before saliva reaches the oral cavity, contribute by continuing sodium resorption and secreting potassium[50]. In addition, myoepithelial cells, which are long cell processes wrapped around acinar cells, contract on stimulation to constrict the acinar. This function, secreting or “squeezing out” accumulating fluid, is the result of a purely neural process[57].

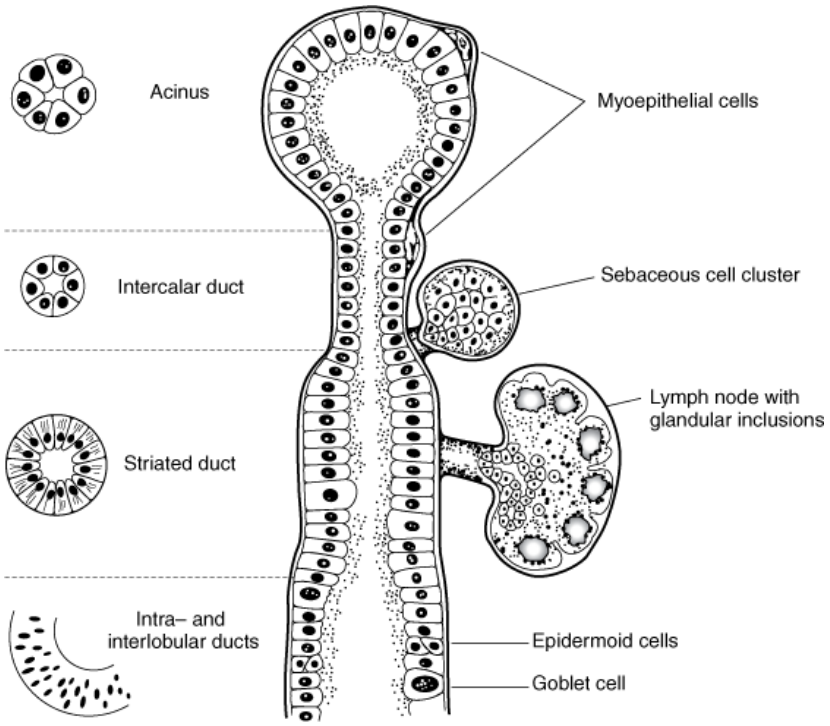

Figure 1.3: Structure of the salivary glands. Diagram of the secretory end piece (acini) and the branched ductal system. Source: Lalwani AK: *Current Diagnosis & Treatment in Otolaryngology* – Head and Neck Surgery, 2nd Edition: http://.www.accessmedicine.com[58]

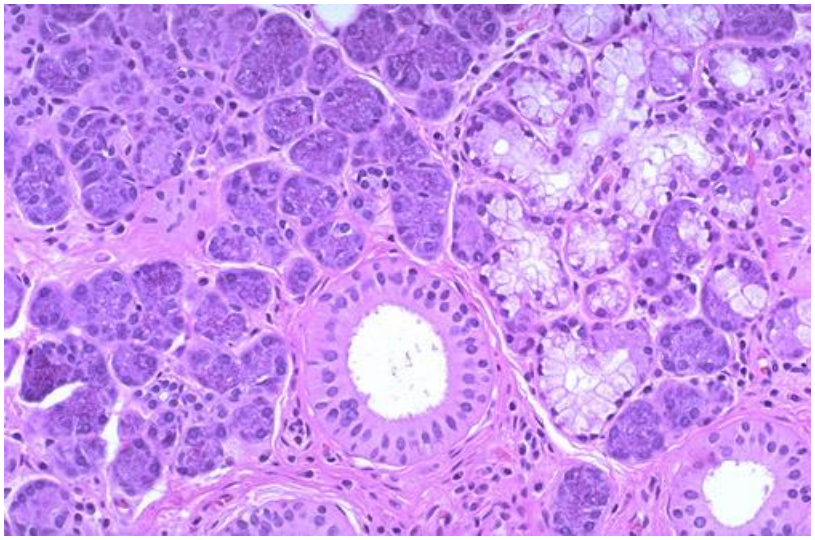

Figure 1.4: Histological image from parotid gland H&E stained. Source: Kumar GS. *Orban's Oral Histology and Embryology*. St Louis: Mosby, 2011[59].

1.4.3 Composition

Whole saliva refers to the complex mixture of fluids from the salivary glands, the gingival fold, oral mucosa transudate, in addition to mucous of the nasal cavity and pharynx, non-adherent oral bacterial, food remainders, desquamated epithelial and blood cells. Saliva is composed of more than 99% water. Saliva also contains a variety of electrolytes, including sodium, potassium, calcium, magnesium, bicarbonate, and phosphates (**Table 1-2**). Also found in saliva are immunoglobulins, proteins, enzymes, mucins, and nitrogenous products, such as urea and ammonia[60].

Proline-rich proteins (PRPs) (acidic PRPs: 20%, basic PRPs: 12% and glycosylated PRPs: 5%), mucins = 20%, amylase = 20%) constitute the most abundant proteins in human saliva. Immunoglobulin (A and G), cystatins, statherins and all others represent 23% of salivary proteins. In conjunction with other organic molecules, such as vitamins and lipids, they perform crucial roles in oral mucosal immunity (anti-viral, anti-bacterial and anti-fungal), protection of teeth and food digestion[61].

Table 1-2: Main saliva composition[60].

Composition of saliva	
Parameter	**Characteristics**
Volume	600-1000mL/day
Electrolytes	Na^{+}, K^{+}, Cl^{-},HCO_3^{-},Ca^{2+}, $Mg2+$,HPO_4^{2-}, SCN^{-}, and F^{-}
Secretory proteins/peptides	Amylase, proline-rich proteins, mucins, histatin, cystatin, peroxidase, lysozyme, lactoferrin, defensis, and cathelicidin-LL37
Immunoglobulins	Secretory immunoglobulin A; immunoglobulins G and M
Small organic	Glucose, amino acids, urea, uric acid, and lipid molecules
Other components	Epidermal growth factor, insulin, cyclic adenosine monophosphate-biding proteins, and serum albumin

1.4.4 Secretion

Acinar cell secretion can be classified as serous (produced mainly from the parotid gland), mucous (minor glands) or mixed (sublingual and submandibular glands). Accumulation of ions in the lumen generates an osmotic gradient driving water through the apical aquaporin-5 channels leading to an isotonic plasma-like fluid. The acinar cells are connected by ducts and the secreted saliva is drained to oral cavity through striated and

excretory ducts. While saliva passes through salivary ducts, Na^{+}/Cl^{-} are reabsorbed and K^{+}/HCO_3^{-} are excreted by active transportation through ion channels[62]. Due to the relative impermeability of the ducts to water, the resulting saliva has a hypotonic characteristic in relation to blood. Some saliva components are locally produced in salivary glands, thus they are not related to plasma concentrations. In this case, the salivary flow rate can influence their salivary concentration[45].

1.4.5 Function of Saliva

Saliva is considered a mirror of body health and is composed of a variety of analytes from systemic sources that reach the oral cavity through various pathways. Saliva plays a key role in the lubrication and repair, formation and swallowing of food bolus, digestion, facilitation of food tasting and control of microbial population. All this versatility is better described in the following sections, while **Figure 1.5** describes the main functions of saliva along with some important of the salivary constituents.

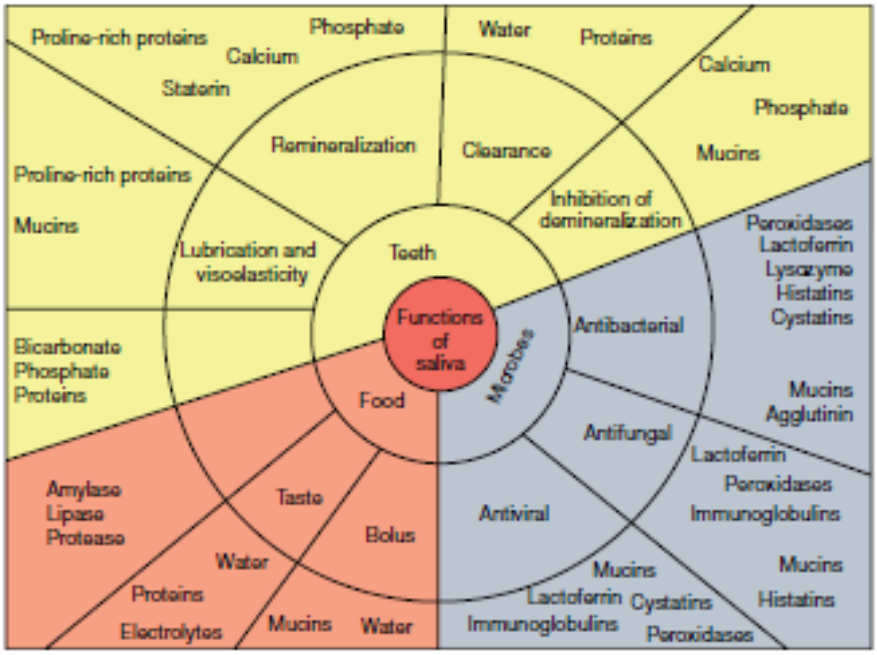

Figure 1.5: The functions of saliva according to specific areas of action and related major components. Source: Kumar GS. *Orban's Oral Histology and Embryology*. St Louis: Mosby, 2011[59].

Protection

Saliva provides a washing action that flushes away bacteria and debris. In particular, the clearance of sugars from the mouth limits their availability to acidogenic plaque microorganisms. Also, the mucins and other glycoproteins provide lubrication, preventing the oral tissues from adhering to one another and allowing them to slide easily over one another. The mucins also form a barrier against noxious stimuli, microbial toxins, and minor trauma[63].

Buffering

The bicarbonate and, to some extent, phosphate in saliva act as an excellent buffer helping to protect the teeth from demineralisation caused by bacterial acids produced during sugar metabolism[64]. Some salivary proteins also may contribute to the buffering action of saliva. The metabolism of salivary proteins and peptides by the native microbiota produces urea and ammonia, which help to increase the pH[65].

Pellicle Formation

Many of the salivary proteins bind to the surfaces of the teeth and oral mucosa, forming a thin film, the salivary pellicle. The composition of the oral mucosal pellicle will presumably determine the types of microorganisms which can attach to the oral mucosa. More recently, several salivary proteins, including the mucins MUC5B and MUC7, have been identified in mucosal pellicle[66].

Regarding the saliva participation in the formation of the enamel pellicle, it is known that several proteins bind calcium and help to protect the tooth surface as well as other proteins

may bind to sites for oral bacteria, providing the initial attachment for organisms that form plaque[67].

Maintenance of Tooth Integrity

Saliva is a bioliquid supersaturated with calcium and phosphate ions. The solubility of these ions is maintained by calcium binding proteins, especially the acidic proline-rich proteins and statherin. At the tooth surface, the high concentration of calcium and phosphate results in a posteruptive maturation of the enamel, increasing surface hardness (mineralisation) and resistance to demineralisation. The concentration of fluoride, responsible for the remineralisation enhancement process, in saliva is only just over 1 mmol/L, but is sufficient to keep the saliva supersaturated with respect to any fluorapatite formed in the tooth as a result of intake of food, drink or oral health products containing fluoride[68].

Antimicrobial Action

Saliva has a major environmental influence on the microorganisms that colonise oral tissues. Associated with the barrier effect provided by mucins, saliva contains several proteins with antimicrobial activity. For example, α-amylase is a growth inhibitor of *Porphyromonas gingivalis*, well known periodontal pathogen[69]. Lysozyme, lactoferrin, peroxidase, and secretory leukocyte protease inhibitor complete the group of main salivary proteins with antibacterial activity[70]. A number of peptides that act by inserting into membranes and disrupting cellular or mitochondrial functions are present in saliva. These include α-defensins and β-defensins, cathelicidin-LL37, and the histatins[71].

In addition to antibacterial activity, several of these proteins and peptides also exhibit antiviral and antifungal activity. The main salivary immunoglobulin, secretory immunoglobulin A (IgA), causes agglutination of specific microorganisms, preventing their adherence to oral tissues and forming clumps that are swallowed, thereby facilitating their removal by swallowing and possibly inhibiting their attachment to oral surfaces. Mucin MUC7, proline-rich proteins, and salivary agglutinin have the same agglutination property[72].

Tissue Repair

The main protein and also digestive enzyme in saliva is α-amylase (1,4-glucan 4-glucanohydrolase), present as six isoenzymes which can split starch into maltose, maltotriose, maltotetrose, and some higher oligosaccharides. A variety of growth factors and other biologically active peptides and proteins are present in small quantities in saliva. Under experimental conditions, many of these substances promote tissue growth and differentiation, wound healing, and other beneficial effects. However, the role of most of these substances in protection of the oral cavity is presently unknown[73].

Digestion

Saliva plays an important early role in digestion in that during the initial chewing of a portion of food, the solubilisation of food substances and the actions of enzymes such as amylase and lipase begin the digestive process. Saliva then contributes to the formation of a cohesive food bolus, covered by a mucin film, which facilitates the swallowing process[74].

1.4.6 Non stimulated versus stimulated saliva

The qualitative and quantitative aspects of saliva vary according to many factors, including the gland type from which it is secreted and another variables such as age, health, diurnal considerations, or sex of individuals. Most studies have focused on individual proteins under specific conditions, with the type of stimulation varying greatly. The average compositions of both non stimulated and stimulated whole saliva can be seen in **table 1-3**[51]. The contribution of each salivary gland in the different method of collections is also further described in **Table 1-4**.

Table 1-3: Major composition of non stimulated and stimulated whole saliva by Edgar *et al*.[51].

	Non stimulated	**Stimulated**
Water	99.55%	99.53%
Solids	0.45%	0.47%
	Mean ± S.D.	**Mean ± S.D.**
Flow rate	0.32 ± 0.23	2.08 ± 0.84
pH	7.04 ± 0.28	7.61 ± 0.17
Inorganic Constituents		
Sodium (mmol/L)	5.76 ± 3.43	20.67 ± 11.74
Potassium (mmol/L)	19.47 ± 2.18	13.62 ± 2.70
Calcium (mmol/L)	1.32 ± 0.24	1.47 ± 0.35
Magnesium (mmol/L)	0.20 ± 0.08	0.15 ± 0.05
Chloride (mmol/L)	16.40 ± 2.08	18.09 ± 7.38

Bicarbonate (mmol/L)	5.47 ± 2.46	16.03 ± 5.06
Phosphate (mmol/L)	5.69 ± 1.91	2.70 ± 0.55
Thiocyanate (mmol/L)	0.70 ± 0.42	0.34 ± 0.20
Iodide (µmol/L)	Not available	13.8 ± 8.5
Fluoride (µmol/L)	1.37 ± 0.768	1.16 ± 0.64
Organic Constituents		
Total protein (mg/L)	1630 ± 720	1350 ± 290
Secretory IgA (mg/L)	76.1 ± 40.2	37. 8 ± 22.5
MUC5B (mg/L)	830 ± 480	460 ± 200
MUC7 (mg/L)	440 ± 520	320 ± 330
Amylase (U=mg	317 ± 290	453 ± 390
maltose/mL/min)	28.9 ± 12.6	23.2 ± 10.7
Lysozyme (mg/L)	8.4 ± 10.3	5.5 ± 4.7
Lactoferrin (mg/L)	4.93 ± 0.61	Not available
Statherin (µmol/L)	51.2 ± 49.0	60.9 ± 53.0
Albumin (mg/L)	79.4 ± 33.3	32.4 ± 27.1
Glucose (µmol/L)	0.20 ± 0.24	0.22 ± 0.17
Lactate (mmol/L)	12.1 ± 6.314	13.6
Total Lipids (mg/L)	780	567
Amino Acids (µmol/L)	3.57 ± 1.26	2.65 ± 0.92
Urea (mmol/L)	6.86	2.57 ± 1.64
Ammonia (mmol/L)		

Table 1-4: Saliva contribution of each gland in non stimulated and stimulated whole saliva collection by *Edgar et al*.[51]

Salivary gland	Unstimulated contribution (%)	Stimulated contribution (%)
Submandibular	65%	35%
Parotid	20%	50%
Sublingual	5%	7%
minor mucous glands	10%	8%

One of the most comprehensive studies comparing whole saliva protein composition using different tastants was performed by Neyraud *et al*[75]. This experiment analysed protein abundance changes from four healthy subjects in whole and parotid saliva following stimulation with different tastants at low concentration and high concentration using two-dimensional gel electrophoresis and mass spectrometry. The respective numbers of differentially expressed proteins in different concentration of tastants (from lower to higher concentration) were 2, 9, 10, and 16. All of the differentially expressed proteins were low in abundance in comparison to total spot volumes and the vast majority of the salivary proteome was, in fact, unchanged by different concentrations of stimulants. However, only the few differently expressed spots were assessed so it is difficult to confirm the validity of these results[75].

Other studies have also examined the effect of changes in the oral environment on unstimulated vs. stimulated protein secretion. An interesting study examined the levels of parotid and submandibular/sublingual salivary IgA in response to experimental gingivitis in humans. They found a statistically significant increase in the IgA secretion rate in stimulated parotid saliva after 6 and 12 days without oral hygiene. This change was not

seen in resting saliva, or in any of the submandibular/sublingual saliva samples. A proposed reason was perhaps that the accumulation of plaque-derived substances or inflammatory products triggered salivary secretion via neural pathways[76].

Also, another study found histatin concentrations in resting saliva to be much higher for parotid than submandibular/sublingual saliva, and upon stimulation, the histatin concentrations decreased in parotid and increased in submandibular and sublingual saliva. Thus, the stimulation was proven to be an influencing factor regarding the saliva quality[77].

It was determined that unstimulated vs stimulated saliva sampling critically affects the amount and composition of detected salivary proteins. Nevertheless, even facing various methodological aspects and preanalytical variables that can affect saliva, these experiments could neither qualify nor specify proteins[78].

In contradiction of the major expected conclusions about the differentiation of stimulated saliva and unstimulated saliva, some studies found no significant time effect during resting and stimulated conditions. As an example, Becerra *et al.* carried out a characterisation of the influence of gustatory stimulation and duration of stimulation on the secretion pattern of salivary mucins and non-mucin glycoproteins in submandibular/sublingual saliva. Samples were analysed using SDS-PAGE, followed by Western blot analysis using polyclonal antibodies against MG 1, MG2, lactoferrin, amylase, and carbonic anhydrase. As final conclusions, both types of saliva did not show quantitative or qualitative differences[79].

Considering the present literature regarding the differences between stimulated and unstimulated saliva, a proper molecular definition for the two sorts of oral fluids still remains uncertain, due to the limitation of the techniques applied for this purpose to date.

1.4.7 Saliva as a diagnostic biofluid

Saliva is gaining increasing interest as a diagnostic fluid, since it represents a non-invasive, safe and cheap source of complex biomolecular information which can easily be obtained from the oral cavity[80]. Furthermore, the past few years have seen the development of salivary diagnostic tools to monitor various oral diseases ranging from periodontal diseases, dental caries to infections and autoimmune diseases. The main challenge of salivary diagnostics is to discover its potential and optimise analytical techniques for the use of this biofluid. The challenge of making salivary diagnostics a clinical reality is in establishing the scientific foundation and clinical validations needed to position it as a highly accurate and feasible technology that can achieve definite point of care assessment of health and diseases states[81].

Saliva may be used not only to detect oral diseases but also systemic ones, showing versatility and merit in diagnostic scope. Salivary biomarkers have already shown promising results in the diagnosis of many diseases, such as periodontitis[82], HIV[83], Hep B[84], and even measles[85]. Immunoassays have been developed to detect secretory IgA and serum-derived IgG (from crevicular fluid) found in saliva for various diseases as well as saliva has shown potential for hormone and drug screening[86].

Proteome-based approaches have been applied over the last three decades to monitor changes in protein expression[87]. Generally, protein expression is primarily analysed by one or two-dimensional polyacrylamide gel electrophoresis (PAGE) which allows separation not only of different molecules with similar molecular weights, but also of different modification patterns or isoforms of the same protein. Along with the development and introduction of mass spectrometry (MS), the PAGE-separated proteins can be more accurately characterised and identified, leading to a wider range of applications for proteomic assays. Proteins that are primarily identified by MS can be

further characterised by ionization methods such as electrospray ionisation (ESI) and matrix-assisted laser desorption ionization (MALDI)[87,88]. Unfortunately, all these techniques usually require labour-intensive sample-preparation procedures and long analysis time.

Other technologies that have been also employed for diagnostics include Enzyme Linked Immunoadsorbent Assay (ELISA), Micro-satellite Analysis, and High-Performance Liquid Chromatography (HPLC), but these techniques suffer from the same limitations.as MS[89].

In contrast, optical methods, such as Raman spectroscopy, are quantitative and more economic in terms of cost and labour[89]. It has been reported that Raman spectroscopy of saliva can be applied for detection of narcotics[90], in forensic medicine[91], cancer[92] and periodontal disease detection[93]. However, all these studies have developed quite costly and complex methodologies using nanoparticle signal enhancers (when performed through surfaced enhanced Raman spectroscopy (SERS)) or modifying the physical form of saliva (dried saliva), leading to undeniable salivary quality loss[93].

The use of Raman spectroscopy for potentially malignant oral lesions and OSCC diagnosis is further discussed in chapter 2a and chapter 2b.

Reference

1. World Health Organisation: The GLOBOCAN 2018 database, http://globocan.iarc.fr.

2. Rivera C. Review Article Essentials of oral cancer. Int J Clin Exp Pathol 2015;8(9):11884-11894.

3. Warnakulasuriya S. Global epidemiology of oral and oropharyngeal cancer. Oral Oncol. 2009 Apr-May;45(4-5):309-16.

4. Kuper H., Adami H.-O, Boffetta P. Tobacco use, cancer causation and public health impact. Journal of Internal Medicine 2002; 251: 455–466.

5. Pfeifer GP, Denissenko MF, Olivier M, Tretyakova N, Hecht SS, Hainaut P. Tobacco smoke carcinogens, DNA damage and p53 mutations in smoking-associated cancers. Oncogene. 2002 Oct 21;21(48):7435-51.

6. Torre LA, Bray F, Siegel RL, Ferlay J, Lortet-Tieulent J, Jemal A. Global Cancer Statistic, 2012. Ca-a Cancer Journal for Clinicians 2015;65:87-108.

7. Honorato J, Rebelo MS, Dias FL, Camisasca DR, Faria PA, Azevedo e Silva G, Lourenço SQ. Gender differences in prognostic factors for oral cancer. Int J Oral Maxillofac Surg. 2015 Oct;44(10):1205-11.

8. Wynder EL, Bross IJ, Feldman RM (1957) A study of the aetiological factors in cancer of the mouth. Cancer 10(6):1300–1323.

9. Nelson DE, Jarman DW, Rehm J, Greenfield TK, Rey G, Kerr WC, Miller P, Shield KD, Ye Y, Naimi TS. Alcohol-Attributable Cancer Deaths and Years of Potential Life Lost in the United States. Am J Public Health. 2013 April; 103(4): 641–648

10. International Agency for Research on Cancer. Alcohol drinking. IARC monographs on the evaluation of carcinogenic risks to humans, vol 44. Lyon: IARC, 1988.

11. Seitz HK, Becker P. Alcohol Metabolism and Cancer Risk. Alcohol Res Health. 2007; 30(1): 38–47.

12. Salaspuro V, Salaspuro M. Synergistic Effect Of Alcohol Drinking And Smoking On In Vivo Acetaldehyde Concentration In Saliva. Int. J. Cancer (2004): 111, 480 – 483.

13. Hashibe M, Brennan P, Chuang S, Boccia S, Castellsague X, Chen C, Curado MP, Maso LD, Daudt AW, Fabianova E, Fernandez L, Wünsch-Filho V, Franceschi S, Hayes RB, Herrero R, Kelsey K, Koifman S, La Vecchia C, Lazarus P, Levi F, Lence JJ, Mates D, Matos E, Menezes A, McClean MD, Muscat J, Eluf-Neto J, Olshan AF, Purdue M, Rudnai P, Schwartz SM, Smith E, Sturgis EM, Szeszenia-Dabrowska N, Talamini R, Wei Q, Winn DM, Shangina O, Pilarska A., Zhang Z, Ferro G, Berthiller J, Boffetta P. Interaction between tobacco and alcohol use and the risk of head and neck cancer: pooled analysis in the INHANCE consortium. Cancer Epidemiol Biomarkers Prev. 2009 Feb; 18(2): 541–550.

14. International Agency for Research on Cancer. Vol. 89. Lyon, France: World Health Organization International Agency for Research on Cancer; IARC Monographs on the Evaluation of Carcinogenic Risks to Humans; 2007. Smokeless Tobacco and Some Tobacco-SpecificN-Nitrosamines.

15. Khan Z, Tönnies J, Müller S. Review Article Smokeless Tobacco and Oral Cancer in South Asia: A Systematic Review with Meta-Analysis. J Cancer Epidemiol. 2014; 2014: 394696.

16. Jeng JH, Chang MC, Hahn LJ. Role of areca nut in betel quid-associated chemical carcinogenesis: current awareness and future perspectives. Oral Oncology 2001;37:477-492.

17. Bhide SV, Shivapurkar NM, Gothoskar SV, Ranadive KJ. Carcinogeneticity of betel quid ingridients – feeding mice with aqueous extract and polyphenol fraction of betel nut. British Journal of Cancer 1979; 40:922-926.

18. D'Souzaa G, Dempseyb A. The role of HPV in head and neck cancer and review of the HPV vaccine. Prev Med. 2011 Oct 1; 53(Suppl 1): S5–S11.

19. Mahmuda A, Ali L, Hassan Z, Khan I. Association of Human Papilloma Virus Infection and Oral Squamous Cell Carcinoma in Bangladesh. J Health Popul Nutr. 2013 Mar; 31(1): 65–69.

20. Manvikar V, Kulkarni R, Koneru A, Vanishree M. Role of human papillomavirus and tumor suppressor genes in oral cancer. J Oral Maxillofac Pathol. 2016 Jan-Apr; 20(1): 106–110.

21. Zini A, Czerninski R, Sgan-Cohen HD. Oral cancer over four decades: epidemiology, trends, histology, and survival by anatomical sites. J Oral Pathol Med. 2010 Apr;39(4):299-305.

22. Markopoulos AK. Current Aspects on Oral Squamous Cell Carcinoma. Open Dent J. 2012; 6: 126–130.

23. Bagan J, Sarrion G Jimenez Y**.** Oral cancer: Clinical features. Oral Oncol. 2010 Jun;46(6):414-7.

24. Singh SP, Ibrahim O, Byrne HJ, Mikkonen JW, Koistinen AP, Kullaa AM, Lyng FM. Recent advances in optical diagnosis of oral cancers: Review and future perspectives. Head Neck. 2016 Apr;38 Suppl 1:E2403-11

25. Abbey LM, Kaugars GE, Gunsolley JC, Burns JC, Page DG, Svirsky JA, Eisenberg E, Krutchkoff DJ, Cushing M. Intraexaminer and interexaminer reliability in the

diagnosis of oral epithelial dysplasia. Oral Surg Oral Med Oral Pathol Oral Radiol Endod. 1995 Aug;80(2):188-91.

26. Pallagatti S, Sheikh S, Aggarwal A, Gupta D, Singh R, Handa R, Kaur S, Mago J. Toluidine blue staining as an adjunctive tool for early diagnosis of dysplastic changes in the oral mucosa. J Clin Exp Dent. 2013 Oct; 5(4): e187–e191.

27. Mendes SF, Ramos GO, Rivero ERC, Modolo F, Grando LJ, Meurer MI. Techniques for Precancerous Lesion Diagnosis. J Oncol. 2011;2011:326094.

28. Zhang H, Graham CM, Elci O, Griswold ME, Zhang X, Khan MA, Pitman K, Caudell JJ, Hamilton RD, Ganeshan B, Smith AD. Locally advanced squamous cell carcinoma of the head and neck: CT texture and histogram analysis allow independent prediction of overall survival in patients treated with induction chemotherapy. Radiology. 2013 Dec;269(3):801-9

29. Lydiatt W, O'Sullivan B, Patel S. Major Changes in Head and Neck Staging for 2018.Am Soc Clin Oncol Educ Book. 2018;23;38:505-514.

30. Anneroth G, Batsakis J, Luna M. Review of literature and recommended system of malignancy grading in oral squamous cell carcinoma. Scand J Dent Res 1984; 92:229-49

31. Akhter M, Hossain S, Rahman QB, Molla MR. A study on histological grading of oral squamous cell carcinoma and its co-relationship with regional metastasis. J Oral Maxillofac Pathol. 2011 May-Aug; 15(2): 168–176.

32. Brown AE, Langdon JD. Management of oral cancer. Ann R Coll Surg Engl. 1995 Nov; 77(6): 404–408.

33. Shah JP, Gil Z. Current Concepts In Management Of Oral Cancer – Surgery. Oral Oncol. 2009 Apr-May; 45(0): 394–401.

34. Carnelio S, Rodrigues GS, Shenoy R, Fernandes D. A Brief Review of Common Oral Premalignant Lesions with Emphasis on Their Management and Cancer Prevention. Indian J Surg (July–August 2011) 73(4):256–261.

35. Pindborg JJ, Reichart, PA, Smith CJ, Van der Waal I. World Health Organization. International Histological Classification of Tumours. Histological Typing of Cancer and Precancer of the Oral Mucosa. Berlin: Springer, 1997.

36. de Souza C, Pawar U, Chaturvedi P. Precancerous Lesions of Oral Cavity. Otorhinolaryngology Clinics: An International Journal, May-September 2009;1(1):7-14

37. Parlatescu I, Gheorghe C, Coculescu E, Tovaru S. Oral leukoplakia - an update. Maedica (Buchar). 2014 Mar;9(1):88-93.

38. Shirani S, Kargahi N, Razavi SM, Homayon S. Epithelial Dysplasia in Oral Cavity. IJMS 2014, 39(5):1.

39. Cho K, and Song JS. Recent Changes of Classification for Squamous Intraepithelial Lesions of the Head and Neck. Archives of Pathology & Laboratory Medicine: July 2018, Vol. 142, No. 7, pp. 829-832.

40. Warnakulasuriya S. Histological grading of oral epithelial dysplasia: revisited. J Pathol 2001; 194: 294–297. DOI: 10.1002 /path.911

41. Watanabe N, Ohkubo T, Shimizu M, Tanaka T. Preneoplasia and carcinogenesis of the oral cavity. Oncology Discovery 2015,(3):5.

42. Cowan JM, Becke MA, Ahmed-Swan S and Weichselbaum RR. Cytogene c evidence of the mul step origin of head and neck squamous cell carcinomas. J Natl Cancer Inst. 1992; 84:793-7.

43. Forastiere A, Koch W, Tro A and Sidransky D. Head and neck cancer. Engl J Med. 2001; 345:1890-900.

44. Ho MW, Risk JM, Woolgar JA, Field EA, Field JK, Steele JC, Rajlawat BP, Triantafyllou A, Rogers SN, Lowe D, Shaw RJ. The clinical determinants of malignant transformation in oral epithelial dysplasia. Oral Oncology 2012;48:969-976.

45. Scully C. Challenges in predicting wich oral mucosal potentially malignant disease will progress to neoplasia. Oral Diseases 2014;20:1-5.

46. Holmstrup P, Vedtofte P, Reibel J, Stolze K. Long-term treatment outcome of oral premalignant lesions. Oral Oncology 2006;42:461-474.

47. Pfaffe T, Cooper-White J, Beyerlein P, Kostner K, Punyadeera C., Diagnostic potential of saliva: current state and future applications. Clinical Chemistry, 2011; 57(5):675–687.

48. Nagler RM, Hershkovich O, Lischinsky S, Diamond E, Reznick AZ. Saliva analysis in the clinical setting: revisiting an underused diagnostic tool. J Investig Med 2002;50(3):214–25.

49. Ellis H. Anatomy of the salivary glands Surgery (Oxford) November 2012;30(11),569–572.

50. Whelton H. Introduction: The anatomy and physiology of salivary glands. In: Edgar M, Dawes C, O'Mullane D, editors. Saliva and Oral Health. 3rd ed. London: British Dental Association; 2004:14.

51. Edgar M, Dawes C, O'Mullane D. Saliva and oral health, 3rd ed., London: British Dental Association, 2004, 6-7.

52. Cummings C. Otolaryngology & head neck surgery. In: Cummings C, editor. Salivary gland. New York: Mosby 1998;1201–9.

53. Beahma DD, Peleaza L, Nussa DW, Schaitkinb B, Sedlmayrc JC, Rivera-Serranob CM, Zanationd AM, Walvekara RR. Surgical approaches to the submandibular gland: A review of literature. Int J Surg. 2009 Dec;7(6):503-9.

54. Wood G, Syyed N, Wales C. Sublingual gland excision: a dissection carried out following adjacent anatomical structures. Br J Oral Maxillofac Surg. 2016 Oct;54(8):927-929.

55. Roth G, Calmes R. Salivary glands and saliva. In: Roth G, Calmes R, editors. Oral Biology. St. Louis: CV Mosby. 1981;196-236.

56. Gray H. Anatomy of the Human Body. Philadelphia: Lea & Febiger, 1918.

57. Humphrey SP, Williamson RT. A review of saliva: normal composition, flow, and function. J Prosthet Dent. 2001 Feb;85(2):162-9.

58. Lalwani AK. Current Diagnosis & Treatment in Otolaryngology – Head and Neck Surgery, 2nd Ed., 2018.

59. Kumar GS. *Orban's Oral Histology and Embryology*. St Louis: Mosby, 2011.

60. de Almeida Pdel V, Grégio AM, Machado MA, de Lima AA, Azevedo LR. Saliva composition and functions: a comprehensive review. J Contemp Dent Pract. 2008 Mar 1;9(3):72-80.

61. Nunes LA, Mussavira S, Bindhu OS. Clinical and diagnostic utility of saliva as a non-invasive diagnostic fluid: a systematic review. Biochem Med (Zagreb). 2015 Jun 5;25(2):177-92.

62. Delporte C, Steinfeld S. Distribution and roles of aquaporins in salivary glands. Biochim Biophys Acta 2006; 1758:1061-70. http://dx.doi.org/10.1016/j.bbamem.2006.01.022

63. Miller N. Ten Cate's oral histology, British Dental Journal. 2012; 8th edition 213, 194.

64. Thaysen JH, Thorn NA, Schwartz IL. Excretion of sodium, potassium, chloride and carbon dioxide in human parotid saliva. Am J Physiol 1954;178(1):155–9.

65. Burne RA, Marquis RE. Alkali production by oral bacteria and protection against dental caries. FEMS Microbiol Lett 2000;193(1):1–6.

66. Gibbins HL, Proctor GB, Yakubov GE, Wilson S, Carpenter GH. Concentration of salivary protective proteins within the bound oral mucosal pellicle. Oral Dis 2014;20(7):707–13

67. Siqueira WL, Zhang W, Helmerhorst EJ, Gygi SP,Oppenheim FG. Identification of protein components in vivo human acquired enamel pellicle using LC–ESI-MS/MS. J Proteome Res 2007;6(6):2152–60.

68. Bruun C, Thylstrup A. Fluoride in whole saliva and dental caries experience in areas with high or low concentrations of fluoride in the drinking water. Caries Res 1984;18(5): 450–6

69. Ochiai A, Harada K, Hashimoto K, Shibata K, Ishiyama Y, Mitsui T, et al. a-Amylase is a potential growth inhibitor of Porphyromonas gingivalis, a periodontal pathogenic bacterium. J Periodont Res 2014;49(1):62–8.

70. Ashby MT. Inorganic chemistry of defensive peroxidases in the human oral cavity. J Dent Res 2008;87(10):900–14.

71. Gorr S-U. Antimicrobial peptides of the oral cavity. Periodontology 2000 2009;51:152–80.

72. Malamud D, Abrams WR, Barber CA, Weissman D, Rehtanz M, Golub E. Antiviral activities in human saliva. Adv Dent Res 2011;23(1):34–7.

73. Woolnough JW, Bird AR, Monro JA, Brennan CS. The effect of a brief salivary a-amylase exposure during chewing on subsequent in vitro starch digestion curve profiles. Int J Mol Sci 2010;11(8):2780–90.

74. Katschinski M. Nutritional implications of cephalic phase gastrointestinal responses. Appetite 2000;34(2):89–96.

75. Neyraud E, Sayd T, Morzel M, Dransfield E. Proteomic analysis of human whole and parotid salivas following stimulation by different tastes. J Proteome Res. 2006 Sep;5(9):2474-80.

76. Seemann R, Hagewald SJ, Sztankay V, Drews J, Bizhang M, Kage A. Levels ofparotid and submandibular/sublingual salivary immunoglobulin A in response to experimental gingivitis in humans. Clin Oral Investig. 2004 Dec;8(4):233-7.

77. Johnson DA, Yeh CK, Dodds MW. Effect of donor age on the concentrations of histatins in human parotid and submandibular/sublingual saliva. Arch Oral Bioi. 2000 Sep;45(9):731-40.

78. Schipper R, Loof A, de Groot J, Harthoom L, Dransfield E, van Heerde W. SELDI TOF-MS of saliva: Methodology and pre-treatment effects. J Chromatogr B Analyt Techno! Biomed Life Sci. 2007 Feb 15;847(1):45-53.

79. Becerra L, Soares RV, Bruno LS, Siqueira CC, Oppenheim FG, Offner GD, et al. Patterns of secretion of mucins and non-mucin glycoproteins in human submandibular/sublingual secretion. Arch Oral Biol. 2003 Feb;48(2): 147-54.

80. Zhang A, Sun H, Wang X. Saliva metabolomics opens door to biomarker discovery, disease diagnosis, and treatment. Appl Biochem Biotechnol. 2012 Nov;168(6):1718-27. doi: 10.1007/s12010-012-9891-5. Epub 2012 Sep 13.

81. Wong DT. Salivary diagnostics powered by nanotechnologies, proteomics and genomics. J Am Dent Assoc. 2006 Mar;137(3):313-21.

82. Miller CS, King CP,Jr, Langub MC, Kryscio RJ, Thomas MV. Salivary biomarkers of existing periodontal disease: A cross-sectional study. J Am Dent Assoc. 2006 Mar;137(3):322-9.

83. Hodinka RL, Nagashunmugam T, Malamud D. Detection of human immunodeficiency virus antibodies in oral fluids. Clin Diagn Lab Immunol. 1998 Jul;5(4):419-26.

84. Fisker N, Georgsen J, Stolborg T, Khalil MR, Christensen PB. Low hepatitis B prevalence among pre-school children in denmark: Saliva anti-HBc screening in day care centres. J Med Virol. 2002 Dec;68(4):500-4.

85. Nigatu W, Jin L, Cohen BJ, Nokes DJ, Etana M, Cutts FT, et al. Measles virus strains circulating in ethiopia in 1998-1999: Molecular characterisation using oral fluid samples and identification of a new genotype. J Med Viral. 2001 Oct;65(2):3 73-80.

86. Cone EJ, Presley L, Lehrer M, Seiter W, Smith M, Kardos KW, et al. Oral fluid testing for drugs of abuse: Positive prevalence rates by intercept immunoassay screening and GC-MS-MS confirmation and suggested cutoff concentrations. J Anal Toxicol. 2002 Nov-Dec;26(8):541-6.

87. Lee Y-H, Wong DT. Saliva: An emerging biofluid for early detection of diseases. American journal of dentistry. 2009;22(4):241-248.

88. Denny P, Hagen FK, Hardt M, Liao L, Yan W, Arellanno M, Bassilian S, Bedi GS, Boontheung P, Cociorva D, Delahunty CM, Denny T, Dunsmore J, Faull KF, Gilligan J, Gonzalez-Begne M, Halgand F, Hall SC, Han X, Henson B, Hewel J, Hu S, Jeffrey S, Jiang J, Loo JA, Ogorzalek Loo RR, Malamud D, Melvin JE, Miroshnychenko O, Navazesh M, Niles R, Park SK, Prakobphol A, Ramachandran P, Richert M, Robinson S, Sondej M, Souda P, Sullivan MA, Takashima J, Than S, Wang J, Whitelegge JP, Witkowska HE, Wolinsky L, Xie Y, Xu T, Yu W, Ytterberg J, Wong DT, Yates JR, 3rd, Fisher SJ. The proteomes of human parotid and submandibular/sublingual gland salivas collected as the ductal secretions. J Proteome Res. 2008;7:1994–2006.

89. Kho KW, Malini O, Shen ZX, Soo KC. Surface Enhanced Raman Spectroscopic (SERS) study of saliva in the early detection of oral câncer, Optical Diagnostics and Sensing. 2005;84:84-91.

90. Dana K, Shende C, Huang H, Farquharson S. Rapid Analysis of Cocaine in Saliva by Surface-Enhanced Raman Spectroscopy. Journal of analytical & bioanalytical techniques. 2015;6(6):1-5. doi:10.4172/2155-9872.1000289.

91. Muro CK, Fernandes LS, Lednev IK. Sex Determination Based on Raman Spectroscopy of Saliva Traces for Forensic Purposes. Anal. Chem. 2016;88(24):12489–12493.

92. Feng S, Huang S, Lin D, Chen G, Xu Y, Li Y, Huang Z, Pan J, Chen R, Zeng H. Surface-enhanced Raman spectroscopy of saliva proteins for the noninvasive differentiation of benign and malignant breast tumors. Int J Nanomedicine. 2015 Jan 12;10:537-47.

93.Gonchukov S, Sukhinina A, Bakhmutov D, Minaeva S. Raman spectroscopy of saliva as a perspective method for periodontitis diagnostics. Laser Phys. Lett. 2012; 9(1): 73-77.

Chapter 2a: Raman Spectroscopy and Diagnostic Applications

2a.1 Raman Spectroscopy

Raman spectroscopy was named in honour of its discoverer, C.V. Raman, who, along with K.S. Krishnan, published the first paper on this technique in 1928[1]. Raman spectroscopy is a versatile method for analysis of a wide range of samples. It resolves most of the limitations of other spectroscopic techniques. It can be used for both qualitative as well as quantitative purposes. Qualitative analysis can be performed by measuring the frequency of scattered radiation while quantitative analysis can be performed by measuring the intensity of scattered radiation[2].

2a.1.1 Diagnostics by Raman Spectroscopy

Raman spectroscopy has been applied in numerous scientific fields, from chemistry and biochemistry to arts and archaeology, as a powerful spectroscopic technique which yields a spectral fingerprint capable of identifying and characterising the structure and function of molecules, materials, cells or tissues [3,4].

Raman spectroscopy, with its molecular specificity and various signal enhancement techniques for increased sensitivity, has been extensively utilised in biomedical and clinical applications[5]. Both *in vivo* and *in situ* measurements have been demonstrated with minimum or no sample preparation[6].

Recent studies with Raman spectroscopy have shown its applicability in the identification of bacterial infection in the urinary tract as well as antibiotic pharmacokinetics for treatment[7]. Furthermore, Raman spectroscopy has been utilised to track nanomaterials moving through the circulation and to detect inhaled nanoparticles in the respiratory tract[8,9]. Coronary atherosclerosis along with blood components have also been

investigated for diagnostic purposes, with promising results[10]. Low level detection of viral pathogens has been also achieved with application of Surface-enhanced Raman scattering (SERS)[11].

2a.1.1.1 *Cancer Diagnosis by Raman Spectroscopy*

Quantitative Raman spectroscopy has also been used for grading the severity of various cancers[12]. The phenomenon of Raman spectroscopy makes it ideal for assessing/probing samples because numerous biological molecules undergo some Raman scattering, allowing one to detect small molecular and architectural changes in the sample that might be associated with cancer, such as an increased nucleus-to-cytoplasm ratio, disordered chromatin, higher metabolic activity, and changes in lipid and protein levels[13].

When aimed at oncological diagnostics, Raman spectroscopy is usually applied through *in vitro*, *ex vivo* and/or *in vivo* approaches, without disrupting the cellular environment. Several studies using *in vitro* cultures have shown encouraging results for the application of Raman spectroscopy for improving the detection and screening of cervical cancer as well as investigating the biochemical changes associated with HPV infection[14,15]. Furthermore, normal and neoplastic lymphocytic cell lines could be distinguished by Raman spectroscopy based on DNA and protein changes[16]. *Ex vivo* essays, which include analysis of histological and cytological specimens, could achieve over 99.5% sensitivity and specificity of classification between normal and malignant in gastrointestinal samples, for example[17]. Similarly, Lyng *et al.* investigated tissue samples from 40 patients using Raman spectroscopy, and a principal components analysis associated with linear discriminant analysis (PCA-LDA) model to classify the samples as normal, cervical intraepithelial neoplasia (premalignant) or invasive carcinoma[18].

The use of *in vivo* Raman detection is still in the exploratory stages with the majority of work being conducted on animal models[19]. However, some researchers have applied this

technique to study a number of *in vivo* health related phenomenon of human tissue samples, such as non-invasive assessment of human corneal hydration, estimation of stratum corneum thickness, and monitoring drug penetration depth inside the skin[20,21,22].

When it comes to cancer diagnostics, skin cancer is arguably one of the most studied forms of neoplasia *in vivo*, *via* Raman spectroscopy, primarily due to the ease of access of suspicious lesions. Clinical studies conducted have already confirmed the ability to distinguish malignant and pre-malignant skin lesions from benign ones, melanomas from nevi (benign pigmented lesions, commonly referred to as moles), and melanomas from seborrheic keratosis[23]. However, the in vivo application of Raman spectroscopy is not confined to skin cancer diagnosis. A variety of endoscopic systems/fiber-based probes have also been developed for investigative work on breast[24], brain[25], colorectal[26], esophageal[27], gastric[28] and lung cancers[29].

The assessment of surgical margins and cancer infiltration has also been investigated using *in* vivo Raman spectroscopy with promising results and easy clinical applicability, although, the small number of subjects involved in these studies may affect the reproducibility and, consequently, can decrease the diagnostic potential of the classifiers[30].

Also, new methodologies of Raman spectroscopy applied for liquid samples have been studied as proposed Bonnier e*t al.*[31]. This approach applied an inverted geometry to improve the quality of the measurements of concentrated serum. The size and shape of the human serum drop analysed had little impact on the data collected using the methodology proposed. Thus, they were able to show that the use of centrifugal filtration devices to remove of low molecular weight proteins, enhances signals and intrinsic spectral reproducibility[31].

2a.1.1.2 *Oral Cancer and Raman Spectroscopy*

Regarding oral cancer specifically, the very first application of Raman spectroscopy started with the analysis of normal and dysplastic tissue in a murine model[32]. Dysplasia was chemically induced in the palate of mice resulting in 100% of both sensitivity and specificity. More recent studies have developed a Raman spectroscopy method with specificity and sensitivity better than 95%, for discrimination of normal and malignant tissues in oral cancers in formalin fixed oral tissues or even epithelial sections [33].

In vivo approaches have been also developed, aimed at the diagnosis of oral dysplasia and oral malignancies. Singh *et al.* have shown the discrimination of normal control, premalignant, and cancerous oral sites from 104 patients with prediction accuracies between 72–96%[34]. In a more recent study, the same group assessed the potential of Raman spectroscopy to detect malignancy changes/cancer field effects in a cohort study. The comparison of non-cancer locations in a smoking and non-smoking population demonstrated prediction accuracies from 75–98%. This work further demonstrates the sensitivity of Raman scattering to subtle biochemical changes which may precede clinical disease[35]. Another group reported the discrimination of normal oral tissue from three separate lesion categories by probing with per-class accuracies ranging from 82–89% in 199 patients and 96% sensitivity and 99% specificities for normal versus malignant and 99% and 98% respectively, for normal versus potentially malignant[36].

Raman spectroscopic analysis of blood samples has also been applied to oral cancers. It has been proven that Raman spectroscopy can be used to distinguish between serum samples from patients that had been diagnosed with buccal mucosa and tongue cancer, and those from healthy volunteers[37]. Amino acids and lipids were the most significant Raman bands affected in the analysis. An efficacy of 85% was found when all spectra

were independently analysed. Also, Raman spectroscopy of serum samples was able to predict a potential reoccurrence of oral cancer[37].

An innovative study for oral diagnosis based on bodily fluids has been also performed[38]. Voided raw urine was collected from 167 patients and evaluated for its chemical components. Molecular vibrations associated with uric acid, specifically C–C stretching at 558 and 649 cm^{-1} and N–H stretching at 798 cm^{-1}, showed elevated intensities in cancer patients compared to healthy volunteers. Four Raman bands related to creatinine also showed increases, while the band at 692 cm^{-1} was only present in cancer patients. Statistical analysis resulted in a diagnostic accuracy of 93.7%[38].

Oral cancer detection has been extended to saliva analysis through SERS. Using a discrimination threshold of 0.5, 23 normal samples (23/30), and 57 cancer samples (57/62) could be discriminated correctly, yielding the diagnostic sensitivity of 91.9%, specificity of 76.7%, and accuracy of 87.0%[39]. Nevertheless, the process to obtain spectral information requires a complex sample preparation of the associated nano particles[39].

2a.1.2 Principle of Raman Spectroscopy

When light interacts with matter, the photons which make up the light may be absorbed or scattered, or may not interact with the material and may pass straight through it. Much of the scattered radiation has a frequency which is equal to the frequency of the incident radiation and constitutes Rayleigh scattering. The Rayleigh scattering process will be the most intense, since most photons scatter this way. However, the scattered light having a frequency different from that of incident light (inelastic scattering) may be used to construct a Raman spectrum. This latter phenomenon was first described by the Indian physicist C.V. Raman in 1928 as a rare process, in that only one in every 10^6–10^8 photons are Raman scattered[40,41].

Raman spectroscopy uses a single frequency of radiation to irradiate the sample and it is the radiation scattered from the molecule, one vibrational unit of energy different from the incident beam, which is detected (**Figure 2a.1**). The Raman scattering process from the ground vibrational state (m) leads to absorption of energy by the molecule and its promotion to a higher energy excited vibrational state (n)[42].

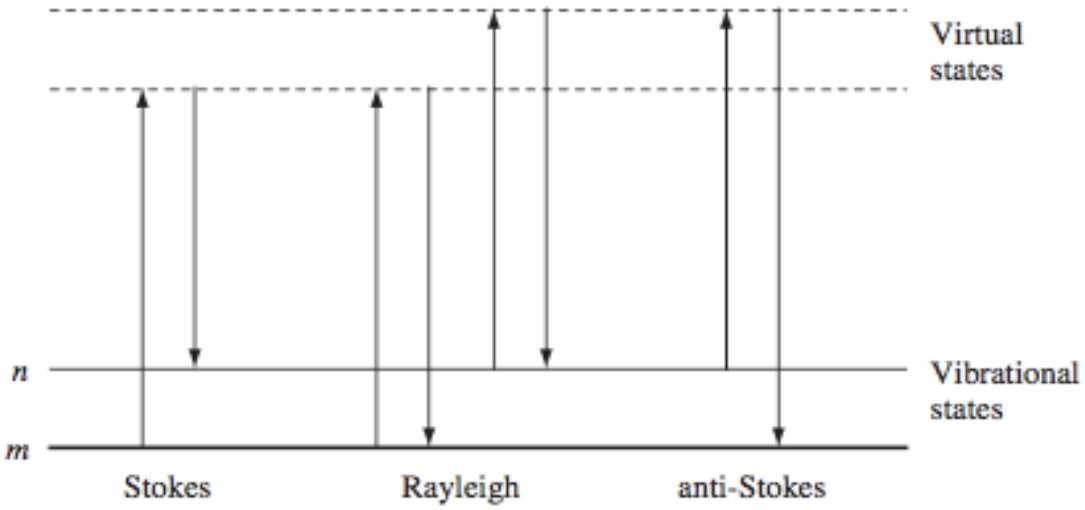

Figure 2a.1: Diagram of the Rayleigh and Raman scattering processes. The lowest energy vibrational state m is shown at the foot with states of increasing energy above it. Source: Hollas JM. *Modern Spectroscopy*. West sussex, England: John Wiley and Sons, 2004[42].

When the frequency of the incident radiation is higher than that of the scattered radiation, Stokes lines appear in the Raman spectrum. But, when the frequency of the incident radiation is lower than that of the scattered radiation, anti-Stokes lines appear in the Raman spectrum. The Raman scattered light can be collected by a spectrometer and displayed as a Raman spectrum, in which peaks (bands) correspond to Raman frequency

shifts (measured in wavenumbers cm^{-1}) caused by the characteristic vibrations in the molecules of a sample[42].

A change in net molecular polarisability must occur for a molecular vibration to be Raman active. The polarisability (α) represents the ability of an applied electric field, E, to induce a dipole moment, μ_0, in an atom or molecule; a process represented mathematically by the following equations:

$$\mu_o = \alpha \mathrm{E}$$

Equation 2a.1

At the molecule's equilibrium nuclear geometry, the polarisability has a value, α_0. In the case of displacement, Δr, away from the molecule's equilibrium geometry, the instantaneous polarisation α is given by:

$$\alpha = \alpha_o \left[\frac{\partial \alpha}{\partial r}\right] \Delta r$$

Equation 2a.2

If the molecule is vibrating in a sinusoidal fashion, Δr can be written as a sinusoidal function in terms of the frequency of the vibration, ν_s, and the time, t:

$$\Delta r = r_{max} \cos\ (2\Delta r = r_{max} \cos(2\pi \nu t)\, \pi \upsilon_{st})$$

Equation 2a.3

Light of a particular frequency, ν_o, has an associated electric field, E, which also has sinusoidal behaviour:

$$\mathrm{E} = \mathrm{E}_{max}\cos\,(2\pi v_o t)$$

Equation 2a.4

Equations 2.1 to 2.4 can thus be written in the form of equation 2.5, in which the first term represents the scattered phenomenon of Rayleigh scattering. The second term represents the Raman scattering of frequency $\nu_0+\nu_s$ (anti-Stokes scattering), when the frequency of the scattered photon increases by molecular motion, ν_s; and the third term represents Stokes scattering of light of frequency $\nu_0-\nu_s$ (Stokes scattering), when the frequency decreases[43].

$$\mu_o = \alpha_o \mathrm{E}_{max}\cos(2\pi\upsilon_o t) + \mathrm{E}_{max} r_{max}\left[\frac{d\alpha}{dr}\right]\cos(2\pi\upsilon_s t)\cos(2\pi\upsilon_o) \Leftrightarrow$$

$$\Leftrightarrow \mu_o = \alpha_o \mathrm{E}_{max}\cos(2\pi\upsilon_o t) + \frac{\mathrm{E}_{max} r_{max}}{2}\left[\frac{\partial\alpha}{\partial r}\right]\{\cos[2\pi t(\upsilon_o + \upsilon_s)] + \cos[2\pi(\upsilon_o - \upsilon_s)]\}$$

Equation 2a.5

2a.1.3 Instrumentation

The common Raman microspectrometer components are detailed in the schematic diagram (**Figure 2a.2**). The laser applied is the source of the monochromatic incident light that can be of different wavelengths, from ultra violet to near infra-red, and its choice is inherent to the application desired. The pin holes, or even sometimes neutral density filters, determine the intensity of the incident light and may be adjustable. Along with

this, the interference filter is a clean-up tool that only allows the laser output through. A microscope coupled to the system holds the sample and makes possible the analysis of samples as the focusing is facilitated with this. Furthermore, the objective lenses deliver the laser as well as collect the backscattered light. The Notch (or Edge) filter reflects the same wavelength as the incident light to remove all the Rayleigh scattered light and everything outside this range is taken as Raman scatter, to be transmitted further. The spectral resolution is determined by the groove density (measured in grooves/mm) of the grating, whereby a higher groove density corresponds to higher resolution. The grating or spectrograph is used to disperse the light and it is generally available in a setup between 300 to 1800 groves / mm. Apart from that, other factors that can influence the spectral resolution are the wavelength and the spectrometer length, which is the distance between the grating and the detector. Very often used in Raman spectroscopy because of its light sensitivity, the charge coupled device (CCD) allows multichannel operation which permits a Raman spectrum be detected in a single acquisition (**Figure 2a.3**).

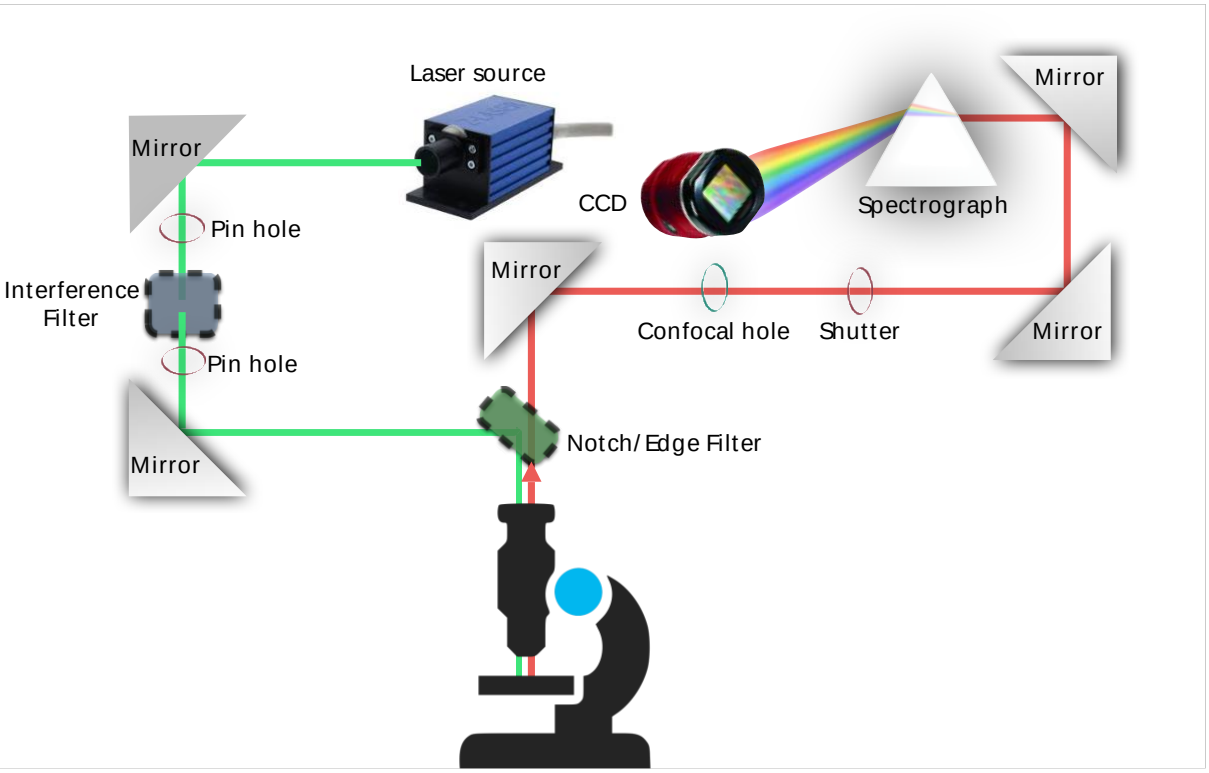

Figure 2a.2: Schematic diagram of a Raman microspectrometer based on the Horiba Jobin Yvon LabRAM HR800.

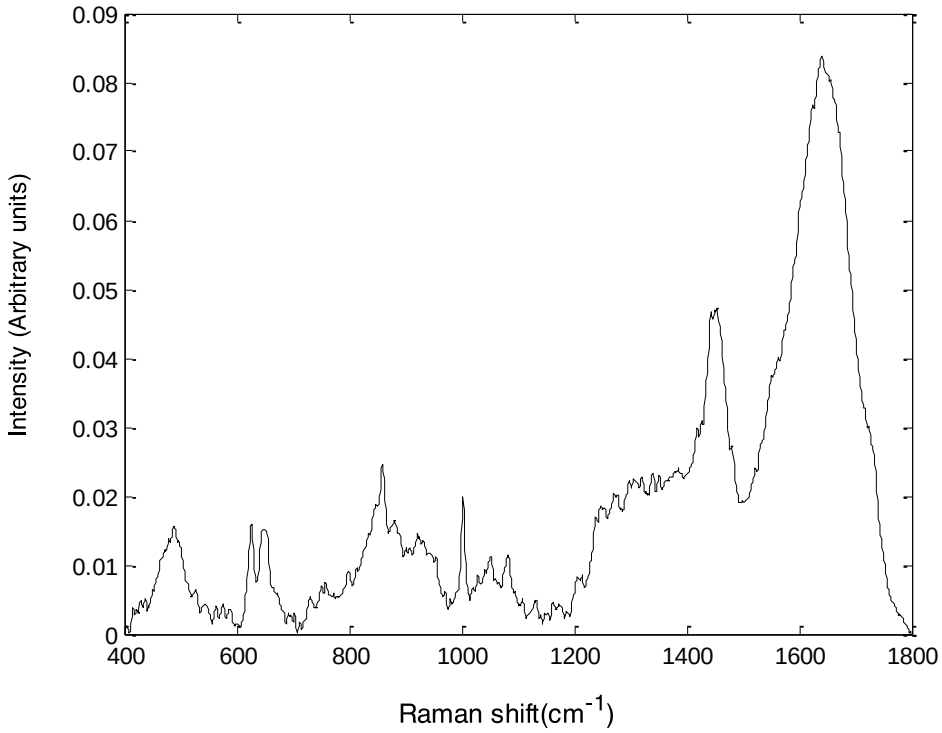

Figure 2a.3: Example of Raman spectrum of unstimulated saliva sample acquired using the instrument setup described above.

2a.1.4 Statistical tools for Raman analysis

2a.1.4.1 *Pre-processing procedures*

Smoothing

Smoothing techniques are commonly used to reduce spectral noise. These noise reduction practices also rely on the fact that spectral noise occurs at high frequency and therefore its transition from point to point on a spectrum is abrupt and random[44]. When utilising the moving average technique, each individual point of a spectrum is averaged with a chosen number of adjacent points. Savitzky–Golay polynomial smoothing can alleviate spectral distortion, as this methodology fits a polynomial function to a section of points around the point of interest. This allows for spectral features, such as a band's height and width, to be conserved[44,45].

Baseline correction

Rubberband baseline correction finds a convex polygonal line whose edges are ''troughs'' within the spectrum. This method fixes the endpoints of the dataset in order to avoid any such alterations from occurring[44].

Normalisation

Another important pre-processing procedure for Raman spectra is intensity normalisation, as this allows for intensities acquired from different spectral acquisitions to be compared. Vector Normalisation (Euclidean or L2-norm) is often used after differentiation, when there is no apparently consistent peak across the spectra in Raman spectroscopy[46].

2a.1.4.2 *Background Removal by Non negative constrained least squares (NNLS) analysis*

Non-negatively constrained least squares analysis (NNLS) is a technique similar to that of Classical least squares (CLS) method developed by Lawson and Hanson[47]. The CLS fitting is a supervised technique used to estimate the weighted contributions of a set of input spectra to a sample spectrum. It assumes that any complex spectrum is the weighted sum of all the base components that contribute to the spectrum[48].

NNLS is used to estimate the weighted contributions of a set of input spectra in a sample spectrum. However, unlike CLS, NNLS introduces non-negative constraints on the weighting co-efficients of the input spectra aiming to minimise the error in fitting the sample spectrum[48].

2a.1.4.3 *Principal Components Analysis (PCA)*

Developed in 1901 by Karl Pearson, principal components analysis (PCA) is a statistical method widely used in exploratory analysis and model prediction. It is an unsupervised data reduction technique used to identify variances within the dataset that may be used to classify objects into groups[49].

PCA involves the calculation of the eigenvalue decomposition of a data matrix, usually after mean centring the data for each attribute. The results of a PCA are usually discussed in terms of component scores and loadings[50].

In Raman spectroscopy, PCA is used to reduce the matrix of spectral data in which objects (individual spectra) are measurements of a large number of variables (wavenumbers), whilst retaining most of the variation within the dataset. It works by (1) subtracting the mean of the dataset to obtain the mean centred matrix, (2) calculating the covariance

matrix (linear relationships between the individual spectra) of the mean centred matrix and (3) finding the eigenvectors and eigenvalues of the covariance matrix[51].

The eigenvector with the highest eigenvalue explains the most variance in the data set and is called the first principal component (PC). The first PC therefore describes the largest source of variance across all the spectra, the second PC the next largest source of variance and so on, all PCs describing mutually independent sources of variance in decreasing proportions of spectral variance[51,52].

2a.1.4.4 *Partial least squares-discriminant analysis (PLSDA)*

PLSDA is considered a supervised technique of multivariate analysis which works as a linear classifier that aims to separate any data into groups using a hyperplane[53]. This form of analysis, similar to PCA, maximises the variance between groups and minimises the variance within groups[53]. It is based, however, on partial least squares regression (PLSR), a method used for constructing predictive models when the factors are many and highly collinear[54]. Conventionally, in the classic PLSR, y is a matrix of continuous variables, while in PLSDA it is categorical and used to assign the observations into classes[53,54]. The loadings of the discriminate hyperplanes or latent variables (LVs) can be visualised to provide more information about the source (component) of the variance[53].

2a.1.4.5 *Leave one patient out cross validation (LOPOCV)*

Cross validation of any spectral classification models is an essential step to avoid over or under-fitting the model due to inappropriate selection of the components used as well as to determine the prediction error of the model.

Leave one patient out cross validation (LOPOCV) is based on the leave one out cross validation (LOOCV) technique. In LOOCV one observation is excluded at a time from the training set and the resulting model is evaluated on the left out observation. The

procedure is repeated for all observations in the data set and the average performance across all interactions is considered the performance of the classification model[51]. However, in LOPOCV, instead of leaving one spectrum out, one patient is left out so that all the spectra of the patient are left out and predicted.

References

1. Raman CV, Krishnan KS. A New Type of Secondary Radiation. Nature . 1928;121:501-502.

2. Bumbrah GS, Sharma RM. Raman spectroscopy – Basic principle, instrumentation and selected applications for the characterization of drugs of abuse. Egyptian Journal of Forensic Sciences 2019;6, 209–215.

3. Krafft C. 2004. Bioanalytical applications of Raman spectroscopy. Analytical and Bioanalytical Chemistry, 2044;378(1):60–62.

4. Baraldi P, Tinti. Raman spectroscopy in art and archaeology. Journal of Raman Spectroscopy, 2008;39(8):963–965.

5. Keating ME, Byrne HJ. Raman spectroscopy in nanomedicine: current status and future perspective. Nanomedicine (Lond). 2013 Aug;8(8):1335-51. doi: 10.2217/nnm.13.108.

6. Kong K, Kendall C, Stone N, Notingher I. Raman spectroscopy for medical diagnostics — From in vitro biofluid assays to in vivo cancer detection. Adv Drug Deliv Rev. 2015 Jul 15;89:121-34. doi: 10.1016/j.addr.2015.03.009. Epub 2015 Mar 22.

7. Kastanos EK, Kyriakides A, Hadjigeorgiou K, Pitris C. A novel method for urinary tract infection diagnosis and antibiogram usinh Raman spectroscopy. Journal of Raman Spectroscopy 2010l;41:958-963.

8. Liu Z, Davis C, Cai W, He L, Chen X, Dai H. Circulation and long-term fate of functionalized, biocompatible single-walled carbon nanotubes in mice probed by Raman spectroscopy. Proc Natl Acad Sci U S A. 2008 Feb 5; 105(5): 1410–1415.

9. Miller MR, Raftis JB, Langrish JP, McLean SG., Samutrtai P, Connell SP, Wilson S, Vesey AT, Fokkens PHB, Boere AJF, Krystek P, Campbell CJ, Hadoke PWF, Donaldson K, Cassee FR, Newby DE, Duffin R, Mills NL. Inhaled Nanoparticles Accumulate at Sites of Vascular Disease. ACS Nano, 2017;11(5: 4542–4552.

10. Chau AH, Motz JT, Gardecki JA, Waxman S, Bouma BE, Tearney GJ. Fingerprint and high-wavenumber Raman spectroscopy in a human-swine coronary xenograft in vivo. Journal of biomedical optics. 2008;13(4):040501. doi:10.1117/1.2960015.

11. Driskell JDm Kwarta KM, Lipert RJ, Porter MD, Neill JD, Ridpath JF. Low-level detection of viral pathogens by surface-enhanced Raman scattering based immunoassay. Analytical Chemistry 2005;77:6147-6154.

12. Rehman S, Movasaghi Z, Tucker AT, Joel SP, Darr JA, Ruban AV, et al.Raman spectroscopic analysis of breast cancer tissues: identifying differences between normal, invasive ductal carcinoma and ductal carcinoma in situ of the breast tissue. J Raman Spectrosc 2007;38:1345-51.

13. Mahadevan-Jansen A, Richards-Kortum RR. Raman Spectroscopy for the detection of cancers and precancers. J. Biomed. Opt. 1(1), 31–70 (1996).10.1117/12.227815

14. Jess PRT, Smith DDW, Mazilu M, Dholakia K, Riches AC, Herrington CS. Early detection of cervical neoplasia by Raman spectroscopy. International Journal of Cancer, 2007;121(12): 2723–2728.

15. Ostrowska KM, Malkin A, Meade A. Investigation of the influence of high-risk human papillomavirus on the biochemical composition of cervical cancer cells using vibrational spectroscopy. Analyst, 2010;135(12):3087– 3093.

16. Chowdary MV, Kumar KK, Thakur K, Anand A, Kurien J, Krishna CM, Mathew S. Discrimination of normal and malignant mucosal tissues of the colon by Raman spectroscopy. Photomed Laser Surg. 2007 Aug;25(4):269-74.

17. Chan JW, Taylor DS, Zwerdling T, Lane SM, Ihara K, Huser T. Micro-Raman Spectroscopy Detects Individual Neoplastic and Normal Hematopoietic Cells. Biophysical Journal. 2006;90(2):648-656. doi:10.1529/biophysj.105.066761.

18. Lyng FM, E. Faola O, Conroy J. Vibrational spectroscopy for cervical cancer pathology, frombiochemical analysis to diagnostic tool. Experimental and Molecular Pathology, 2007;82(2):121–129.

19. Austin LA, Osseiran S, Evans CL. Raman technologies in cancer diagnostics. Analyst. 2016 Jan 21;141(2):476-503. doi: 10.1039/c5an01786f.

20. Bauer NJC, Hendrikse F, March WF. In vivo confocal Raman spectroscopy of the human cornea. Cornea 1999;18:483–488.

21. Egawa M, Hirao T, Takahashi M. In vivo estimation of stratum corneum thickness from water concentration profiles obtained with Raman spectroscopy. Acta. Derm. Venereol 2007; 87:4–8.

22. Caspers PJ, Williams AC, Carter EA, Edwards HGM, Barry BW, Bruining HA, Puppels GJ. Monitoring the Penetration Enhancer Dimethyl Sulfoxide in Human Stratum Corneum in Vivo by Confocal Raman Spectroscopy. Pharmaceutical Research 2002;19(10):1577–1580.

23. Wang H, Zhao J, Lee AMD, Lui H, Zeng H. Improving skin Raman spectral quality by fluorescence photobleaching. Photodiagn.Photodyn. Ther., 2012;9:299–302.

24. Li Q, Gao Q, Zhang G. Classification for breast cancer diagnosis with Raman spectroscopy. Biomedical Optics Express. 2014;5(7):2435-2445. doi:10.1364/BOE.5.002435.

25. Beljebbar A, Dukic S, Amharref N, Manfait M. Ex vivo and in vivo diagnosis of C6 glioblastoma development by Raman spectroscopy coupled to a microprobe. Analytical and Bioanalytical Chemistry, 2010;398(1):477–487.

26. American Cancer Society, Breast Cancer Facts & Figures 2009–2010, American Cancer Society, Atlanta, Ga, USA.

27. Garai E, Sensarn S, Zavaleta CL, et al. A Real-Time Clinical Endoscopic System for Intraluminal, Multiplexed Imaging of Surface-Enhanced Raman Scattering Nanoparticles. Chen X, ed. PLoS ONE. 2015;10(4):e0123185. doi:10.1371/journal.pone.0123185.

28. Shi H, Chen S-Y, Lin K. Raman spectroscopy for early real-time endoscopic optical diagnosis based on biochemical changes during the carcinogenesis of Barrett's esophagus. World Journal of Gastrointestinal Endoscopy. 2016;8(5):273-275. doi:10.4253/wjge.v8.i5.273.

29. Bergholt MS, Zheng W, Ho KY, Teh M, Yeoh KG, So JB, Shabbir A, Huang Z. Fiber-optic Raman spectroscopy probes gastric carcinogenesis in vivo at endoscopy. J Biophotonics. 2013 Jan;6(1):49-59. doi: 10.1002/jbio.201200138.

30. Short MA, Lam S, McWilliams AM, Ionescu DN, Zeng H. Using laser Raman spectroscopy to reduce false positives of autofluorescence bronchoscopies: a pilot study. J Thorac Oncol. 2011 Jul;6(7):1206-14. doi: 10.1097/JTO.0b013e3182178ef7.

31. Bonnier F, Petitjean F, Baker MJ, Byrne HJ. Improved protocols for vibrational spectroscopic analysis of body fluids. J Biophotonics. 2014 Apr;7(3-4):167-79. doi: 10.1002/jbio.201300130.

32. Bakker Schut TC, Witjes MJ, Sterenborg HJ, Speelman OC, Roodenburg JL, Marple ET, Bruining HA, Puppels GJ. In vivo detection of dysplastic tissue by Raman spectroscopy. Anal Chem. 2000 Dec 15;72(24):6010-8.

33. Olivo M, Bhuvaneswari R, Keogh I. Advances in Bio-Optical Imaging for the Diagnosis of Early Oral Cancer. Pharmaceutics, 2011;3:354-378. doi:10.3390/pharmaceutics3030354

34. Singh SP, Deshmukh A, Chaturvedi P, Murali Krishna C. In vivo Raman spectroscopic identification of premalignant lesions in oral buccal mucosa. J Biomed Opt. 2012 Oct;17(10):105002. doi: 10.1117/1.JBO.17.10.105002.

35. Chen P, Shimada R, Yabumoto S,2 Okajima H, Ando M, Chang C, Lee L, Wong Y, Chiou A, Hamaguchib H. Automatic and objective oral cancer diagnosis by Raman spectroscopic detection of keratin with multivariate curve resolution analysis. Sci Rep. 2016; 6: 20097.

36. Krishna H, Majumder SK, Chaturvedi P, Sidramesh M, Gupta PK. In vivo Raman spectroscopy for detection of oral neoplasia: a pilot clinical study. J Biophotonics. 2014 Sep;7(9):690-702. doi: 10.1002/jbio.201300030. Epub 2013 Jul 2.

37. Sahu A, Sawant S, Mamgain H, Krishna CM. Raman spectroscopy of serum: an exploratory study for detection of oral cancers. Analyst. 2013 Jul 21;138(14):4161-74. doi: 10.1039/c3an00308f. Epub 2013 Jun 4.

38. Elumalai B., Prakasarao A., Ganesan B., Dornadula K., and Singaravelu G. (2014) Raman spectroscopic characterization of urine of normal and oral cancer subjects, J. Raman Spectrosc., 46; pages 84–93, doi: 10.1002/jrs.4601.

39. Feng S, Lin D, Lin J, Huang Z, Chen G, Li Y. Saliva analysis combining membrane protein purification with surface-enhanced Raman spectroscopy for nasopharyngeal cancer detection. Appl Phys Lett. 2014;104:073702. doi: 10.1063/1.4866027.

40. Skoog DA, Holler FJ, Crouch SR. Principles of instrumental analysis. 6th ed. Cengage Learning; 2006.

41. Smith E, Dent G. Modern Raman spectroscopy: a practical approach. England, Chichester: John Wiley & Sons; 2005.

42. Hollas JM. Modern Spectroscopy. West sussex, England: John Wiley and Sons, 2004:483.

43. Ball DW. Theory of Raman Spectroscopy. Spectroscopy, 2001;16(11).

44. Gemperline P. Practical Guide To Chemometrics 2nd edn CRC Press, 2006.

45. Savitzky A, Golay MJE. Smoothing and Differentiation of Data by Simplified Least Squares Procedures. Anal. Chem. In Analytical Chemistry, Vol. 36, No. 8. (1 July 1964), pp. 1627-1639, doi:10.1021/ac60214a047

46. Trevisan J, Angelov PP, Carmichael PL, Scott AD, Martin FL. Extracting biological information with computational analysis of Fourier-transform infrared (FTIR) biospectroscopy datasets: current practices to future perspectives. Analyst. 2012 Jul 21;137(14):3202-15. doi: 10.1039/c2an16300d.

47. Lawson CL, Hanson RJ. Solving Least Squares Problems, Prentice-Hall, Englewood Cliffs, NJ 1974.

48. Ibrahim O, Maguire A, Meade AD, Flint S, Toner M, Byrne HJ, Lyng FM. Improved protocols for pre-processing Raman spectra of formalin fixed paraffin preserved tissue sections. Anal. Methods. 2017,9:4709-4717.

49. Pearson K. On Lines and Planes of Closest Fit to Systems of Points in Space. Philiosophical Magazine, 1901;2:559–572.

50. Martens H, Næs T.. Multivariate Calibration, John Wiley & Sons, Inc. 1989.

51. Gautam R, Vanga S, Ariese F, Umapathy S. Review of multidimensional data processing approaches for Raman and infrared spectroscopy EPJ Techniques and Instrumentation, 2015;2(8):1-38.

52. Bonnier F, Traynor D, Kearney P, Clarke C, Knief P, Martin C, O'Leary JJ, Byrned HJ, Lyng F. Processing ThinPrep cervical cytological samples for Raman spectroscopic analysis. Anal. Methods, 2014,6, 7831-7841

53. Richard G. Brereton Gavin R. Lloyd. Partial least squares discriminant analysis: taking the magic away. Volume28, Issue4 Special Issue: Conferentia Chemometrica, 2014, 213-225.

54. Tobias R D. An introduction to partial least squares regression. SAS Conf Proc SAS Users Gr Int 20 (SUGI 20), 1995:2-5.

Chapter 2b: Raman Spectroscopic Analysis of Saliva samples for the Diagnosis of Oral Cancer: A Systematic Review

Adapted from 'Calado, G., Behl, I., Daniel, A., Byrne H. J., Lyng, F. M. Raman Spectroscopic Analysis of Saliva samples for the Diagnosis of Oral Cancer: A Systematic Review' accepted for publication in Translational Biophotonics (DOI: 10.1002/tbio.201900001).

Genecy Calado conducted all the systematic analysis and was primary author of the article, with contribution and guidance from the other authors.

2b.1 Abstract

Oral squamous cell carcinoma (OSCC) is one of the most common malignancies worldwide, and new protocols for routine and early detection are required. Raman spectroscopy is an optical based method that can provide sensitive and non-invasive real time detailed information on the biochemical content of a sample like saliva, through the unique vibrations of its constituent molecules and this is sensitive to changes associated with disease. A comprehensive systematic review of the available scientific literature related to Raman spectroscopy of human saliva for diagnosis of OSCC was performed. The 785 nm laser line was most applied wavelength along with principal components analysis (PCA) associated with linear discriminant analysis (LDA). The main salivary components possibly associated with the presence of OSCC were proteins and lipids. Measurement in the liquid physical state, and with no addition of nanoparticles for signal enhancement, seemed to best conserve the salivary integrity. However, in terms of

sampling protocols, no differentiation was generally made between stimulated and non stimulated saliva. Raman spectroscopy of saliva holds a promising future for clinical applications such as early detection of OSCC. However more systematic analyses are still required for a better elucidation regarding sampling procedure, storage and degradation.

2b.2 Introduction

Oral Squamous cell carcinoma (OSCC) is one of the most frequently encountered malignant tumours worldwide, and its incidence is expected to reach around 350,000 new cases per year[1]. In 2018, OSCC, the histopathological variant present in more than 95% of tumours of the head and neck region, was also responsible for more than 150,000 thousand deaths[1]. Furthermore, an exponential growth of the mortality rate related to this pathologic entity can be foreseen for the coming years[1-3].

OSCC, along with other head and neck tumours such as oropharygeal cancer, is the 6th most common malignant tumour worldwide[2]. This neoplasm seems to be more prevalent in males, in a ratio of 1.5 male:1 female[2]. This gender difference could be explained by the more frequent exposure to predisposing factors (such as tobacco and alcohol) and those associated with occupational conditions[2,3].

Early detection followed by appropriate treatment can increase cure rates in 80-90% of OSCC cases and significantly improve patient quality of life, minimising the need for extensive and debilitating treatments[4]. In addition, the medical and scientific community currently recognises that, without the development and implementation of new standardised screening procedures, the vast majority of cases of oral cancer are found in the late stage, often presenting peripheral metastases and infiltration of the regional liphonodal chain[5,6].

Usually, the clinical diagnosis of head and neck neoplasias, including oral cancer, is performed through invasive biopsies followed by an expensive histological examination of excised tissue. This may result in psychological trauma and risk of infection for patients. In addition, it is well accepted that this type of diagnostic method is limited as it is a subjective histological gradation of the pathology in question, as represented by morphological abnormalities in the tissue[7]. In addition, clinically innocuous premalignant lesions, or even "hidden" lesions (such as lesions located in the retromolar region), can easily go undetected by routine clinical examination.

Adjuvant techniques for the early detection and diagnosis of oral cancer include exfoliative cytology, toluidine blue staining, chemiluminescence and optical mapping[8,9]. Although some of these diagnostic aids show some promise for clinical everyday application, none have yet demonstrated better performance than conventional visual examination[9]. Thus, the accepted gold-standard method for diagnosis of oral cancer and potentially malignant lesions is still clinical examination and histopathological examination of the biopsied tissue[10-12]. However, given the difficulty of early detection of oral cancer and the increased prevalence of this type of neoplasm worldwide, any method that improves or contributes to the diagnostic process should also improve screening capacity across a large population. Significant efforts have been devoted to development of less invasive and at the same time effective diagnostic modalities for the early diagnosis of oral cancer[13,14]. In this context, optical techniques that are efficient, precise, low-cost, portable and easy to handle seem to overcome most of the present difficulties in this process and are of great value in clinical applications[15,16].

Raman spectroscopy is a technique that consists basically of the analysis of light scattering[17]. It has been known as a means of studying molecular structural properties of solids, liquids and gases since its discovery in 1928 by C. V. Raman and K. S. Krishnan.

The impact of the light onto molecules results in either elastic scattering (same frequency as that of the incident light and known as Rayleigh) and inelastic scattering (frequency different from that of the incident light). By interacting with vibrations in the material, the dispersed photon can either lose energy (a phenomenon known as Stokes scattering) or gain energy (known as anti-Stokes) (**Figure 2b.1**). Finally, the Raman spectrum shows the energy difference between incident photons and dispersed photons as a variation in intensity associated with the range of vibrational modes in the material[16,17].

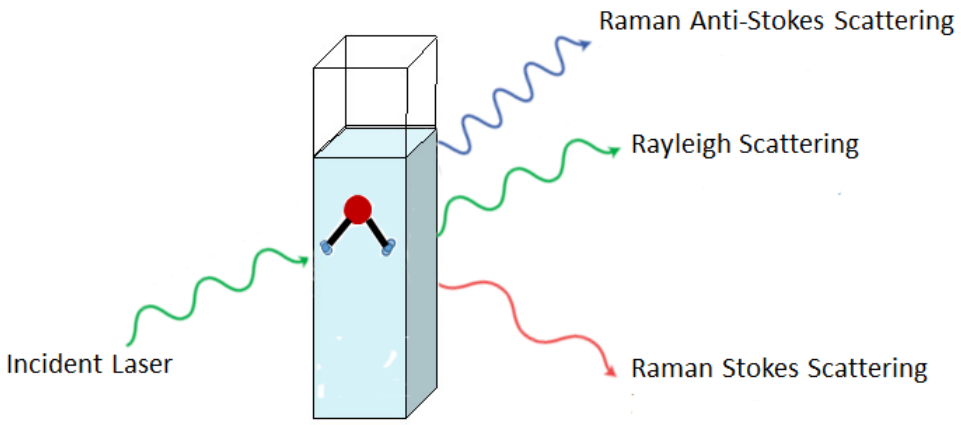

Figure 2b.1: Schematic illustration of Rayleigh and Raman scattering processes.

The Raman spectroscopic signature is a set of several characteristic peaks that represent the most important and specific spectral variations of the sample being studied. The application potential of these multidimensional signatures obtained is almost unlimited and may also be used for the spectral typing of a heterogeneous sample, such as saliva samples. Furthermore, newer modalities of Raman analysis, such as Surface-Enhanced Raman spectroscopy (SERS), have been applied recently, aiming to obtain a better performance regarding spectral acquisition as well as to increase the sensitivity and specificity of this technique[13]. SERS takes advantage of the enhancement of the local field in the regions of surface plasmon resonances on the surfaces of many metals, such as

gold, silver or copper, which can result in increases in the Raman signals by many orders of magnitude[13].

A Raman spectrometer, coupled to a light microscope, is capable of characterising the molecular structure of the salivary components through the incidence of light (laser) at a specific wavelength, and detecting the energy that is dispersed due to the vibration of the respective salivary molecules[16]. As a result, a specific spectral signature (or fingerprint) is acquired containing peaks/bands (shown in cm^{-1} or nm) which, as a whole, could be taken into account for the development of a multivariate analysis algorithm for the classification of saliva from, and consequent diagnosis of, patients with OSCC, for example[16].

Recent Raman spectroscopic studies have achieved specificity and sensitivity of > 90% for differentiating normal and neoplastic specimens of malignant tumours of the mouth in oral tissues based on the water content values from OSCC[18]. Also, Hole *et al.*[20] established a confusion matrix that enables the correct classification of 82% and 92% of tumour and oral cell spectra, respectively, when a spectra-wise cross validation was performed. In a subject-wise cross validation, 100% of oral normal cells and 90% of oral tumour cells spectra were correctly classified. These results are based on a large number of plasma and tissue proteins indicative of malignancy, supporting the application of Raman spectroscopy for the diagnostic purpose for this type of malignant neoplasm[21,22].

While spectroscopic analysis of tissues and cells for clinical applications has been explored over at least two decades, analysis of bodily fluids has emerged more recently[23,24]. In this sense, human saliva has gradually gained interest from researchers and scientists as a means of diagnosis because it represents a non-invasive source of safe, low-cost complex biomolecular information that can easily be obtained from the oral cavity[25]. Recent studies have shown that saliva can be used as a diagnostic medium not

only for diseases of the oral cavity, but also for systemic diseases, exhibiting versatility and merit in the diagnostic field[26]. However, although the development of diagnostic tools for salivary analysis to monitor diseases of the oro-maxillo-mandibular complex has been witnessed in recent years, the main challenge of clinical diagnosis from saliva is the discovery of the varied potential of this type of sample and the standardization/confirmation of analytical techniques for the correct use of this biofluid[27].

Knowing the importance and urgency of the implementation of more accurate and less expensive diagnostic methods such as Raman spectroscopy, and the clinical versatility of the salivary sample, it is important to develop methodologies for this type of sample. However, studies involving spectral analysis of human saliva through Raman spectroscopy for the diagnosis of oral cancer are still limited and diverse in terms of methodology and results. Therefore, this work aims to perform a systematic review of the literature on the application of Raman spectroscopy for human saliva analysis for the diagnosis of OSCC. It also aims to describe aspects that concern the instrumentation and preparation of saliva which could translate to a better standardised and reproducible protocol, a better assessment of the technique itself, as well as to describe spectral salivary components of verifiable significance for the applicability of this technique for routine clinical diagnosis.

2b.3 Methodology

The parameters adopted for this systematic review were based upon the PRISMA (Preferred Reporting Items for Systematic reviews and Meta-analyses) system[28]. An extensive electronic search was conducted in the Pubmed, B-On and other domains (eg. Scopus, Google, Google Scholar, etc.) using the following terms: “Raman Spectroscopy”, “Oral Cancer”, “Oral dysplasia” and “Saliva”. In addition, the Boolean terms "AND" and

"OR" were used to combine keywords. Only scientific articles in English were considered for this bibliographic review.

All the identified articles were initially assessed by title and respective abstract. When such elements were unclear or not available, full articles were retrieved and examined. Studies that appeared in more than one database, or appeared more than once in the same database, were considered only once. Titles/abstract screening was performed by one reviewer and full text articles collected. Full text articles were independently assessed for eligibility by two reviewers. The bibliographic research was carried out between August 2018 and February 2019.

Review articles, opinion articles, and articles that were not related to oral cancer/oral epithelial dysplasia diagnosed with Raman spectroscopy through salivary samples were initially excluded from the proposed systematic review. Theses of any nature were also considered in this systematic review. Due to the scarcity of the literature on the proposed theme, no criteria of temporal restriction of the publication of the chosen articles were applied.

Scientific articles involving the use of saliva as a biological sample in the diagnosis of some type of cancer through the use of Raman spectroscopy were included for the systematic analysis of the treatment (methodology) of the sample (saliva). However, only studies that aimed at the diagnosis of oral cancer or oral epithelial dysplasia were analysed in relation to the biological component of the salivary spectral profile as well as to the sensitivity, specificity and/or classificatory efficiency (also known as accuracy and described as the capability of efficiently detect the true positive and true negative samples over all observations)[29] of the mathematical models.

2b.4 Results

The bibliographic search identified a total of 828 scientific articles (**Figure 2b.2**). Duplicate studies were then excluded (n = 65), resulting in a total of 763 articles. After a thorough review of the title and/or abstracts, a total of approximately 525 articles were excluded because they were not consistent with the systematic review topic. Associated with this, literature reviews of any nature were also excluded from the final systematic analysis (n=230). Finally, only eight studies were deemed to be fully consistent with the proposed theme[30-37], including those that did not specifically diagnose oral cancer (n=3) but used salivary samples for Raman spectroscopy[33,35,36].

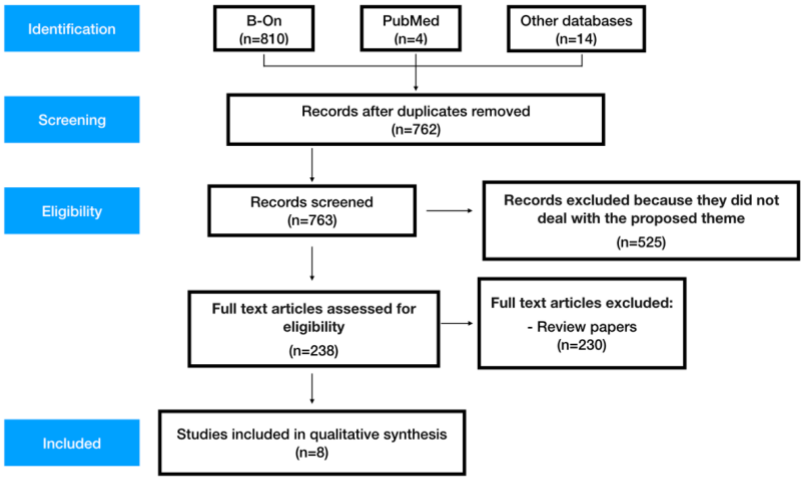

Figure 2b.2: Flowchart showing the results of the research and the selection procedure of the papers included for analysis.

Important aspects of each study were also analysed, including the year of the study, sample size, the nature of saliva collection, the physical state of the sample at the time of analysis, the laser wavelength used as source, the use of nano particles as enhancers for Raman analysis (SERS), the type of statistical analysis adopted, whether principal components analysis associated with linear discriminant analysis (PCA-LDA), partial least squares discriminant analysis (PLSDA) or support vector machines (SVM) were used, and the size of the spectral range analysed (**Table 2b-1**). Further details related to

the type of nanoparticles, and the incorporation state (colloid or substrate) of these particles listed by each of the groups was also noted and are presented in the same table (**Table 2b-1**). Statistical results related to the differentiation between the group of patients with OSCC and control group of each study (**Table 2b-2**) were defined as sensitivity and specificity and/or classification efficiency (accuracy) (not necessarily present in every analysis, but mandatory when sensitivity and specificity were not mentioned) and were also noted as important features of each study. In addition, the spectral profile of the predominant salivary components responsible for differentiation of the same groups (**Table 2b-3**) were also indicated and, based on the spectral profile of isolated components, were correlated with possible biochemical salivary associations found in the current literature.

Table 2b-1: List of articles that formed this systematic review, according to the year of publication and the number of participants in each study. Also, information was collected regarding the type of collection of the salivary sample (stimulated or non stimulated), the physical state of the sample at the time of collection, the wavelength of the laser source applied, the use or not of nanoparticle enhancers (SERS), the statistical method used by each study and the spectral range selected for analysis.

Authors	Year	Participants (patients/ controls)	Saliva collection type	Physical state of the sample	Laser-line (nm)	Type of Raman technique	Type of nanoparticle (incorporation)	Statistical method	Fingerprint region (cm^{-1})
Kho *et al.*	2005	10 (5/5)	Not mentioned	Dry	632.8	SERS	Gold (colloid)	No statistical tool was used	400-1800
Feng *et al.*	2014	92 (62/30)	Not mentioned	Liquid	785	SERS	Silver (colloid)	PCA-LDA	500-1750
Feng *et al.*	2015	64 (31/33)	Not mentioned	Liquid	785	SERS	Silver (colloid)	PLSDA	500-1800
Qiu *et al.*	2015	62 (32/30)	Not mentioned	Dry	785	SERS	Silver (colloid)	PCA-LDA	400-1750
Connolly *et al.*	2016	36 (18/18)	Not mentioned	Dry	785	SERS	Silver (substrate)	PCA-LDA	400-1,750
Jaychandran, Meenapriya and Ganesan	2016	158 (137/21)	Not mentioned	Not mentioned	785	Conventional	No particle was applied	PCA-LDA	600-1000
Rekha *et al.*	2016	83 (61/23)	Non stimulated	Liquid	785	Conventional	No particle was applied	PCA-LDA	800-1800
Quian *et al.*	2018	127(61/66)	Not mentioned	Dry	785	SERS	Gold (substrate)	SVM	400-1800

Table 2b-2: Statistical results of the mathematical models in the salivary sample classification process of patients with OSCC/ oral epithelial dysplasia.

Authors	Sensitivity/Specificity (%)	Classification efficiency (%)
Connolly *et* al.	89 / 57	Not mentioned
Jaychandran, Meenapriya and Ganesan	Not mentioned	91.3
Rekha *et* al.	Not mentioned	55.4

Table 2b-3: Main peak positions and tentative vibrational mode assignments of saliva components associated to OSCC/oral epithelial dysplasia.

Wavenumber (cm^{-1})	Biological Assignments	Reference
444	Protein	Jaychandran, Meenapriya and Ganesan
752	Glycoproteins	Jaychandran, Meenapriya and Ganesan
870	Amino acid	Rekha *et al.*
885	Protein	Connolly et *al.*
918	Glycoprotein	Rekha *et al.*
948	Proline rich proteins	Rekha *et al.*
969	Proline rich proteins	Rekha *et al.*
986	Amino acids	Rekha *et al.*
1015	Phenylalanine (proteins)	Rekha *et al.*
1126	Protein	Connolly *et al.*
1158	Lipids	Jaychandran, Meenapriya e Ganesan
1204	Phenylalanine (proteins)	Connolly *et al.*
1224	Amide III	Connolly *et al.*
1275	Amide III	Connolly *et al.*
1288	Amide III	Rekha *et al.*
1409	Glycoproteins	Connolly *et al.*
1417	C=C stretching	Connolly *et al.*
1525	Lipids	Jaychandran, Meenapriya and Ganesan
1636	Amide I (glycoproteins)	Rekha *et al.*

In general, the work of Kho *et al.* was the only one to mention the method of collection of the saliva samples (non stimulated)[30]. Saliva in the liquid state was used by Feng *et al.*[31,32] and Rekha *et al.*[33] while dried saliva (after evaporation of water) was used in four studies, Kho *et al.*[30], Qiu *et al.*[34], Connolly *et al.*[35] and Quian *et al.*[37] (**Table 2b-1**). One of the groups did not mention the physical state of the samples that were analysed[33].

The wavelength of 785 nm was chosen for sample excitation in almost all salivary sample studies (**Table 2b-1**). Kho *et al.* was the only group to apply a laser source of 632.8 nm for spectral analysis[30].

In relation to the use of nano particles for spectral enhancement (SERS), Kho *et al.*[30], Feng *et al.*[31,32], Qiu *et al.*[34], Connolly *et al.*[35] and Quian *et al.*[37] used metal nanoparticles to enhance the vibrational signal from saliva, while Jaychandran, Meenapriya and Ganesan[36] and Rekha *et al.* [33] did not use SERS to enhance the Raman signal of their samples (**Table 2b-1**).

The type of nano particles varied in the different studies, as well as how they were incorporated (**Table 2b-1**). Silver nano particles were the most common spectral enhancer and were used in four studies[31,32,34,35] while gold nano paticles were used in two studies [30,37]. The particles were used as a colloidal solution in four of the studies[30,31,32,34] while only two studies used nanoparticles incorporated in the substrate[35,37]. Notably, however, none of the studies indicated whether the choice of the type of metal nanoparticle and/or the wavelength were correlated.

The choice of PCA-LDA was almost common amongst all studies involving analysis of saliva for the diagnosis of cancer through the use of Raman spectroscopy (**Table 2b-1**). Only Feng *et al.*[31] and and Quian *et al.*[37] used PLSDA and SVM, respectively, as the

statistical method of choice. Kho *et al*. perfomed a simple visual comparison between mean spectral profile of saliva from healthy people and patients with oral cancer[30].

The spectral range of analysis, however, was quite diverse across all studies (**Table 2b-1**). Kho *et al.*[30] and Quian *et al.*[37] used a broad fingerprint region (between 400-1800 cm^{-1}), while Jaychandran, Meenapriya and Ganesan[36] used the smallest range in fingerprint region of all the studies analysed (600-1000 cm^{-1}).

Studies involving the use of saliva samples for the diagnosis of oral cancer through Raman spectroscopy were restricted to three studies (**Table 2b-2**): Connolly *et al*[35], Jaychandran, Meenapriya and Ganesan[36] and Rekha *et al*.[33]. Connolly *et al*.[35] were able to obtain a sensitivity and specificity of 89 and 57%, respectively, when using Raman spectroscopy for differentiation between salivary samples from patients with oral cancer and from healthy controls (**Table 2b.2**). In addition, according to this analysis, some specific spectral features of saliva components were assigned as responsible for the classification obtained – 870, 1126 (proteins), 1204 (phenylalanine), 1224, 1275, (starch), 1409 (glycoproteins), and 1417 cm^{-1} (C=C bonds) (**Table 2b-3**).

On the other hand, Jaychandran, Meenapriya and Ganesan[36] report the following bands as establishing the difference between patients with oral cancer (or some form of oral epithelial dysplasia) and the control group: 444 (mucin), 752 (glycoproteins), 1158 and 1525 cm^{-1} (lipids) (**Table 2b-3**). Nevertheless, a classification efficiency of approximately 91% was obtained between the two groups (**Table 2b-2**).

A lower classification efficiency obtained between the groups was determined by Rekha *et al*.[33] of approximately 55% (**Table 2b-2**). Although not statistically significant, this study found that the amino acid-associated (870, 986 cm^{-1}), glycoproteins (918 cm^{-1}), proline rich proteins (948, 969 cm^{-1}), phenylalanine (1015 cm^{-1}), starch III (1288 cm^{-1})

and starch I (1636 cm^{-1}) bands appeared to be associated with the presence of OSCC (**Table 2b-3**).

2b.5 Discussion

Human saliva is considered a "mirror" of body health and plays an important role in the repair and lubrication of soft and hard tissues, formation and ingestion of the alimentary bolus, digestion, taste and control of the microbial population[38].

Schipper *et al*. determined, through mass spectroscopy, that the salivary collection method seems to be very important for the variability and concentration of proteins and substances detected in each type of saliva[39]. An interesting study examined the levels of parotid and submandibular/sublingual salivary IgA through ELISA (enzyme-linked immunosorbent assay) in response to experimental gingivitis in humans, where a statistically significant increase in the IgA secretion rate in stimulated parotid saliva was observed after 6 and 12 days without oral hygiene, not seen in resting parotid saliva[40].

The literature has also reported that Raman spectroscopy for saliva analysis can be applied for the detection of narcotics in forensic medicine and periodontal disease[41,42].

In terms of salivary nature, several factors can influence salivary secretion and composition, such as non stimulated and stimulated saliva collection. Salivary collection is basically termed non stimulated (resting) when no exogenous or pharmacological stimulation is present and termed stimulated when secretion is promoted by mechanical or gustatory stimuli or by pharmacological agents. When the secretion is stimulated mechanically, inert stimuli are commonly used (chewing of paraffin wax or rubber bands)[43].

The studies identified in this systematic review were not conclusive or used only one form of salivary collection for analysis, consequently, limiting a more detailed analysis of the spectral profile of each type of sample. Calado *et al.* recently published an abstract in which a better and comprehensive analysis of the type of collection of saliva was performed[44]. In this study, stimulated saliva was considered as the sample type of choice for analysis with Raman spectroscopy, as it is more suited to the standard operating procedure for clinical applications and results in a more prominent Raman signal from the saliva samples.

The physical state of the sample would also be a very important element in the process of instrumentation and analysis. Feng *et al.*[31], Qiu *et al.*[34], Connolly *et al.*[35], Jaychandran, Meenapriya and Ganesan[36] and Quian *et al.*[37] used solid (dry) or liquid samples for analysis by SERS. Such methodologies using enhancement particles (SERS), or modifying the physical state of the saliva, add complexity to the sample preparation and/or resulting in indubitable loss of salivary quality when in a physical state other than the one of origin[41,45].

SERS is a special type of Raman spectroscopy, in which irregular or patterned metal substrates or metal nanocolloids are used for signal enhancement[46-48]. Typically, the best enhancement effect is achieved with silver induced SERS[49]. As a substance, silver holds antimicrobial properties and, consequently, may affect the sample under inspection, which could be the reason for the widespread use of silver nanoparticles in the studies reviewed. However, it is chemically quite reactive, and the stability and reproducibility of the silver substrates and colloids can also be an issue[46,47]. On the other hand, gold is preferred in microbe detection having the optimal excitation wavelength in the near-infra red region[47].

In terms of spectral resemblance or peak compatibility among studies with SERS, some similarities in spectral features and profile were observed, such as cancer saliva proteins showing higher intensities at 1004, 1340, 1134 cm^{-1} [31,32]. However, the SERS studies found in this review did not show major similarities regarding the general spectral pattern, possibly due to the fact that they detect different histopathological entities. Also, the variability in intensity is an intrinsic property of SERS measurements. It is already known that the aggregation and adsorption mechanisms cause constant fluctuations in the intensity in a time-independent manner[50].

PCA-LDA was the method of choice for the statistical analysis of the obtained spectra. In Raman spectroscopy, PCA is used to reduce a mathematical matrix based on the spectral data of measured objects (in this case the individualised spectra), with a large number of variables (wavelength of each peak/band), while retaining the variability within the probabilistic data[51]. The LDA method, when used in conjunction with PCA, uses the PCA scores as latent variables to find a linear hyperplane that best classifies one or two groups of PCA scores[51].

PLSDA, another method of statistical analysis, can also represent a tool of classification. Similar to PCA-LDA, PLSDA is a supervised form of multivariate analysis which works as a linear classifier that aims to maximise the variance between groups and minimise the variance within groups. It is based on partial least squares regression (PLSR), a method used for constructing predictive models when the factors are many and highly collinear[52].

In a similar way, the use of SVM is considered an effective method for building a classifier. It aims to create a decision boundary between two classes that enables the prediction of labels from one or more feature vectors. This decision boundary, known as the hyperplane, is orientated in such a way that it best differentiates the identified classes. These closest points are called support vectors[53].

Despite the widespread use of PCA-LDA for human saliva analysis through Raman spectroscopy of the studies reviewed, other studies have already demonstrated that PLSDA or SVM can also provide excellent or even superior classification efficiency to PCA-LDA between samples analysed by Raman spectroscopy, for example 90% accuracy for colon diagnosis[54] and 96.72% sensitivity for lung cancer[37].

The precedent of previous studies employing PCA-LDA to categorise spectral profiles of samples could explain the continued preference over PLSDA or SVM in the reviewed studies, in spite of the similar statistical basis of these three different techniques. Notably, there have been no reports of a direct comparison of the three approaches applied to the same dataset.

In terms of sensitivity and specificity, the studies involving Raman analysis of saliva for detection of oral cancer/oral dysplasia have revealed significant discrepancies related to the detection capabilities, even using the same statistical analysis method (PCA-LDA), the reported classification efficiency ranging from 55.4% to 91.3%[33,36]. The use of SERS did not seem improve this performance to any great extent, yielding sensitivity of 89% and specificity of 57% in the SERS study of Connolly *et al.*[35], compared to 91.3% of classification efficiency in other studies[36].

Among the SERS studies that analysed saliva, independent of the tumour type, the highest sensitivity and specificity achieved were 95.08 and 100%, respectively[37]. The similarity of results obtained by conventional Raman and SERS analysis therefore brings into question the need or benefit of SERS for the analysis of saliva. Due to the lack of analysis in some of the SERS studies, the sensitivity and specificity could not be further correlated to use of a specific metal nanoparticle (gold or silver). However, the SERS incorporation in colloid state can usually reach a slightly better sensitivity[55] as highlighted by Feng *et al.*[31], yielding a diagnostic sensitivity of 91.9%.

Regarding the source wavelength, 785 nm was the most commonly used for saliva analysis, but no reasonable explanations have been addressed in order to clarify its use. This situation could be explained by the "convenience factor" of not having other laser lines available. Notably, the Raman scattering efficiency scales according to 1/(wavelength)^4, and so, the shorter the wavelength the better, but, at shorter wavelengths, Rayleigh and Mie scattering also increase, increasing the background, and the chance of being resonant with fluorophores also increases[56].

The fingerprint region selected by the studies reviewed was very variable. In Raman spectroscopy, the fingerprint region 400–1800 cm^{-1} can detect the majority of biological components of a sample. A smaller fingerprint range, consequently, can limit the information acquired from the sample in question[57].

In the case of SERS, different kinds of metallic enhancement material, silver, gold, or copper, on substrates or in colloidal form, can be used, enabling this technique to be applied in a Raman setup[58]. The enhancement effect derives from the resonant excitation of the surface plasmon of the nanoparticle, which varies according to the constituent metal, the nanoparticle size, and aggregation state[59]. This means that the optimum type of metal particle is directly correlated to the wavelength applied or vice-versa. However, no specific rationale governing choice of nanoparticle type/size or state was provided by the studies covered in this review.

The reported spectral profiles of saliva are usually complex and show contributions of multiple chemical compounds. The spectral bands correlated with the salivary composition of all studies are suggestions based on available literature on specific components previously isolated and analysed. In the studies included in the analysis, peaks related to Amide I and Amide III of proteins were among the main biochemical

components associated with the differentiation between saliva samples of patients with OSCC or oral dysplasia and the control group.

Many salivary proteins and glycoproteins have already been reported as biomarkers for the diagnosis of OSCC[60]. The current literature is rich in reports that correlate proteins such as c-erbB2, CA-125 and P53 as well as some antibodies, such CA15-3 antigen, in saliva to the development of OSCC and so act as biomarkers to detect this type of neoplasm[61]. In addition, other studies have also detected an overexpression of zinc-α-2-glycoprotein in the saliva of patients through matrix-assisted laser desorption ionization-quadrupole-time-of-flight (MALDI-Q-TOF) and mass spectrometry[62].

Results indicative of associations between C=C and C-H vibrations from the salivary Raman spectrum have also been previously reported in the clinical profile of epithelial cells or in the detection of lung cancer[63]. In addition, Feng *et al*. reported that those vibrational features are correlated with proteins that were involved in the salivary response of breast cancer patients[32]. The vibrational signals were seen to be stronger in benign breast tumour samples, indicating that the amount of proteins increases in the saliva samples from patients this type of lesion[32].

Specifically related to OSCC, biological vibration assignments from saliva can also be seen in some other Raman studies involving different types of oral samples. *In vivo* and *ex vivo* Raman studies, for example, have described the similar prominence of other similar protein Raman spectral bands in oral tissue such as 1126 and 1204 cm^{-1}. They have also reported that the protein content of these samples was also responsible (in 86%) for the differentiation of dysplastic samples from controls[64,65]. Furthermore, Guze *et al.* have described other the prominence similar protein/glycoprotein bands in oral tissue specimens, such as 758 and 1288 cm^{-1} [66]. This study has also shown that peaks in the range 850–950 cm-1 (protein backbone vibrations) and 1200-1300 cm^{-1} (Amide III) were

more intense in the tumour region, particularly within the nucleus[66]. Results like these reinforce the importance of the protein content of saliva/oral tissues for the diagnosis process of these neoplasms as well as the Raman capability of detecting these alterations.

Raman spectroscopy has already shown its versatility for the diagnosis of other types of cancers based on protein differentiation. Lyng *et al.* demonstrated the ability of Raman spectroscopy to classify cervical cancer based on relevant changes of essential proteins[67]. Sensitivity and specificity values could be calculated as high as 99.5% and 100% respectively for normal tissue and 98.5% and 99% respectively for invasive cervical carcinoma. Also, Raman spectroscopy was able to demonstrate that the secondary structures of serum proteins and the contents of amino acids can change during cancer colorectal progression[68].

It is important to highlight the fact that, even though Raman spectroscopy is a highly accurate and sensitive vibrational technique, the biochemical compositions correlated to the Raman vibrations of saliva have been assigned through the spectral profile of components acquired and present in the published literature. Raman spectroscopy, unlike other techniques such as mass spectroscopy or other molecular biology techniques, when used for salivary analysis, fully analyses the entire salivary molecular profile. The greatest advantage of Raman spectroscopy, often neglected by those working in the area of microscopy/molecular biology, is in the label free definition of saliva as a whole for the determination, through mathematical models, of the presence of early-stage OSCC (or dysplastic lesions) without any visible clinical and/or histopathological alterations, bringing possibilities for the development of technologies derived for application *in vivo* not only in the diagnosis of OSCC but also for biopsy guidance for example.

2b.5 Conclusion

The current systematic review serves as a basis for a more complete methodological approach to salivary samples by means of Raman spectroscopy for future investigations, besides signaling its promising application in the oral cancer diagnosis process, even in the face of differences in the instrumentation setups and statistical analysis applied.

Regarding the sample collection process, the nature/collection of the saliva samples from each study was not highlighted as an important factor for the adopted methodologies nor its correlation with the results obtained. However, new research indicates that stimulated salivary samples appear to have more diagnostic potential in terms of the number of biological components present and of greater clinical applicability for analysis by Raman spectroscopy according to the results obtained[44]. In addition, it is expected that SERS methodologies are more costly for a possible routine clinical application. In the same way, drying the sample prior to analysis undeniably results in a loss of salivary component quality.

The most used wavelength for application of Raman technology was 785 nm according to the great majority of the studies examined. Also, it was confirmed that PCA-LDA was the most applied statistical method for analysis of the salivary spectrum, able to obtain values in sensitivity, specificity and/or classification efficiency higher than 90% when in the diagnosis of OSCC.

The peaks/bands correlated with the salivary components such as proteins, glycoproteins and lipids appeared to be altered and they were possibly associated with the presence of OSCC/oral epithelial dysplasia in all the studies reviewed.

Notable, however, is the inconsistency of the methodologies employed to date, and there is need for a systematic approach to optimisation of analysis protocols, to establish a

standard Raman setup for saliva samples as well as to better clarify factors correlated to the sampling procedure, such as type of collection, degradation and etc.

Finally, once more clearly elucidated, an optimised methodology based on salivary analysis through Raman spectroscopy may contribute to the implementation of this technique in routine clinical diagnosis.

ACKNOWLEDGEMENTS

This research was supported in part by Science without Borders (Brazil).

CONFLICT OF INTEREST

The authors declare no financial or commercial conflict of interest.

References

1. World Health Organization: The GLOBOCAN 2018 database, http://globocan.iarc.fr.

2. Warnakulasuriya S. Histological grading of oral epithelial dysplasia: revisited. J Pathol 2001; 194: 294–297. DOI: 10.1002 /path.911

3. Rivera C. Review Article Essentials of oral cancer. Int J Clin Exp Pathol 2015;8(9):11884-11894.

4. Mager DL, Haffajee AD, Devlin PM, Norris CM, Posner MR, Goodson JM. The salivary microbiota as a diagnostic indicator of oral cancer: a descriptive, non-randomized study of cancer-free and oral squamous cell carcinoma subjects. J Transl Med. 2005 Jul 7;3:27.

5. Papamarkakis K, Bird B., Schubert JM, Miljković M, Wein R, Bedrossian K, Laver N, Diem M. Cytopathology by optical methods: spectral cytopathology of the oral mucosa. Lab Invest. 2010 Apr;90(4):589-98.

6. Scully C. Oral cancer aetiopathogenesis; past, present and future aspects. Med Oral Patol Oral Cir Bucal. 2011 May 1;16 (3):e306-11.

7. de Carvalho LFCS, Sato ET, Almeida JD, Martinho HS. Diagnosis of inflammatory lesions by high-wavenumber ft-raman spectroscopy. Theor. Chem. Acc. 130, 1221–1229 (2011).10.1007/s00214-011-0972-2.

8. Bagan J, Sarrion G, Jimenez Y. Oral cancer: clinical features. Oral Oncol. 2010 Jun;46(6):414-7.

9. Shin D, Vigneswaran N, Gillenwater A, Richards-Kortum R. Advances in fluorescence imaging techniques to detect oral cancer and its precursors. Future Oncol. 2010 Jul;6(7):1143-54. doi: 10.2217/fon.10.79. PubMed PMID: 20624126; PubMed Central PMCID: PMC2929485.

10. Ram S, Siar CH. Chemiluminescence as a diagnostic aid in the detection of oral cancer and potentially malignant epithelial lesions. Int J Oral Maxillofac Surg. 2005 Jul;34(5):521-7. Epub 2005 Jan 26.

11. Fedele S. Diagnostic aids in the screening of oral cancer. Head Neck Oncol. 2009 Jan 30;1:5. doi: 10.1186/1758-3284-1-5. PubMed PMID: 19284694; PubMed Central PMCID: PMC2654034.

12. Schwarz RA, Gao W, Stepanek VM, Le TT, Bhattar VS, Williams MD, Wu JK, Vigneswaran N, Adler-Storthz K, Gillenwater AM, Richards-Kortum R. Prospective evaluation of a portable depth-sensitive optical spectroscopy device to identify oral neoplasia. Biomed Opt Express. 2010 Dec 8;2(1):89-99.

13. Kah JC, Kho KW, Lee CG, James C, Sheppard R, Shen ZX, Soo KC, Olivo MC. Early diagnosis of oral cancer based on the surface plasmon resonance of gold nanoparticles. Int J Nanomedicine. 2007;2(4):785-98.

14. Olivo M, Bhuvaneswari R, Keogh I. Advances in bio-optical imaging for the diagnosis of early oral cancer. Pharmaceutics. 2011 Jul 11;3(3):354-78.

15. Ferlay J, Shin HR, Bray F, Forman D, Mathers C, Parkin DM. Estimates of worldwide burden of cancer in 2008: GLOBOCAN 2008. Int J Cancer. 2010 Dec 15;127(12):2893-917.

16. Singh SP, Ibrahim O, Byrne HJ, Mikkonen JW, Koistinen AP, Kullaa AM, Lyng FM. Recent advances in optical diagnosis of oral cancers: Review and future perspectives. Head Neck. 2016 Apr;38 Suppl 1:E2403-11.

17. Raman CV, Krishnan KS. A Change of Wave-length in Light Scattering. Nature, 1928, 121:619-619.

18. Barroso EM, Smits RW, Bakker Schut TC, ten Hove I, Hardillo JA, Wolvius EB, Baatenburg de Jong RJ, Koljenović S, Puppels GJ. Discrimination between oral cancer and healthy tissue based on water content determined by Raman spectroscopy. Anal Chem. 2015 Feb 17;87(4):2419-26. doi: 10.1021/ac504362y. Epub 2015 Feb 5.

20. Hole A, Tyagi G, Sahu A, Shaikh R, Krishna M. Chemometric analysis of integrated FTIR and Raman spectra obtained by non-invasive exfoliative cytology for the screening of oral cancer. Analyst, 2019,144, *1309-1325*.

21. Malini R., Venkata Krishna K., Kurien J., Keerthilatha M. Pai., Lakshmi Rao., Kartha VB and C. Murali Krishna “Discrimination of normal inflammatory, pre-malignant and malignant oral tissue: A Raman Spectroscopy Study” Biopolymers, 2006, 81:179-193.

22. Krishna H1, Majumder SK, Chaturvedi P, Sidramesh M, Gupta PK. In vivo Raman spectroscopy for detection of oral neoplasia: a pilot clinical study. J Biophotonics. 2014 Sep;7(9):690-702. doi: 10.1002/jbio.201300030.

23. Byrne HJ, Baranska M, Puppels GJ, Stone N, Wood B, Gough KM, Lasch P, Heraud P, Sulé-Suso J, Sockalingum GD. Spectropathology for the next generation: quo vadis? Analyst. 2015 Apr 7;140(7):2066-73. doi: 10.1039/c4an02036g.

24. Baker MJ, Byrne HJ, Chalmers J, Gardner P, Goodacre R, Henderson A, Kazarian SG, Martin FL, Moger J, Stone N, Sulé-Suso J. Clinical applications of infrared and Raman spectroscopy: state of play and future challenges. Analyst. 2018 Apr 16;143(8):1735-1757.

25. Fábián TK, Fejérdy P, Csermely P. Salivary Genomics, Transcriptomics and Proteomics: The Emerging Concept of the Oral Ecosystem and their Use in the Early Diagnosis of Cancer and other Diseases. Curr Genomics. 2008 Mar;9(1):11-21.

26. Hu S, Arellano M, Boontheung P, Wang J, Zhou H, Jiang J, Elashoff D, Wei R, Loo JA, Wong DT. Salivary proteomics for oral cancer biomarker discovery. Clin Cancer Res. 2008 Oct 1;14(19):6246-52.

27. Wong DT. Salivary diagnostics powered by nanotechnologies, proteomics and genomics. J Am Dent Assoc. 2006 Mar;137(3):313-21.

28. Moher D, Liberati A, Tetzlaff J, Altman DG; PRISMA Group. Preferred reporting items for systematic reviews and meta-analyses: the PRISMA statement. PLoS Med. 2009 Jul 21;6(7):e1000097.

29. Baratloo A, Hosseini M, Negida A, El Ashal G. Part 1: Simple Definition and Calculation of Accuracy, Sensitivity and Specificity. Emerg (Tehran). 2015 Spring;3(2):48-9.

30. Kho KW, Malini O, Shen ZX, Soo KC. Surface enhanced Raman spectroscopic (SERS) study of saliva in the early detection of oral cancer. Proceedings of SPIE. 2005;5702:84–91. doi: 10.1117/12.590142.

31. Feng SY, Lin D, Lin JQ et al. Saliva analysis combining membrane protein purification with surface-enhanced Raman spectroscopy for nasopharyngeal cancer detection. Appl Phys Lett 2014; 104: 238– 43.

32. Feng S, Chen R, Lin J, Pan J, Chen G, Li Y, Cheng M, Huang Z, Chen J, Zeng H. Nasopharyngeal cancer detection based on blood plasma surface-enhanced Raman spectroscopy and multivariate analysis. Biosens. Bioelectron. 201025, 11:2414–2419 ().

33. Rekha P, Aruna P, Brindha E, Koteeswaran D, Baludavid M, Ganesan S. Near-infrared Raman spectroscopic characterization of salivary metabolites in the discrimination of normal from oral premalignant and malignant conditions. J Raman Spectrosc. 2015, 47:763-772.

34. Qiu S, Xu Y, Huang L, Zheng W, Huang C, Huang S, Lin J, Lin D, Feng S, Chen R, Pan J. Non-invasive detection of nasopharyngeal carcinoma using saliva surface-enhanced Raman spectroscopy. Oncol Lett. 2016 Jan;11(1):884-890.

35. Connolly JM, Davies K, Kazakeviciute A, Wheatley AM, Dockery P, Keogh I, Olivo M. Non-invasive and label-free detection of oral squamous cell carcinoma using saliva surface-enhanced Raman spectroscopy and multivariate analysis. Nanomedicine. 2016 Aug;12(6):1593-601. doi: 10.1016/j.nano.2016.02.021. Epub 2016 Mar 23.

36. Jaychandran S, Meenapriya PK, Ganesan S. Raman Spectroscopic Analysis of Blood, Urine, Saliva and Tissue of Oral Potentially Malignant Disorders and Malignancy-A Diagnostic Study. Int J Oral Craniofac Sci 2016, 2(1): 011-014.

37. Qian K, Wang Y, Hua L, Chen A, Zhang Y. New method of lung cancer detection by saliva test using surface-enhanced Raman spectroscopy. Thorac Cancer. 2018 Nov;9(11):1556-1561.

38. Miller N. Ten Cate's oral histology, 8th edition. British dental journal. 2012, 213. 194.

39. Schipper R, Loof A, de Groot J, Harthoorn L, Dransfield E, van Heerde W. SELDI-TOF-MS of saliva: methodology and pre-treatment effects. J Chromatogr B Analyt Technol Biomed Life Sci. 2007 Feb 15;847(1):45-53.

40. Seemann R, Hägewald SJ, Sztankay V, Drews J, Bizhang M, Kage A. Levels of parotid and submandibular/sublingual salivary immunoglobulin A in response to experimental gingivitis in humans. Clin Oral Investig. 2004 Dec;8(4):233-7.

41. Gonchukov S, Sukhinina A, Bakhmutov D, Minaeva S. Raman spectroscopy of saliva as a perspective method for periodontitis diagnostics. Laser Phys. Lett. 2012, 9:73.

42. Dana K, Shende C, Huang H, Farquharson S. Rapid Analysis of Cocaine in Saliva by Surface-Enhanced Raman Spectroscopy. J Anal Bioanal Tech. 2015;6(6):1–5. doi:10.4172/2155-9872.1000289

43. Muddugangadhar BC, Sangur R, Rudraprasad IV, Nandeeshwar DB, Kumar BH. A clinical study to compare between resting and stimulated whole salivary flow rate and pH before and after complete denture placement in different age groups. J Indian Prosthodont Soc. 2015;15(4):356–366. doi:10.4103/0972-4052.164907.

44. Calado G, Behl I, Ibrahim O, Byrne HJ, Lyng FM. Development Of Methodologies For Raman Spectral Analysis Of Human Saliva For Detection Of Oral Cancer. Oral Surg Oral Med Oral Pathol Oral Radiol Endod, 2017, 124(2):e142.

45. Bonnier F, Petitjean F, Baker MJ, Byrne HJ. Improved protocols for vibrational spectroscopic analysis of body fluids. J Biophotonics. 2014 Apr;7(3-4):167-79. doi: 10.1002/jbio.201300130. Epub 2013 Oct 17.

46. Anker JN, Hall WP, Lyandres O, Shah NC, Zhao J, Van Duyne RP. Biosensing with plasmonic nanosensors. Nat Mater. 2008 Jun;7(6):442-53. doi: 10.1038/nmat2162.

47. Bantz KC, Meyer AF, Wittenberg NJ, Im H, Kurtuluş O, Lee SH, Lindquist NC, Oh SH, Haynes CL. Recent progress in SERS biosensing. Phys Chem Chem Phys. 2011 Jun 28;13(24):11551-67. doi: 10.1039/c0cp01841d.

48. Bibikova O, Popov A, Bykov A, Prilepskii A, Kinnunen M, Kordas K, Bogatyrev V, Khlebtsov N, Vainio S, Tuchin V. Optical properties of plasmon-resonant bare and silica-coated nanostars used for cell imaging. J Biomed Opt. 2015 Jul;20(7):76017.

49. Liu Y, Chen YR, Nou X, Chao K. Potential of surface-enhanced Raman spectroscopy for the rapid identification of Escherichia coli and Listeria monocytogenes cultures on silver colloidal nanoparticles. Appl Spectrosc. 2007 Aug;61(8):824-31.

50. Muehlethaler C, Leona M, Lombardi JR. Towards a validation of surface-enhanced Raman scattering (SERS) for use in forensic science: repeatability and reproducibility experiments. Forensic Sci Int. 2016 Nov;268:1-13. doi: 10.1016/j.forsciint.2016.09.005.

51. Gautam R, Vanga S, Ariese F, Umapathy S. Review of multidimensional data processing approaches for Raman and infrared spectroscopy. EPJ Techniques and Instrumentation, 2015,2(1):8.

52. Liu W., Sun Z, Chen J, Jing C. Raman Spectroscopy in Colorectal Cancer Diagnostics: Comparison of PCA-LDA and PLS-DA Models. J Spectroscopy 2016, 2016:1-6.

53. Huang S, Cai N, Pacheco PP, Narrandes S, Wang Y, Xu W. Applications of Support Vector Machine (SVM) Learning in Cancer Genomics. Cancer Genomics Proteomics. 2018;15(1):41–51. doi:10.21873/cgp.20063

54. Bergholt MS, Zheng W, Lin K, Wang J, Xu H, Ren JL, Ho KY, Teh M, Yeoh KG, Huang Z. Characterizing variability of in vivo Raman spectroscopic properties of different anatomical sites of normal colorectal tissue towards cancer diagnosis at colonoscopy. Anal Chem. 2015 Jan 20;87(2):960-6.

55. Besner S, Kabashin, AV, Meunier M. Fragmentation of colloidal nanoparticles by femtosecond laser-induced supercontinuum generation. Appl. Phys. Lett. 2006,89:1–4.

56. Tuschel D. Photoluminescence Spectroscopy Using a Raman Spectrometer *Spectroscopy*, **2016**, 31(9):14–21.

57. Hesse M, Meier H, Zeeh B, Spektroskopische Methoden in der organischen Chemie Pharmazie, 1996, l25(4):220-220.

58. Cardinal MF, Vander Ende E, Hackler RA, McAnally MO, Stair PC, Schatz GC, Van Duyne RP. Expanding applications of SERS through versatile nanomaterials engineering. Chem Soc Rev. 2017 Jul 3;46(13):3886-3903.

59. Tian F, Bonnier F, Casey A, A. Shanahana E, Byrne HJ. Surface enhanced Raman scattering with gold nanoparticles: effect of particle shape. Anal. Methods, 2014,6:9116-9123.

60. Castagnola M, Scarano E, Passali GC, Messana I, Cabras T, Iavarone F, Di Cintio G, Fiorita A, De Corso E, Paludetti G. Salivary biomarkers and proteomics: future diagnostic and clinical utilities. Biomarkers e proteomica salivari: prospettive future cliniche e diagnostiche. Acta Otorhinolaryngol Ital. 2017 Apr;37(2):94-101.

61. Wong DT. Salivary diagnostics. Oper Dent. 2012 Nov-Dec;37(6):562-70.

62. Vidotto A, Henrique T, Raposo LS, Maniglia JV, Tajara EH. Salivary and serum proteomics in head and neck carcinomas: before and after surgery and radiotherapy. Cancer Biomark. 2010-2011;8(2):95-107.

63. Simonova D, Karamancheva I. Application of Fourier Transform Infrared Spectroscopy for Tumor Diagnosis. Biotechnol Biotechnol Equi., **2013, 27(6):**4200-4207.

64. Cals FLJ, Bakker Schut TC, Caspers PJ, Baatenburg de Jong RJ, Koljenović S, Puppels GJ. Raman spectroscopic analysis of the molecular composition of oral cavity squamous cell carcinoma and healthy tongue tissue. Analyst. 2018 Aug 20;143(17):4090-4102.

65. Guze K, Pawluk HC, Short M, Zeng H, Lorch J, Norris C, Sonis S. Pilot study: Raman spectroscopy in differentiating premalignant and malignant oral lesions from normal mucosa and benign lesions in humans. Head Neck. 2015 Apr;37(4):511-7. doi: 10.1002/hed.23629.

66. Guze K, Short M, Zeng H, Lerman M, Sonis S. Comparison of molecular images as defined by Raman spectra between normal mucosa and squamous cell carcinoma in the oral cavity. J Raman Spectroscopy, 2011, 42(6):1232-1239.

67. Lyng FM, Faoláin EO, Conroy J, Meade AD, Knief P, Duffy B, Hunter MB, Byrne JM, Kelehan P, Byrne HJ. Vibrational spectroscopy for cervical cancer pathology, from biochemical analysis to diagnostic tool. Exp Mol Pathol. 2007 Apr;82(2):121-9.

68. Wang J, Lin D, Lin J, Yu Y, Huang Z, Chen Y, Lin J, Feng S, Li B, Liu N, Chen R. Label-free detection of serum proteins using surface-enhanced Raman spectroscopy for colorectal cancer screening. J Biomed Opt. 2014 Aug;19(8):087003.

Chapter 3: Raman measurement optimisation for saliva analysis

3.1 Introduction

Raman spectroscopy may be able to holistically analyse saliva by giving a unique biochemical profile. This study aims to use Raman spectroscopy in the clinic to screen and diagnose OSCC and potential malignant oral lesions. This chapter had as its objective the determination of the best strategy to record Raman spectra from whole saliva for diagnostic purposes, keeping the liquid nature of the sample and without the use of nanoparticle enhancers.

3.2 Methodology – Measurement optimisation

3.2.1 Water measurements

Initially, measurements of water were performed to facilitate a future Raman set up for artificial saliva and real saliva. Ultrapure water was used for this initial stage. The Raman signal from water could be evaluated according to the noise aspect/appearance and spectral information (peaks), whether present. A low and a high magnification were used for each laser line; objectives 10X and 50X for the upright microscope and 10X and 60X (with a drop of water) for the inverted microscope. High wavenumbers were also recorded to make sure that the water content was visible for the respective laser line. A standard cuvette, a 96 well-plate (polystyrene) and a 96 well-plate with glass bottom no.1 (Thermo Fisher, around 0.17mm thickness) were used as substrates.

3.2.2 Artificial Saliva Preparation

Attempting to mimic the biological behaviour of human saliva, artificial saliva was prepared according to the formula of Klimek *et* al.[1], (**Table 3-1**) using high-purity chemicals and distilled water, at 28 ± 1°C. The pH of 6.8 to 7.5 was maintained by the manual addition of H_3PO_4. The order of addition followed the order of listing in the table. Furthermore, different concentrations of artificial saliva (0, 25, 50, 75 and 100% more concentrated, respectively based on the absolute concentration presented in the **Table 3-1**) were prepared, aiming to overcome the natural "weak" spectral profile of saliva during the acquisition of the Raman spectra[50].

Table 3-1: Chemical composition for 1000ml of Artificial Saliva according to *Klimek et al*.[1]

Chemical Substance	Mass (g)
Ascorbic Acid	0,002
Glucose	0,03
Sodium Chloride	0,58
Calcium Chloride	0,17
Ammonium Chloride	0,16
Sodium Thiocyanate	0,16
Monopotassium Chloride	1,27
Monopotassium phosphate	0,33
Urea	0,20
Mucin	2,70
Sodium Phosphate dibasic	0,34

3.2.3 Raman spectral acquisition

Optimisation of the different parameters required for Raman spectral acquisition was carried out using a HORIBA Jobin-Yvon HR-800 confocal Raman microspectrometer (**Figure 3.1**).

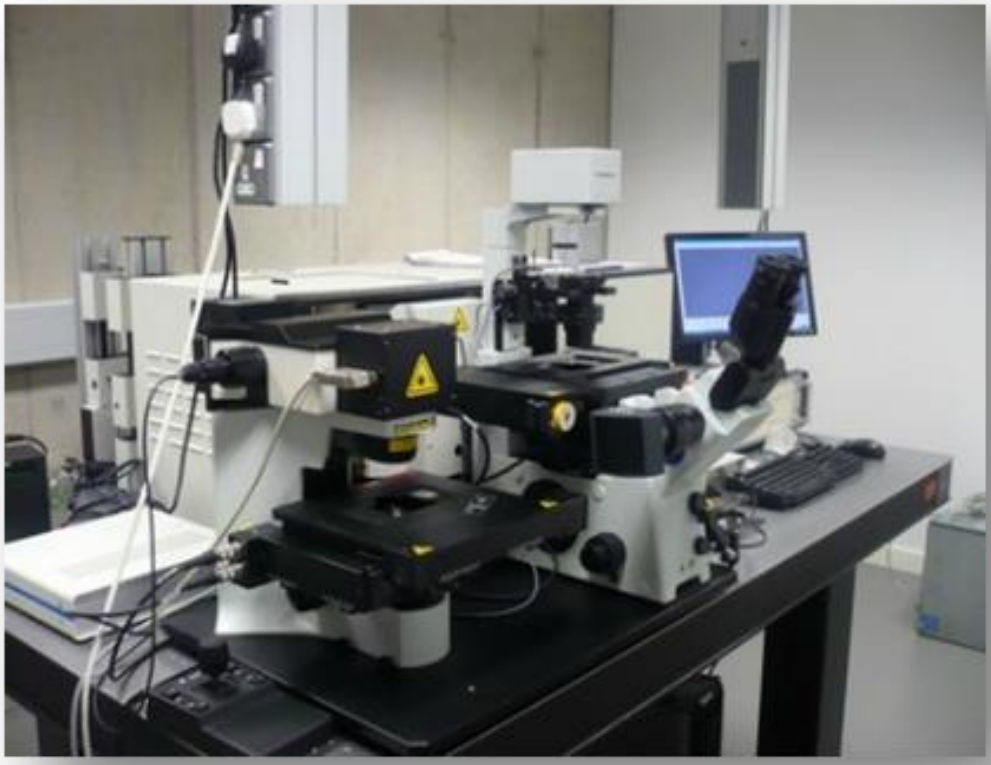

Figure 3.1. The Horiba Jobin-Yvon LabRAM HR system used for the Raman spectral acquisition of the artificial saliva samples.

The Raman spectra were recorded using two different wavelengths (532nm and 785nm), various objectives (10X, 50X and 60X) and a diffraction grating of 600 grooves/mm coupled with a charge couple device (CCD). Manual calibration of the grating was carried out using the 520.7cm^{-1} Raman line of crystalline silicon. Moreover, upright and inverted geometries were both tested and different substrates, including cuvettes, 96 well-plate (polystyrene) and 96 well-plate with no. 1 cover glass bottom. Raman spectra were

acquired in the 400 to 1800 cm^{-1} region with an integration time of 40 seconds per spectrum, and averaged over three accumulations. Dark current measurement and recording of the substrate and optics signal was also performed, for further corrections.

3.2.4 Real saliva collection and centrifugal filtration

A sample of human non stimulated whole saliva was collected from a healthy volunteer according to the procedure approved by ethical committee of Technological University Dublin (fully detailed in chapter 4, section 4.3.3). Following collection, 0.5 mL of the saliva sample was centrifugal-filtered using Amicon Ultra- 0.5ml centrifugal filter devices (Merck, Germany), according to the method demonstrated by Bonnier *et al* [2]. In the case of centrifugally filtered devices, the 3 kDa device was employed, and 0.5 mL of the saliva was placed in the device and centrifuged at 14,000 g for 30 minutes. The filtrate was mostly composed of water and molecules smaller than 3kDa molecular weight, while the remainder of the saliva (concentrate) is retained in the filter device. The filter device was then placed upside down in a new Eppendorf and spun down at 1000g for 2 minutes. The resultant is a concentration by a factor of 10 for the remaining saliva, with a resultant concentrate volume of ~70 mL.

3.2.5 Data Processing

The data processing was carried out using Matlab (Mathworks, US) with the PLS-Toolbox (Eigenvector Research Inc.) and in-house algorithms. The raw Raman spectra were first smoothed using a Savitsky-Golay filter (13 points, 9^{th} order). The baseline correction was applied using the rubberband method, and the spectra were vector normalised aiming to reduce any variability caused by the fluctuation of excitation power.

3.3 Results

3.3.1 Water measurements

Upright geometry

For the initial experiments with water, a quartz cuvette (3.5 mL) completely filled with ultrapure water was used as a substrate to initially explore the optimisation of the Raman measurement protocol. A full range from 400cm-1 to 3800cm-1 was acquired through a 10X objective, using 785nm as the laser source (**Figure 3.2**). The resulting spectrum obtained from water using a cuvette had a noisy aspect, which seemed to compromise the Raman signal from water (**Figure 3.2**).

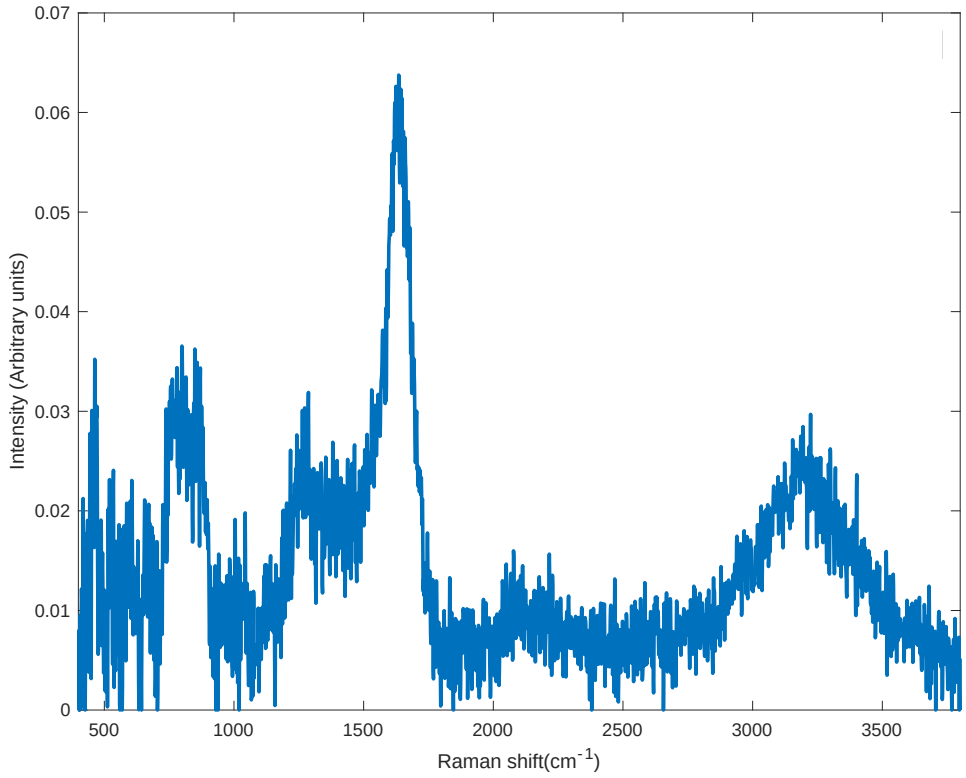

Figure 3.2: 785nm Raman full range spectrum of water in an upright geometry focused by a 10X objective using a quartz cuvette as substrate.

A second laser line (532 nm) was also used with the same set up above described. The Raman spectrum obtained from water was of very good quality with high signal to noise (**Figure 3.3**). It exhibits the two major water bands around 1640cm-1 and 3200-3400cm-1.

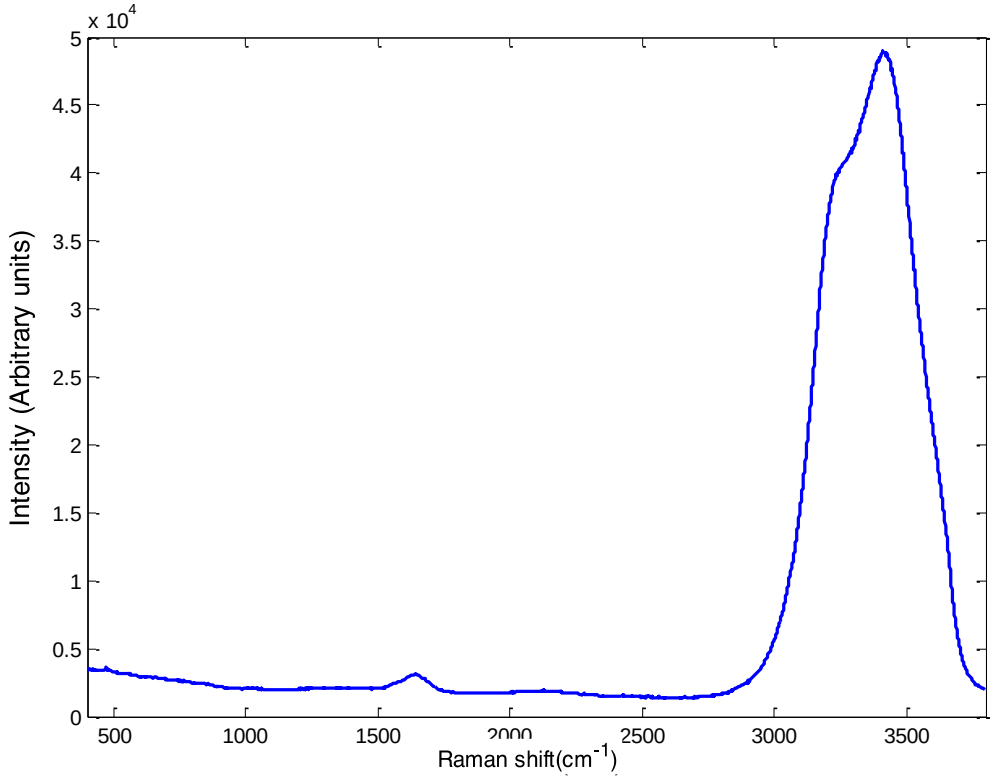

Figure 3.3: 532nm Raman full range spectrum of water in an upright geometry focused by a 10X objective using a quartz cuvette as substrate.

However, when adopting cuvettes as substrate to analyse saliva samples, the amount of sample needed to completely fill the cuvette (3.5 mL) had to be taken into consideration. In clinical conditions, an individual saliva sample (after sample preparation) would not be able to fill the required cuvette volume.

Given these limitations related to the cuvette for Raman instrumentation, a 96 well-plate (made of polystyrene) was subsequently applied as substrate. 300 µL of water was poured

into one of the wells to completely fill it. Again, a 10X objective was also used to acquire the Raman spectrum of water, using 532nm as laser source. Although not very evident in the high wavenumber region (**Figure 3.4b**), contamination from polystyrene can clearly be seen to contribute to the sample (water) spectrum (**Figure 3.4a**). This association to contamination of the spectrum by polystyrene features can be further confirmed in **Figure 3.5** showing the pure spectra of the polystyrene base of the 96 well-plate and water in the range 400-3800cm^{-1}.

The polystyrene contribution could be attributed to the fact that the focal depth of the 10X objective is often too long, in comparison to the well depth. Trying to minimise this contribution, a higher magnification (50X), and lower focal depth objective were also explored. The interference (polystyrene) could be apparently completely eliminated, resulting in a good quality water spectrum (**Figure 3.6**).

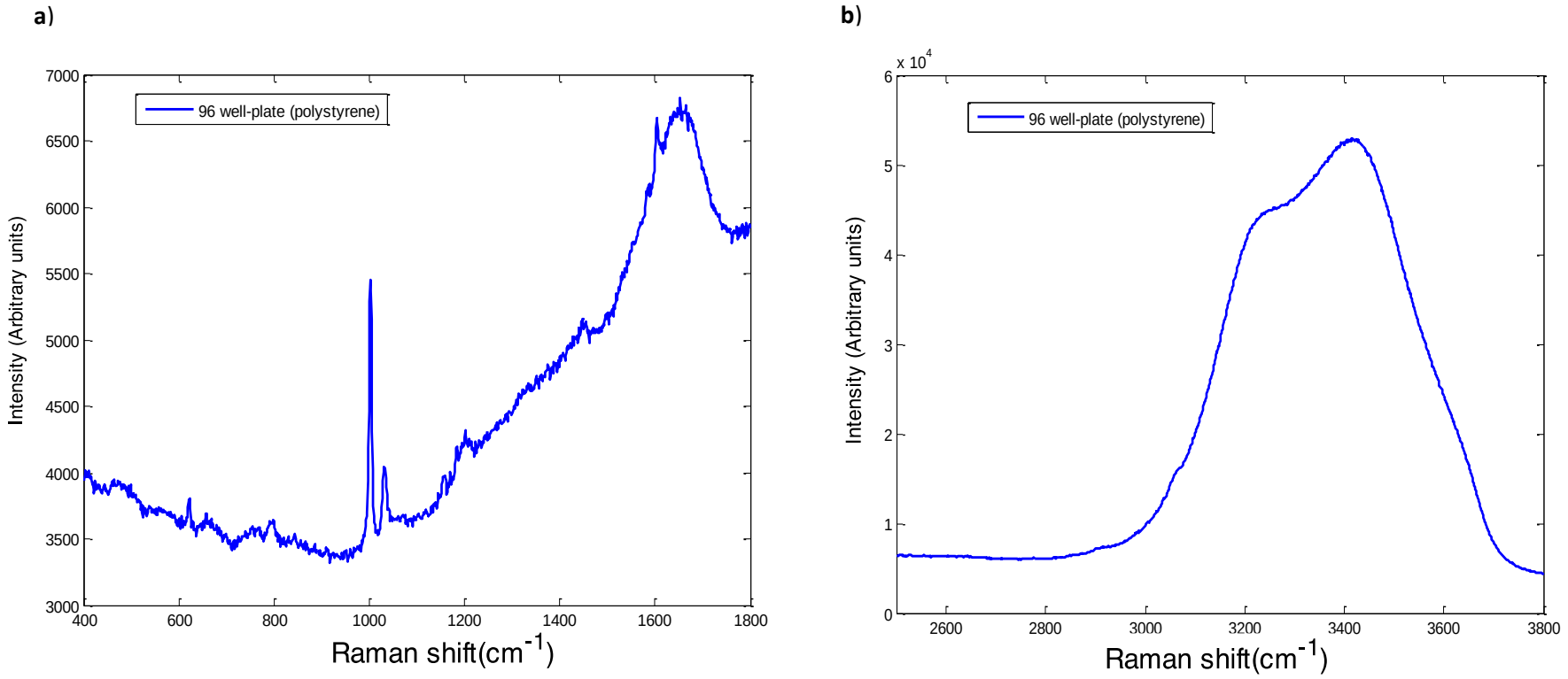

Figure 3.4: 532nm Raman spectrum of water in an upright geometry focused by a 10X objective using a 96 well-plate (polystyrene) substrate. (**a**) The fingerprint region (400-1800cm-1) and (**b**) the high wavenumber fingerprint (2500-3800cm-1) show the influence of polystyrene contributions to the spectrum.

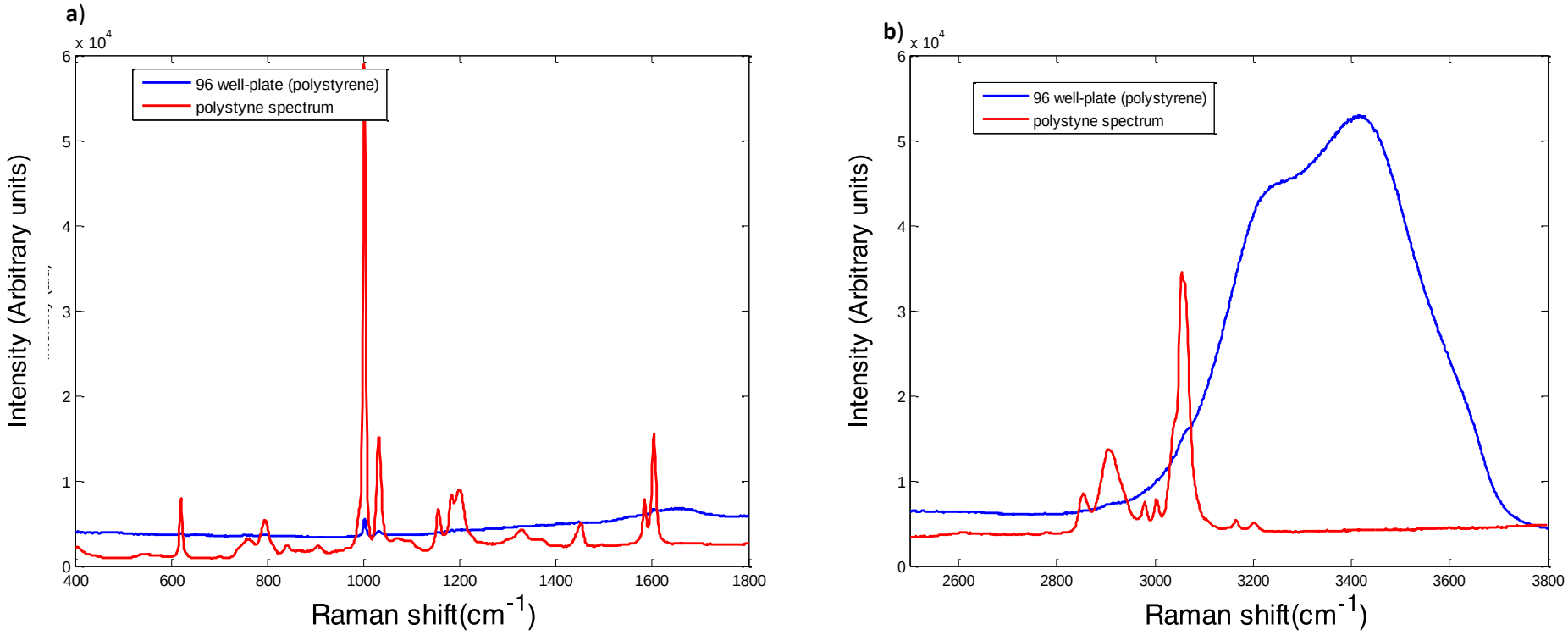

Figure 3.5: 532nm Raman spectra of water in an upright geometry focused by a 10X objective using a 96 well-plate (polystyrene) substrate along with polystyrene spectrum. (**a**) fingerprint region and (**b**) high wavenumber region.

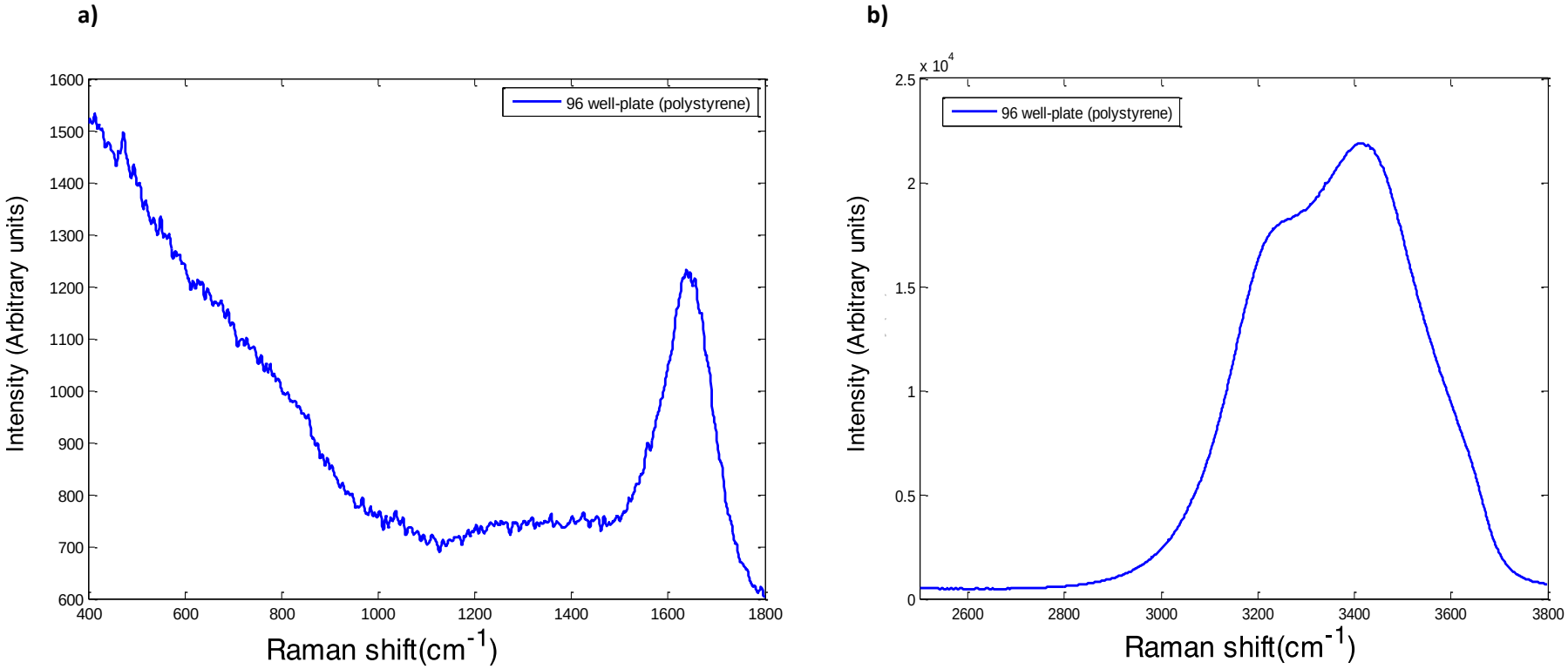

Figure 3.6: 532nm Raman spectrum of water in an upright geometry focused by a 50X objective using a 96 well-plate (polystyrene) substrate. (**a**) The fingerprint region (400-1800cm^{-1}) and (**b**) the high wavenumber fingerprint (2500-3800cm^{-1}) shows no influence from the background over the water spectrum.

The use of a lower magnification, such as 10X objective, increases the focal depth, consequently, making it possible to analyse larger working volumes. Therefore, in the case of saliva samples, the working volume provided by the 10X objective allows a complete scan of the sample. However, the increased working volume can also contribute to signal contamination from the substrate, as seen with polystyrene. In contrast to this, the higher magnification (50X) avoids the contamination from background (polystyrene or other) due to the reduced focal depth of the objective lens.

Inverted geometry

As an alternative, the inverted geometry was investigated, as it has previously been reported to give optimal signals for serum measurement[2]. In an attempt to eliminate the high substrate interference from polystyrene seen in the upright measurements, a new 96 well-plate glass bottom no.1 was then adopted for the inverted geometry.

Using the inverted instrumentation configuration, the Raman signals from water using 10X objective were initially acquired using the 785 nm laser source. The signal was in general very noisy and fluorescence compromised the spectral profile of water (**Figure 3.7**). Also, the high wavenumber region did not show the bands related to water at this wavelength due to fluorescence influence and software autocorrection.

The higher magnification (60X water immersion) was subsequently applied. The signal was clearly improved and the noise decreased, but the fluorescence interference remained, compromising the Raman signal (**Figure 3.8**). This sort of fluorescence response has also been reported in other studies, where this phenomenon was well documented as an effect from the substrate when 785 nm lasers are applied[3,4].

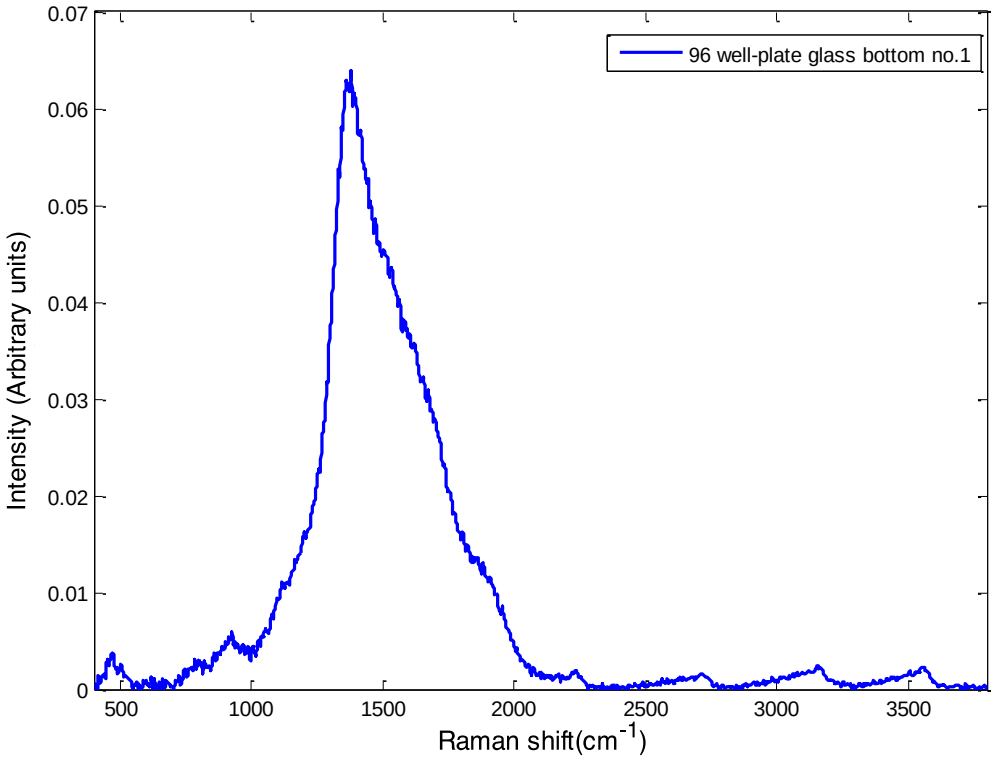

Figure 3.7: 785nm full range Raman spectrum of water in an inverted geometry focused by a 10X objective using 96 well-plate glass bottom no.1.

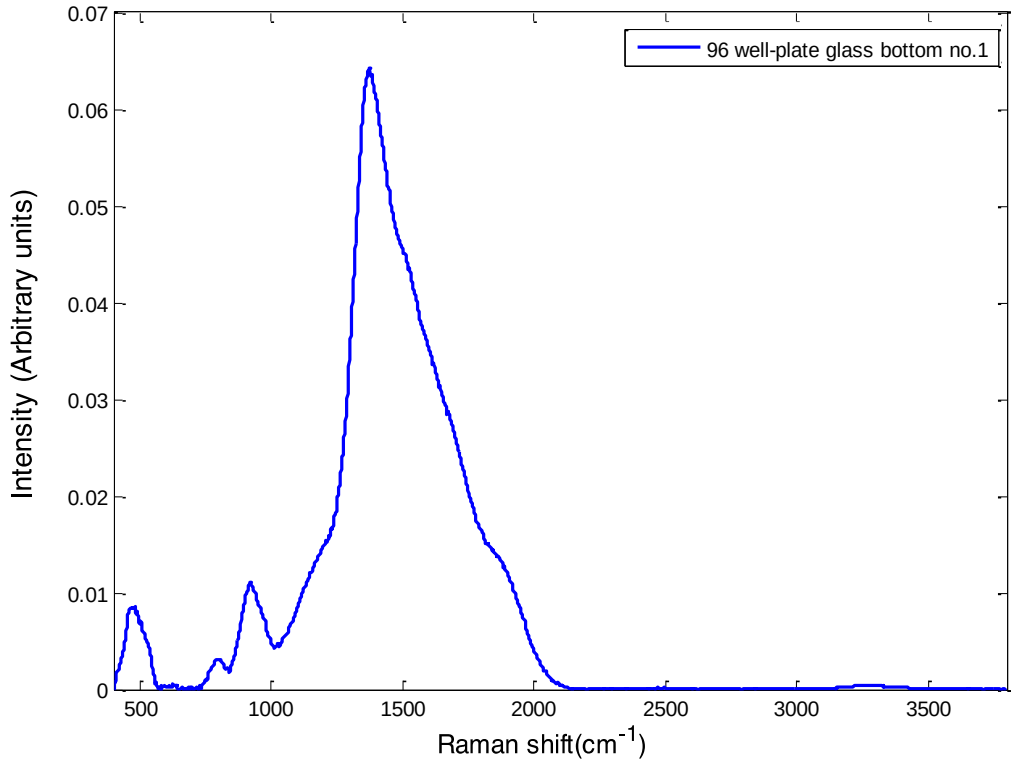

Figure 3.8: 785nm full range Raman spectrum of water in an inverted geometry focused by a 60X objective (water immersion) using 96 well-plate glass bottom no.1.

A 60X water immersion objective was applied to the inverted set up (**Figure 3.9**). Bonnier *et al.* have already demonstrated that when working in immersion using a 60X or 100X water immersion objectives, the working distance is increased to about 2 mm2. Thus, the 60X objective coupled to water immersion might increase the signal resolution from saliva samples.

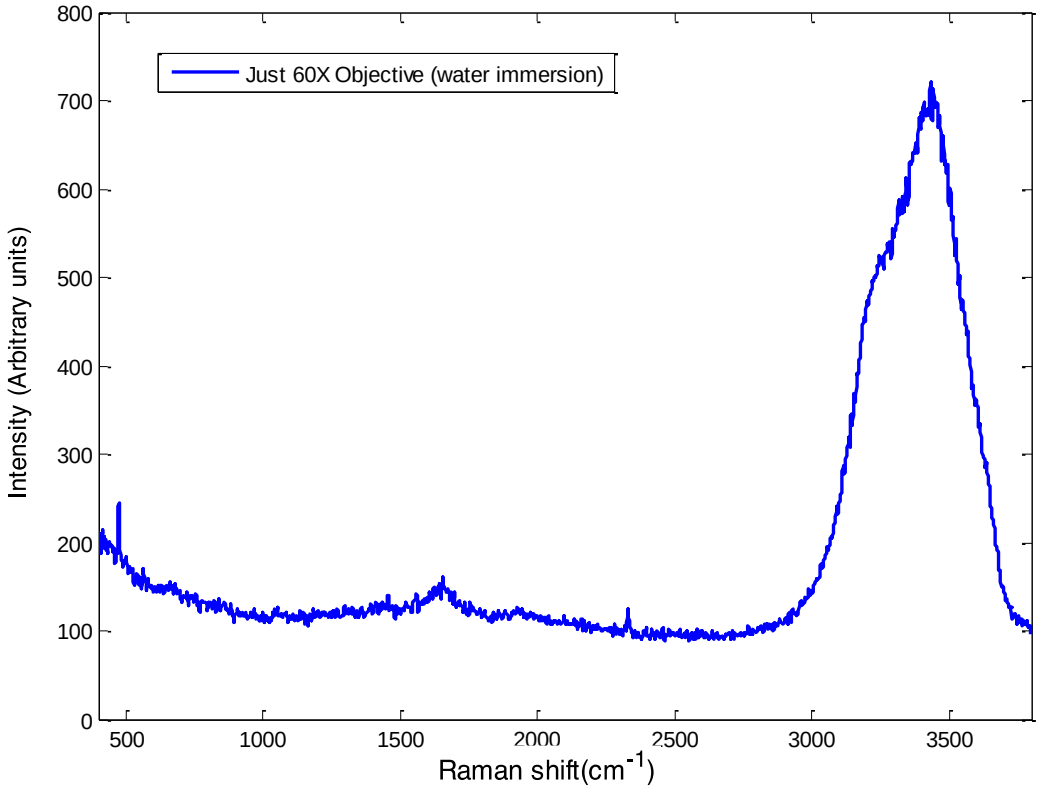

Figure 3.9: 532nm Raman full range spectrum from 60X water immersion objective by itself.

Keeping the higher magnification (60X water immersion objective), the 532 nm laser source was then applied for Raman signal acquisition from an empty well of 96 well-plate glass bottom no.1. The Raman signal was recorded in different stages, from the point at which the focus of the water immersion objective had not yet reached the substrate; then, at different points as the focus was translated through the substrate (**Figure 3.10**). This measurement practice allowed the identification of the best focus point above the

substrate at which the contribution of the glass as well as the water droplet on the immersion objective itself was minimised.

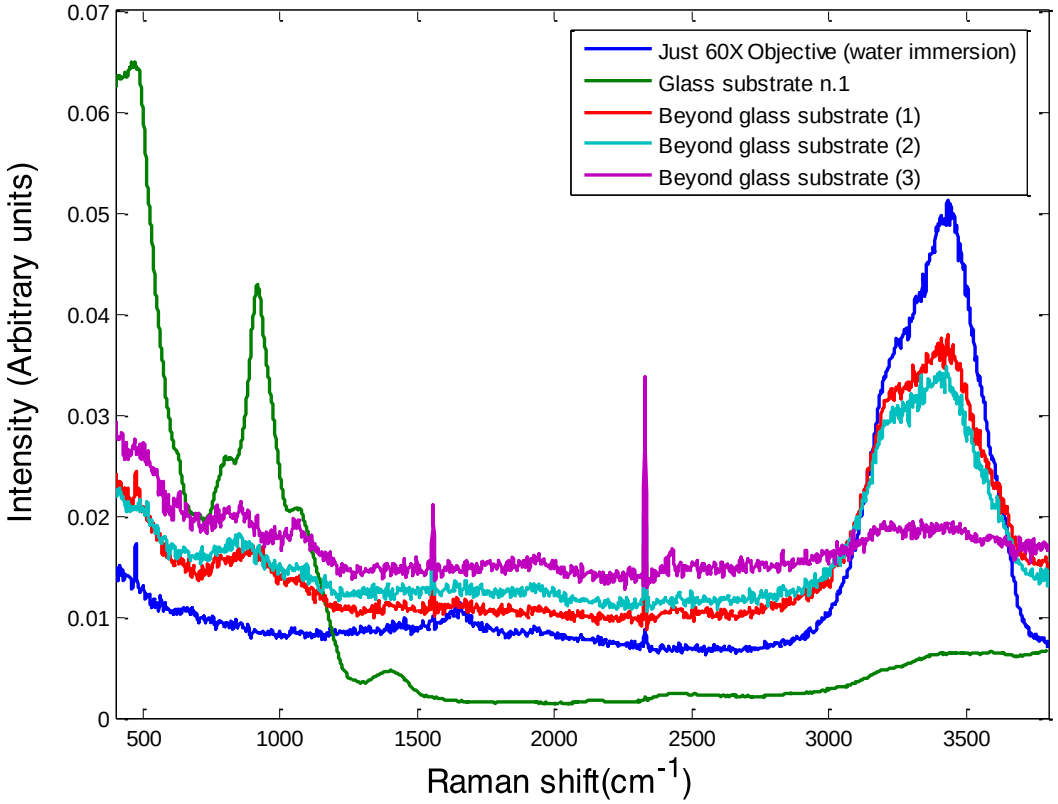

Figure 3.10: 532nm Raman full range spectrum 60X water immersion objective, glass substrate, and 3 different focus points beyond the bottom of an empty well in inverted geometry, respectively.

Once the optimum focus point was reached, different amounts of water were added (from 0 to 70 µL) into the well in an attempt to find the minimum sample amount required for the set up proposed (**Figure 3.11**). The minimum amount was determined based on the water band intensity at 3400cm-1 as the water was added into the well (**Figure 3.12**).

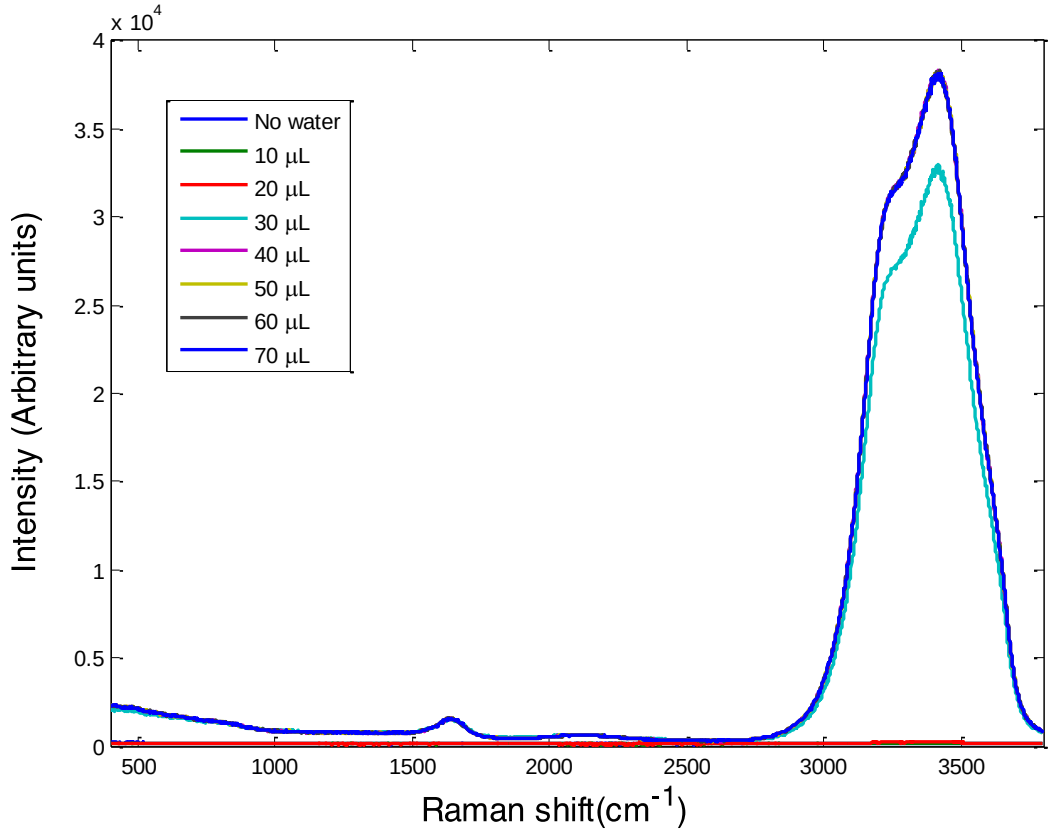

Figure 3.11: 532nm Raman full range spectrum of an empty well and different amounts (10-70 µL) of water in an upright geometry focused by a 60X water immersion objective using a 96 well-plate glass bottom no.1 substrate.

The intensity of water peak at 3400cm-1 reached its highest after 40 µL of water was added into the well. At this volume, the spectrum using the 60X water immersion in the upright geometry, the 532nm laser line, and a 96 well-plate glass bottom no.1 as substrate, was effective in eliminating any visible glass contribution from the water spectrum (**Figure 3.13**). The set up showed the feasibility of application for limited amounts of sample (saliva) as low as 40 µL

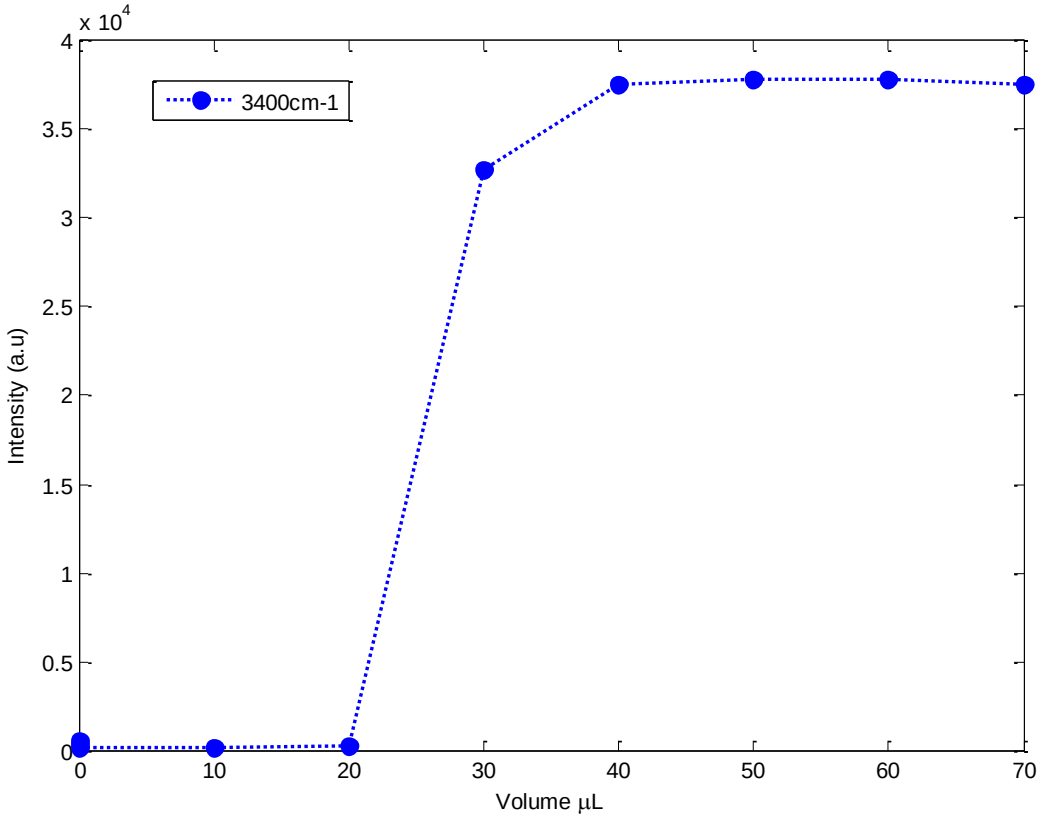

Figure 3.12: Raman intensity variation of different volume of water between 0-70 µL at 3400cm1 in an upright geometry focused by a 60X water immersion objective using a 96 well-plate glass bottom no.1 substrate.

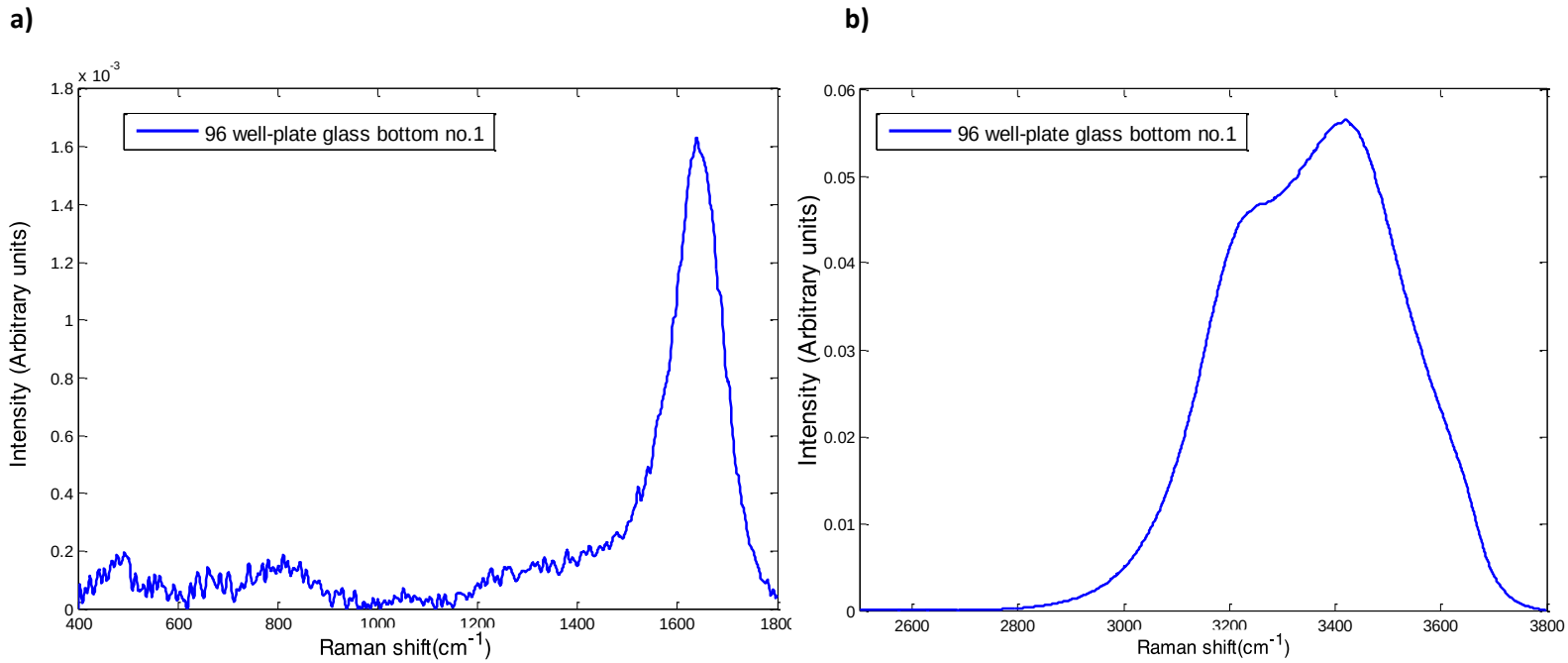

Figure 3.13: 532nm Raman full range spectrum of water in an inverted geometry focused by a 60X water objective using a 96 well-plate glass bottom no. 1 as substrate.

3.3.2 Artificial saliva measurements

Artificial Saliva in different concentrations (Inverted Geometry)

Following further analysis using inverted inverted geometry as the most suitable for liquid samples, different concentrations of artificial saliva were prepared aiming to obtain relevant Raman spectra signal which could not be detected with relevant biological signal information. The substrate (96 well-plate with glass bottom no. 1) and the previous wavelength (532nm) were adopted as this setup was demonstrated to be a suitable setup for saliva samples.

The Raman spectral quality could be improved as long as the sample concentration was increased. Among five formulations, the spectral definition and relevant information (peaks) were more visible from artificial saliva when 75% (1:1.75) or more concentrated compared to lower concentrations (**Figure 3.14**).

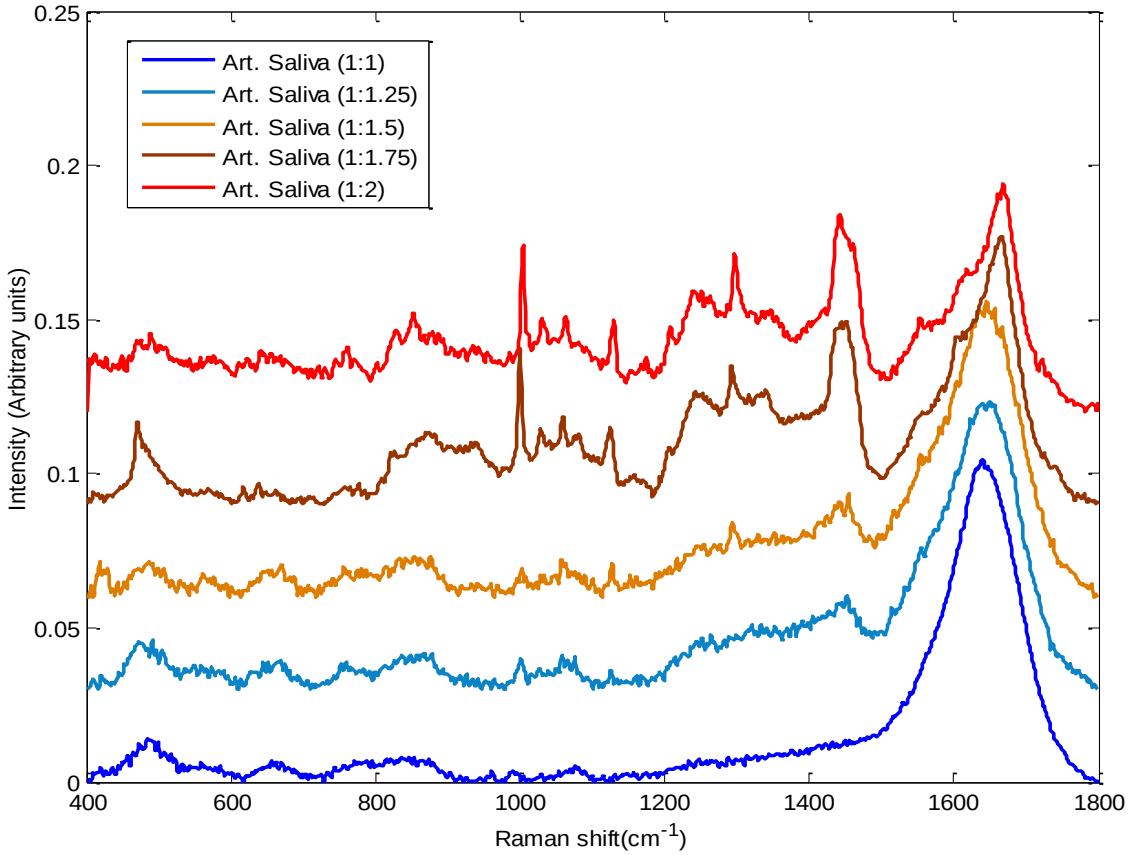

Figure 3.14: Off-set plot of 532nm Raman spectrum focused by a 60X objective onto a sample of artificial saliva 1:1, 1:1.25, 1:1.5, 1:1.75 and 1:2 (or 0, 25%, 50%, 75% and 100% more concentrated, respectively) in an inverted geometry focused by a 60X water objective using a 96 well-plate with glass bottom no. 1 as substrate.

785nm – laser line

The information obtained from artificial saliva sample using a 785nm laser line could not show same relevant Raman spectral information compatible with the molecular composition of the artificial sample recorded when using a 532 nm laser line (**Figure 3.15**).

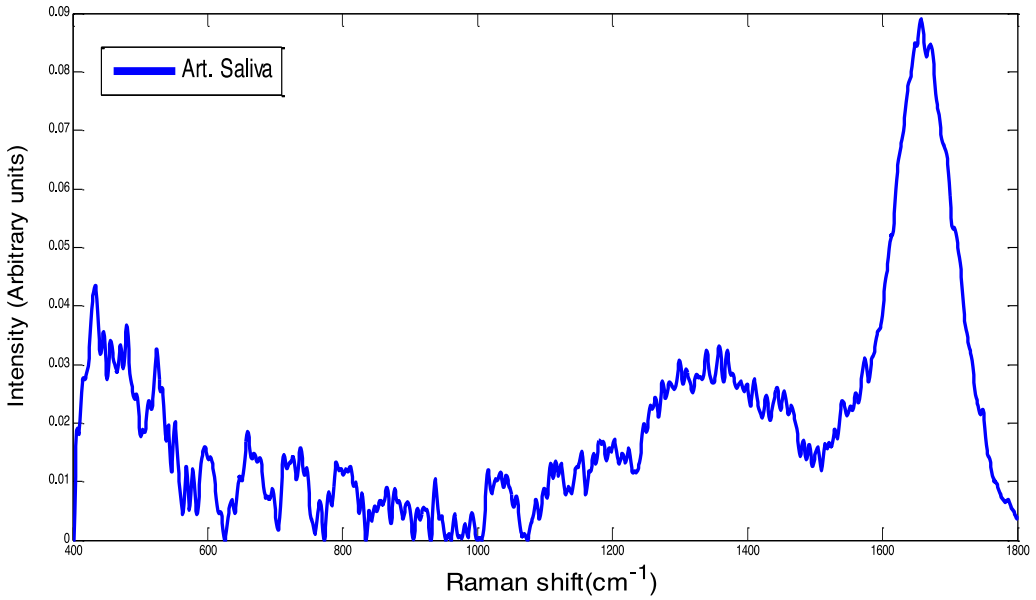

Figure 3.15: 785nm Raman spectrum focused by a 60X water objective onto a sample of artificial saliva in an inverted geometry using a 96 well-plate with glass bottom no. 1 as substrate. A noisy Raman signal was obtained with limited spectral information.

3.3.3 Real Saliva

A real stimulated whole saliva sample from a healthy donor (Technological University Dublin) was analysed by previous protocols applied in the artificial samples. Centrifugal filtration using 3kDa centrifugal filtering devices seemed to provide a relevant Raman signal revealing biomolecular information in the spectra valuable for future analysis for oral cancer detection (**Figure 3.16**).

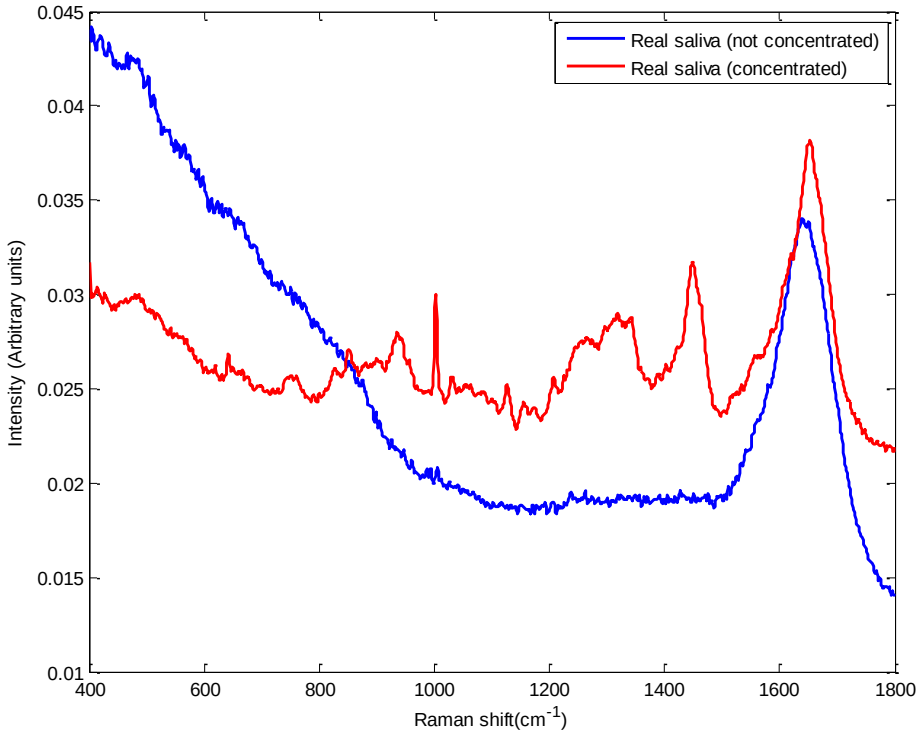

Figure 3.16: 532nm raw Raman spectrum focused by a 60X water objective onto a sample of real saliva (around 75% more concentrated by centrifugal filtration) (blue) and a samples of real saliva not concentrated (before centrifugal filtration) (red) in an inverted geometry focused by a 60X water objective using a 96 well-plate with glass bottom no. 1 as substrate.

Moreover, the pre-processing data analysis can express the effectiveness of the protocol when comparing the pre-processed artificial concentrated saliva spectral profile to real saliva spectrum (**Figure 3.17**).

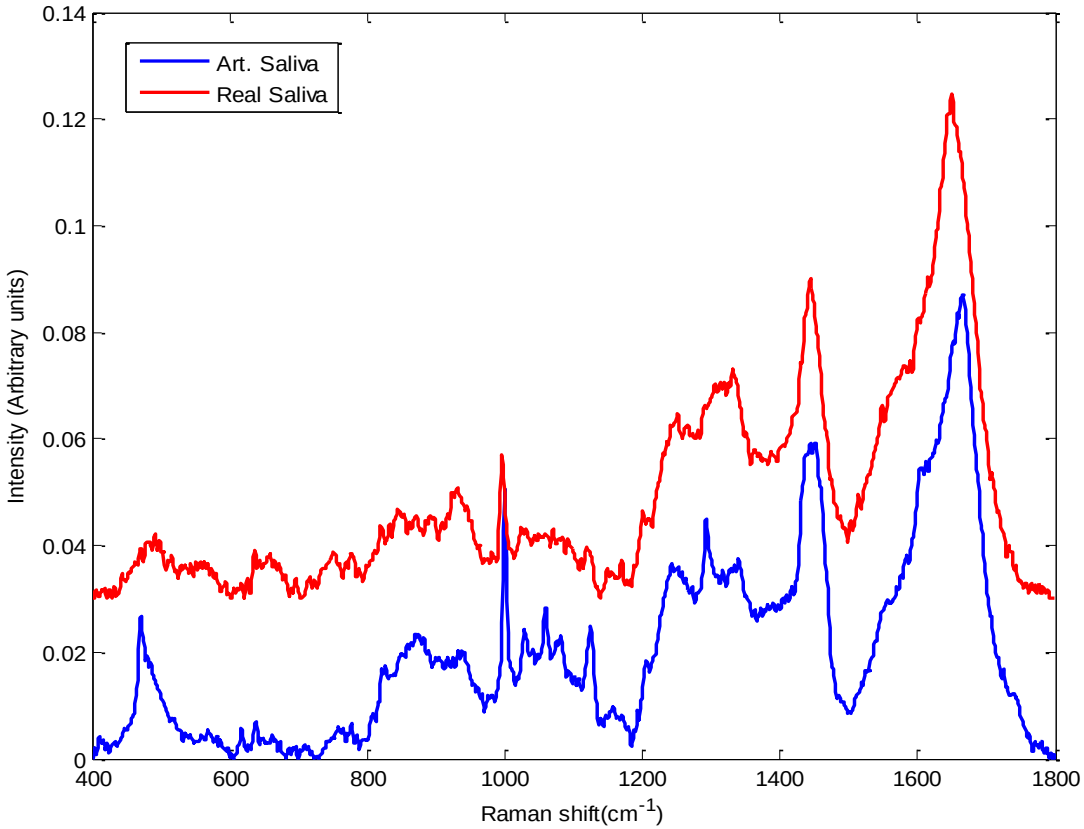

Figure 3.17: Off-set plot of Raman spectrum acquired from real saliva samples previously centrifuged using 3kDa devices in comparison to artificial saliva 1:2 (100% more concentrated) after pre-processing in an inverted geometry focused by a 60X water objective using a 96 well-plate with glass bottom no. 1 as substrate. Similarities can be seen between both spectra confirming the effectiveness of the standardisation protocol for real saliva samples.

Sample stabilisation study

For a better understanding regarding sample stability, a pilot study regarding the effects of time on a saliva sample was also carried out. As the temperature effect from the Raman laser applied to the liquid saliva samples remains unknown in the current literature, one random stimulated saliva sample from a healthy volunteer (n=1) was analysed over one hour by the protocol established in this chapter, using the same substrate and instrumentation setup, and processing stages. A Raman spectrum was acquired every 2 minutes over 1 hour, resulting in a total of 30 spectra.

The plot of Raman spectra as a function of time shows the variance of the spectra obtained (**Figure 3.18**). Briefly, many of the peaks related to the biochemical composition of saliva decreased as the time passed.

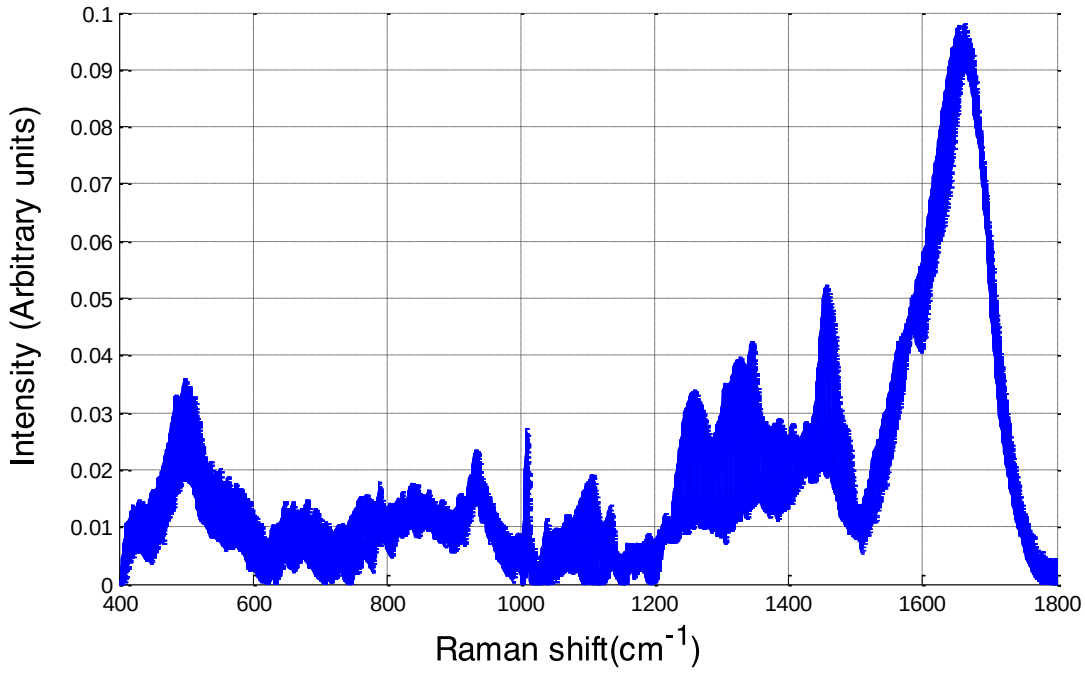

Figure 3.18: Raw Raman spectral changes of one liquid saliva sample over one hour.

The area under the curve of each spectrum was also calculated by the trapezoidal numerical integration method. Although showing noise variances, **Figure 3.19** shows that the overall intensity of the Raman fingerprint of saliva has considerably decreased with time. Also, an off-set plot of each of the spectra over time (**Figure 3.20**) shows that the loss was basically restricted to protein bands.

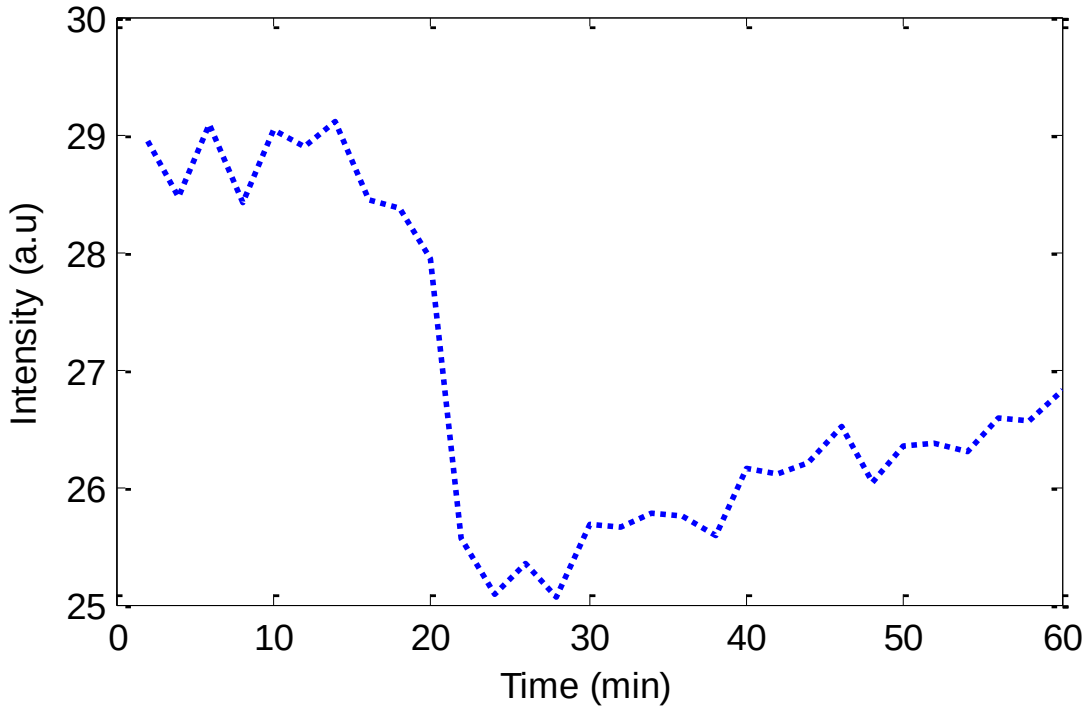

Figure 3.19: Plot of the variation of the area under the curve over one hour.

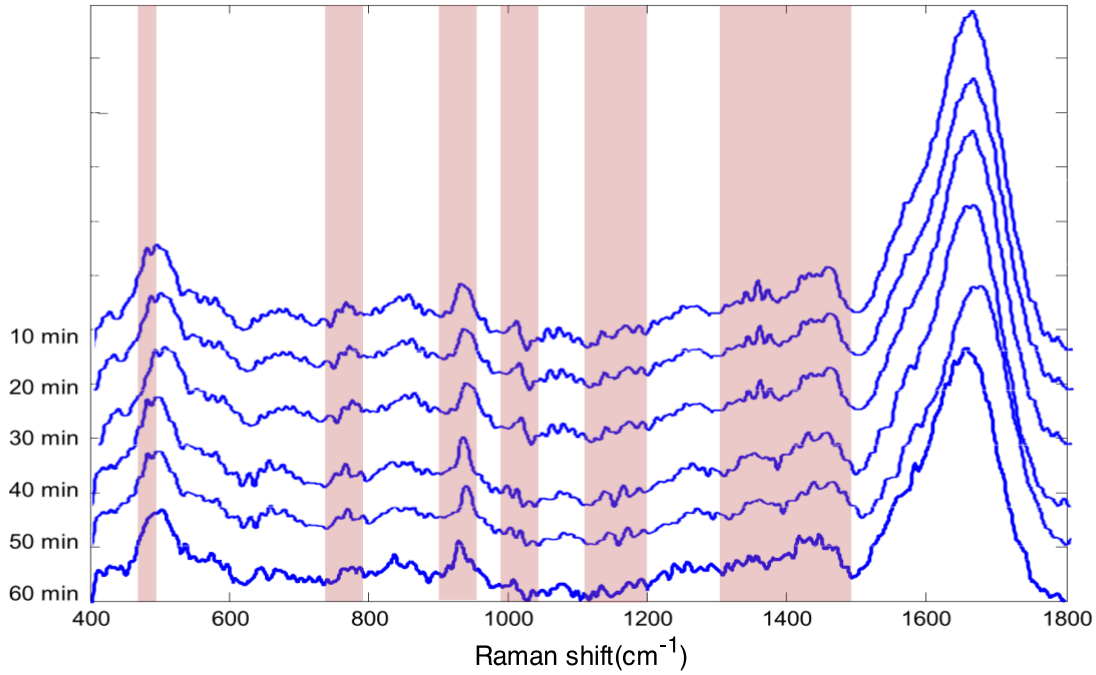

Figure 3.20: Off-set plot highlighting spectral regions related to proteins and significant loss over time.

According to the results obtained, the 10 first spectra, which represent the first 20 minutes, did not show any major spectral changes (degradation). After 20 minutes, the bands related to the biochemical profile of the sample had almost completely disappeared. These results can be due to possible degradation caused by the laser throughout the Raman acquisition process. It might be related to the fact that the laser can overheat the sample causing salivary protein degradation.

These results complement and validate the current methodology, according to which only the first 10 saliva spectra of each sample can be safely used for Raman analysis.

3.4 Discussion

Vibrational spectroscopy techniques, such as Raman spectroscopy, hold the advantage of minimal sample preparation for analysis of biological samples. The methodology in this

current study aimed to optimise the Raman instrumentation and substrates rather than saliva preparation.

The Klimek *et al*. formula of artificial saliva is considered the most similar to human saliva as it contains inorganic components as well as organic components, such as mucin[1]. Other formulae for artificial saliva preparation have also been used in different studies, although these formulations only contain inorganic components, which could represent a lack of biomolecular information for the Raman spectral recording[5,7].

It is very important to highlight the importance of this study in the vibrational spectroscopy field due to the effort in trying to find the best Raman instrumentation setup specifically for saliva analysis. The methodology proposed uses only different substrates and minimal sample preparation (as saliva was still kept in the liquid physical state) compared to other experiments, where enhancers were applied, such as nanoparticles; or the saliva sample was completely dried to facilitate the signal acquisition[7,8,9].

Although demonstrating the potential of saliva as a sample, most of the studies involving Raman microspectroscopy and saliva analysis on its own have dried the sample, resulting in a predictable biochemical information loss[10,11]. Studies have been carried out showing the saliva properties and Raman diagnostic capability for breast, nasopharyngeal and lung malignancies[9,10,11]. To diagnose nasopharyngeal cancer for example, the results suggested that the SERS signals attributed to proteins are significantly different between saliva from controls and nasopharyngeal cancer patients, and high diagnostic accuracy of 90.2% could be abtained[8]. Similarly, an accuracy of 82.47% and 80% were obtained when comparing saliva from healthy controls to saliva from patients with breast and for lung cancer, respectively[7,8]. However, all the methodologies performed in those studies involved preparation of enhancers (nano particles) that could be costly as well as difficult to translate to a clinical environment.

In summary, the Raman setup using the 532 nm laser line, 96 well-plate with glass bottom no.1 in an inverted microscope geometry, has been demonstrated to be effective for the measurement of artificial saliva, revealing significant biochemical spectral information from real saliva samples in an effective and less costly when in comparison to other techniques. In view of its potential for precise and rapid analysis of saliva, Raman spectroscopy can be used as a potential method for oral dysplasia diagnostics**.**

Reference

1. Klimek J, Hellwig E, Ahrens G. Effect of plaque on fluoride stability in the enamel after amine fluoride application in the artificial mouth. Dtsch Zahnarztl Z. 1982;10:836-40.

2. Bonnier F, Petitjean F, Baker MJ, Byrne HJ. Improved protocols for vibrational spectroscopic analysis of body fluids. J Biophotonics. 2014 Apr;7(3-4):167-79. doi: 10.1002/jbio.201300130.

3. Fullwood LM, Griffiths D, Ashton K, Dawson T, Lea RW, Davis C, Bonnier F, Byrne HJ, Baker MJ. Effect of substrate choice and tissue type on tissue preparation for spectral histopathology by Raman microspectroscopy. Analyst. 2014 Jan 21;139(2):446-54. doi: 10.1039/c3an01832f.

4. Kerr LT, Byrne HJ, Hennellyac BM. Optimal choice of sample substrate and laser wavelength for Raman spectroscopic analysis of biological specimen. Anal. Methods, 2015;(7):5041-5052.

5. Batista GR1, Rocha Gomes Torres C, Sener B, Attin T, Wiegand A. Artificial Saliva Formulations versus Human Saliva Pretreatment in Dental Erosion Experiments. Caries Res. 2016;50(1):78-86. doi: 10.1159/000443188. Epub 2016 Feb 13.

6. Levine MJ, Aguirre A, Hatton MN, Tabak LA. Artificial salivas: present and future. J Dent Res. 1987 Feb;66 Spec No:693-8.

7. Feng S, Huang S, Lin D, Chen G, Xu Y, Li Y, Huang Z, Pan J, Chen R, Zeng H. Surface-enhanced Raman spectroscopy of saliva proteins for the noninvasive differentiation of benign and malignant breast tumors. Int J Nanomedicine. 2015 Jan 12;10:537-47. doi: 10.2147/IJN.S71811. eCollection 2015.

8. Qiu S, Xu Y, Huang L, Zheng W, Huang C, Huang S, Lin J, Lin D, Feng S, Chen R, Pan1 J. Non-Invasive Detection Of Nasopharyngeal Carcinoma Using Saliva Surface-Enhanced Raman Spectroscopy. Oncol Lett. 2016 Jan; 11(1): 884–890.

9. Li X, Yang T, Lin J. Spectral analysis of human saliva for detection of lung cancer using surface-enhanced Raman spectroscopy. J Biomed Opt. 2012 Mar;17(3):037003. doi: 10.1117/1.JBO.17.3.037003.

10. Gonchukov S, Sukhinina A, Bakhmutov D, Minaeva S. Raman spectroscopy of saliva as a perspective method for periodontitis diagnostics. Laser Phys. Lett. 2012; 9(1): 73-77

11. Virkler K, Lednev IK, Forensic body fluid identification: The Raman spectroscopic signature of saliva, Analyst, 2010;35:512–517.

Chapter 4: Raman spectroscopic characterisation of non stimulated and stimulated human whole saliva: a new methodology.

Chapter adapted from 'Calado G, Behl I, Byrne HJ, Lyng FM. Raman spectroscopic characterisation of non stimulated and stimulated human whole saliva: a new methodology' submitted for publication in Analyst (September/2019).

Genecy Calado conducted all the experiment and data analysis, and was primary author of the article, with contributions and guidance from the other authors.

4.1 Abstract

Human saliva is a unique biofluid which can reflect the physiopathological state of an individual. The wide spectrum of molecules present in saliva, compounded by the close association of salivary composition to serum metabolites, can provide valuable information for clinical diagnostic applications through highly sensitive vibrational spectroscopic techniques such as Raman spectroscopy. However, the nature of saliva, in terms of collection and patient-related characteristics, can be considered factors which may strongly affect the Raman spectral profile of salivary samples and disrupt the search for specific salivary biomarkers in the detection of diseases. The main objective of this study, dealing with the processing of Raman spectra of saliva from 20 donors, concentrated by centrifugal filtration, was to highlight spectral features associated with the type of collection in an intra- and inter-patient patient approach. The methodology adopted for liquid saliva, showed consistency in the qualitative analysis of the groups,

confirming the reproducibility of this Raman spectroscopic approach. Using principal component analysis (PCA) and partial least squares – discriminant analysis (PLSDA), non stimulated saliva could be differentiated from stimulated saliva in both intra- and inter-patient analysis, with a classification efficiency of 77 and 87%, respectively. The bicinchoninic acid (BCA) assay showed a similar trend in terms of total protein concentration, showing a slight increase in stimulated saliva samples. These results are valuable in the process of developing and establishing Raman spectroscopy as a novel diagnostic tool in the future as well as controlling variabilities, in order to determine specific spectroscopic markers related to a multifactorial disease for diagnostic or follow-up purposes.

4.2 Introduction

Saliva is considered a dynamic biological fluid that has a large range of constituents, including proteins, polypeptides, nucleic acids, electrolytes, and hormone[1]. It is categorised as an exocrine secretion of the salivary glands, which is hypotonic in nature, with a pH of 7.2–7.4, or in some conditions slightly acidic[1]. Whole saliva is unique and complex, both in its sources and composition. It consists not only of secretions from the three major salivary glands (parotid, submandibular and sublingual) and the minor glands, but also gingival crevicular fluid, oral mucosa transudate, secretions from nasal and pharyngeal mucosa, keratin debris and blood cells[2,3].

Interest in human saliva as a potential diagnostic and prognostic fluid is steadily increasing because it provides access not only to relevant oral but also systemic disease information[4,5]. Saliva has been identified as functionally equivalent to blood serum, reflecting the physiological state of the body, including hormonal, nutritional, and metabolic variations, for example[6], and its composition can be linked with traditional

biochemical parameters which appear in the serum[7]. Salivary collection is usually considered as one of the easiest methods of collection of bodily fluids, due to its noninvasive nature, which also does not require specialised equipment or supervision. Further, saliva collection is usually a well accepted procedure, from the patients' point of view, and is a cost-effective approach. Oral fluid sampling is also safe for both the operator and the patient and is amenable to repeated and voluminous sampling in short intervals of time. Considering these advantages, saliva is identified as a potential source of biological sample to be employed for specific patient as well as routine diagnostic screening[8,9].

It is very important, however, to highlight the fact that the composition of each saliva sample tends to vary and depend on the type of gland of origin and, consequently, the type of collection employed to obtain these samples[10]. Its composition differs according to the contribution of each gland in order to obtain the total unstimulated saliva secretion, and can vary from 65%, 23%, and 8% to 4% for the submandibular, parotid, and sublingual glands, for example[11].

When resting, without exogenous or chemical stimulation, non stimulated saliva is characterised by its low and continuous salivary flow, denoted basal unstimulated secretion, present in the form of a film that covers, moisturises, and lubricates the oral tissues. In contrast, stimulated saliva is produced by a range of mechanical, gustatory, olfactory, or pharmacological stimuli, and contributes to around 80% to 90% of daily salivary production[12].

Clinically, the most practical way to differentiate between non stimulated and stimulated saliva is usually by its salivary flow rate. In adults, normal total stimulated salivary flow ranges from 1 to 3 mL/min, low ranges from 0.7 to 1.0 mL/min, while hyposalivation is characterised by less than 0.7 mL/min[13,14]. In normal, non stimulated salivary function, it

ranges from 0.25 to 0.35 mL/min, low ranges from 0.1 to 0.25 mL/min, while hyposalivation is characterised by a salivary flow of less than 0.1 mL/min[14]. However, although widely adopted in clinics, the values denoted “normal” for stimulated and non stimulated salivary flow exhibit large biological variation[14].

Despite the complexity of the salivary milieu and the anatomy of salivary glands, the analysis of saliva and its different collection forms represent a promising approach to establishing potential biomarkers for several pathological conditions[15]. In this context, the scientific development of new technologies and associated “omics” approaches provide opportunities for the determination of new biomarkers for the diagnosis, staging, or prognosis of diseases[16].

Vibrational spectroscopy is one such evolving set of techniques which allows analysis of a multitude of biological samples, including saliva[17-20]. Recently, vibrational spectroscopic analysis of saliva has proven efficient to differentiate chronic periodontitis from aggressive periodontitis[21], diagnose type 2 diabetes and psoriasis[22], detect drugs[23], and discriminate smoking from non-smoking patients[24]. Amongst the vibrational spectroscopic methods, Raman spectroscopy can be considered a unique non-invasive laser-based analytical technique that aids biochemical component analysis[25]. Raman spectroscopy is based on the molecular vibrations that are specific to certain types of biomolecules, including proteins, nucleic acids and lipids[25]. The Raman effect is based on vibration transitions under inelastic scattering of monochromatic light in visible, near ultraviolet or near infrared ranges. Raman spectroscopy can thus provide a characteristic fingerprint of the molecular vibrations that are specific to certain types of biomolecules, including proteins, nucleic acids and lipids[25]. Raman spectroscopy, in contrast to conventional biochemical methods, is a label-free and rapid technique, which usually requires only a small quantity of a sample without any preparation[26].

It has been reported that Raman Spectroscopy of saliva can be used for narcotic usage detection[27], for cancer diagnosis[28,29], and in forensic medicine[30]. It is notable, however, that the current literature lacks technical information regarding the methodologies employed[31]. Thus, there is an urgent need for a systematic optimisation of analysis protocols governing Raman spectroscopy analysis of saliva samples. Most studies reported to date have focused on individual proteins under specific conditions, with the type of stimulation varying greatly[32]. Studies looking at protein changes in human saliva have typically analysed samples from individual glands, not whole saliva[33]. Notably, the literature is particularly scant on details regarding the sample collection protocols, and differentiation of stimulated and unstimulated production of saliva and on human whole saliva composition.

In an attempt to establish a standard Raman spectroscopy protocol for analysis of saliva samples, as well as to better clarify factors correlated to the sampling procedure, such as type of collection, the aim of the present study was to develop, based on Raman spectra of saliva samples, a preanalytical workflow to highlight spectral features associated with intra- and inter-patient characteristics which could further help to extract specific salivary diagnostic signatures of systemic or local pathological conditions.

4.3 Methodology

4.3.1 Subjects

Ethical approval to collect saliva samples from healthy donors was granted by the Technological University Dublin Research Ethics Committee (REC ref: 15/104). Written informed consent was obtained from each donor and the study was conducted in accordance with ethical principles founded in the Declaration of Helsinki.

4.3.2 Collection of saliva samples

Saliva samples were collected by both non stimulated and stimulated techniques. In both techniques of saliva collection, all subjects were instructed to refrain from smoking, eating, drinking and tooth brushing for 1h prior to saliva collection. In each case, saliva was collected between 9:00 a.m. and 12:00 a.m., to minimise any interference of food. The participants rinsed their mouth with distilled water prior to collection for one minute, and waited five minutes before the collection commenced.

Resting drooling (minimal oral movements), known as the non stimulated collection method, was used to collect about 2 mL of whole saliva from the oral cavity of healthy volunteers from Technological University Dublin. The saliva providers were asked to sit comfortably in an upright position and tilt their heads down slightly to pool saliva in the floor of the mouth. The first expectoration was discarded to eliminate food debris and unwanted substances which may contaminate the sample and cause analytical inaccuracy. Subsequently, the samples were expectorated into a pre-labelled, sterile, 15 mL plastic container (Nalgene, Eppendorf).

Stimulated whole saliva was also collected, by asking the volunteers to chew on a tasteless piece of parafilm (5x5cm, 0.30 g; Parafilm ‘M’; American National CAL, Chicago, IL, USA). The first expectoration was discarded and the chewing-stimulated saliva was also expectorated into test tubes, every 30s for two minutes. During the saliva collection period, the subjects chewed at their natural pace.

A total number of 30 saliva samples were collected from 20 volunteers. Non stimulated saliva and stimulated saliva were both collected from each of 10 of the donors, such that stimulated and non stimulated samples from the same donors could be compared. The remaining 10 samples were collected according to the stimulated protocol from 10

different donors, such that stimulated and non stimulated samples from different donors could be compared. From each sample (donor), 10 spectra were acquired.

All salivary samples were aliquoted directly into 1 mL cryotubes and stored at -80°C, aiming to preserve the samples. They were further subjected to a freeze–thaw cycle to break down mucopolysaccharides[34], consequently reducing viscosity and minimising pipetting errors. Before spectroscopic measurement, the saliva sample was allowed to rest for around 10 minutes to completely defrost in a 4 C° refrigerator.

4.3.3 Centrifugal filtration of saliva samples

Commercially available centrifugal filtration devices, Amicon Ultra- 0.5 mL (Millipore – Merck, Germany), with cut-off points at 3 kDa, were employed in this study. Reported by Bonnier et al., the centrifugal filtration methodology was then adapted to concentre the saliva samples, as they retain constituent components only above a size of 3 kDa, allowing much of the aqueous sample pass to the filtrate[35].

As indicated by the manufacturer, the ultrafiltration membranes in Amicon® Ultra-0.5 devices "contain trace amounts of glycerine, which, as demonstrated by Bonnier *et al.*[36], can contaminate spectral analysis. Washing of the centrifugal devices prior to saliva analysis was therefore carried out by spinning the Amicon Ultra-0.5 mL once with a solution of NaOH (0.1 M) followed by two rinses with Milli-Q water (Millipore Elix S). For both washing and rinsing, 0.5 mL of the respective liquid was added to the filters and the centrifugation was applied for 30 minutes at 14000g followed by a spinning with the devices upside down at 1000 × g for two minutes in order to remove any residual solution contained in the filter.

For the sample concentration, 0.5 mL of saliva was placed in a 3K Centrifugal filtration device and centrifuged at 14 000 × g for 30 minutes. The filter devices were then placed

upside down in a new Eppendorf and spun down at 1000g for 2 minutes in order to collect the remainder of the saliva (concentrate) retained in the filter devices. The concentrating factor is of the order of 10, with a resultant concentrate volume of ~70 μL. As a result, one fraction was obtained, representing proteins/components with a molecular weight higher than 3 kDa.

4.3.4 Instrumentation

A Raman Horiba Jobin Yvon LabRam HR 800, inverted, confocal Raman spectroscopic microscope was used to record the spectra from the concentrated saliva samples. The microscope has an automated xy stage and is coupled to a Peltier cooled CCD detector. A 50 mW diode laser with 532 nm wavelength was used, with a grating of 600 grooves/mm, while the confocal hole was set at 100 μm. A 96 well-plate with glass bottom (Thermo Fisher number 1, 0.17 mm thickness) was used as substrate. For the acquisition, 10 different regions were selected randomly using a 60X objective (MPLAN N Olympus, Japan), which also collected the backscattered light. The spectra were acquired over 3 accumulations, totalling 2 minutes per spectrum. A spectral fingerprint range from 400 to 1800cm^{-1} was recorded for further analysis.

4.3.5 BCA assay

Total protein concentration of 9 randomly selected saliva samples (3 non stimulated samples and 3 stimulated samples from the same donors, and 3 stimulated samples from different donors) was estimated via the bicinchoninic acid (BCA) protein assay (Micro BCA Protein Assay Kit - Thermo Scientific) by following the instructions of the manufacturer. The BCA assay is colorimetric based, giving a dark purple colour when two molecules of BCA chelate with protein and form a compound of the cuprous ion. The absorbance of the complex was measured at 562 nm using a microplate reader (Beckman Coulter Co.). BCA standard reagents A, B and C were freshly mixed in the ratio of

25:24:1. Bovine serum albumin (2 mg/ml) was used as a standard, with 13 working standards 0.5–2000 μg/mL. All the tubes (standards, test samples, and blank) were incubated at 37°C for 2 hours. After incubation, absorbance was measured at 562 nm against a reagent blank. The concentration of test samples was measured with reference to standards for further analysis.

4.3.6 Data Analysis

Pre-processing procedures

The spectral data processing was carried out using Matlab (Mathworks, US) with the PLS-Toolbox (Eigenvector Research Inc.) and in-house algorithms. The raw Raman spectra were first smoothed using a Savitsky-Golay filter (13 points, 9th order). The baseline correction was applied using the rubberband method[37], and the spectra were vector normalised, aiming to reduce any variability caused by the fluctuation of measurement conditions or instrumental parameters.

Spectral correction method by non-negative least squares (NNLS)

To deal with possible interferences from the background that may mask important biological features, the non-negative least squares method was used to remove glass and/or water residuals in the saliva spectra. This in-house model considers the spectral data obtained as linear functions resulting from the underlying saliva components and the water background and glass substrate[38]. It aims to reconstitute a vector x that explains the observed spectra as well as possible, based on known observations. So, given the spectra obtained and a set of known observations, such as a matrix of (1) 60 glass spectra and 60 water spectra recorded from the model set samples considered in the study (see **Supplemental Figure S1**) and (2) a selection of 9 saliva components (from a pool of 11

components used to prepare artificial saliva according to the formula of Klimek *et al.*[39]), which were recorded at their maximum concentration in water (see **Supplemental Figure S2**, **Figure S3** and **Table S1**) following the same parameters of instrumentation used for saliva samples; it is possible to find a nonnegative vector that estimates the contribution of these known observations to the spectra. The known observations are then multiplied by the nonnegative vector before being subtracted from the initial spectral matrix, correcting for both the glass and water contributions in saliva samples.

This method of correction was also successfully applied for wax and glass removal in formalin fixed paraffin preserved tissues by Ibrahim *et al.*[38]. Also, a recent study has demonstrated the same versatility of the NNLS method for glass correction in oral cytological samples[40].

The formula of Klimek *et al.*[39] was designed mainly to study dental erosion in *in vitro* models. Only 9 out of 11 saliva components were recorded due to their suitable chemical properties allowing a Raman signal to be acquired. Sodium chloride and monopotassium chloride were rapidly dissociated in water affecting the Raman spectra and essentially providing a spectrum corresponding to water. As a result, the individual spectra of these components were not considered. Also, due to the inability of the mucin component to adequately represent the glycoprotein/protein content in the saliva spectrum (see **Supplemental Figure S2**), the spectrum of an extra component (IgG – solubility 50 mg/L), was also included in the unsupervised analysis (**Supplemental Figure S2**). This component was used to better understand the protein content of saliva through the analysis of the weight of each component used in NNLS, and was also used in the unsupervised analysis. Concomitantly, the spectral information of the constituents of artificial saliva was used for peak assignment in analysis the real saliva samples, where appropriate.

Statistical Analysis

The pre-processed and corrected spectra of saliva samples were initially subjected to Principal Components Analysis (PCA) to allow an unsupervised evaluation of the variability existing in the data sets itself, as well as among non stimulated saliva and stimulated saliva.

Furthermore, partial least squares discriminant analysis (PLSDA) was also used for further classification. Similar to PCA, PLSDA is a form of multivariate analysis which works as a linear classifier that aims to maximise the variance between groups and minimise the variance within groups, albeit in a supervised way. It is based on partial least squares regression (PLSR)[41]. Also, leave one patient out cross validation (LOPOCV) was applied by leaving out all the spectra from each patient (in this case, donor) in turn during the cross validation setoff the classifier. Saliva spectral datasets of both groups were mean centered to exclude any common variances.

To further evaluate the performance of the PLSDA algorithm for differentiating between the three saliva groups, receiver operating characteristic (ROC) curves were also generated. Sensitivity was calculated from the fraction of in class spectra while the specificity was calculated from the fraction of not in class spectra for a given threshold. The cross validated ROC curves follow the same method, except the class predicted when the spectra are left out during cross validation is used.

Data obtained from the BCA assay was subjected to statistical analysis (2 paired t-test) and $p<0.05$ was deemed to be significant.

4.4 Results

As the intrinsic contribution of water from each sample and possible residual contribution from the glass in the finger print region (400-1800 cm^{-1}) could interfere with the acquisition of the overall Raman spectra (**Figure 4.1**), those bands were removed using the NNLS method.

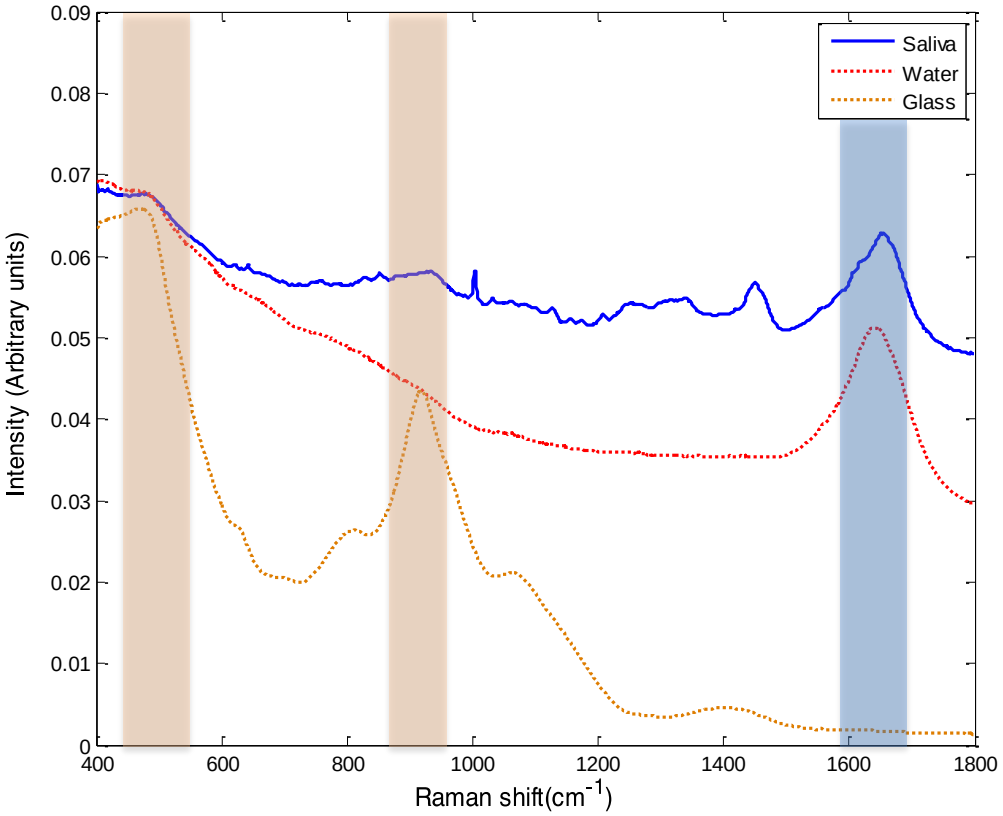

Figure 4.1: Raw Raman spectrum of a sample of saliva (blue spectrum), water spectrum (red spectrum) and glass coverslip no. 1 (orange spectrum). The blue rectangular region denotes the strong influence of water on the important protein finger-print range. The orange rectangular region denotes the possible finger-print range where there could be spectral glass contamination.

Due to the inability of mucin to account for the spectral profile in the protein regions in saliva (e.g. the Amide I region ~1500- 1800cm^{-1}) (see **Supplemental Figure 4.S5**), IgG was included along with 9 saliva components to analyse the weight of the components in different saliva groups (see Supplemental **Figure 4.S6**). The weighted sum of all components was acquired by the combination of components associated with least residual error and it was compared to each corresponding group mean spectrum.

Although the "fit" is still far from perfect, the inclusion of IgG in the spectral analysis significantly improves the correspondence, particularly in the region of the Amide I. In the non stimulated saliva samples, the least residual error showed that the component that best fit was IgG (glycoprotein) followed by mucin. In contrast, both groups of stimulated saliva samples (from same donors and different donors) had more contribution of mucin followed by IgG. These results support the use of IgG also for correction along with the other nine saliva components.

After the required pre-processing and corrections, the mean Raman spectra of the groups analysed; (i) non stimulated saliva, (ii) stimulated saliva (from the same donors as the non stimulated samples) and (iii) the second group of stimulated saliva (different donors), can be seen in **Figure 4.2**. The major vibrational assignments for all three groups, based on literature data[26,30,42,43], can be seen in **Table 4-1**. The NNLS correction model seems to confer a significant improvement, in this case, on the water and glass subtraction.

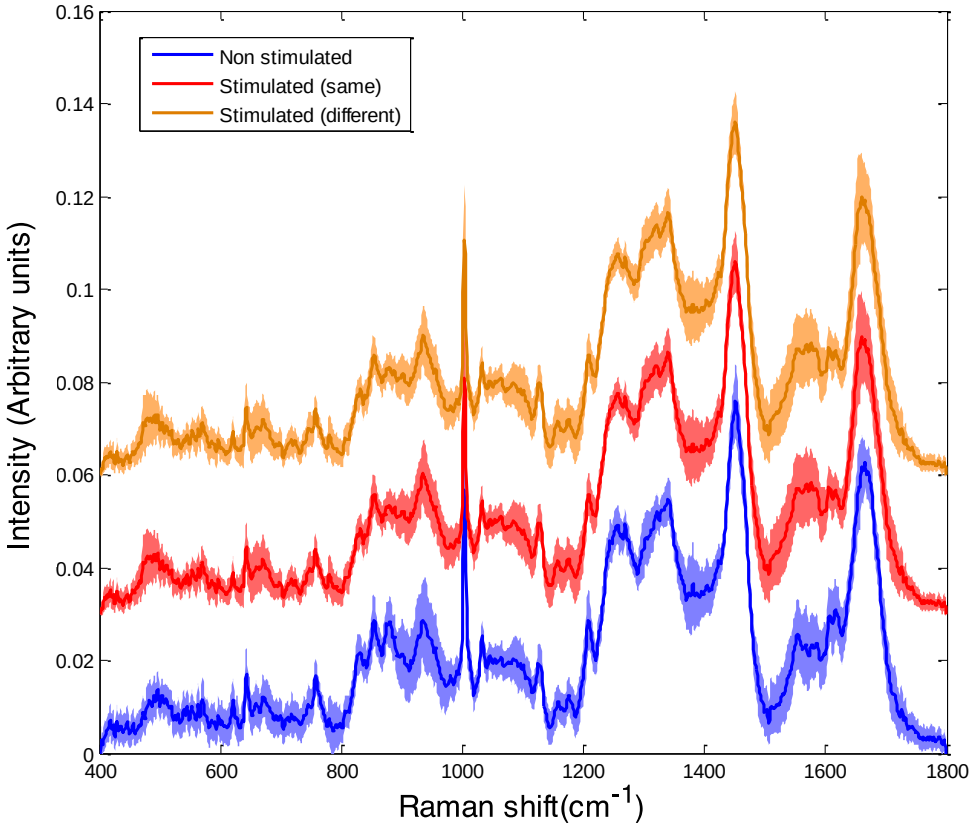

Figure 4.2: Mean Raman spectra of non stimulated saliva (blue), stimulated saliva from the same donors as non stimulated saliva (red), and stimulated saliva from different donors (orange). Spectra have been offset for clarity and the shading denotes standard deviation.

Table 4-1: Assignment of the main saliva proteins in the Raman bands to biomolecules[26,30,42,43].

Raman shift/cm^{-1}	Major assignments
502	S-S disulphide stretching band (collagen)
654	Phenylalanine
760	Tryptophan
852	Proline/tyrosine
878	Hydroxyproline
938	Proline
1003	Phenylalanine
1032	Phenylalanine
1127	C-N stretching (proteins)
1208	Tryptophan
1268	Amide III
1340	Collagen
1450	Proteins
1552	Tryptophan
1658	Amide I

Qualitative analysis

In terms of composition, it is clear that the saliva mean fingerprint from each sample set is dominated by the polypeptide backbone of protein, represented by the amide I, C-H deformation bands and aromatic ring breathing peaks at 1658 cm^{-1}, 1450 cm^{-1} and 1003cm^{-1}, respectively. Based on the current literature, these bands can be related to various glycoproteins that are known to be constituents of saliva, especially mucin matrices[43]; when correlated to the panel of saliva components recorded and available (see

Supplemental Figure 4.S2), these peaks show compatibility with spectral features of IgG and mucin, reaffirming the high presence of glycoproteins/proteins.

There are also some peaks, including those in the low wavenumber range of 400-550 cm^{-1}, that indicate the presence of saccharide. The salivary mucus is rich in mucopolysaccharides, also known as glycosaminoglycans, which can explain this possible assignment[30]. When linked to the components(present in **Supplemental Figure 4.S2**), glucose, for example, shows similar spectral features, such as peaks at 422, 448 and 520 cm^{-1}, as does mucin (as it is also a protein with agglutination properties). Furthermore, considering again the saliva components used for NNLS correction (see **Supplement Figure 4.S3**), some peaks in this range could also potentially represent some salivary electrolytes (in other words the buffer content of saliva), such as sodium phosphate (540 cm^{-1}), potassium phosphate (516 cm^{-1}) and calcium chloride (480 cm^{-1}).

Saliva is also known for its high concentration of proline-rich proteins. These type of proteins are one of the major components of the saliva from the parotid and submandibular gland in humans but mainly secreted by the submandibular gland[44]. The Raman peaks at 852 cm^{-1}, 878 cm^{-1} and 938 cm^{-1} are known to be correlated to proline presence and can also be easily assigned in the mean spectra of non stimulated saliva[30].

The bands at 760 cm^{-1}, 1032 cm^{-1}, 1208 cm^{-1} and 1340 cm^{-1} are bands related to a wide range of proteins and lipids. When compared to the panel of artificial saliva components used for correction, these peaks also show some correlation with spectral bands of IgG (glycoproteins). Furthermore, the 1127 cm^{-1} peak seems to be related to carbohydrate, very commonly found in the oral environment[30].

Unsupervised analysis of non stimulated saliva versus stimulated saliva

PCA was applied to gain more information on the differences between the non stimulated and stimulated saliva samples in general (**Figure 4.3a** and **Figure 4.3b**)

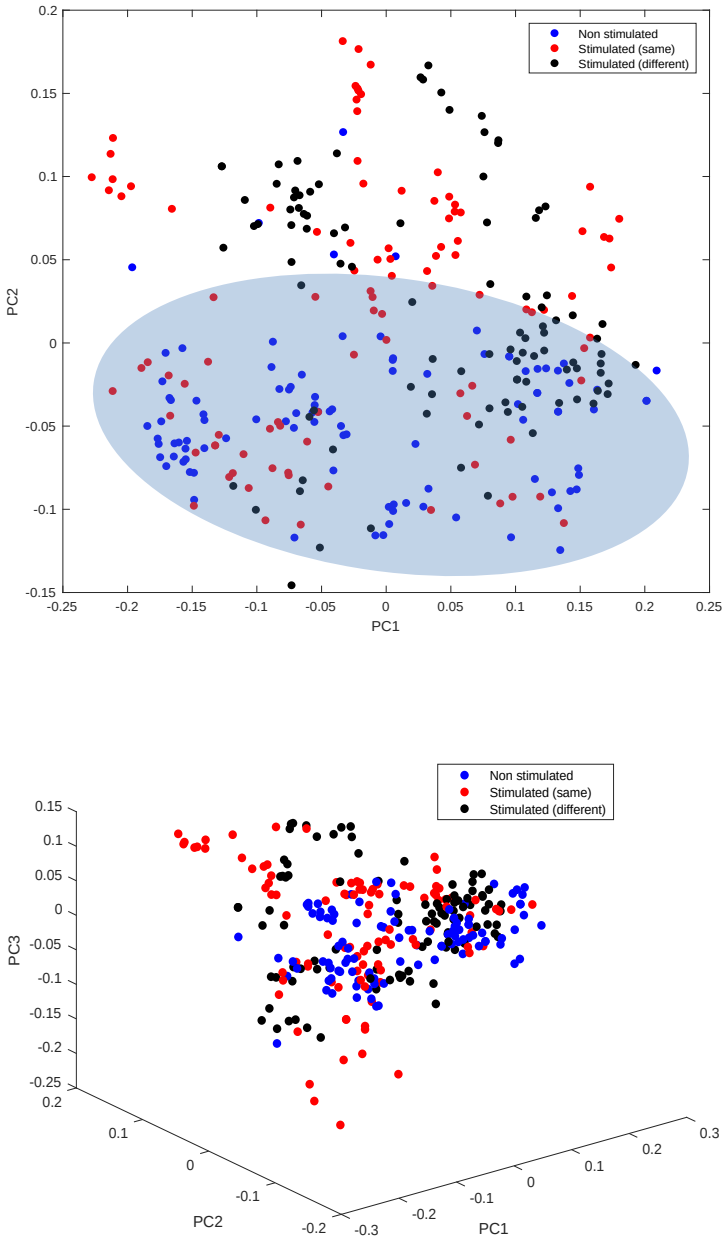

Figure 4.3: PCA of non stimulated and stimulated saliva from the same and different donors showing overlap between the groups according to PC1 in (**a**) 2D scatterplot and (**b**) 3D scatterplot. The PC2 axis shows, however, some degree of differentiation of the non stimulated saliva samples, as denoted by the blue ellipse.

PCA revealed a significant variance amongst the groups, indicating that the biochemical features of the saliva samples, either stimulated or non stimulated, from the same or different donors, leads to little or no differentiation with respect to the PC1 axis, (**Figure 4.3**). Similar behaviour can be seen in a PCA of the dataset, following NNLS correction without IgG (**Supplemental Figure 4.S2**). However, with respect to the PC2 axis, the non stimulated saliva group seems to be more tightly aggregated, showing more biochemical homogeneity (**Figure 4.3a**).

Although no clear differentiation of the sample types was achieved, the PC1 loading indicates that the variability across the samples could be correlated to protein (**Figure 4.4**), featuring prominent protein bands such as 938 cm^{-1}, 1004 cm^{-1}, 1128 cm^{-1}, 1384 cm^{-1}, 1450 cm^{-1}, 1565 cm^{-1} and 1652 cm^{-1}, mentioned previously in the qualitative analysis. The same behaviour could be seen in the PC1 loading where the NNLS correction did not include IgG (**Supplemental Figure 4.S8**).

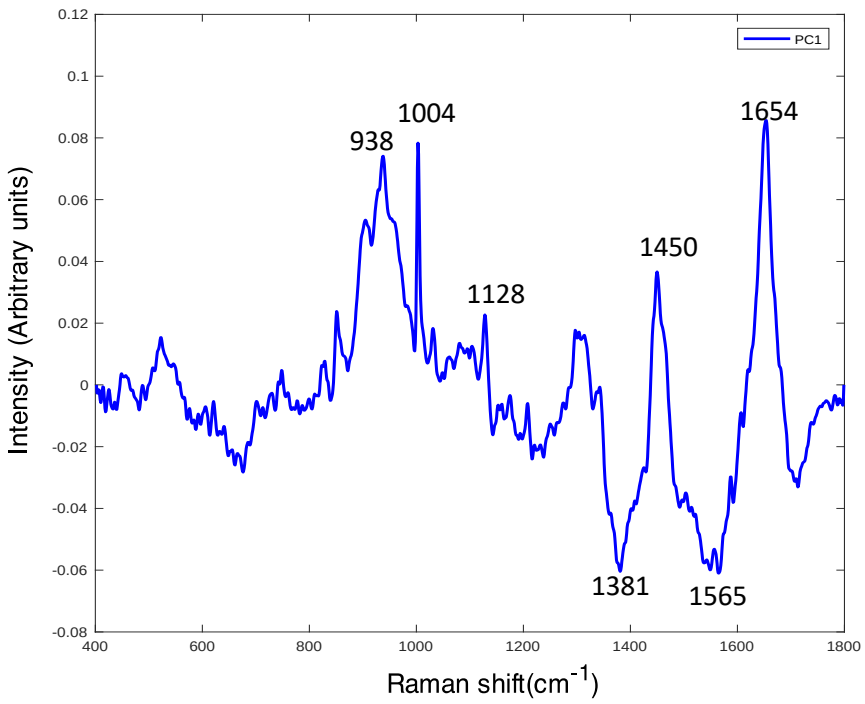

Figure 4.4: PC1 loading from PCA analysis.

The PC2 loading (**Figure 4.5**), for which a more clear differentiation of the non stimulated saliva samples was achieved, suggests that the higher intensity of the major negative peaks (1004, 1450, 1450 and 1669 cm^{-1}) could be mostly assigned to higher concentration of glycoprotein/proteins in the non stimulated saliva, directly correlated to the Raman bands of IgG from the panel of components used in the NNLS correction (see **Supplemental Figure S3**).

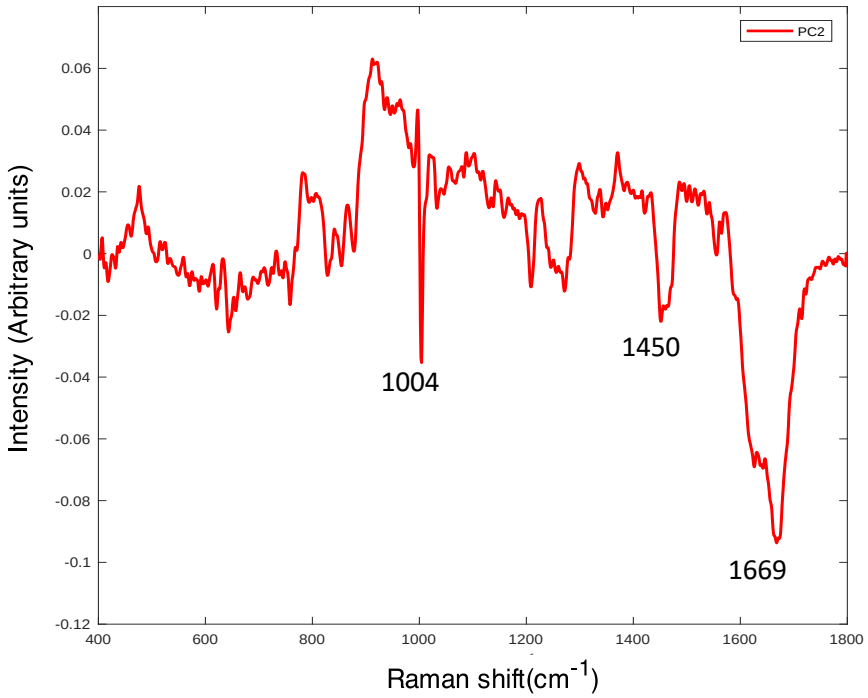

Figure 4.5: PC2 loading from PCA analysis.

The inclusion of IgG to represent the glycoprotein content of saliva samples, although it does not significantly improve the discrimination power of PCA for the stimulated saliva samples, was considered important for the classification of the non stimulated samples due not only to the improved "fit" with this component but also due to a clearer discrimination according to PC2 (**Supplemental Figure 4.S7**), and was consequently used for in the supervised analysis.

The distribution of the different groups of saliva samples in PCA (**Figure 4.3**) suggests that non stimulated saliva seems to be, in an overall analysis, biochemically distinct (negative side of PC2), while stimulated saliva might represent a "mixture" of stimulated and non stimulated, composition-wise (spread across the negative and the positive side of PC2). Notably, the mean of the distributions of stimulated and non stimulated samples in PCA are offset, with respect to PC2, and therefore it is more appropriate to compare the mean spectra of the different groups to further analyse its composition.

Stimulated and non stimulated saliva from the same donors showed very similar Raman spectral features when compared (**Figure 4.6**), apart from the spectral range around 1575 cm^{-1} (glycoprotein related). Visually comparing the mean spectrum from each group (**Figure 4.6**), all the same major peaks are displayed in both, and in general the spectra appear very similar to each other.

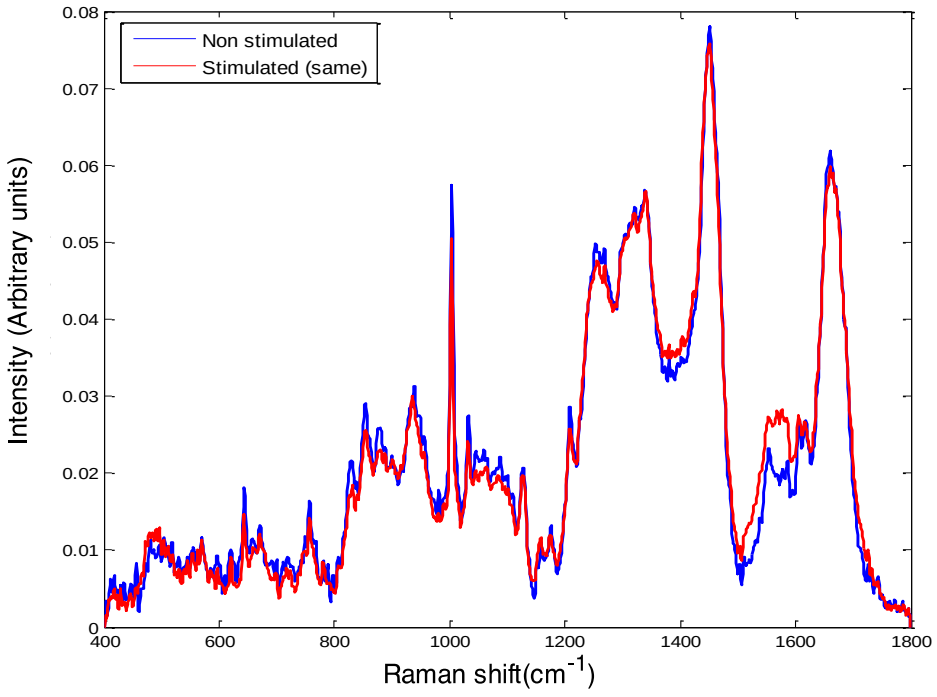

Figure 4.6: Mean spectra of non stimulated saliva and stimulated saliva from the same donors.

These differences in intensity are further confirmed when the mean spectra of the non stimulated saliva group was subtracted from the mean spectra of the stimulated saliva group (same donors) (**Figure 4.7**), showing again a higher presence of glycoproteins (1575 cm^{-1}) associated with the stimulated saliva.

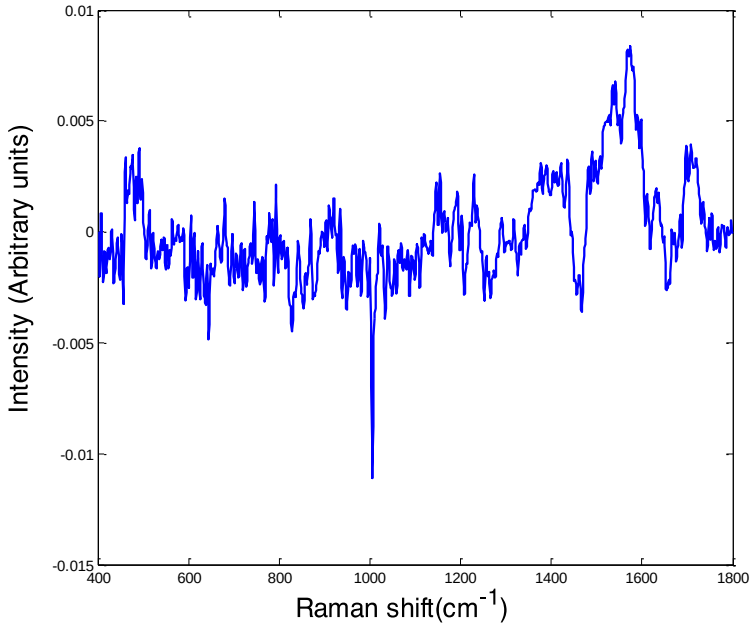

Figure 4.7: Difference spectrum of non stimulated saliva mean spectrum subtracted from stimulated (same donors) mean spectrum.

Supervised analysis of non stimulated saliva versus stimulated saliva – same donors

PLSDA, along with LOPOCV method, was subsequently utilised as a classification algorithm employed to quantitatively differentiate stimulated from non stimulated saliva from the same donors. The resultant, cross validated, probability prediction plot indicates that it is possible to classify and separate the non stimulated saliva group from the stimulated saliva group, although they come from the same donors (**Figure 4.8**). In the same way, the confusion matrix obtained (in a balanced analysis of 100 spectra collected) indicates sensitivity and specificity of 77% and 78%, respectively (**Table 4-2**).

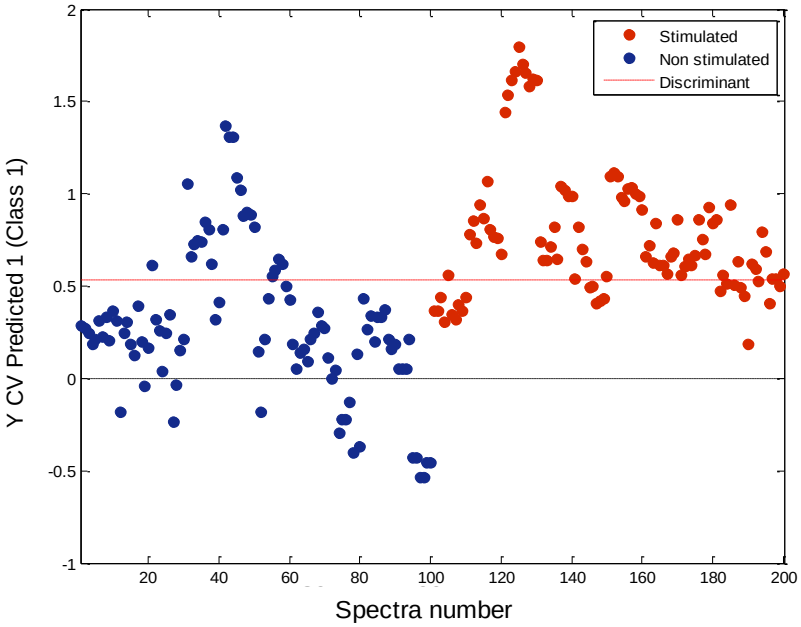

Figure 4.8: Cross validated probability prediction plot showing the discrimination between non stimulated saliva and stimulated saliva from the same donors. The discriminant (red line) is considered as the latent variable where the data best classifies.

Table 4-2: Sensitivity and specificity from PLSDA classification between non stimulated saliva and stimulated saliva from the same donors.

Sensitivity (%)	**78%**
Specificity (%)	**77%**

Based on the ROC curves (**Figure 4.9a** and **Figure 4.9b**), the classifier was able to obtain excellent discrimination between non stimulated saliva (AUC=0.844) and stimulated saliva (AUC=0.844).

a) **b)**

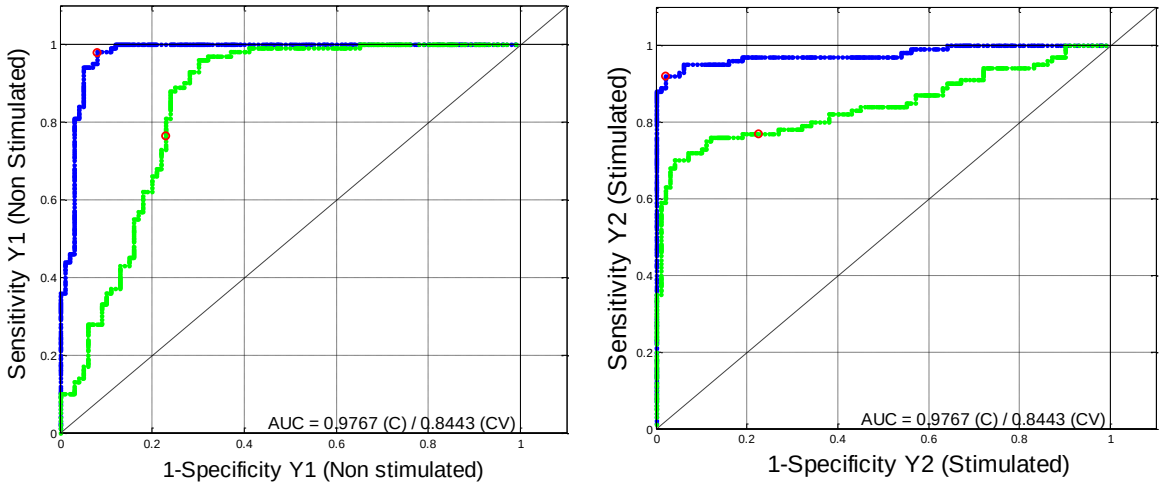

Figure 4.9: ROC curves for (**a**) non stimulated saliva samples and (**b**) stimulated saliva samples from the same donors. AUC is a measure of accuracy of the classifier, (C) is calibrated and (CV) is the cross validated AUC. The red dots represent the calculated sensitivity and 1-specificity on the y and x axis, respectively.

Supervised analysis of non stimulated saliva versus stimulated saliva – different donors

As a second approach aiming to further classify these samples, the saliva samples from different donors were compared, non stimulated saliva samples from 10 donors (used in the first analysis), and stimulated from a new group of 10 different donors. Consistent with the analysis of samples from the same donors, only the intensity of some peaks seemed to change while the general spectral appearance of the salivary profile of the non stimulated and stimulated groups continued to be very similar (**Figure 4.10**).

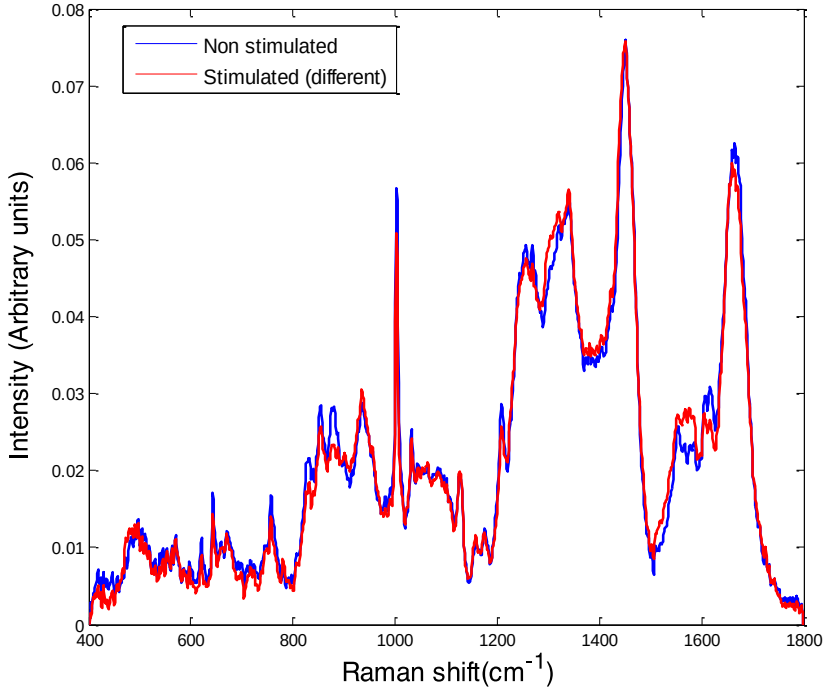

Figure 4.10: Mean spectra of non stimulated saliva and stimulated saliva from different donors.

Following the analysis with the same donors, similar differences in intensity could be further confirmed when the mean spectra of the non stimulated saliva group was subtracted from the mean spectra of the stimulated saliva group (different donors) (**Figure 4.11**), showing this time a reduced presence of proteins (1575 cm^{-1}) associated with the stimulated saliva from different donors. It is, however, important to highlight a higher intensity on proline related peak (938 cm^{-1}) associated with the non stimulated saliva.

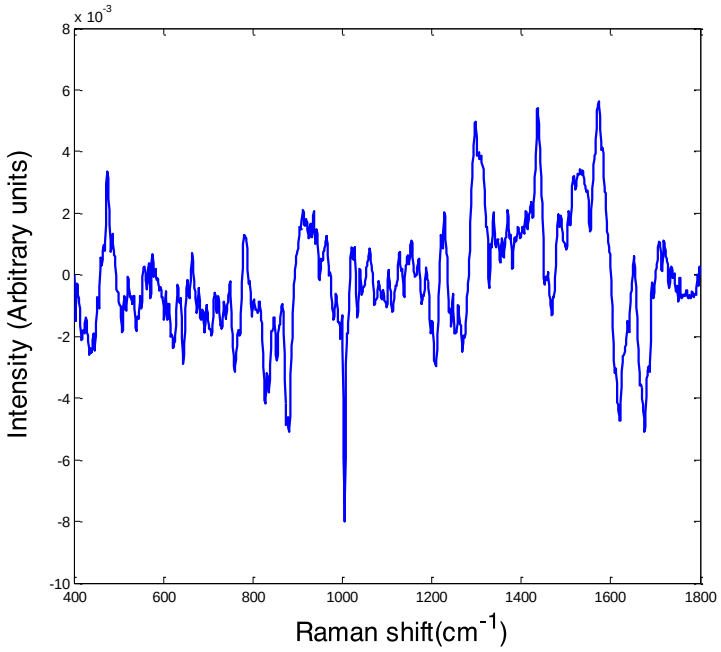

Figure 4.11: Difference spectrum of non stimulated saliva mean spectrum subtracted from stimulated (different) mean spectrum.

To further assess the accuracy of saliva spectra, spectral differences of non stimulated saliva and stimulated saliva from different donors were mean centered and also explored in detail by the PLSDA multivariate algorithm and LOPOCV. The cross validated probability prediction plot from the different donors (**Figure 4.12**) could show an efficient classification between the groups which was confirmed with sensitivity and specificity (in a balanced analysis of 100 spectra) of 88% and 86%, respectively (**Table 4-3**).

Table 4-3: Sensitivity and specificity from PLSDA classification between stimulated saliva and non timulated saliva from distinct donors.

Sensitivity (%)	**88%**
Specificity (%)	**86%**

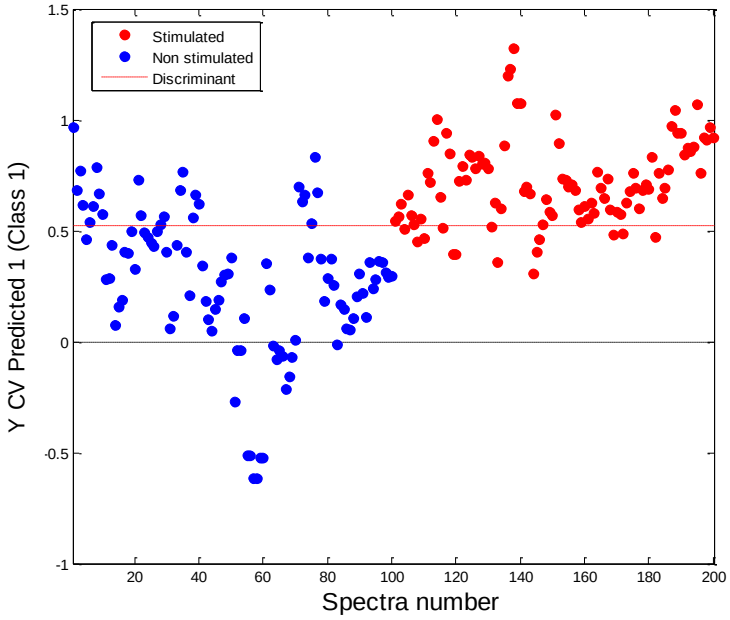

Figure 4.12: Cross validated probability prediction plot showing the discrimination between non stimulated saliva and stimulated saliva from different donors.

The ROC curve plot for the second analysis showed that the classifier had an even better accuracy (AUC=0.8550) for both classes (non stimulated and stimulated) of samples from different donors (**Figure 4.13a** and **Figure 4.13b**).

a) **b)**

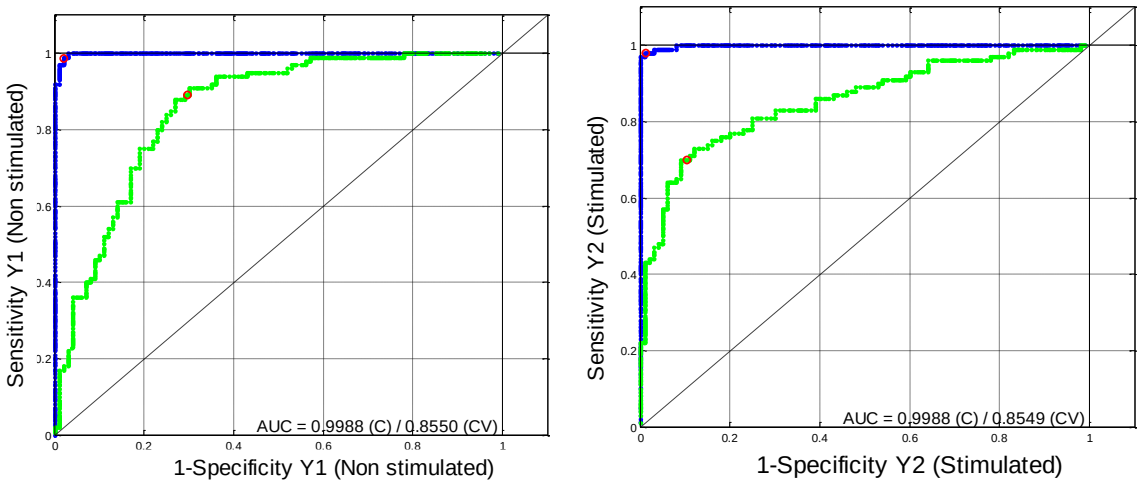

Figure 4.13: ROC curves for (**a**) non stimulated saliva samples and (**b**) stimulated saliva samples from distinct donors.

In terms of estimation of the total concentration of proteins, the BCA assay results did not show a significant difference between the non stimulated saliva samples and the stimulated saliva samples from the same donors (p = 0.584) or different donors (p = 0.370). However, the mean concentration of total proteins was slightly increased in stimulated saliva from the same donors (**Figure 4.14a)** and different donors (**Figure 4.14b**).

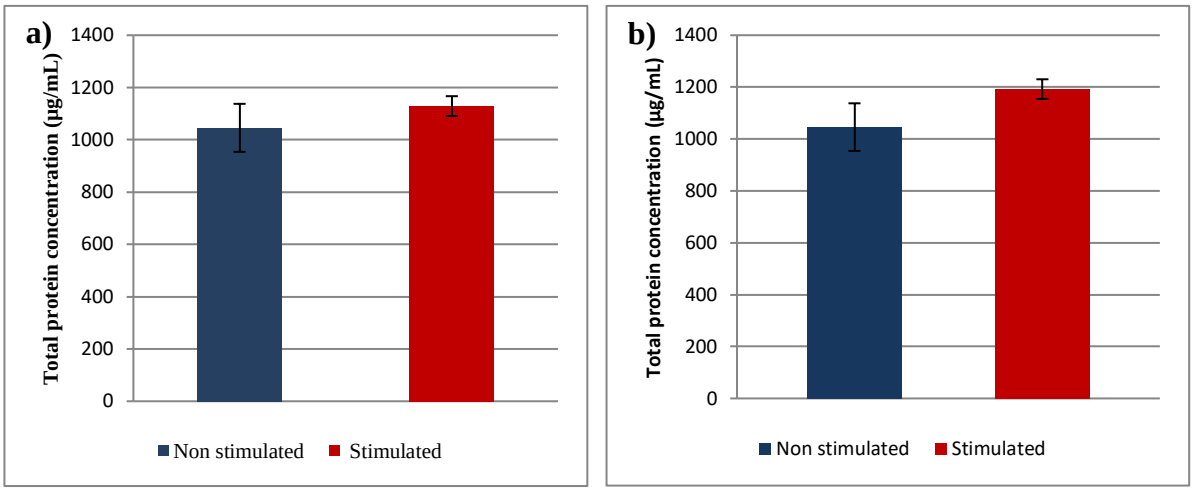

Figure 4.14: BCA assay showing the mean total protein concentration (µg/mL) and standard deviation (error bars = 95% confidence intervals) according to the different types of saliva in the same donors (**a**) and different donors (**b**).

4.5 Discussion

In the development of label free spectroscopic methodologies for potential screening of biofluids for biomedical applications, standardisation of sample collection and analysis protocols is critical. In the case of saliva, sample collection can be performed under two conditions: stimulated and non stimulated. Non stimulated saliva is collected by drooling the saliva in the mouth and draining it in a wide bore sterile vessel or by swabbing or suction methods. Stimulated whole saliva is collected by masticatory action, that is,

chewing paraffin wax or by gustatory stimulation by applying acetic acid in the mouth followed by collection of saliva[1,45].

Few reports have explored the effect of stimulation on human whole saliva composition. Most studies have focused on individual proteins under specific conditions, with the type of stimulation varying greatly. In an attempt to use non stimulated saliva to detect juvenile idiopathic arthritis, despite small divergences, no differences in the protein salivary status between patients and the control group were found[46]. Studies looking at protein changes in human saliva have typically analysed samples from individual glands, not whole saliva and many of these studies did not account for important variables, such as intra- and inter-patient differences[47]. Nevertheless, protein concentration is known to be influenced by type of stimulation, glandular source, etc [48].

Discriminating chemometrically between non stimulated whole saliva and stimulated whole saliva is an important step to confirm and standardise the applicability of Raman spectroscopy for diagnostic purposes. To the best of our knowledge, this is the first study of its kind to compare the composition of stimulated and non stimulated saliva based on the Raman spectral features as well as the individual spectral biochemical fingerprint based on an intra- and inter-patient approach.

The spectral components of saliva are complex, and have contributions from multiple constituent chemical species. For both saliva types, the spectra are dominated by water, proteins and electrolytes. These results consequently correlate with several literature sources, where the cited majority chemical components of saliva in the highest concentrations are electrolytes, mucus, antibacterial compounds, and various enzymes, and water[49-51].

As part of the preprocessing procedure, water can be removed using NNLS fitting, using spectra of constituents of a known artificial saliva formulation. It was noted however, that the combined spectra of the formulation did not account well for the protein content evident in the saliva spectra, and thus IgG was added to the mix of constituents. Also, it is important to highlight the fact that the artificial saliva formulation of Klimek *et al.*, although representing a comprehensive mixture of saliva components, might not be representative enough for the complex spectroscopic band assignment, as this formula was primarily created to see the *in vitro* effects of dental erosion[39]. This explains the need for IgG as the salivary glycoprotein representative for improvement of the spectral fit (see **Supplemental Figure 4.S5** and **4.S6**).

When comparing the two different saliva groups, the qualitative analysis (spectral composition) of non stimulated saliva and stimulated saliva initially showed that, in both the intra-patient and inter-patient approach, the mean spectra of the different saliva groups had similar features. From the intra-patient approach, these results would be expected due to the fact that each saliva sample had the same donor source, despite being collected in a different way, which would mean a minimal variation in terms of biological composition of these samples. Thus, the same behaviour would also be expected from the inter-patient analysis due to the essential components of saliva being still quite similar even when collected from different individuals[50].

Generally the intensity of some bands, as seen in the mean spectra of each group, changed, and this is understandable since the relative contribution of the chemical species in saliva will likely change with each donor and can even change within the same donor throughout the day [30]. Besides, it is important to highlight the fact that, for example, the proline band at 938 cm^{-1} had a higher intensity in the non stimulated group which could be explained by the major contribution of the submandibular gland in non stimulated samples as

compared to stimulated samples[44]. However, differences such as the higher intensity of glycoprotein related peaks, such as those at 1575 cm^{-1}, in the difference spectra of the groups can suggest that stimulated saliva also contain valuable protein contributions in its composition for possible clinical analysis.

It is already known that the average daily flow of whole saliva varies in healthy individuals between 1 and 1.5 L and the type of collection/stimulation. Percentage contributions of the different salivary glands during unstimulated flow are 20% from parotid, 65% from submandibular, 7% to 8% from sublingual, and less than 10% from numerous minor glands. Stimulated high flow rates drastically change the percentage contributions from each gland, with the parotid contributing more than 50% of total salivary secretions[52].These different contributions might be responsible for the overlapping distribution of the stimulated saliva samples with the non stimulated saliva samples in PCA.

Since the structure and composition of saliva is complex, and given that the spectral profile from different groups based on stimulation and non stimulation are very similar, it was necessary to develop a more sophisticated and robust diagnostic model based on PCA and PLSDA by utilising the entire spectrum to determine the most diagnostically significant spectral features for classification of the saliva. However, there is of course a potential for a large variety of contaminants in any saliva sample due to the eating habits of a particular donor[48], but these interferences do not appear to affect the spectroscopic signature.

In an unsupervised analysis, PCA did not provide a clear differentiation between the different saliva samples regardless of NNLS correction with IgG. However, PC1 of both analyses has shown that the slight differences in spectral profiles could be attributed to bands at 1004, 1128, 1450, 1655 cm^{-1}. As expected, these bands seem to correspond to

the bond stretching of ν_s (C-C) of phenylalanine and Amide I which could be used to identify salivary proteins[43]. These results are also consistent with contributions from mucin and IgG (glycoproteins) spectral features from the recorded components, providing confirmation of such assignments.

Furthermore, the overall spectral profile of stimulated saliva seemed to have more influence from peaks at 938, 1442-50 cm^{-1} which could be correlated to proline and lipids in comparison to non stimulated samples from different donors. These results indicate that proline-rich proteins which are found in abundance in non stimulated saliva, can be subject to inter-patient variation in salivary composition. However, a possible association with calcium chloride and urea, according to our own panel of components, may open a possibility that Raman spectroscopy was able to detect possible differences in the microbiome of stimulated saliva, as urea is a resultant component of bacterial proliferation in the oral environment; and calcium chloride (present in the acquired pellicle) could be a result of the mechanical action during collection[54].

PCA showed that stimulated saliva was quite diverse (as mixture of both stimulated and non stimulated components), whereas non stimulated saliva was more homogeneous (or pure). According to the PC2 loading, non stimulated saliva also seemed to be strongly influenced by a peak at 1669 cm^{-1}, to which amino acids could be correlated[55]. On the other hand, the difference spectra of both groups could highlight the higher concentration in other glycoproteins in stimulated saliva[52].

To further complement the Raman spectral analysis, the BCA assay results seemed to be consistent with the fact that there are no major differences in the protein concentration of the two types of saliva samples. Although not statistically significant, stimulated samples had a slightly increased protein concentration in comparison to the non stimulated samples. This result is in accordance with some variability in intensity of some protein

peaks, such as 1575 cm^{-1} seen in the difference spectrum. Ultimately, BCA results were able to confirm the rich general content of protein in saliva samples but could not differentiate the two groups based on protein concentration specifically. This could be attributed not only to the inter-patient issues but perhaps also attributed to the reduced number of samples used in this biochemical test.

Several factors may modify the salivary concentration. Thus, the composition of unstimulated saliva is different from stimulated saliva (which is more similar in composition to plasma)[56]. For example, an increase in the salivary flow rate, obtained by stimulation with acidic food, increases the concentrations of sodium, chloride and bicarbonate and decreases the concentration of salivary potassium and phosphate, compared with unstimulated saliva[57].

Stimulated saliva has certain drawbacks as the foreign substances which stimulate the saliva tend to modify the pH and the water phase of salivary secretion. However, for practical reasons, stimulated saliva samples may be preferred over non stimulated saliva samples, as these can be collected in higher volumes and considerably faster than non stimulated saliva samples or when in a clinical environment[1]. Not surprisingly, the proteomic profile of stimulated saliva samples has been reported to be diluted when compared with non stimulated saliva samples, which is why non stimulated saliva samples are preferred for proteomic analysis of saliva[58,59]. Others studies, however, have reported the salivary protein content increased with stimulated saliva samples[60].

4.6 Conclusion

The field of salivary diagnostics has undeniable translational and clinical potential. Continuing advancements in vibrational spectroscopy technologies have revealed unprecedented insights toward understanding salivary composition as part of the body's overall health. Correct interpretation and utilization of this information may be useful not only for identifying local and systemic disorders but also, perhaps, to aid in the treatment strategies.

Raman spectroscopy can be of real interest for diagnostic purposes in case of complex diseases with multiple confounding factors. This is even more the case for salivary extracts whose biochemical composition may be affected by several conditions, not only the type of collection but also comorbidities related to complex diseases.

The qualitative results show that the specificity of the Raman signature of liquid saliva samples and its potential ability to be used as an identification technique for diagnostic purposes in the future due to its reproducibility even in different conditions of collection and considering inter-patient (donor) variability.

In an unsupervised analysis, PCA was not able to differentiate the different saliva samples, showing minimal changes inherent to individual saliva composition. However, it did indicate that non stimulated saliva was significantly more biochemically homogeneous, compared to stimulated saliva.

The good sensitivity and specificity obtained by PLSDA revealed that, even with high spectral similarities correlated to the salivary composition, the classifiers could provide differentiation between the groups, mainly between non stimulated samples and stimulated samples from different donors.

With the help of a standardised collection procedure and protocol, the use of salivary samples for Raman spectroscopy can be a promising diagnostic method that can allow a novel non invasive and cost-effective approach. Also, having set guidelines standardising the procedure, as the method proposed by this study, could resolve any confounding issues between studies and alleviate some of the inherent variability among individuals and populations when using saliva samples for Raman spectroscopic clinical analysis.

References

1. Sindhu S, Jagannathan N. Saliva: A Cutting Edge in Diagnostic Procedures. Journal of Oral Diseases, 2014, 2014:1-8.

2. Castagnola M, Picciotti PM, Messana I, Fanali C, Fiorita A, Cabras T, Calo L, Pisano E, Passali GC, Iavarone F, Paludetti G, Scarano E: Potential applications of human saliva as diagnostic fluid. Acta Otorhinolaryngol Ital 2011, 31(6):347–57.

3. Cheng YS, Rees T, Wright J. A review of research on salivary biomarkers for oral cancer detection. Clin Transl Med. 2014 Feb 24;3(1):3. doi: 10.1186/2001-1326-3-3. PMID: 24564868; PMCID: PMC3945802., 3:3

4. Gonzalez-Begne M, Lu B, Han X, Hagen FK, Hand AR, Melvin JE, Yates JR. Proteomic analysis of human parotid gland exosomes by multidimensional protein identification technology (MudPIT). J Proteome Res. 2009 Mar;8(3):1304-14.

5. Buduneli N, Kinane DF. Host-derived diagnostic markers related to soft tissue destruction and bone degradation in periodontitis. J Clin Periodontol 2011;38(Suppl. 11):85–105.

6. Lee YH, Wong DT. Saliva: an emerging biofluid for early detection of diseases. Am J Dent. 2009 Aug;22(4):241-8.

7. Silvia C, Giorgia A, Rosalba G, Elio F, De Palo EF. Saliva specimen: a new laboratory tool for diagnostic and basic investigation. Clinica Chimica Acta, 2007, 383(1-2):30–40,.

8. Malamud D. Saliva as a diagnostic fluid. Dent Clin North Am. 2011 Jan;55(1):159-78. doi: 10.1016/j.cden.2010.08.004.

9. Streckfus CF, Bigler LR. Saliva as a diagnostic fluid. Oral Dis. 2002;8(2):69–76.

10. S. Hu, P. Denny, P. Denny et al., “Differentially expressed protein markers in human submandibular and sublingual secretions,” International Journal of Oncology, vol. 25, no. 5, pp. 1423–1430, 2004.

11. Chiappin S, Antonelli G, Gatti R, De Palo EF. Saliva specimen: a new laboratory tool for diagnostic and basic investigation. Clin Chim Acta. 2007 Aug;383(1-2):30-40.

12. de Almeida Pdel V, Grégio AM, Machado MA, de Lima AA, Azevedo LR. Saliva composition and functions: a comprehensive review. Contemp Dent Pract. 2008 Mar 1;9(3):72-80.

13. Tenovuo J, Lagerlöf F. Saliva. In: Thylstrup A, Fejerskov O. Textbook of clinical cariology. 2nd ed. Copenhagen: Munksgaard; 1994. 2.

14. Edgar M, Dawes C, O’Mullane D. Saliva and oral health. 3rd ed. London: BDJ Books; 2004.

15. Baker MJ, Hussain SR, Lovergne L, Untereiner V, Hughes C, Lukaszewski RA, Thiéfin G, Sockalingum GD. Developing and understanding biofluid vibrational spectroscopy: a critical review. Chem Soc Rev. 2016;45:1803–18.

16. Kuku G, Saricam M, Akhatova F, Danilushkina A, Fakhrullin R, Culha M. Surface-enhanced Raman scattering to evaluate nanomaterial cytotoxicity on living cells. Anal Chem. 2016;88: 9813–20.

17. Baker MJ, Hussain SR, Lovergne L, Untereiner V, Hughes C, Lukaszewski RA, et al. Developing and understanding biofluid vibrational spectroscopy: a critical review. Chem Soc Rev. 2016;45:1803–18.

18. Kuku G, Saricam M, Akhatova F, Danilushkina A, Fakhrullin R, Culha M. Surface-enhanced Raman scattering to evaluate nanomaterial cytotoxicity on living cells. Anal Chem. 2016;88: 9813–20.

19. Mikkonen JJ, Raittila J, Rieppo L, Lappalainen R, Kullaa AM, Myllymaa S. Fourier Transform Infrared Spectroscopy and Photoacoustic Spectroscopy for Saliva Analysis. Appl Spectrosc. 2016,70:1502-1210,

20. Derruau S Gobinet C, Mateu A, Untereiner V, Lorimier S, Piot O. Shedding light on confounding factors likely to affect salivary infrared biosignatures. Anal Bioanal Chem. 2019 Apr;411(11):2283-2290.

21. Simsek Ozek N, Zeller I, Renaud DE, Gümüş P, Nizam N, Severcan F, Buduneli N, Scott DA. Differentiation of chronic and aggressive periodontitis by FTIR spectroscopy. J Dent Res. 2016;95:1472-8.

22. Bottoni U, Tiriolo R, Pullano SA, Dastoli S, Amoruso GF, Nisticò SP, Fiorillo AS. Infrared saliva analysis of psoriatic and diabetic patients: similarities in protein components. IEEE Trans Biomed Eng. 2016;63:379-84.

23. Armenta S, Garrigues S, de la Guardia M, Brassier J, AlcalaÃÄ M, Blanco M. Analysis of ecstasy in oral fluid by ion mobility spec- trometry and infrared spectroscopy after liquid-liquid extraction. J Chromatogr A. 2015;1384:1-8.

24. Bottoni U, Tiriolo R, Pullano SA, Dastoli S, Amoruso GF, Nistico SP, et al. Infrared saliva analysis of psoriatic and diabetic patients: similarities in protein components. IEEE Trans Biomed Eng. 2016;63:379-84.

25. Gonchukov SA, Lonkina TV, Minaeva SA, Sundukov AV, Migmanov TE, Lademann J, Darvin ME and Bagratashvili VN: Confocal Raman microscopy of pathologic cells in cerebrospinal fluid. Laser Phys Lett 2014, 11(1):1-4.

26. Gonchukov SA, Sukhinina A, Bakhmutov D, Minaeva S. Raman spectroscopy of saliva as a perspective method for periodontitis diagnostics. 2012, 9(1):73-77.

27. Chen AY, Hua L, Liu JH, Cui ZJ, Jiao Y, Qu D, Guo X, Liu CW, Huang W, Wang H. IFMBE Proc. 2009,25(7):71.

28. Kah JCY, Kho KW, Lee CGL, Sheppard CJR, Shen ZX, Soo KC, Olivo MC. Early diagnosis of oral cancer based on the surface plasmon resonance of gold nanoparticles. International Journal of Nanomedicine, 2007, 2:785–798.

29. Farquharson S, Shende C, Inscore FE, Maksymiuk P, Gift A. Analysis of 5-fluorouracil in saliva using surface-enhanced Raman spectroscopy. J.Raman Spectrosc. 2005, 36(3):208-212.

30. Virkler K, Lednev IK. Forensic body fluid identification: the Raman spectroscopic signature of saliva. Analyst. 2010 Mar;135(3):512-7. doi: 10.1039/b919393f. Epub 2009 Dec 15.

31. Calado G, Behl I, Daniel A, Byrne HJ, Lyng FM. Raman spectroscopic analysis of saliva for the diagnosis of oral cancer: a systematic review. Translational Biophotonics. Accepted for publication in August/2019.

32. Fang X, Yang L, Wang W, Song T, Lee CS, DeVoe DL, et al. Comparison of electrokinetics-based multidimensional separations coupled with electrospray ionizationtandem mass spectrometry for characterization of human salivary proteins. Anal Chern. 2007 Aug 1;79(15):5785-92.

33. Walz A, Stuhler K, Wattenberg A, Hawranke E, Meyer HE, Schmalz G, et al. Proteome analysis of glandular parotid and submandibular-sublingual saliva in comparison to whole human saliva by two-dimensional gel electrophoresis. Proteomics. 2006 Mar;6(5):1631-9.

34. Mohamed R, Campbell JL, Cooper-White J, Dimeski G, Punyadeera C. The impact of saliva collection and processing methods on CRP, IgE, and Myoglobin immunoassays. Clin Transl Med. 2012;1(1):19. Published 2012 Sep 5. doi:10.1186/2001-1326-1-19

35. Bonnier F, Petitjean F, Baker MJ, Byrne HJ. Improved protocols for vibrational spectroscopic analysis of body fluids. J Biophotonics. 2014 Apr;7(3-4):167-79. doi: 10.1002/jbio.201300130.

36. Bonnier F, Baker MJ, Byrne HJ. Vibrational spectroscopic analysis of body fluids: avoiding molecular contamination using centrifugal filtration. Anal. Methods, 2014,6:5155-5160

37. Trevisan J, Angelov PP, Carmichael PL, Scott AD, Martin FL Extracting biological information with computational analysis of Fourier-transform infrared (FTIR) biospectroscopy datasets: current practices to future perspectives. Analyst. 2012 Jul 21;137(14):3202-15.

38. Ibrahim O, Maguire A, Meade AD, Flint S, Toner M, Byrne HJ, Lyng FM. Improved protocols for pre-processing Raman spectra of formalin fixed paraffin preserved tissue sections. Anal. Methods. 2017,9:4709-4717.

39. Klimek J, Hellwig E, Ahrens G. Effect of plaque on fluoride stability in the enamel after amine fluoride application in the artificial mouth. Dtsch Zahnarztl Z. 1982;10:836-40.

40. Behl I, Calado G, Ibrahim O, Malkin A, Flint S, Byrne HJ, FM Lyng. Development of methodology for Raman microspectroscopic analysis of oral exfoliated cells. Analytical Methods 2017:9(6):937-948.

41. Tobias RD. An introduction to partial least squares regression. SAS Conf Proc SAS Users Gr Int 20 (SUGI 20). 1995:2-5.

42. Movasaghi Z, Rehman S, and Rehman IU. Raman Spectroscopy ofBiological Tissues. Applied Spectroscopy Reviews 2007;42(5):493-541.

43. Feng S, Huang S, Lin D, Chen G, Xu Y, Li Y, Huang Z, Pan J, Chen R, Zeng H. Surface-enhanced Raman spectroscopy of saliva proteins for the noninvasive differentiation of benign and malignant breast tumors. Int J Nanomedicine. 2015 Jan 12;10:537-47.

44. Bennick A. Salivary proline-rich proteins. Mol Cell Biochem. 1982 Jun 11;45(2):83-99.

45. Navazesh M. Methods for collecting saliva. Annals of the New York Academy of Sciences, 1993, 694:72–77.

46. Kobus A, Kierklo A, Zalewska A, et al. Unstimulated salivary flow, pH, proteins and oral health in patients with Juvenile Idiopathic Arthritis. BMC Oral Health. 2017;17(1):94. Published 2017 Jun 2. doi:10.1186/s12903-017-0386-1

47. Benedek-Spät E. The composition of stimulated human parotid saliva. Arch Oral Biol. 1973 Sep;18(9):1091-7.

48. Humphrey SP, Williamson RT. A review of saliva: normal composition, flow, and function. J Prosthet Dent. 2001 Feb;85(2):162-9.

49. Dawes C, Jenkins GN. Stimulus effects on protein and electrolyte concentrations in parotid saliva. J. Physiol., 1964;170:86–100.

50. Streckfus CF, Dubinsky WP. A Review on Salivary Genomics and Proteomics Biomarkers in Oral CancerExpert Rev. Proteomics, 2007;4:329–332.

51. Dawes C. Circadian rhythms in human salivary flow rate and composition. J Physiol 1972;220:529–545.

52. Edgar WM. Saliva and dental health. Clinical implications of saliva: report of a consensus meeting. Br Dent J. 1990 Aug 11-25;169(3-4):96-8.

53. Walsh MC, Brennan L, Malthouse JP, Roche HM, Gibney MJ. Effect of acute dietary standardisation on the urinary, plasma, and salivary metabolomic profiles of healthy humans. Am. J. Clin. Nutr., 2006, 84:531-539.

54. Gomar-Vercher S, Simón-Soro A, Montiel-Company JM, Almerich-Silla JM, Mira A. Stimulated and unstimulated saliva samples have significantly different bacterial profiles. PLoS One. 2018;13(6):e0198021.

55. Byrne H, Sockalingum, G, Stone N. Raman Spectroscopy: Complement or Competitor? In Moss, D. (ed.) Biomedical Applications of Synchrotron Infrared Microspectroscopy. Royal Society of Chemistry, RCS Analytical Spectroscopy Monographs, 2011, 11:105-142. doi:10.1039/9781849731997-00105

56. Loo JA, Yan W, Ramachandran P, Wong DT. Comparative human salivary and plasma proteomes. J Dent Res. 2010;89 (10):1016–1023. doi:10.1177/0022034510380414

57. Jensdottir T, Nauntofte B, Buchwald C, Bardow A. Effects of sucking acidic candy on whole-mouth saliva composition. Caries Res. 2005;39: 468–74.

58. Yakob M, Fuentes L, Wang MB, Abemayor E, Wong DT. Salivary biomarkers for detection of oral squamous cell carcinoma current state and recent advances. Curr Oral Health Rep 2014;1:133-41.

59. Schafer CA, Schafer JJ, Yakob M, Lima P, Camargo P, Wong DT. Saliva diagnostics: utilizing oral fluids to determine health status. Monogr Oral Sci 2014; 24:88-98.

60. Nayak A, Carpenter GH. A physiological model of tea-induced astringency. Physiol Behav. 2008 Oct 20;95(3):290-4. doi: 10.1016/j.physbeh.2008.05.023. Epub 2008 Jun 5.

Chapter 4: Supplemental

Supplemental 1

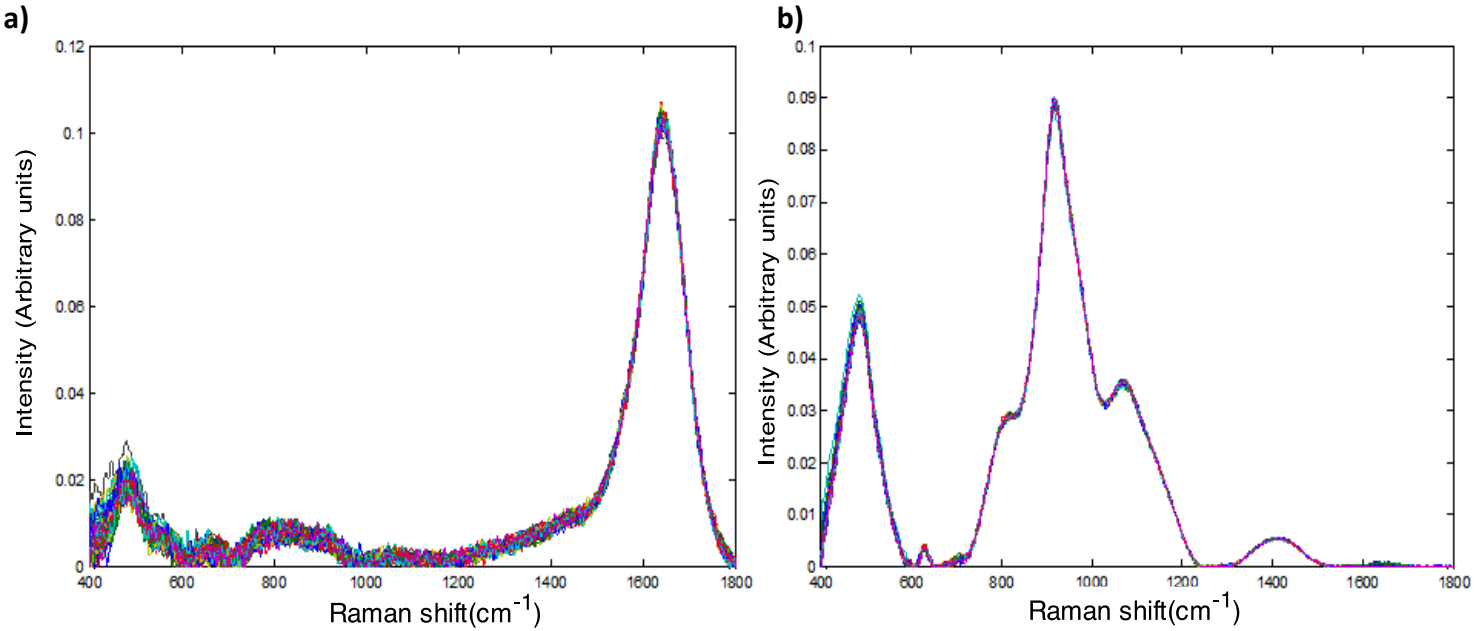

Figure 4.S1: 60 Pre-processed spectra of ultrapure water **(a)** and glass coverslip no. 1 **(b)** for NNLS correction

Supplemental 2 (part 1)

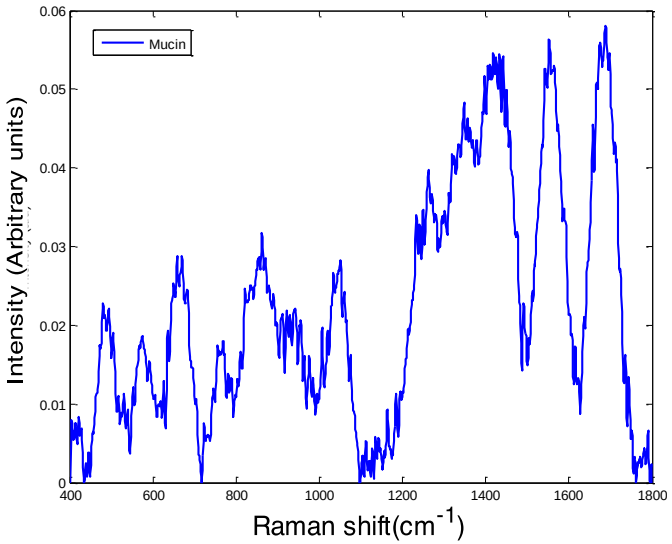

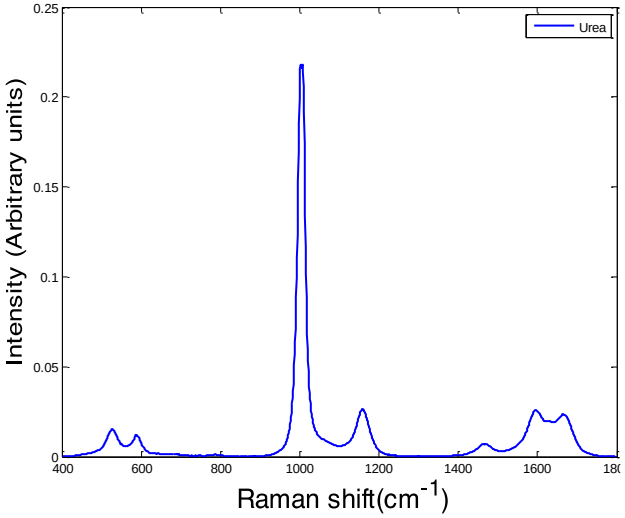

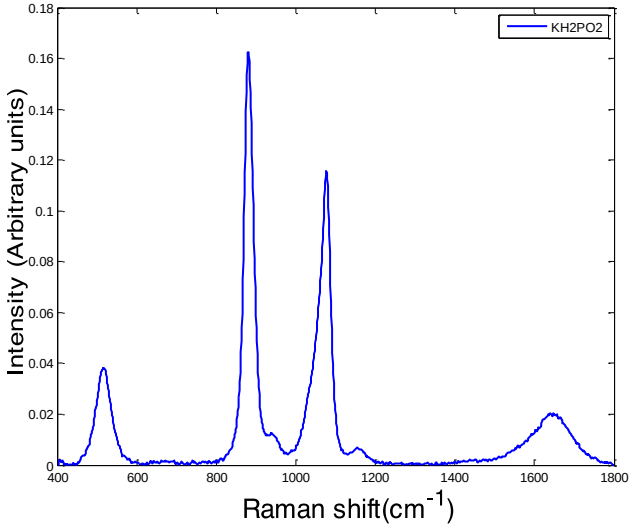

Supplemental 2 (part 2)

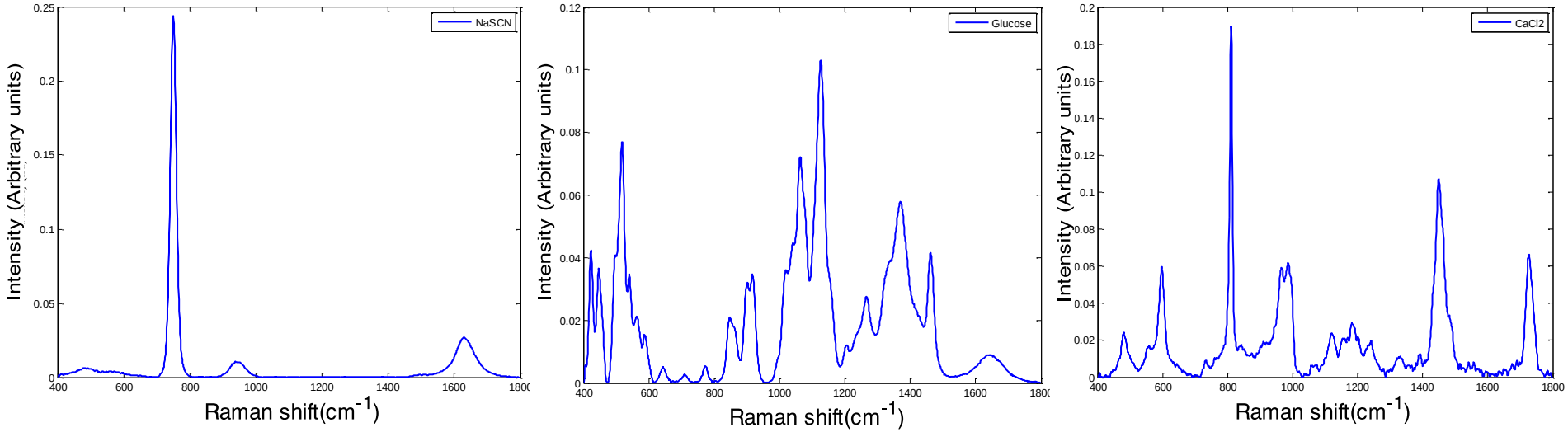

Supplemental 2 (part 3)

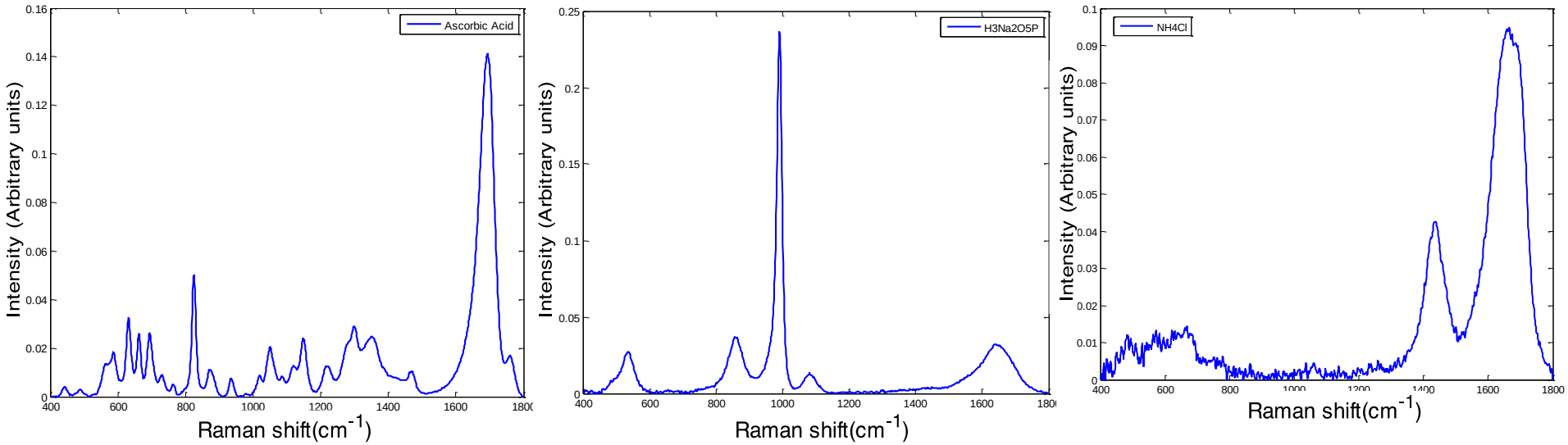

Supplemental 2 (part 4)

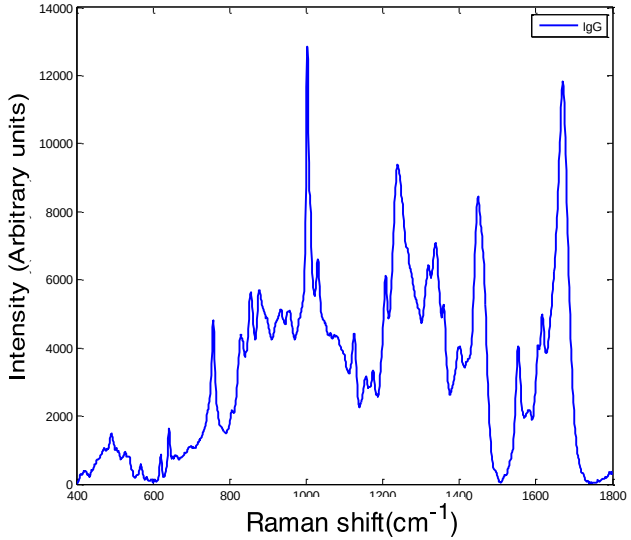

Figure 4.S2: 9 artificial saliva components according to the formula of Klimek *et al.*[39] recorded individually plus IgG.

Supplemental 3

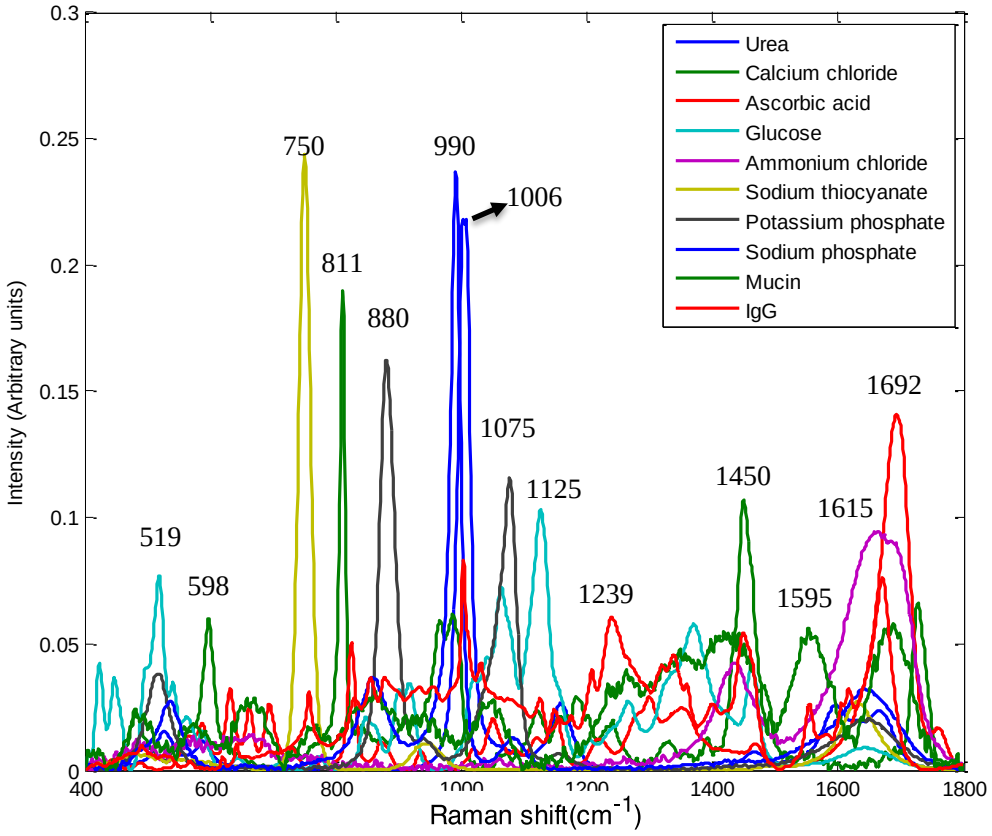

Figure 4.S3: Raman spectra from 9 saliva components plus IgG used as reference for NNLS correction for water and glass and selected bands used for reference in the mathematical correction process.

Supplemental 4

Table 4-S1: Saliva components used as reference for NNLS correction for water and glass and the maximum solubility of each component in water according to the supplier (Sigma Aldrich).

Saliva Components	Maximum solubility indicated by the supplier (at room temperature)
Urea	1 g/mL
Calcium chloride	219.1 g/L
Ascorbic Acid	176 g/L
Glucose	133 mg/mL
Ammonium chloride	100 mg/mL
Sodium thiocyanate	1,000 g/L
Monopotassium phosphate	22.6 g/100 mL
Disodium phosphate	7.7 g/100 ml
Mucin	20 mg/mL

Supplemental 5

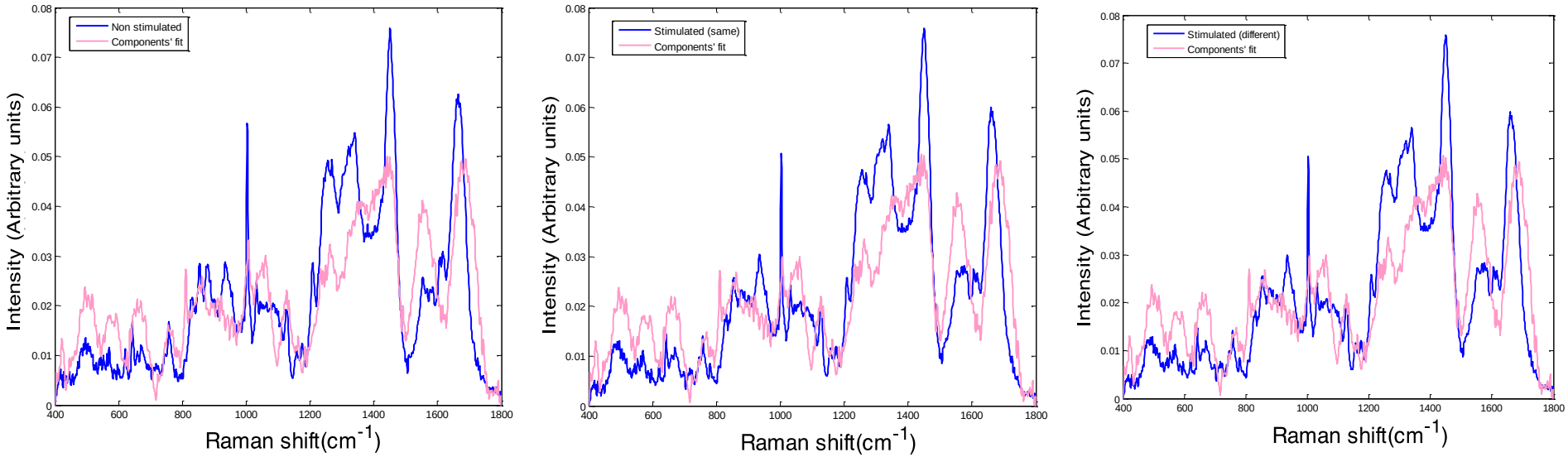

Figure 4.S5: Non stimulated mean spectrum and spectrum of the weighted components without IgG (components' fit) after NNLS correction (**a**); stimulated (same donors) mean spectrum and spectrum of the weighted components (components' fit) after NNLS correction (**b**); and stimulated (different donors) mean spectrum and spectrum of the weighted components (components' fit) after NNLS correction (**c**).

Supplemental 6

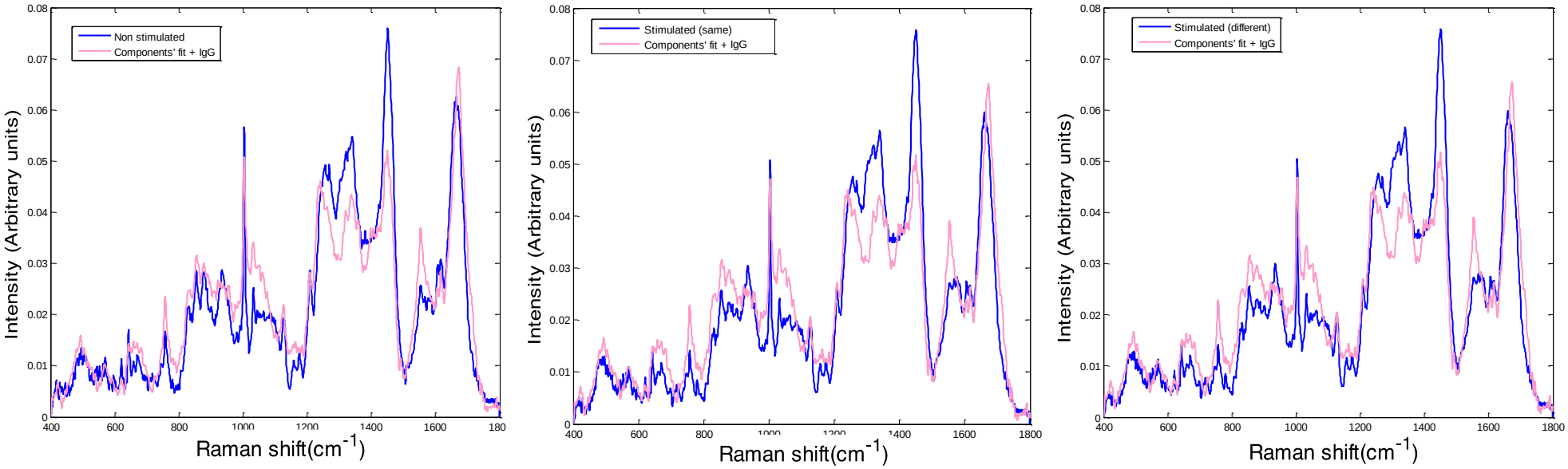

Figure 4.S6: Non stimulated mean spectrum and spectrum of the weighted components including IgG (components' fit) after NNLS correction (**a**); stimulated (same donors) mean spectrum and spectrum of the weighted components including IgG (components' fit) after NNLS correction (**b**); and stimulated (different donors) mean spectrum and spectrum of the weighted components plus IgG (components' fit) after NNLS correction (**c**).

Supplemental 7

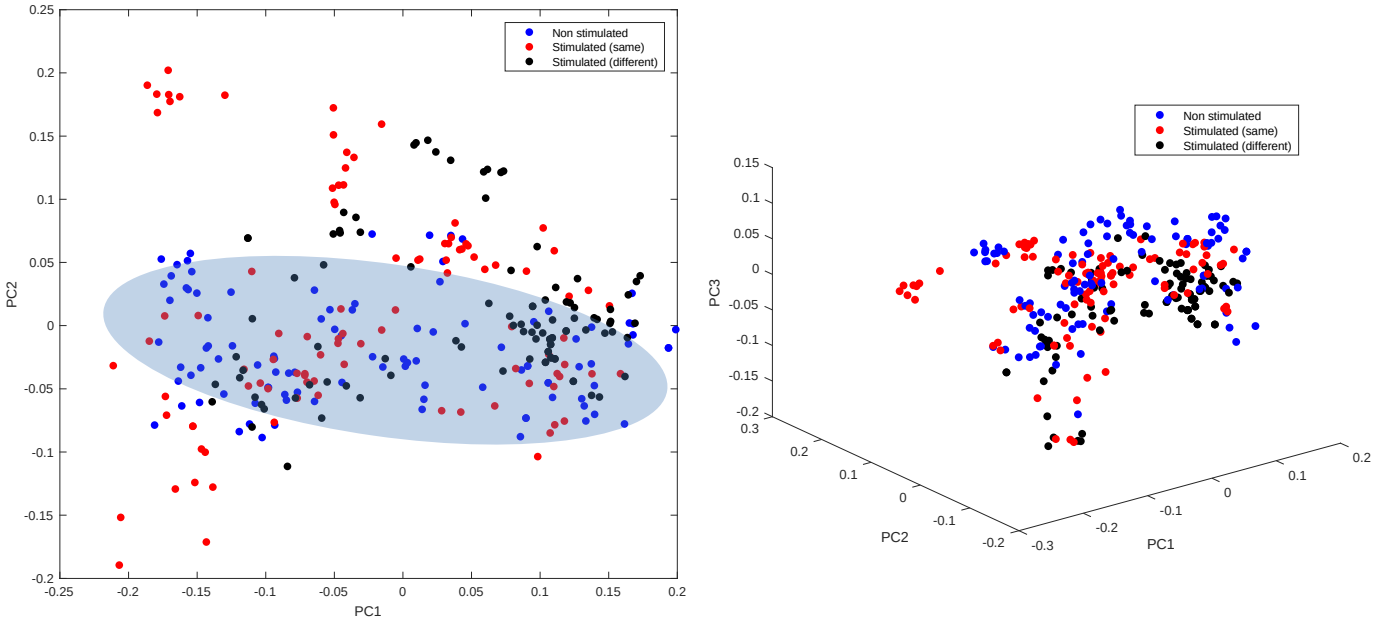

Figure 4.S7: PCA of non stimulated and stimulated saliva from same (**a**) and different donors (without IgG) showing general misclassification and, consequently, non-differentiation, by PC1 perspective. 3D plot corroborates the misclassification (**b**). PC2 axis shows, however, sort of differentiation of non stimulated saliva samples, as denotes the blue ellipse.

Supplemental 8

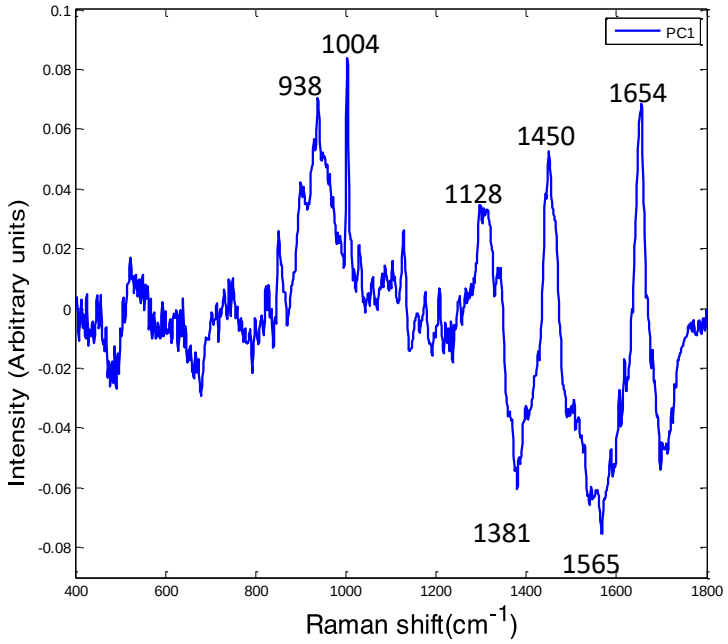

Figure 4.S8: PC1 loading from analysis without IgG.

Chapter 5: Raman spectroscopy for identification of potential malignant oral lesions and oral squamous cell carcinoma through saliva analysis

5.1 Introduction

It is undeniable that oral squamous cell carcinoma (OSCC) causes significant rates of mortality and morbidity in patients diagnosed with this type of tumour, especially when discovered late in the course of the disease onset and/or progression. In a clinical context, OSCC can be considered in terms of a "natural history", which originates from non-aberrant keratinocytes which are chronically exposed to a stimulus that disrupts their homeostasis, leading to epithelial hyperplasia, dysplasia of different degrees, carcinoma in situ (CIS) and ultimately invasive carcinoma, which can give rise to the generation of remote metastases[1], with the consequent clinical manifestations.

The 2005, the World Health Organisation defined a three-tier classification system of epithelial dysplasia grades of potential malignant oral lesions (PMOL) as mild, moderate and severe[2]. This is based on the architectural and cytological alterations, whereby, in mild dysplasia, the architectural disturbances, with cytological atypia, are present only in the lower third of the epithelium. In moderate dysplasia, the criteria stipulate that architectural disturbance extends into the middle third of the epithelium, but the degree of cytological atypia may require upgrading the classification to "severe dysplasia". In severe dysplasia, architectural disturbances are observed in greater than two thirds of the epithelium, with cytological atypia which now can also include CIS, characterised by full thickness or almost full thickness of epithelial architectural disturbance in the viable cell layers accompanied by pronounced cytological atypia[2,3].

More recently, in an attempt to simplify the clinical application of this grading system, the Working Group coordinated by the WHO Collaborating Centre for Oral Cancer also recommended a 2-tier classification of low risk (hyperplasia and mild dysplasia) and high risk (moderate, severe and CIS)[4]. Thus, in the more recent evolution of the WHO grading system (2017), features of "squamous hyperplasia (acanthosis and basal cell hyperplasia)" and "CIS", considered in the 2005 WHO classification, have been removed from the oral epithelial dysplasia grading[5]. The term CIS is now used synonymously with severe dysplasia. Some cytological/cellular features in the 2005 WHO classification have been dropped, while others have now been included in the new classification. For example, the "increase in nuclear size" has been dropped, while the architectural feature "loss of epithelial cell cohesion" has been included in 2017 WHO diagnostic criteria[6]. However, the biological significance of this system needs to be validated in longitudinal studies to explore its value in the prediction of malignant transformation risk of oral epithelial dysplasia.

The grading for oral epithelial dysplasia (PMOLs with histopathological epithelial dysplasia present), has always been considered one of the most ill-defined and unfocused fields in oral and maxillofacial pathology and, unfortunately, the new WHO grading does not seem to improve this scenario[6]. Added to this, the histopathological classification as such is prone to inter- and intra-observer errors and, in some situations, the progression of dysplasia is not a linear process, so the degree of dysplasia attributed is not necessarily a predictor for malignant transformation[7]. Furthermore, although it is accepted that PMOLs are statistically more likely to progress to cancer, the actual mechanisms are still poorly understood and it is not inevitable that a dysplastic lesion will progress to cancer. Hence, there are still no clear molecular markers which enable us to distinguish lesions that may progress from those that will not[7].

From a diagnostic perspective, researchers postulate that blood-derived molecules could potentially influence the molecular constituency of oral fluids[8,9,10]. This suggests that circulating biomarkers absorbed by the salivary glands may possibly alter the biochemical composition of saliva. Consequently, whole saliva may contain complex but characteristic molecular information capable of communicating an individual's current state of health[11].

Based on the results obtained from healthy volunteers to differentiate the two types of saliva collection in Chapter 4, Raman spectroscopy may be able to integrally analyse saliva, giving a faithful and distinct biochemical profile and be used to clinically screen and diagnose OSCC and PMOL. This chapter explores the use of Raman spectroscopy to discriminate between mild, moderate and severe dysplasia as well as high and low dysplasia grades based on the spectral profile of saliva samples through partial least squares discriminant analysis (PLSDA) for possible clinical application of this technique in the near future.

5.2 Methodology

5.2.1 Ethics and volunteer questionnaire

Ethical approval to collect saliva samples from healthy donors was granted by the Dublin Institute of Technology (now Technological University Dublin) Research Ethics Committee (REC ref: 15/104) (**Appendix I**), as mentioned in chapter 4. A medical and oral health status questionnaire was also used to obtain further information regarding biological factors that could potentially influence the analysis (**Appendix II**). Some of the data will be further exploited in chapter 6, to better understand the influence of individual/clinical factors, such as smoking and alcohol consumption.

Ethical approval was also obtained from the St James' Hospital/Dublin Dental University Hospital Research Ethics Committee to collect saliva samples from patients with histopathologically diagnosed PMOL/OSCC (REC ref: 2013/23/05) (**Appendix III**). Written informed consent was obtained from each donor and the study was conducted in accordance with ethical principles founded in the Declaration of Helsinki.

5.2.2 Collection of saliva samples

Due to the practicality of the method in the clinical environment and the results obtained in chapter 4, stimulated saliva collection was the methodology of choice for patient samples. Stimulated whole saliva was collected, pre-processed, stored and concentrated following the same procedures elucidated in *Stimulated saliva collection* in chapter 4 (section 4.3.2).

In total, saliva samples of 45 patients were collected and included; of which 18 were mild oral epithelial dysplasia, 17 moderate oral epithelial dysplasia, 6 severe oral epithelial dysplasia/carcinoma *in situ* and 4 invasive OSCC (**Table 5-1**). To counter-balance the study, 45 saliva samples from healthy volunteers (controls) were collected (**Table 5-2**). The average age for the patients was 63 ±12.8 years while that of the controls was 34 ± 10.49 years. Regarding gender, 46.66% (n=21) of the patients were female and 53.33% (n=24) were male, while 33.33% (n=15) of the healthy volunteers were male and 66.66% (n=30) were female.

Table 5-1: Information on patients' clinical profile.

Patient	Gender	Age	Histopathological diagnosis
1	F	54	Moderate dysplasia
2	M	62	Moderate dysplasia
3	M	70	Moderate dysplasia
4	M	65	Moderate dysplasia
5	F	68	Mild dysplasia
6	F	72	OSCC
7	F	71	Moderate dysplasia
8	F	91	OSCC
9	F	50	CIS
10	F	59	Mild dysplasia
11	F	56	Mild dysplasia
12	F	65	Moderate dysplasia
13	F	49	Moderate dysplasia
14	M	63	Moderate dysplasia
15	M	63	OSCC
16	M	73	Mild dysplasia
17	F	70	Mild dysplasia
18	M	77	Mild dysplasia
19	M	80	Mild dysplasia
20	F	40	Mild dysplasia
21	F	48	Mild dysplasia
22	M	80	Moderate dysplasia
23	M	35	Moderate dysplasia
24	F	72	CIS
25	F	70	Severe dysplasia
26	M	55	Mild dysplasia
27	F	73	Mild dysplasia
28	M	74	Mild dysplasia
29	F	34	Severe dysplasia
30	M	73	Mild dysplasia
31	F	67	Mild dysplasia
32	M	69	Mild dysplasia
33	F	64	Moderate dysplasia
34	M	62	Mild dysplasia
35	M	45	Moderate dysplasia
36	M	61	Severe dysplasia
37	F	86	Moderate dysplasia
38	M	66	Moderate dysplasia
39	M	58	Moderate dysplasia
40	M	71	Moderate dysplasia
41	M	52	OSCC
42	M	49	Moderate dysplasia
43	M	61	Severe dysplasia
44	F	60	Mild dysplasia
45	M	63	Mild dysplasia

Table 5-2: Relevant information on healthy volunteers.

Healthy volunteers (controls)	Gender	Age
1	M	30
2	F	27
3	F	39
4	F	35
5	M	27
6	F	38
7	F	27
8	F	29
9	M	34
10	F	27
11	F	32
12	M	31
13	F	32
14	F	32
15	F	38
16	F	27
17	M	33
18	F	41
19	F	29
20	F	50
21	M	28
22	M	34
23	F	40
24	F	31
25	M	70
26	M	32
27	F	56
28	F	35
29	F	26
30	M	27
31	F	26
32	M	30
33	F	27
34	M	30
35	F	63
36	M	32
37	F	29
38	M	65
39	F	25
40	F	25
41	F	32
42	F	26
43	F	27
44	M	29
45	F	32

5.2.3 BCA assay

Total protein concentration of stimulated saliva samples of 9 patients (3 mild, 3 moderate and 3 severe/CIS) was estimated by the bicinchoninic acid (BCA) protein assay (Micro BCA Protein Assay Kit - Thermo Scientific). This assay was performed as described in section 4.3.5 in chapter 4.

5.2.4 Instrumentation

Following the methodology proposed in chapter 3, a confocal Raman Horiba Jobin Yvon LabRam HR 800 Raman (inverted) microspectroscope was used to record the spectra from the concentrated saliva samples from patients and healthy volunteers. The instrument and setup properties, and substrate choice, were applied as described in section 4.3.4 in chapter 4. For every sample, 10 different random regions (within the sample area) were spectrally recorded such that the depth (z axis) was kept constant, as explained in chapter 3.

5.2.5 Data Analysis

The data analysis was carried out using Matlab (Mathworks, US) with the PLS-Toolbox (Eigenvector Research Inc.) and in-house algorithms. The spectral preprocessing and correction steps have been described in *Pre-processing procedures* section 4.3.6 in chapter 4.

In the same way as the data analysis of chapter 4, PLSDA with leave one patient out cross validation (LOPOCV) was used to build the classifier and discriminate the samples according to dysplasia grade and/or presence of malignancy.

Similar to chapter 4, ROC curves were also graphed for each class tested. The accuracy was measured by the area under the curve (AUC), so the closer the curve towards the left

and the border, the more accurate the classifier. Conversely, the close to its diagonal (baseline), the higher the misclassification rate and the lower the accuracy.

The data obtained from the BCA assay was subjected to 2 paired t-test to compare values across two groups, or one-way analysis of variance (ANOVA) to compare values across three groups (with Tukey post hoc, if needed). $p<0.05$ was deemed to be significant.

5.3 Results

Analysis of saliva samples from healthy volunteers and from patients with PMOL and OSCC

The mean spectra from saliva of the healthy volunteers and of the patients with mild, moderate, severe (which also includes CIS) oral epithelial dysplasia and OSCC, as expected, appeared to be very similar (**Figure 5.1**), demonstrating the need for more sophisticated multivariate analysis techniques, such as PLSDA, to discriminate the presence of different dysplasia grades and the presence of OSCC or not.

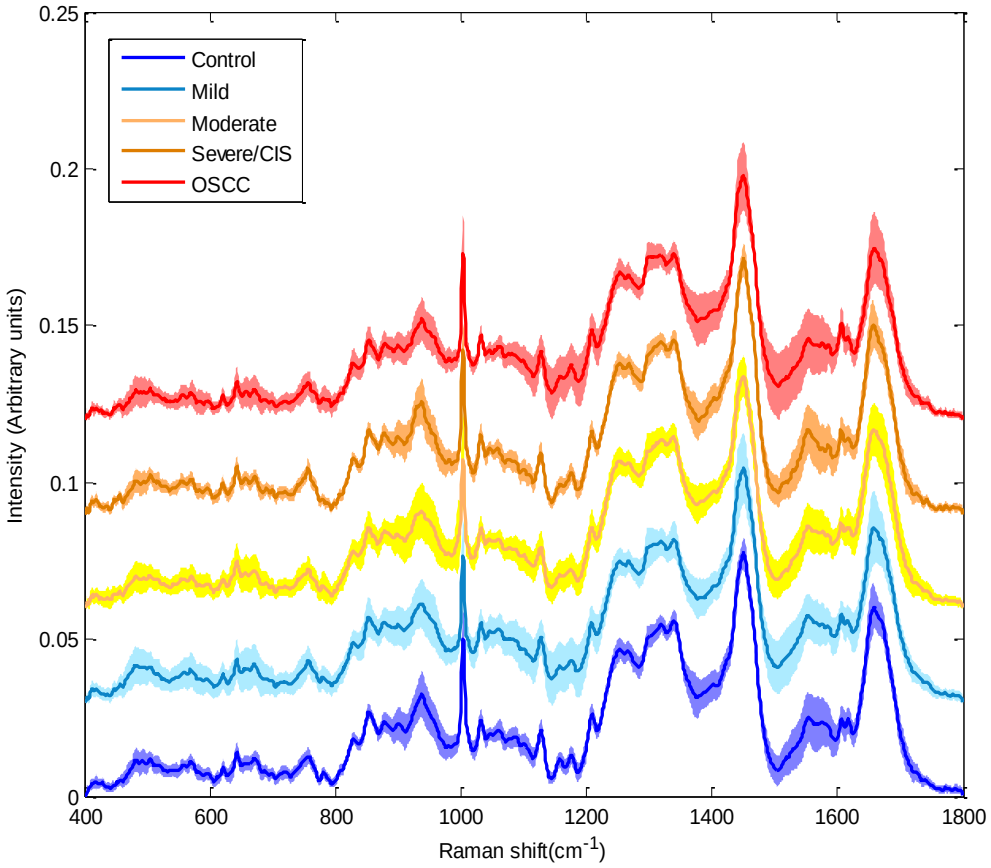

Figure 5.1: Mean Raman spectra of control, mild, moderate, severe oral epithelial dysplasia and OSCC. The spectra have been off set for clarity and shading denotes standard deviation.

Firstly, to detect the presence or not of dysplasia, a general model involving the entire dataset (450 spectra from healthy volunteers and 450 spectra from patients, which included PMOLs and OSCC) was created. The results from the PLSDA classification show a very good discrimination based on the two classes assigned, as seen through the cross validated probability predicted plot (**Figure 5.2**). This was further ratified by the sensitivity and specificity of the classifier (**Table 5-3**).

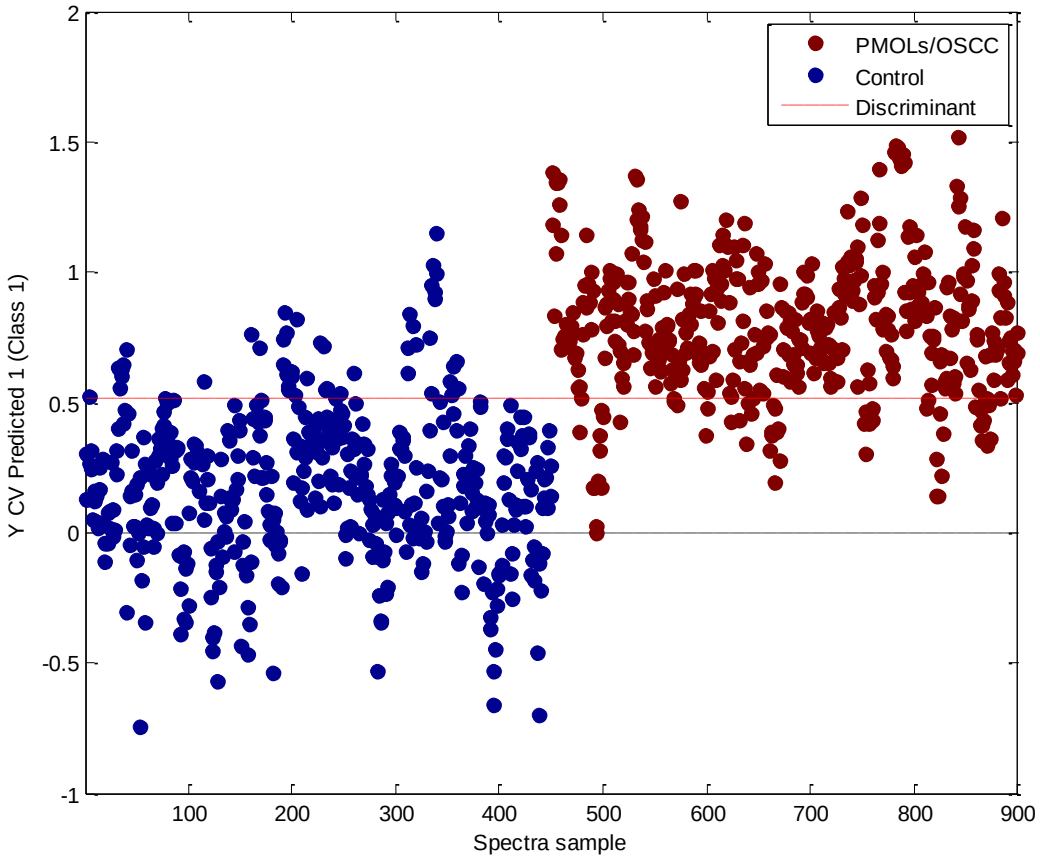

Figure 5.2: Cross validated probability prediction plot showing the discrimination between the control group and the PMOLs/OSCC group.

Table 5-3: Sensitivity and specificity from PLSDA classification between control group and PMOLs/OSCC group.

Sensitivity (%)	**86%**
Specificity (%)	**89%**

In an attempt to better understand the classification obtained, the cross validated probability prediction plot was then patient-coloured to identify any possible clinical correlation to the misclassification (outliers) present (**Figure 5.3**). In this perspective,

mild dysplasia samples that were clinically regressing after biopsy or removal of aetiological factors (such as smoking/alcohol consumption) and one sample of mild epithelial dysplasia from semi-labial mucosa seemed to be the reason for misclassification towards the controls.

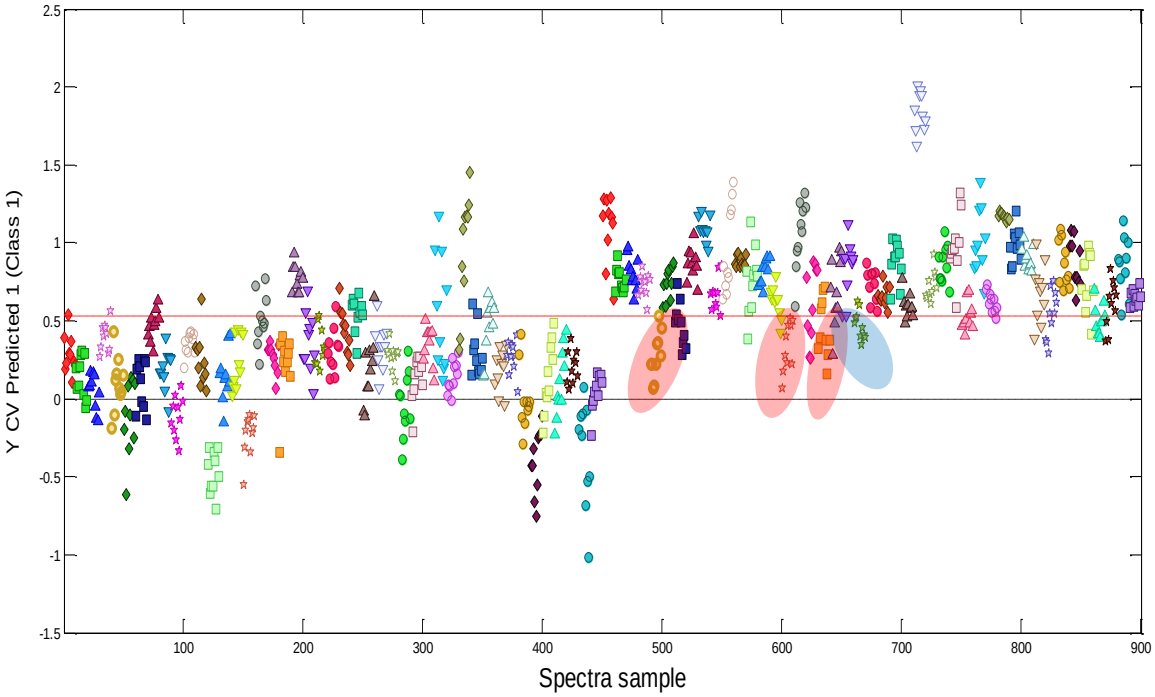

Figure 5.3: Cross validated probability prediction plot showing the discrimination between the control group and the PMOLs/OSCC group coloured by sample. Red ellipse denotes mild dysplasia samples that were clinically regressing after biopsy and/or removal of aetiological factors. Blue ellipse denotes one sample of mild epithelial dysplasia located in semi-labial mucosa.

The results from the ROC curves reveal an excellent degree of accuracy (AUC=0.9211) for discrimination of both groups by the classifier (**Figure 5.4**).

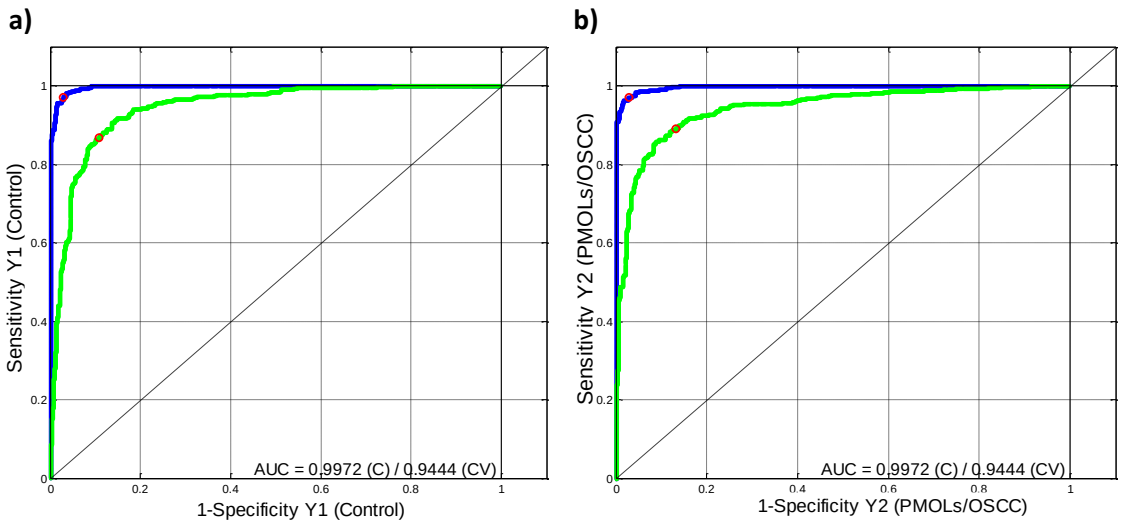

Figure 5.4: ROC curves for (**a**) control group and (**b**) PMOLs /OSCC group from Raman analysis of saliva samples.

To better evaluate the factors responsible for the discrimination between the different classes, the latent variable (LV-1), responsible for 24.70% of the variance, was plotted (**Figure 5.5**). Positive peaks, mostly correlated to oral dysplasia in general, were observed at 938 (proline rich proteins[12]), 1004, 1450 and 1655 cm^{-1} (proteins and glycoproteins[13]). The major bands on the negative of LV-1 were observed to be at 1375 and 1342 cm^{-1} (amino acids/acetates[13]).

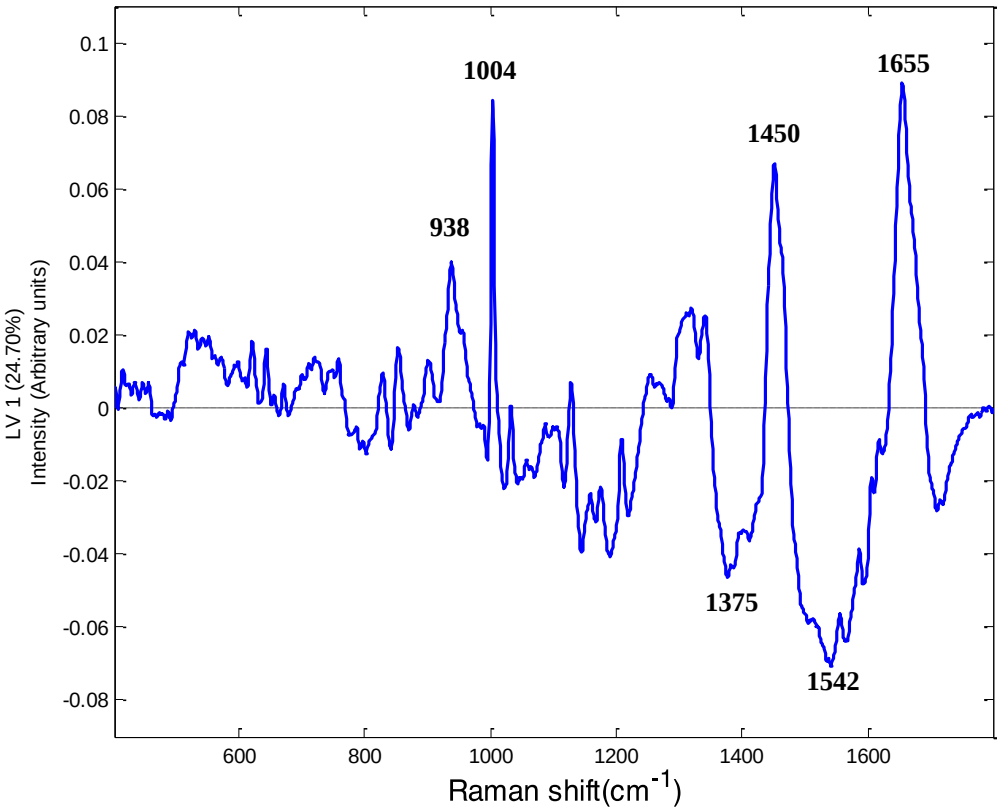

Figure 5.5: LV-1 of PLSDA model which included control group and oral dysplasia/OSCC group.

Although not statistically significant (p = 0.1537), the BCA assay showed an increase in total protein concentration in the oral dysplasia/OSCC group in general when compared to the control group, complementing the results from the Raman analysis (**Figure 5.6**).

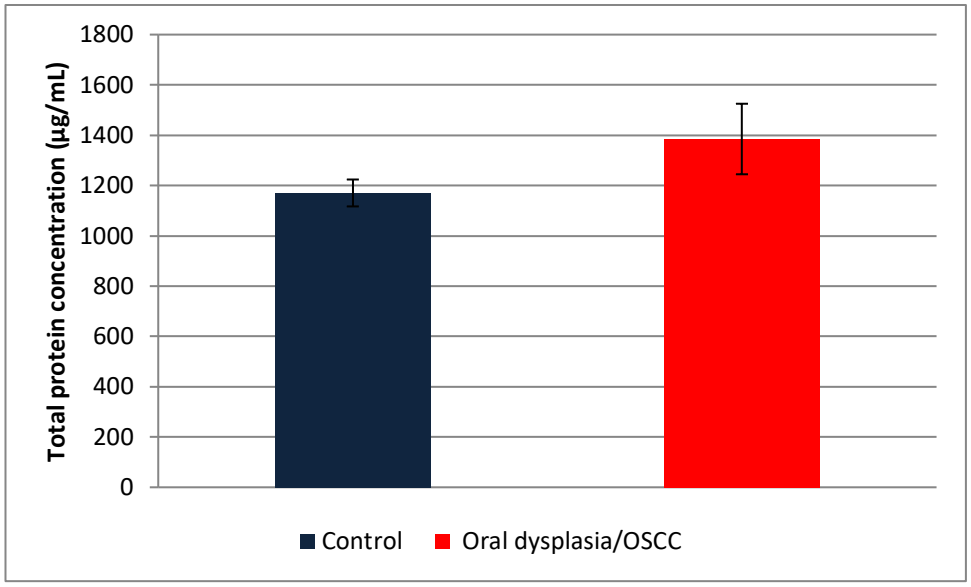

Figure 5.6: BCA assay showing the mean total protein concentration (µg/mL) and standard deviation (error bars = 95% confidence intervals) of saliva samples from the control group and from the oral dysplasia/OSCC group.

Aiming to better analyse the capability of discrimination of the classifier, four extra models were created to better visualise the differentiations between the control group and the different dysplasia grades or OSCC.

The model dedicated to discriminating control saliva samples (n=45) from mild dysplasia saliva samples (n=18), exhibited the same trend of differentiation as the general model. The cross validated probability predicted plot (**Figure 5.7a**) showed a noticeable differentiation, while the differentiating LV-1 (**Figure 5.7b**) exhibited primarily the same features as that of the general model. The ROC curves (**Figure 5.8a** and **Figure 5.8b**) complemented those results by showing a good accuracy (AUC=0.8348) for both groups obtaining also a very good specificity, although a substantially reduced sensitivity of 63% (**Table 5-4**).

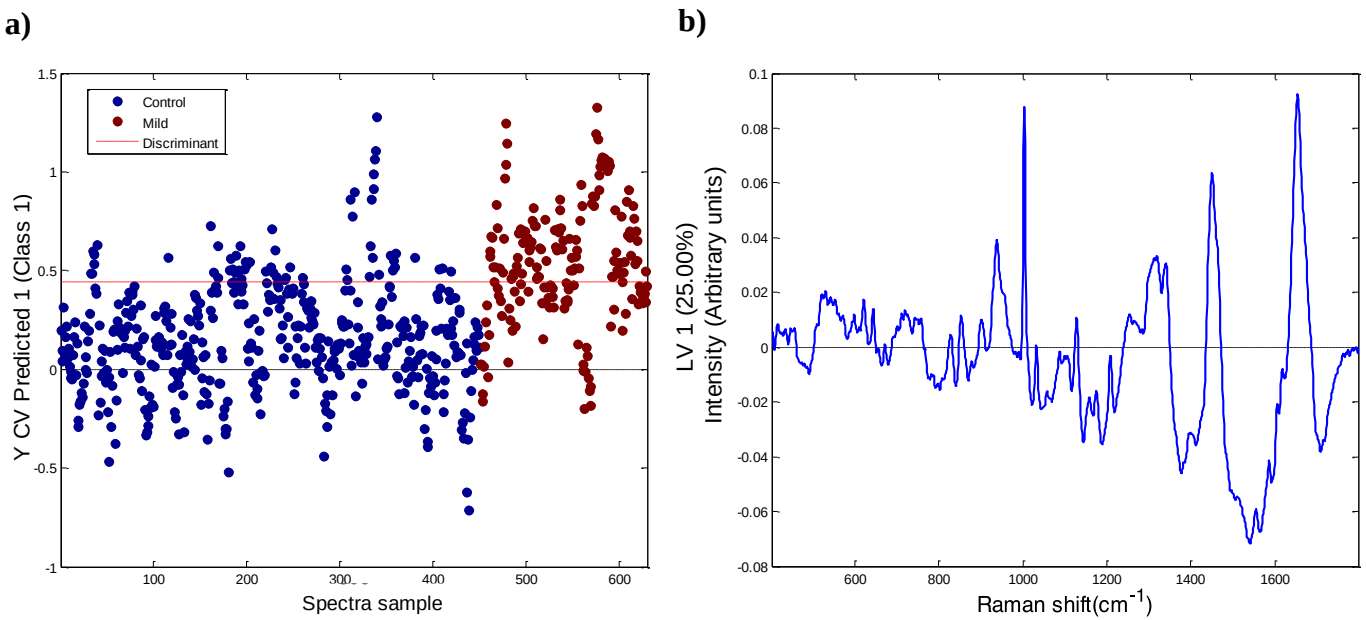

Figure 5.7: Plot of the (**a**) cross validated probability prediction and (**b**) PLSDA LV-1 showing the discrimination between the control group (n=45) and the mild epithelial dysplasia group (n=18).

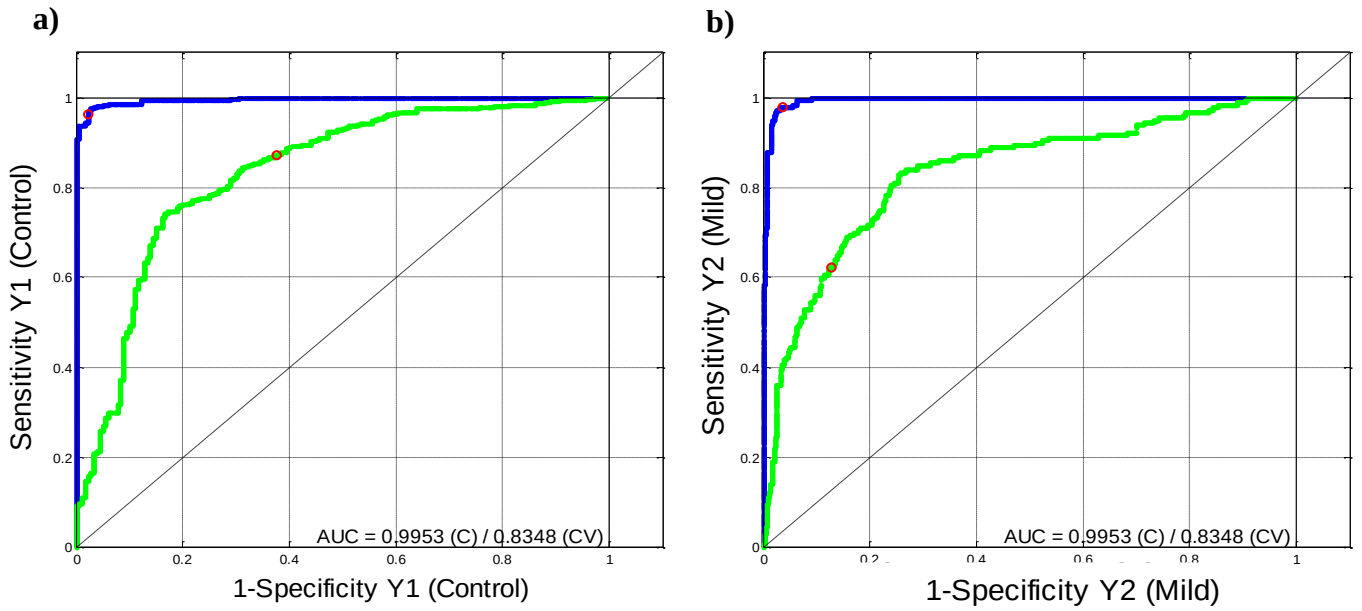

Figure 5.8: ROC curves of the control group (n=45) (**a**) and the mild epithelial dysplasia group (n=18) (**b**).

Table 5-4: Sensitivity and specificity from PLSDA classification between the control group and the mild dysplasia group.

Sensitivity (%)	**63%**
Specificity (%)	**87%**

The second model was designed to differentiate the control group (n=45) from the moderate epithelial dysplasia group (n=17). Once more, PLSDA could provide good specificity, albeit with a low sensitivity (**Table 5-5**). The cross validated probability prediction plot (**Figure 5.9a**) shows similar differentiation, based on the same LV-1 characteristics cited before (**Figure 5.9c**), with the exception of the peak at 1000 cm^{-1}. Also, the ROC curves (**Figure 5.10a** and **Figure 5.10b**) showed good accuracy (AUC=0.72690) for both classes.

Table 5.5: Sensitivity and specificity from PLSDA classification between the control group and the moderate dysplasia group.

Sensitivity (%)	**58%**
Specificity (%)	**78%**

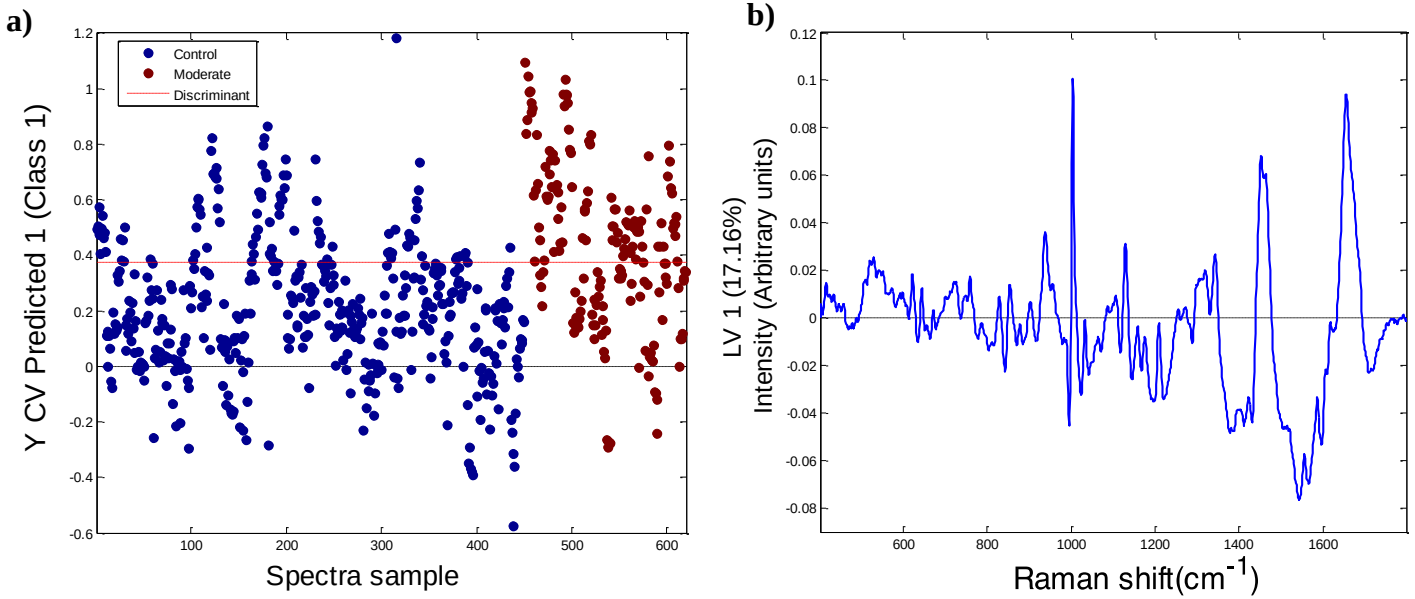

Figure 5.9: Plot of the (**a**) cross validated probability prediction and (**b**) PLSDA LV-1 showing the discrimination between control group (n=45) and the moderate epithelial dysplasia group (n=17).

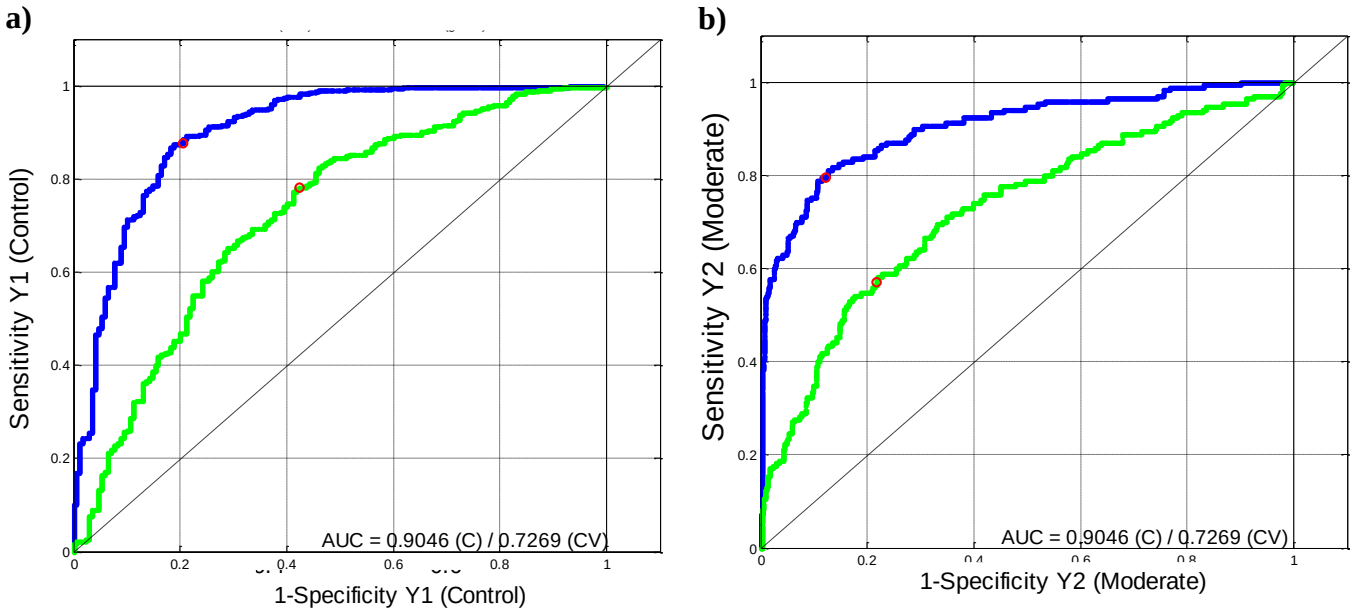

Figure 5.10: ROC curves of the control group (n=45) (**a**) and the moderate epithelial dysplasia group (n=17) (**b**).

When differentiating the control group (n=45) from the severe dysplasia group (n=6), PLSDA resulted in relatively poor discrimination, that can be seen by the cross validated probability prediction plot (**Figure 5.11a**) and good specificity (**Table 5-6**). However, LV-1 (**Figure 5.11b**), responsible for 21.53% of the variance, showed the same bands as those found in the lower grade dysplasia groups, including the peaks at 783 (nucleic acid/surgar[13,14]), 1382 (amino acids), 1557 and 1707 cm^{-1} (acetates/amino acids[14]). Furthermore, the ROC curve (**Figure 5.12a** and **Figure 5.12b**) still showed excellent discriminant power of the classifier, albeit with a poor sensitivity of 59%.

Table 5-6: Sensitivity and specificity from PLSDA classification between the control group and the severe dysplasia group.

Sensitivity (%)	**59%**
Specificity (%)	**83%**

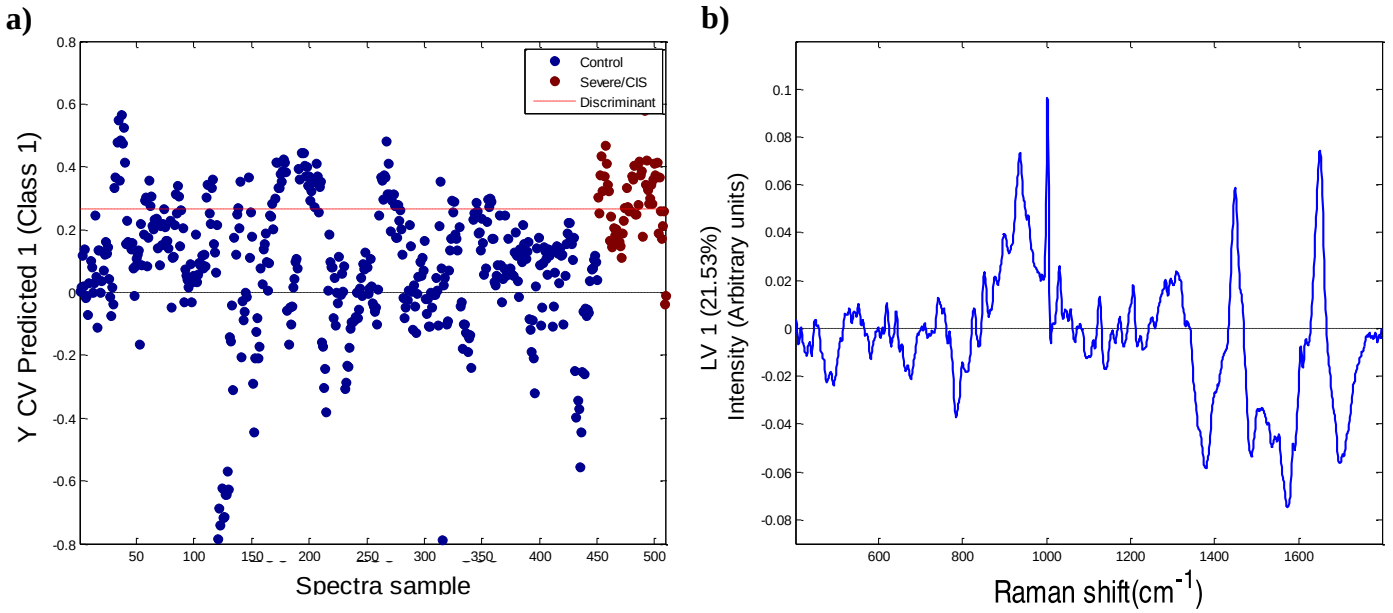

Figure 5.11: Plot of the (**a**) cross validated probability prediction and (**b**) PLSDA LV-1 showing the discrimination between the control group (n=45) and the severe epithelial dysplasia group (n=6).

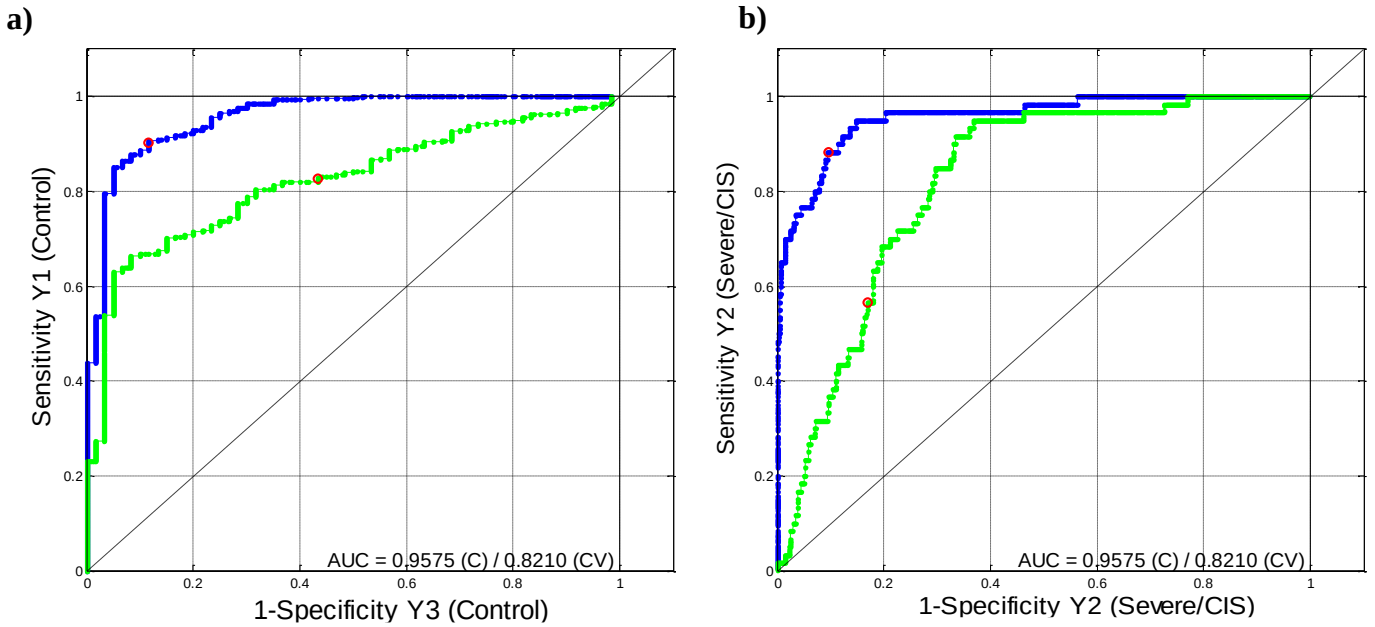

Figure 5.12: ROC curves of the control group (n=45) (**a**) and the severe epithelial dysplasia group (n=6) (**b**)

Finally, the PLSDA results from the discrimination between control (n=45) and OSCC (n=4) showed no visible separation in the cross validated probability prediction plot (**Figure 5.13a**). The LV-1 (**Figure 5.13b**), responsible for 16.01% of variance, showed a similar pattern to the LVs of the previous models, with major intensity differences, this time, on the negative side and a higher influence of the peak 671 cm^{-1} (nucleic acid/sugars[13]) on the positive side. However, the ROC curves (**Figure 5.14a** and **Figure 5.14b**) still showed good accuracy (AUC=0.7133) for both classes and the specificity was high, although the sensitivity was low (**Table 5-7**).

Table 5-7: Sensitivity and specificity from PLSDA classification between the control group and the OSCC group.

Sensitivity (%)	**50%**
Specificity (%)	**88%**

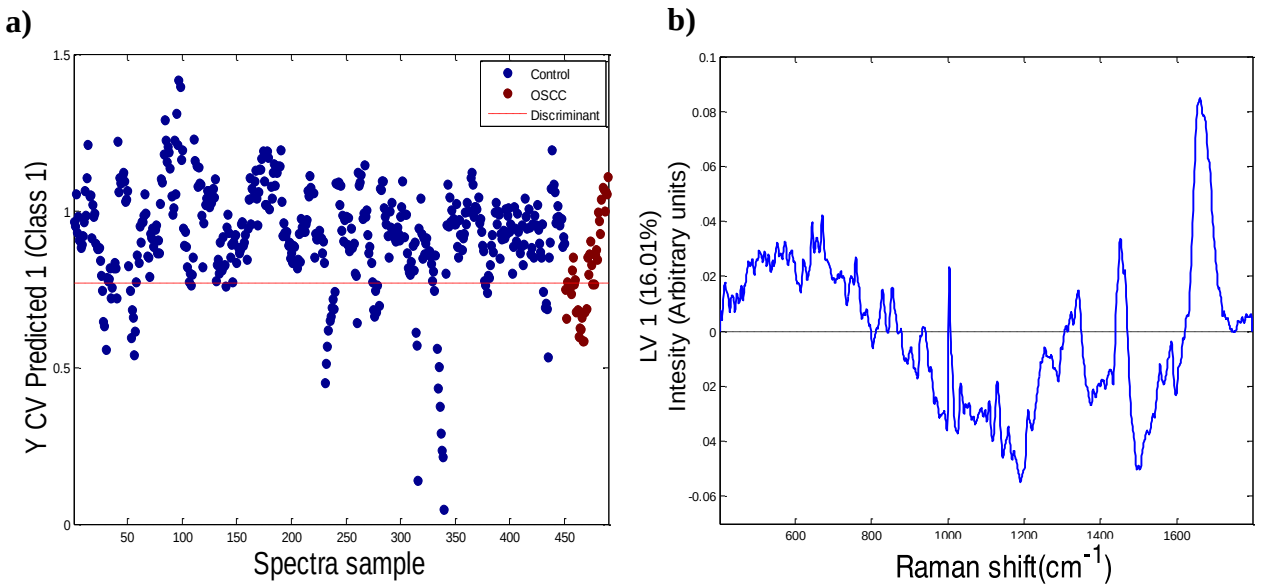

Figure 5.13: Plot of the (**a**) cross validated probability prediction and (**b**) PLSDA LV-1 showing the discrimination of the control group (=45) and the OSCC group (n=4).

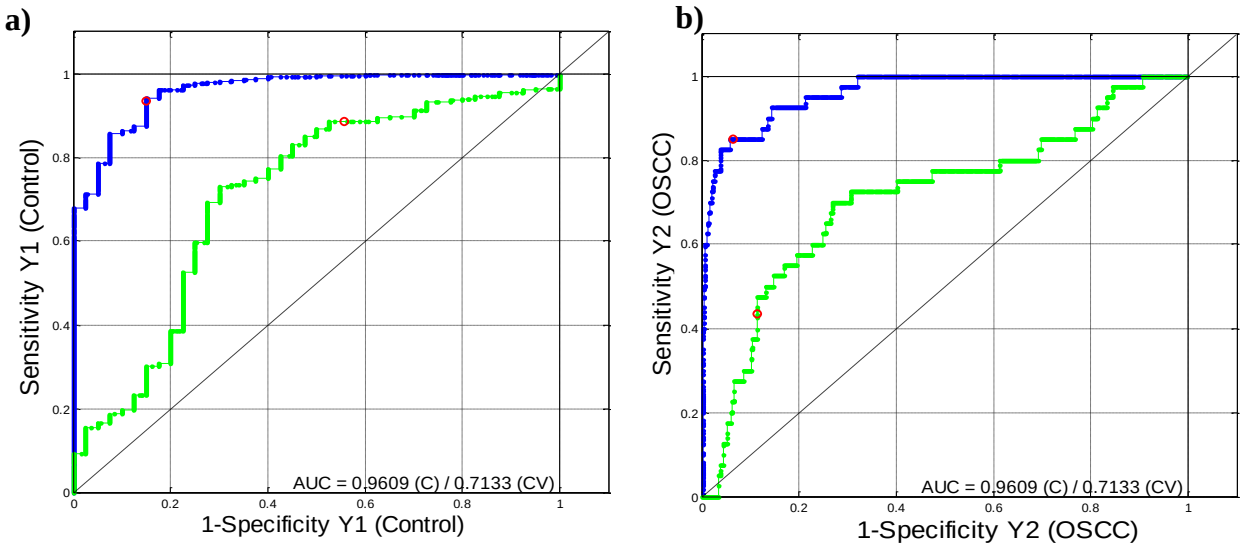

Figure 5.14: ROC curves of the control group (=45) (**a**) and the OSCC group (n=4) (**b**).

Analysis of dysplasia grade (WHO classification)

To assess whether it affects the classification efficiency, the oral epithelial dysplasia groups, classified according to the WHO criteria (2017), were compared to each other, to evaluate the sensitivity of the Raman technique over the histopathological grading given to each sample/group. In a primary qualitative analysis, based on the mean spectra of the different groups of dysplasia (**Figure 5.15**), differences could not be noticed, calling for a supervised analysis, such as PLSDA.

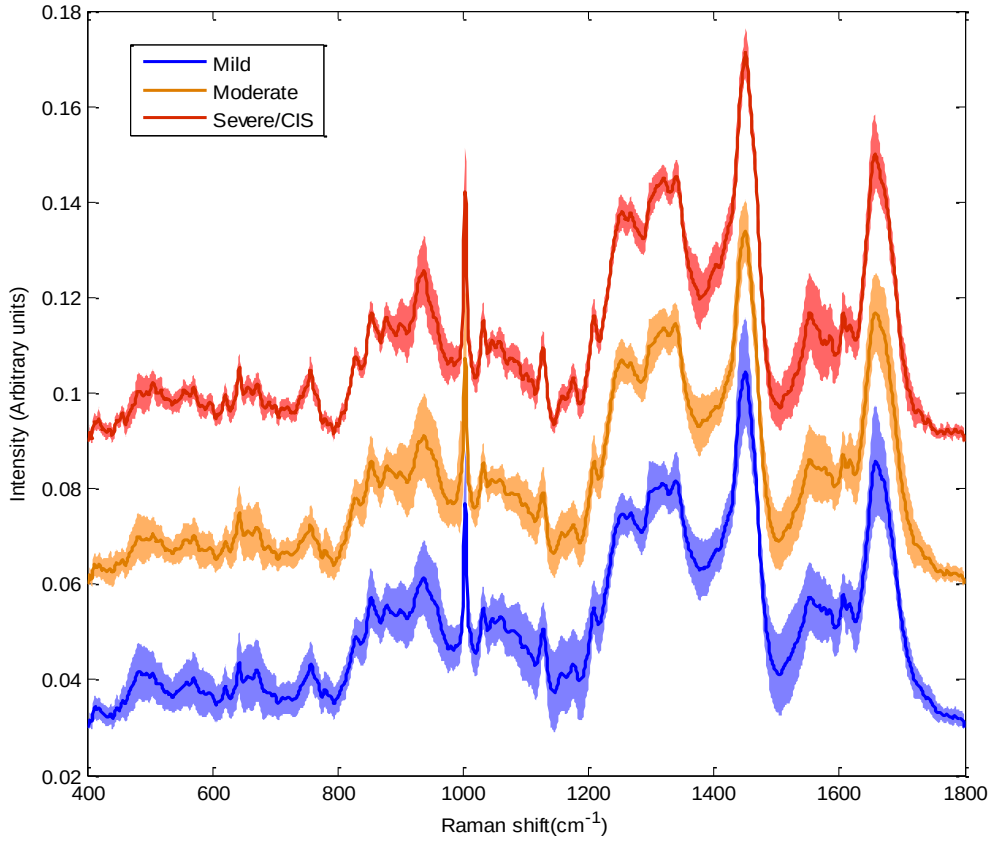

Figure 5.15: Mean Raman spectra of mild, moderate and severe/CIS oral epithelial dysplasia groups. The spectra have been off set for clarity and shading denotes standard deviation.

In a more complex approach, PLSDA was applied to the three classes at once: mild (n=18), moderate (n=17) and severe (n=6). A very low sensitivity but good specificity was observed for the mild dysplasia group, while, in contrast, the discrimination of moderate and severe dysplasia groups yielded high sensitivity although with poor specificity (**Table 5-8**).The cross validated probability prediction plot (**Figure 5.16a**) did not show any separation by the discriminant analysis, while LV-1 (**Figure 5.16b**), 23.88% of variance, showed the same spectral features as those cited in the LV-1 of the general model (**Figure 5.5**).

Table 5-8: Sensitivity and specificity from PLSDA classification between the mild, moderate and severe/OSCC groups.

	Mild	**Moderate**	**Severe/CIS**
Sensitivity (%)	**30**	**72**	**77**
Specificity (%)	**74**	**20**	**38**

The ROC curves (**Figure 5.17a** and **Figure 5.17b**) did not show a high degree of accuracy in general, the highest accuracy being achieved for the severe/CIS group (**Figure 5.17c**).

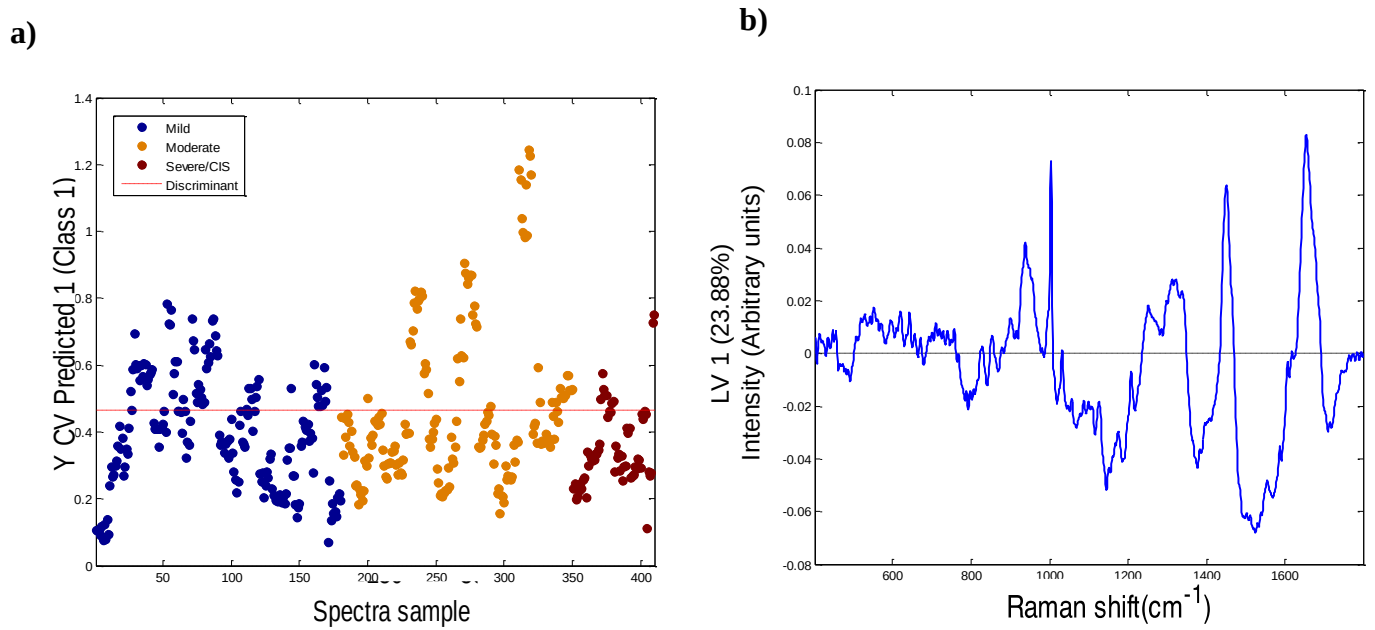

Figure 5.16: (**a**) cross validated probability prediction and (**b**) PLSDA LV-1 plot showing the discrimination between the three classes.

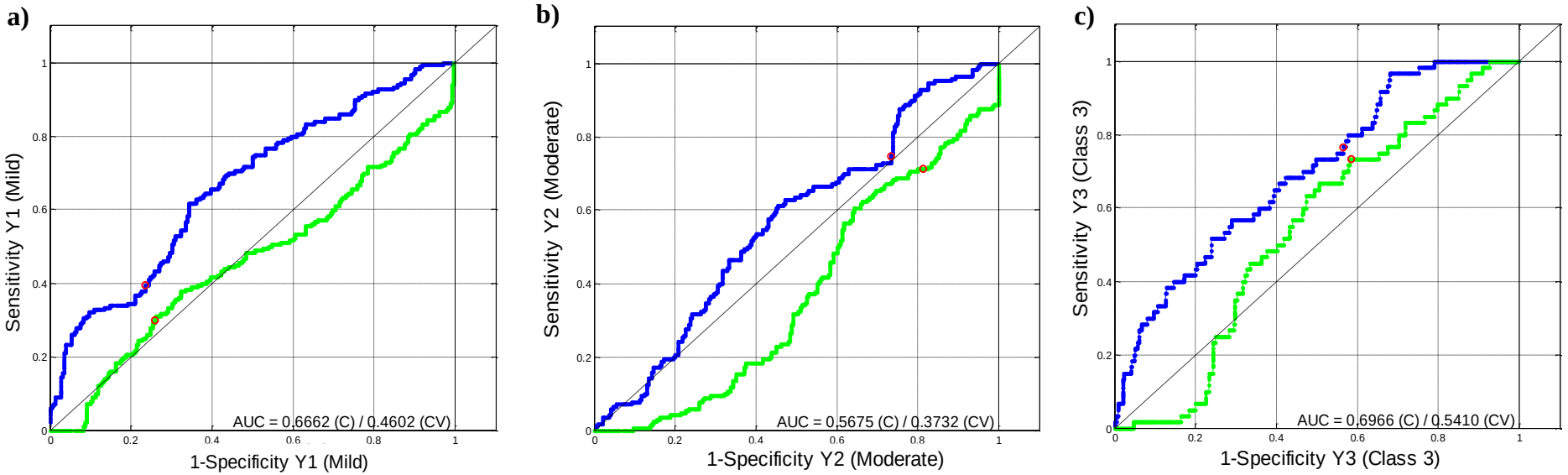

Figure 5.17: ROC curves for the (**a**) mild, (**b**) moderate and (**c**) severe oral epithelial dysplasia groups.

By plotting the means of the scores on LV-1 of each PMOL sample (**Figure 5.18**), the analysis could show that there is a degree of progression detected by Raman spectroscopy, in terms of variability amongst the three grades of dysplasia from saliva samples, mainly between the mild and higher grades.

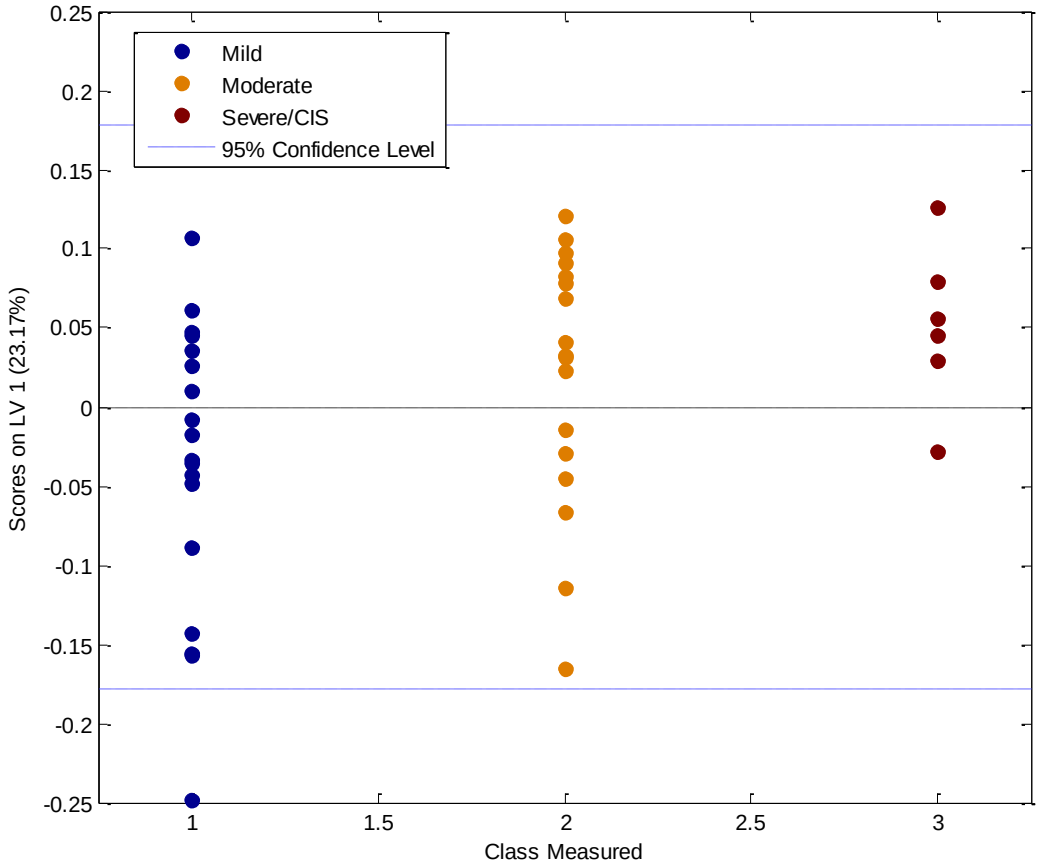

Figure 5.18: Mean (each PMOL sample) of PLSDA scores of LV-1.

The results from BCA assay (**Figure 5.19**) did not show any statistical difference (p=0.428313). However, the general levels of protein indicated a similar tendency of progression visualised by the increase of the mean total protein concentration at higher dysplasia grades.

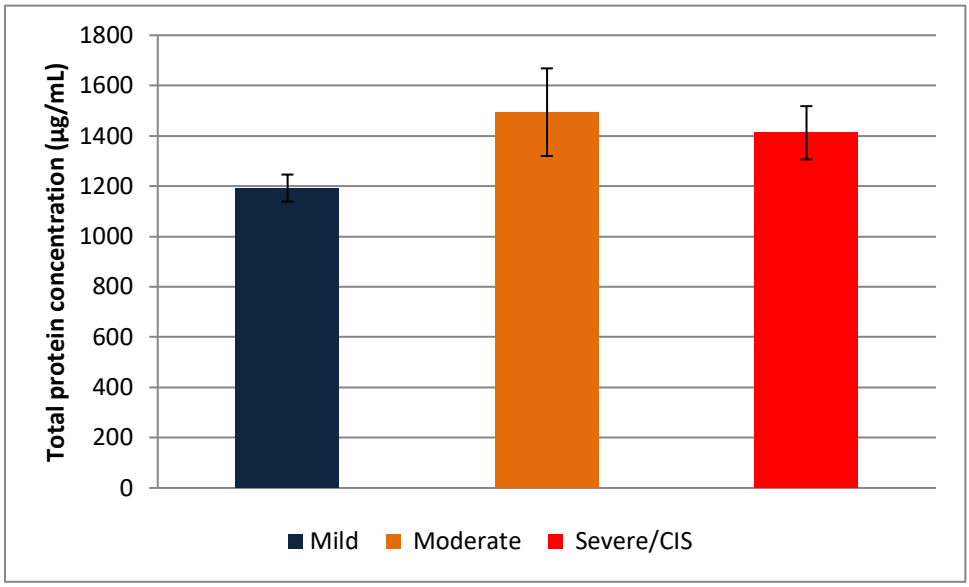

Figure 5.19: BCA assay showing the mean total protein concentration (µg/mL) and standard deviation (error bars = 95% confidence intervals) from saliva samples of control, mild, moderate and severe/CIS groups.

Analysis of dysplasia grade (binary classification)

In an attempt to achieve a better classification based on the results of the previous section, analysis according to the new suggested WHO binary grading analysis was also performed. However, no discrimination could be seen based on the cross validated probability prediction plot (**Figure 20a**); although LV-1 showed similar spectral features to those seen previously, with no new spectral features apparent (**Figure 5.20b**). Also, the classifier showed a low accuracy for both classes (**Figure 5.21**). Nevertheless, it is important to highlight that the sensitivity of this model was considerably higher (**Table 5-9**).

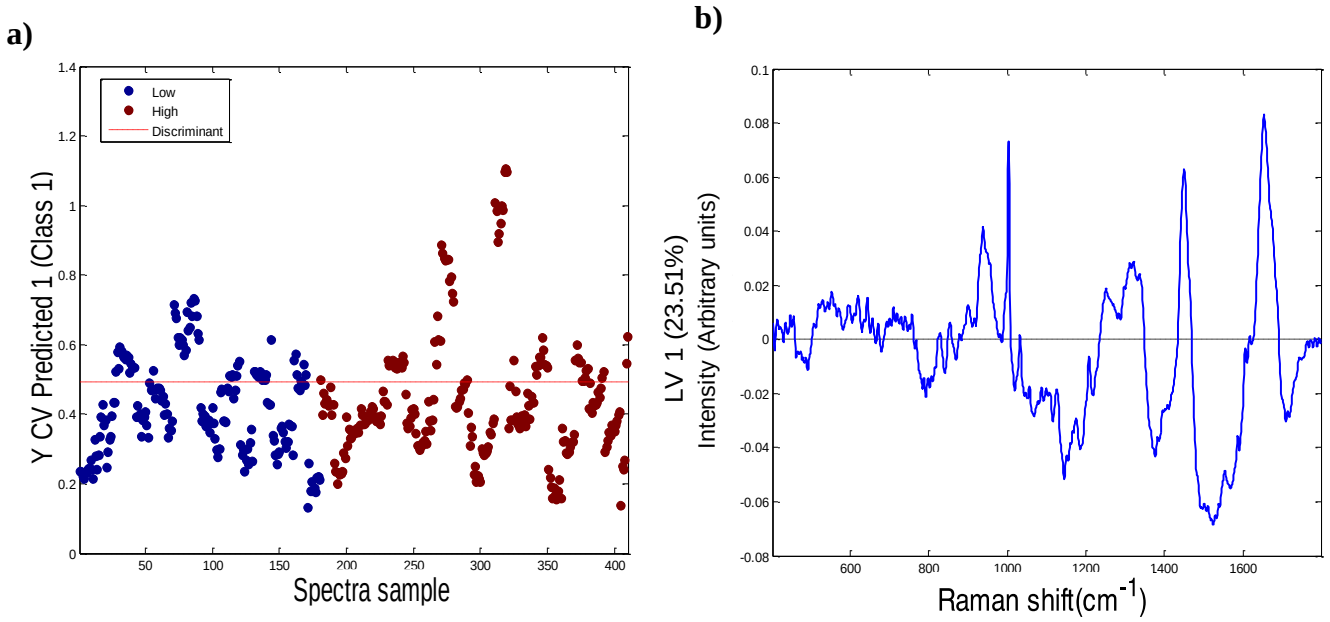

Figure 5.20: Plot of the (**a**) cross validated probability prediction and (**b**) PLSDA LV-1 showing the discrimination between low and high dysplasia groups.

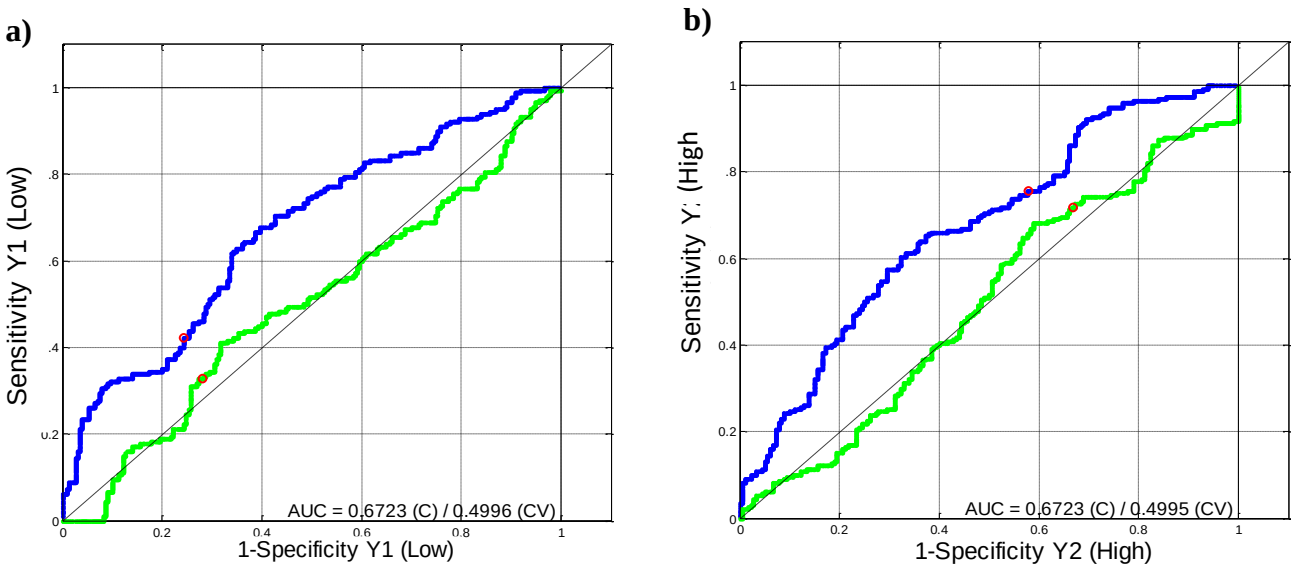

Figure 5.21: ROC curves of (**a**) low and (**b**) high dysplasia groups.

Table 5-9: Sensitivity and specificity from PLSDA classification between low and high dysplasia groups.

Sensitivity (%)	**72%**
Specificity (%)	**33%**

OSCC analysis

PLSDA was also applied to examine the differences between the PMOLs (n=41) and OSCC (n=6) groups. Taking into consideration all the data from the oral epithelia dysplasia (410 spectra) and OSCC (40 spectra), PLSDA was not able to find statistical discrimination of these two groups. This can be seen through the results of the cross validated probability prediction plot (**Figure 5.22a**), the ROC curves (**Figure 5.22b** and **Figure 5.22c**) and the sensitivity (**Table 5-10**). For the same reason, LV-1 was not generated for this analysis.

Table 5-10: Sensitivity and specificity from PLSDA classification between PMOLs and OSCC.

Sensitivity (%)	**37%**
Specificity (%)	**83%**

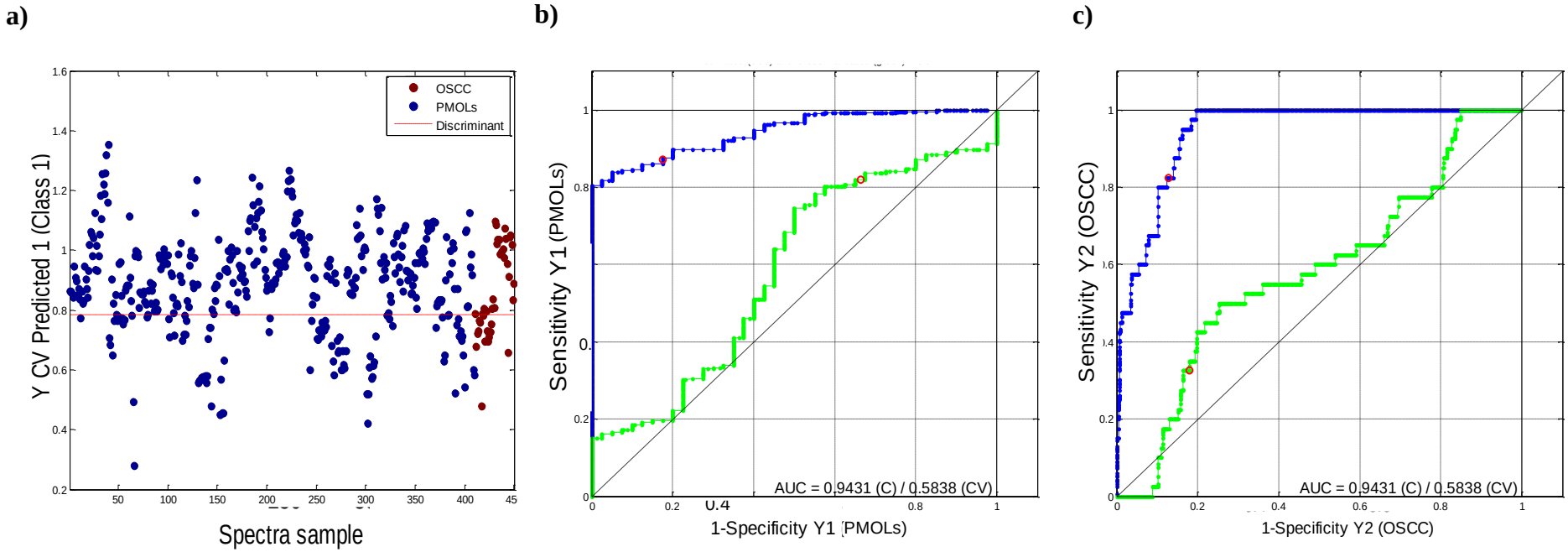

Figure 5.22: Plot of the (**a**) cross validated probability prediction showing the discrimination between the classes and ROC curves of (**b**) dysplasia and (**c**) OSCC groups.

It should be noted that, in this exploratory, proof of concept study, the patient numbers are rather limited, and when subdivided into grades, even more so, and notably, they become unbalanced with respect to the control dataset, which can impact the data analysis protocol[15]. In an attempt to evaluate the groups in a more realistic way, PLSDA was once more applied to differentiate saliva samples from oral epithelial dysplasia and OSCC groups. However, in order to balance the dataset sizes, a new matrix with spectra of saliva samples of oral dysplasia was randomly created through the use of random integers generation (Matlab), taking into account that at least one patient data of these generated numbers should be from each dysplasia grade, mild (n=1), moderate (n=1) and severe/CIS (n=1), and the last observation should be randomly selected by the algorithm from any of the remaining data. To keep the model consistent, this randomisation process was performed five consecutive times to ensure the consistency of the results.

In this approach, PLSDA was able to show clear discrimination between saliva samples from PMOLs and OSCC groups, as apparent in the cross validated probability prediction plot (**Figure 5.23a**), and the model showed good sensitivity and specificity (**Table 5-11**) when differentiating saliva samples from OSCC and oral epithelial dysplasia groups. The LV-1 (**Figure 5.23b**), responsible for 37.74% of the variance, described by negative peaks at 1376 and 1489 cm^{-1} (amino acids[13]). Other negative peaks for this analysis, also associated to the presence of OSCC, were observed at 481, 668, 537, 758, 852 (nucleic acid/sugars[13]) and 1655 cm^{-1} (amino acids[14]). Notably, the spectral profile of LV-1 is significantly different from most of the previous LVs, in which the classification seemed to be based on the protein content. The ROC curves (**Figure 5.24a** and **Figure 5.24b**) also show excellent accuracy (AUC=0.8025) for both classes.

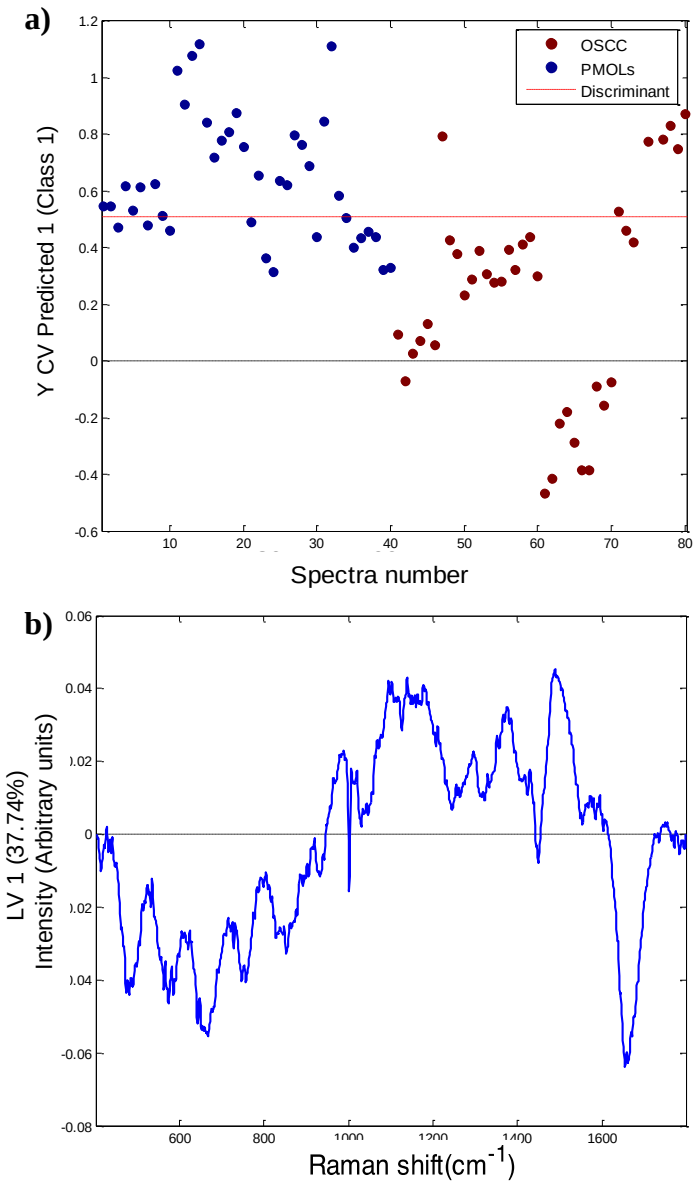

Figure 5.23: Plot of the (**a**) cross validated probability prediction and (**b**) PLSDA LV-1 showing the discrimination between the dysplasia and OSCC groups.

Table 5-11: Sensitivity and specificity from PLSDA classification between PMOLs and OSCC groups in a paired analysis.

Sensitivity (%)	**75%**
Specificity (%)	**72%**

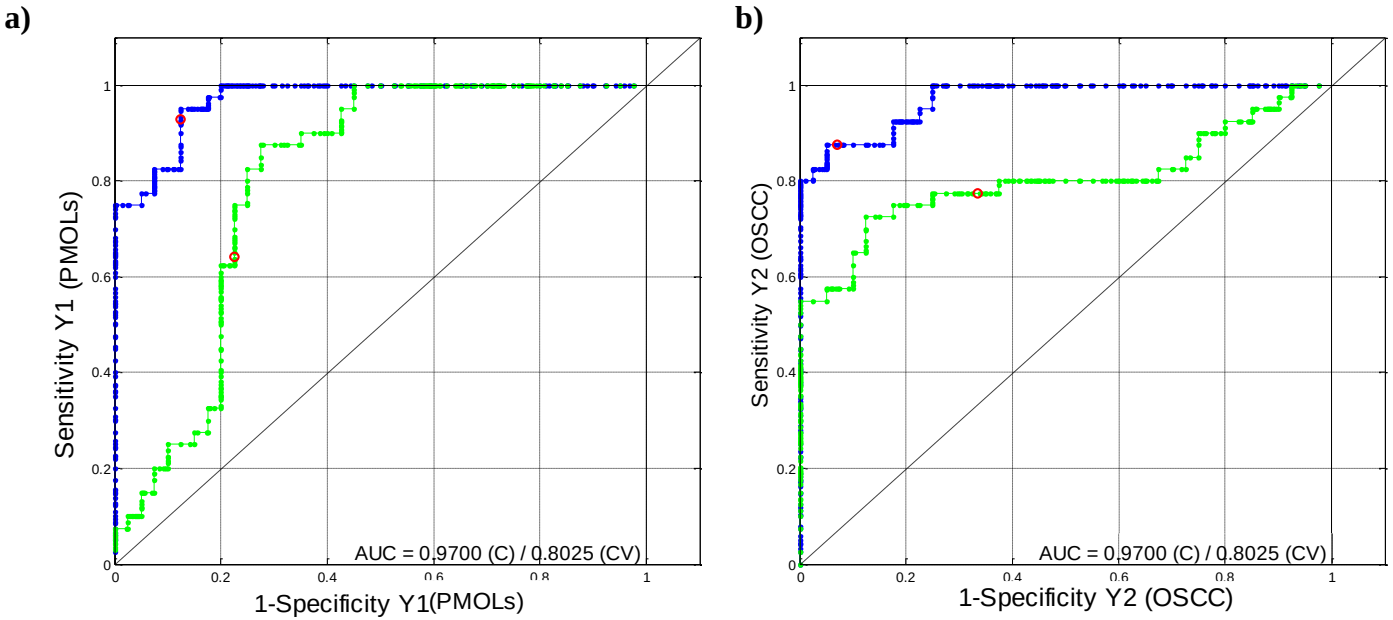

Figure 5.24: ROC curves of (**a**) dysplasia and (**b**) OSCC groups in a paired analysis

5.4 Discussion and conclusions

PMOLs are usually associated with a variable rate of malignant progression, with the detection of oral epithelial dysplasia by tissue biopsy remaining the gold standard in guiding management[6]. However, many grading systems, including the current one proposed by WHO, have been put forward in an attempt to obtain objectivity in grading oral epithelial dysplasia. Despite these efforts, variability and subjectivity remains unresolved.

Diagnosing any oral dysplastic lesion is vital to provide an early treatment and consequently better prognosis. As shown by the general PLSDA model, Raman spectroscopy could provide, through the salivary profile of patients, this discrimination with an excellent degree of accuracy. The results from PLSDA have shown this differentiation can primarily be attributed to higher levels of glycoproteins and proteins.

Some proteomic studies have already reported elevated levels of salivary defensin-1 as an indication for the detection of OSCC, since higher concentrations of salivary defensin-1 were detected in patients with OSCC compared with healthy controls, for example[16]. In another study, soluble CD44 was elevated in the majority of patients with OSCC and distinguished cancer from benign disease with a high specificity[17]. Furthermore, a well-known panel of proteins, such as p53 and growth factor proteins, are widely reported to be present in higher concentrations in the presence of oral dysplasia[18,19].

Compared to the general analysis, the dysplasia grade analysis results obtained through PLSDA did not show, in a general perspective, very good discrimination, even using two different grading systems to analyse the saliva spectra. However, it is important to note that, when good sensitivity/accuracy was achieved, the models seemed to correlate the spectral changes with amino acids. These results are consistent with previous studies which reported markedly higher levels of salivary concentration of leucine, isoleucine,

tryptophan, valine, threonine, histidine, alanine and phenylalanine in OSCC patients than in healthy individuals[20].

In the OSCC analysis, it was possible to observe that, in a paired analysis, the discrimination obtained by PLSDA could be associated with the content of sugars. Nucleic acids have been already reported in saliva by some researchers, i.e. circulating tumour DNA, which is cell-free DNA of 180–200 base pairs in length that sheds from tumour cells into the circulatory system and has been detected in various bodily fluids, including saliva[21].

Also, different and important factors should be taken in consideration when using machine learning systems or classifiers. As observed in the different analyses, the results had a broad range in terms of accuracy/sensitivity/specificity and seemed to be influenced by sample dataset size and balance. The potential impact of these factors on the PLSDA modelling process was therefore explored. Following the same protocol of analysis as the results section of this chapter, the initial model containing the whole set of controls (n=45) and patients (n=45) was tested in different situations of parity and number (**Figure 5.25**), whereby the sensitivity and specificity of the original analysis was kept for reference (and standard deviations by 95% confidence interval based on the distribution of the confusion matrix from the analysis) and other situations, including randomly decreasing the dimension of the patient group, or matching the numbers of both classes; or even increasing artificially the patient data to reach parity with the control data.

When the patient data was reduced, the number of controls were retained (n=45), and different reduced dimensions were tested: 12, 8, and 4 patients. These dimensions were strategically selected to mimic the reduced numbers of some of the patient data subsets, for example OSCC (n=4). When paired by decreasing the dimensions of both classes, the data number was determined by the smallest group (4 patients with OSCC, requiring then

4 from the other classes – totalling 12). Also, the final composition of each matrix (control or patients) was determined random integers generation algorithm in each round.

In a similar way, when artificially increased, the same algorithm was applied to select the uniform composition of each grade (having at least 4 patients for each class) and randomly increased making sure that each subset (mild, moderate, severe/CIS and OSCC) appeared at least three times (n=36), leaving the 9 remaining observations (needed to complete the 45) to be again randomly selected by the algorithm. In this case, the controls were all retained (n=45).

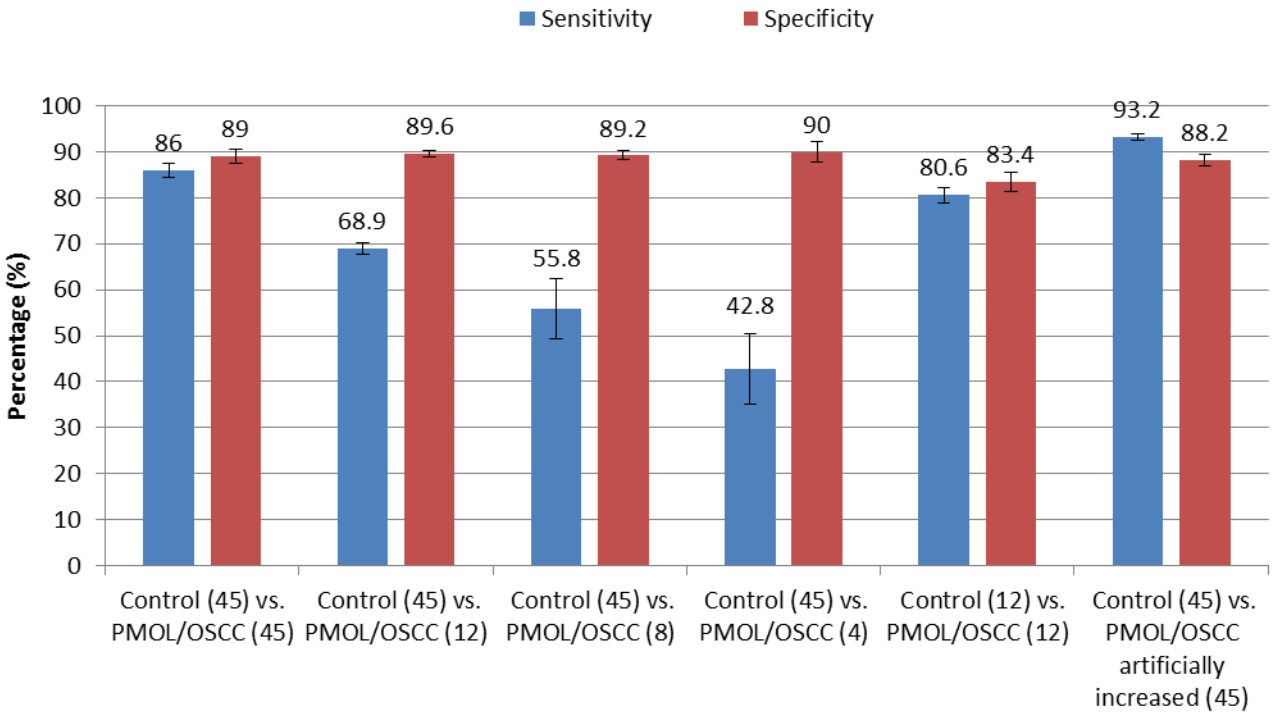

Figure 5.25: Bar-graph showing simulations of analyses involving the dataset from controls and patients. The first two columns (L-R) represent the original sensitivity (blue) and specificity (red) from the original model associated with standard deviations acquired based on the Clopper-Pearson confidence interval (95%) over the distribution of the PLSDA confusion matrix. The rest of the columns represent different situations in which the patient data could be reduced, matched by decreasing the control data or matched by artificially increasing the patient data. In these cases, the sensitivity, specificity and standard deviation of each situation were acquired by the average of these values throughout 5 rounds of PLSDA analysis (where the dimension of the classes was randomised by using of random integers generation algorithm).

In the case of the analyses in which the dimension of the group was decreased (or matched by decreasing the patient data), the values for sensitivity and specificity were obtained by taking the average percentage value of five consecutive analyses where each patient data (or control, in case of decreasing the control data) was randomly selected, by random integers generation algorithm (Matlab), to compose the matrix in question before analysis. The standard deviation, in these analyses, was obtained based on the values of discrepancies during the five rounds of analysis.

These analyses were performed to mimic the situation of the data available to this study, in which the dimensions of the control group is larger than the patient group, such that having an extremely unbalanced dataset could somehow lower the power of disease detection of the multivariate analysis. Matching the data (by decreasing the controls) somewhat underestimates the sensitivity/specificity, while artificially increasing the patient data (to match with the number of controls) overestimates these values, although, without major analytical discrepancies.

In fact, when the multivariate analysis was applied with a reduced number of "diseased" samples in comparison to a fixed number of control samples, the values of sensitivity tended to decrease, as the analysis found it more difficult to assimilate the small number of observations as true positives, while the true negatives (directly correlated to the specificity) had no major discrepancies. This scenario could be important to infer that matching group dimensions or even artificially increasing the small groups to match with the general dimensions of the classes could show a less detrimental impact on the classification than a scenario where the dimensions are not matched.

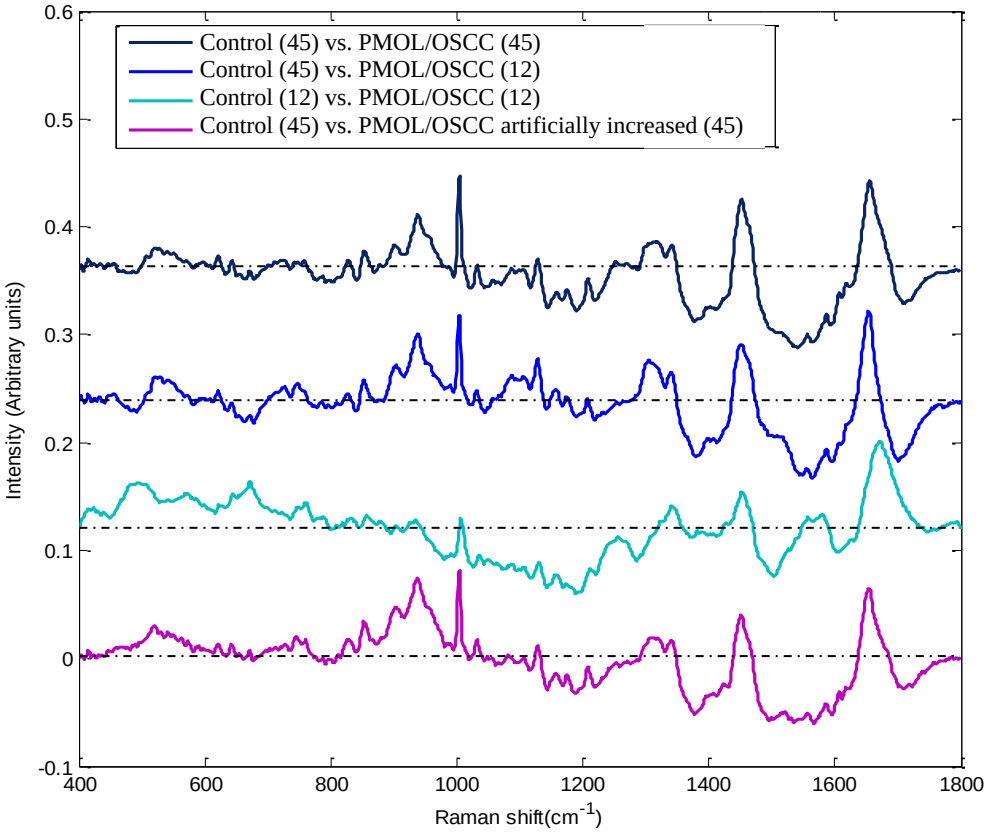

Figure 5.26: Representative LV-1s from each PLSDA analysis simulation involving the dataset of controls and patients according to the average of sensitivity and specificity of each.

The validity of the "simulated" approach was investigated by examination of the consistency of the LV-1 of the respective analyses (**Figure 5.26**). The similarities of the LVs indicates (taken from the most representative analysis, amongst the five rounds, in terms of the average sensitivity and specificity values) that the PLSDA analyses, although providing different values for sensitivity and specificity, based its classifications on similar spectral components (peaks), the peaks of which were also previously highlighted in the results section of this chapter (**Figure 5.5**). However, it is important to highlight that the LV-1 obtained from a "naturally" balanced PLSDA analysis (controls decreased to meet the number of patients' data - control 12 vs. 12 PMOL/OSCC) was the most

different LV-1 to the original model (Control 45 vs. PMOL/OSCC 45); while the artificially increased (Control 45 vs. PMOL/OSCC artificially increased 45) had more spectral similarities, in terms of intensity, with the original results.

These observations could open a precedent to fully evaluating PLSDA analysis and how the group dimensions can influence the general results. Further analyses were also performed following the same experimental principles of group dimension and parity used for the analysis of the entire data. This time, the analyses followed the classes in the analysis of controls vs. each PMOL/OSCC (**Figure 5.27**), the analysis of WHO dysplasia grade (**Figure 5.28**) and PMOLs vs. OSCC (**Figure 5.29**). No simulations were performed using the binary dysplasia classification (low and high dysplasia) due to the high number already present in each class seen in the results section of this chapter, in the results section (binary classification).

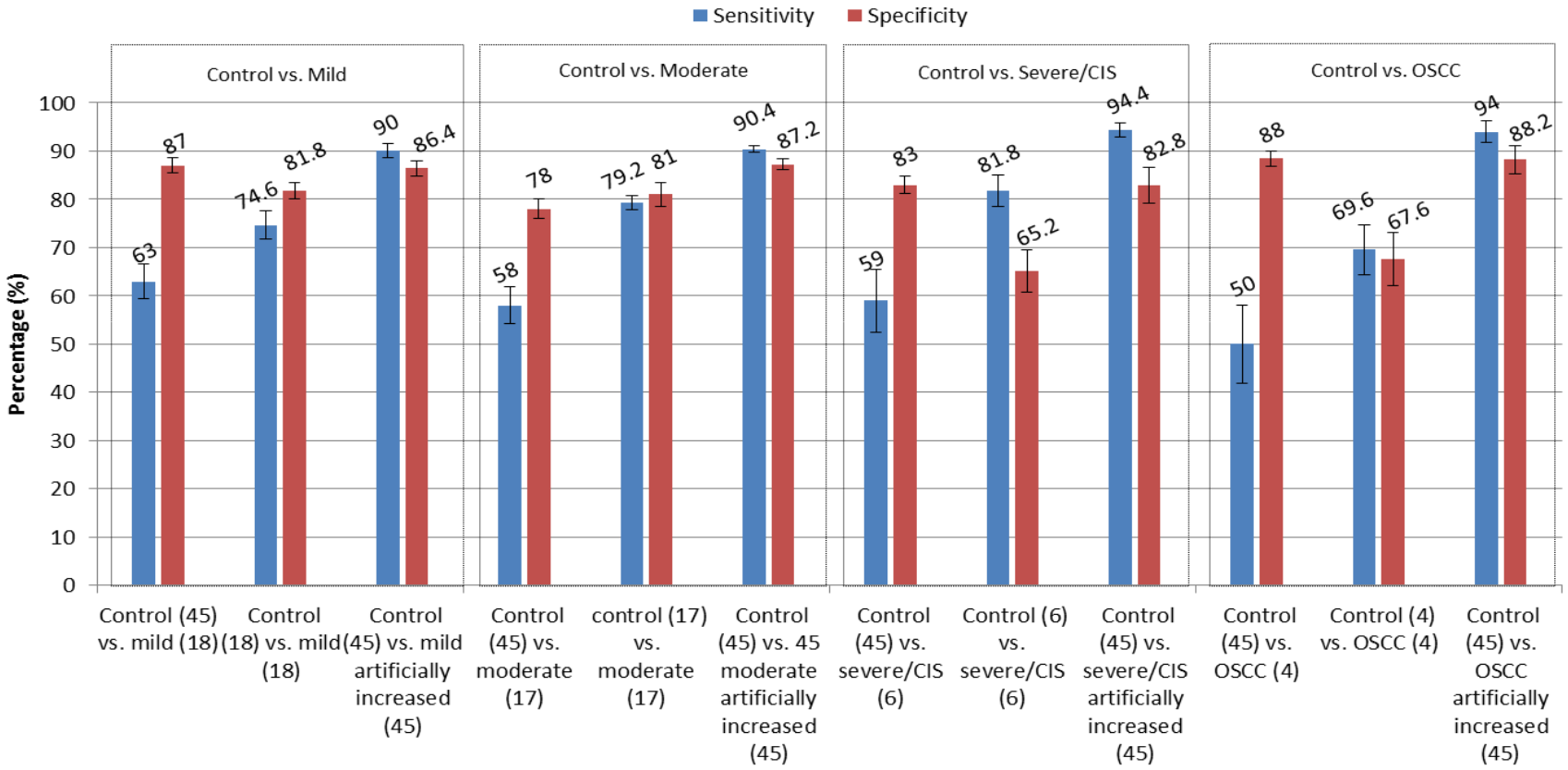

Figure 5.27: Bar-graph showing simulations of analyses involving the dataset from controls and the different dysplasia grades (WHO classification). The first three columns (L-R) represent the original sensitivity (blue) and specificity (red) from the original model associated with standard deviations acquired based on the Clopper-Pearson confidence interval (95%) over the distribution of the PLSDA confusion matrix. The rest of the columns represent different situations where the patients' data (separated each dysplasia grade) could be reduced, paired by decreasing the number of controls or paired by artificially increasing the number of patients' data. In these cases, the sensitivity, specificity and stand deviation of each situation were acquired by the average of these values throughout 5 rounds of PLSDA analysis (where the dimension of the classes were randomised by using of random integers generation algorithm).

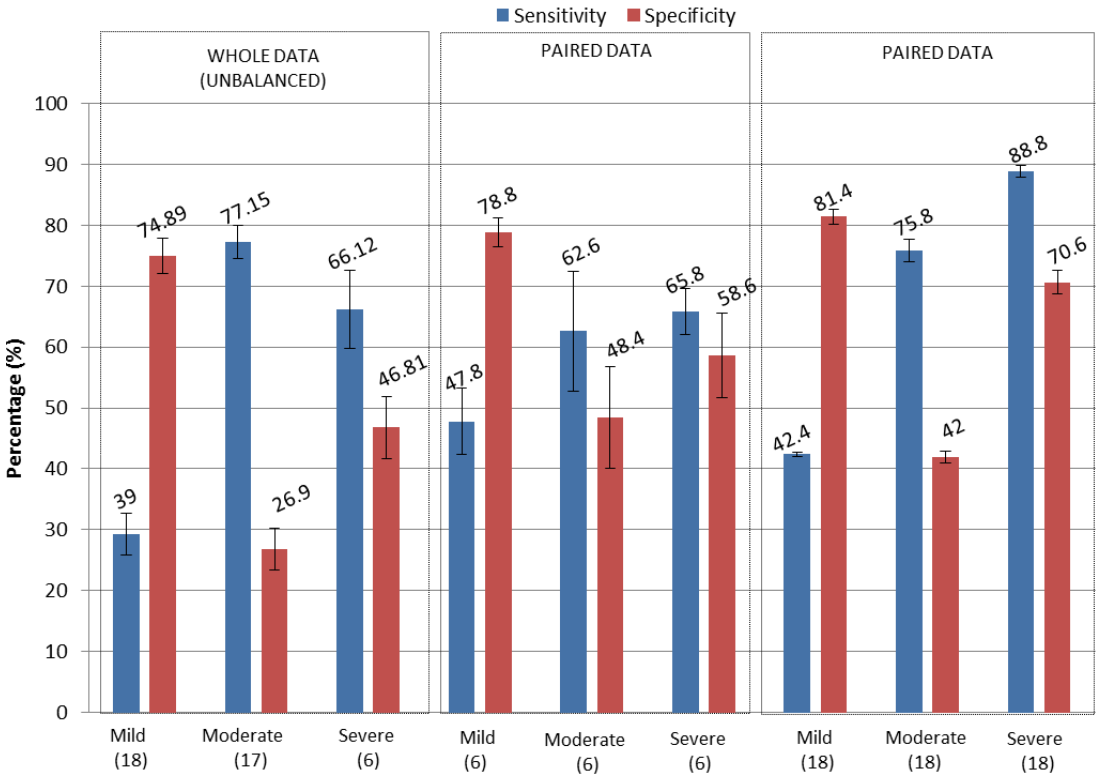

Figure 5.28: Bar-graph showing simulations of analyses involving the dataset from patients according to each dysplasia grade. The first three columns (whole data) represent the original sensitivity (blue) and specificity (red) from the original model associated with standard deviations acquired based on the Clopper-Pearson confidence interval (95%) over the distribution of the PLSDA confusion matrix. The rest of the columns represent different situations where the different classes could have different dimensions, paired by decreasing the number of larger dimension classes (mild and moderate), or paired by artificially increasing the number of the smaller classes (moderate and severe/CIS). In these cases, the sensitivity, specificity and standard deviation of each situation were acquired by the average of these values throughout 5 rounds of PLSDA analysis (where the dimension of the classes was randomised by using the random integers generation algorithm).

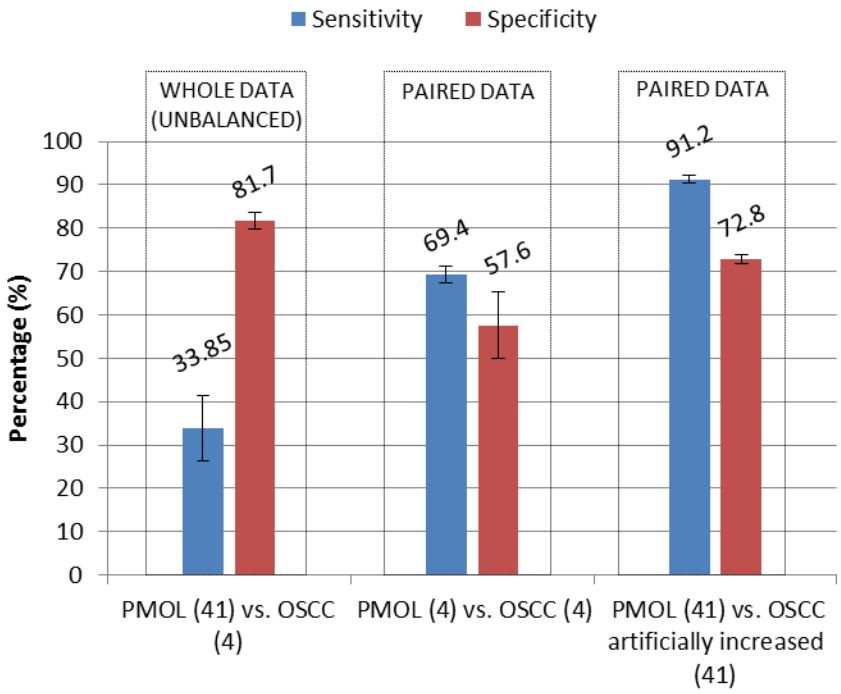

Figure 5.29: Bar-graph showing simulations of analyses involving the dataset from patients with PMOLs vs. OSCC. The first two columns (whole data) represent the original sensitivity (blue) and specificity (red) from the original model associated with standard deviations acquired based on the Clopper-Pearson confidence interval (95%) over the distribution of the PLSDA confusion matrix. The rest of the columns represent different situations where the different classes could have different dimensions, paired by decreasing the number of the larger dimension class (PMOL), or paired by artificially increasing the number of the smaller class (OSCC). In these cases, the sensitivity, specificity and standard deviation of each situation were acquired by the average of these values throughout 5 rounds of PLSDA analysis (where the dimension of the classes was randomised by using the random integers generation algorithm).

These further experimental test/results seemed to follow the same pattern of sensitivity/specificity values among the PLSDA analyses. Some of the poor values initially obtained in the results section of this chapter can now be clearly explained and

associated with the sample size and the paired/unpaired conditions. The smaller the size of the sample, the harder it is to build a representative model[21]. Even with an underestimation, an analysis approach in which the larger dimension classes were reduced to produce parity/balance, seemed to be a better analytical approach in comparison to PLSDA analyses with small dimension/unpaired classes. However, this new overview regarding group dimension, which could for example be performed by artificially increasing a small patient dataset, might represent a new alternative to overcome these usual analytical problems, as the spectral results from the LV-1s comparison show that the classifications with artificially increased data was provided based on a very similar spectral profile and, consequently, similar biochemical composition.

Finally, it should also be noted that all the analysis explored here were based on results from the histopathological diagnosis provided by the hospital pathologists following associated grading systems. The severity of dysplasia is arrived at based on the grading of dysplasia in the lesion in question. However, it has been established that dysplasia grading suffers from intra- and inter-observer variability[23] and thus the classifications of the "gold standard" should in themselves be open to question.

Finally, other factors that can have influence on the Raman spectrum and classification will be further explored in chapter 6.

Reference

1. Tanaka T, Ishigamori R. Understanding carcinogenesis for ghting oral cancer. J Oncol 2011; 2011:603740.

2. El-Naggar AK, Chan JK, Grandis JR, Takata T, Slootweg PJ. WHO Classification of Head and Neck Tumors. WHO/IARC Classification of Tumours. International Agency for Research on Cancer (IARC) press; 2017, 4, 9.

3. van der Waal I. Potentially malignant disorders of the oral and oropharyngeal mucosa; terminology, classification and present concepts of management. Oral Oncol. 2009 Apr-May;45(4-5):317-23.

4. Kujan O, Oliver RJ, Khattab A, Roberts SA, Thakker N, Sloan P. Evaluation of a new binary system of grading oral epithelial dysplasia for prediction of malignant transformation. Oral Oncol 2006;42:987-93.

5. Barnes L, Eveson JW, Reichart, P, Sidransky D. World Health Organization Classification of tumours: Pathology and genetics of tumours of the head and neck. IARC Press, Lyon, 2005.

6. Ranganathan K, Kavitha L. Oral epithelial dysplasia: Classifications and clinical relevance in risk assessment of oral potentially malignant disorders. J Oral Maxillofac Pathol. 2019;23(1):19–27. doi:10.4103/jomfp.JOMFP_13_19

7. Scully C, Sudbo J, Speight PM. Progress in determining the malignant potential of oral lesions. J Oral Pathol Med 2003;32:251–56

8. Drobitch RK, Svensson CK. 1992. Therapeutic drug monitoring in saliva: an update. Clin. Pharmacokinet. 23:365–379.

9. Haeckel R, Hanecke P. The application of saliva, sweat, and tear fluid for diagnostic purposes. Ann. Biol. Clin., 1993, 51:903–910.

10. Jusko WJ, Milsap RL. Pharmacokinetic principles of drug distribution in saliva. Ann. N. Y. Acad. Sci. 1993,694:36 – 47.

11. Yoshizawa JM, Schafer CA, Schafer JJ, Farrell JJ, Paster BJ, Wong DT. Salivary biomarkers: toward future clinical and diagnostic utilities. Clin Microbiol Rev. 2013;26(4):781–791. doi:10.1128/CMR.00021-13

12. Feng S, Huang S, Lin D, Chen G, Xu Y, Li Y, Huang Z, Pan J, Chen R, Zeng H. Surface-enhanced Raman spectroscopy of saliva proteins for the noninvasive differentiation of benign and malignant breast tumors. Int J Nanomedicine. 2015 Jan 12;10:537-47. doi: 10.2147/IJN.S71811. eCollection 2015.

13. Movasaghi Z, Rehman S, and Rehman IU. Raman Spectroscopy ofBiological Tissues. Applied Spectroscopy Reviews 2007;42(5):493-541.

14. Virkler K, Lednev IK. Forensic body fluid identification: the Raman spectroscopic signature of saliva. Analyst. 2010 Mar;135(3):512-7. doi: 10.1039/b919393f. Epub 2009 Dec 15.

15. Bonnier F, Byrne HJ. Understanding the molecular information contained in Principal Component Analysis of Vibrational Spectra of Biological Systems, Analyst, 2012, 137:322-332.

16. Mizukawa N, Sugiyama K, Fukunaga J, Ueno T, Mishima K, Takagi S, et al. Defensin-1, a peptide detected in the saliva of oral squamous cell carcinoma patients. Anticancer Res 1998;18:4645-9.

17. Franzmann EJ, Reategui EP, Pedroso F, Pernas FG, Karakullukcu BM, Carraway KL, et al. Soluble CD44 is a potential marker for the early detection of head and neck cancer. Cancer Epidemiol Biomarkers Prev 2007;16:1348-55.

18. Li Y, Zhang J. Expression of mutant p53 in oral squamous cell carcinoma is correlated with the effectiveness of intra-arterial chemotherapy. Oncol Lett. 2015;10(5):2883–2887. doi:10.3892/ol.2015.3651

19. Krishna A, Singh S, Kumar V, Pal US. Molecular concept in human oral cancer. Natl J Maxillofac Surg. 2015;6(1):9–15. doi:10.4103/0975-5950.168235

20. Reddy I, Sherlin HJ, Ramani P, Premkumar P, Natesan A, Chandrasekar T. Amino acid profile of saliva from patients with oral squamous cell carcinoma using high performance liquid chromatography. J Oral Sci. 2012 Sep;54(3):279-83.

21. Patel KM, Tsui DW, The translational potential of circulating tumour DNA in oncology, Clin. Biochem 2015,48(15):957–961.

22. Beleites C, Neugebauer U, Bocklitz T, Krafft C, Popp J. Sample Size Planning for Classification Models. Analytica Chimica Acta, 2013,760:25–33.

23. Geetha KM, Leeky M, Narayan TV, Sadhana S, Saleha J. Grading of oral epithelial dysplasia: Points to ponder. J Oral Maxillofac Pathol. 2015;19(2):198–204. doi:10.4103/0973-029X.164533

Chapter 6: Influence of patient factors and potential confounding factors on Raman spectroscopic classification through saliva analysis

6.1 Introduction

Following from the analysis in chapter 5, clinical features and/or patient factors that might represent an influence on the statistical classification using Raman spectroscopy are now explored. As discussed in detail in section 1.2.2 of chapter 1, it has long been accepted that tobacco consumption, including smokeless tobacco, and heavy alcohol consumption are the principal aetiologic factors for the development of oral cancer[1] and it has also been demonstrated that they can have a synergistic effect[1-3]. In addition, a variety of suspected risk factors such as chronic irritation, poor oral hygiene, viral infection, occupational exposure, malnutrition and genetic factors, have also been correlated to the development of oral cancer[4,5].

Beyond those factors inherent to the disease itself, there are several others that can influence the salivary profile of an individual. The amount and composition of secreted human saliva depends on factors such as flow rate, circadian rhythm, type and size of the salivary gland, type of the stimulus, diet, drugs, age, sex, blood type, physiological status, and several others[6].

As the study of chapter 5 was based on heterogeneous groups of healthy volunteers and patients of different gender, age, habits and medical histories, the aim of this chapter was to discern whether these factors have any influence on the classification using Raman spectroscopy.

6.2 Methodology

6.2.1 Ethics, saliva collection and volunteer questionnaire

Ethical approval for collection of saliva samples healthy volunteers (collected in FOCAS Research Institute, Technological University Dublin) and patients with potentially malignant lesions or OSCC (from Dysplasia Clinic at Dublin Dental University Hospital) is fully detailed in section 5.2.1 from chapter 5.

A medical and oral health status questionnaire was also used to obtain further information regarding biological factors that can influence the analysis classification, such as gender, age, and others, to better understand these variances over the classifier (**Appendix III**).

A stimulated whole saliva collection method was used, as described in section 4.3.2 of this thesis.

6.2.2 Raman Spectroscopic Instrumentation

The Raman spectroscopic instrument and recording setup have been described in section 4.3.4 of chapter 4. The spectra acquired for chapter 5 were used for this study.

6.2.3 Data analysis

Metadata on the healthy volunteers (control) and patients included in chapter 6 is provided in **Table 6-1** and **Table 6-2**, respectively. This was used to divide all healthy volunteers (control) and patients, regardless of histopathological diagnosis, into groups according to gender, smoking habits, alcohol consumption and site of the lesion for the patient group. The spectra acquired for the study of chapter 5, were analysed using PLSDA with LOPOCV, as described in section 5.2.5.

Table 6-1: Information on healthy volunteer (control) factors.

Healthy volunteer (control)	Gender	Age	Smoking	Alcohol Consumption
1	M	30	No	No
2	F	27	No	Yes/0-2 units per week
3	F	39	No	Yes/0-7 units per week
4	F	35	No	Yes/0-8 units per week
5	M	27	No	Yes/0-30 units per week
6	F	38	No	Yes/25 units per week
7	F	27	No	Yes/Occasionally
8	F	29	No	Yes/2 units week
9	M	34	No	Yes/25 units per week
10	F	27	No	Yes/20 units per week
11	F	32	No	No
12	M	31	Yes	Yes
13	F	32	Yes	Yes
14	F	32	Yes/2 cpw	Yes/2 per week
15	F	38	No	No
16	F	27	No	Yes/0-1
17	M	33	Yes	Yes/4 units per week
18	F	41	No	No
19	F	29	No	Yes/0-2 units per week
20	F	50	No	Yes
21	M	28	No	Yes/2 units per week
22	M	34	No	No
23	F	40	No	No
24	F	31	No	Yes/0-1 per week
25	M	70	Yes	Yes
26	M	32	No	Yes/1unit per month
27	F	56	No	Yes/5 units per week
28	F	35	No	No
29	F	26	No	Yes/0-2 units week
30	M	27	No	Yes/10 units per week
31	F	26	Yes/2cpd	Yes/4 units per week
32	M	30	No	No
33	F	27	No	No
34	M	30	No	Yes/3 units week
35	F	63	No	Yes/11 units per week
36	M	32	No	Yes/1 unit per week
37	F	29	No	No
38	M	65	No	Yes/8 units per week
39	F	25	No	Yes/2 units per week
40	F	25	No	Yes/1 unit per week
41	F	32	No	No
42	F	26	Yes/4cpd	Yes/6 units per week
43	F	27	No	No
44	M	29	No	No
45	F	32	No	No

n/a, information was not available; cpd, cigarettes per day; cpw, cigarettes per week.

Table 6-2: Information on patient factors and clinical features.

Patient	Gender	Age	Smoking	Alcohol Consumption	Site of Lesion
1	F	54	Ex-smoker	Yes/7 units per week	Buccal mucosa
2	M	62	No	No	Gingiva
3	M	70	5 cpd	Yes/minimal	Buccal mucosa
4	M	65	Ex-smoker	Yes/8 units per week	Gingiva
5	F	68	No	Yes/10 units per week	Tongue
6	F	72	No	Yes/2 units per week	Gingiva
7	F	71	Ex-smoker	Yes/12 units per week	Buccal mucosa
8	F	91	No	Yes/2 units per week	Floor of mouth
9	F	50	No	Yes/10 units per week	Tongue
10	F	59	10 cpd	Yes/4 units per week	Buccal mucosa
11	F	56	Ex-smoker	Yes/12 units per week	Tongue
12	F	65	No	n/a	Tongue
13	F	49	Ex-smoker	n/a	Tongue/ buccal mucosa
14	M	63	15 cpd	Yes/15 units per week	Buccal mucosa
15	M	63	Ex-smoker	Yes/14 units per week	Tongue
16	M	73	30 cpd	No	Floor of mouth
17	F	70	Ex-smoker	Yes/6-7 units per week	Hard palate
18	M	77	Ex-smoker	Yes/2 units per week	Labial mucosa
19	M	80	Ex-smoker	No	Tongue
20	F	40	Ex-smoker	No	Buccal mucosa
21	F	48	No	Yes/1 units per week	Buccal mucosa
22	M	80	Ex-smoker	No	Buccal mucosa
23	M	35	Ex-smoker	Yes/5-10 units per week	Alveolus
24	F	72	15 cpd	Yes/10 units per week	Floor of mouth
25	F	70	No	Yes/1 units per week	Gingiva
26	M	55	25-30 cpd	Yes/8 units per week	Alveolus
27	F	73	Ex-smoker	Yes/8 unitsper week	Tongue
28	M	74	Ex-smoker	n/a	Buccal mucosa
29	F	34	No	No	Tongue
30	M	73	No	Yes/1 unit per week	Tongue
31	F	67	20 cpd	No	Soft palate
32	M	69	60 cpd	Yes/60 units per week	Tuberosity
33	F	64	20 cpd	Yes/6 units per week	Soft palate
34	M	62	Ex-smoker	Yes/8 units per week	Tongue
35	M	45	No	No	n/a
36	M	61	3-4 cpd	No	Labial mucosa
37	F	86	No	No	Palate
38	M	66	20 cpd	No	Tongue
39	M	58	20-30cpd	Yes/100 units per week	Buccal mucosa
40	M	71	No	No	Gingiva
41	M	52	5 cpd	Yes/80 units per week	Floor of mouth
42	M	49	No	No	Labial mucosa
43	M	61	20 cpd	Yes/6 units per week	Tongue
44	F	60	10 cpd	Yes/10 units per week	Floor of mouth
45	M	63	Ex-smoker	Yes/20 units per week	Tongue

n/a, information was not available; cpd, cigarettes per day; cpw, cigarettes per week.

It is important to highlight that the PLSDA analyses of the factors/clinical features were performed using paired dimension classes (by decreasing the dimension of larger higher group data randomly, as detailed in chapter 5). Each statistical analysis was performed five times for the different factors, in order to ensure the consistency of the results .

6.3 Results

6.3.1 Gender

Taking into consideration the clinical information from the entire dataset of healthy volunteers and patients (**Table 6-1** and **Table 6-2**), the analysis was paired according to the smallest group available (15 males from control group) and the data organised according to gender into: females from control group (n=15), males from control group (n=15), females from patient group (n=15) and males from patient group (n=15). The PLSDA did not show any statistical influence of the gender of the groups, which was further confirmed through the cross validated probability prediction plot (**Figure 6.1**). However, some outliers (misclassification) could be seen in the control group in comparison to the patient group, perhaps due to the higher variability of healthy volunteers samples and the smaller variability of PMOLs/OSCC saliva samples. The sensitivity and specificity obtained by this model was generally poor, and illustrated in **Table 6-3**.

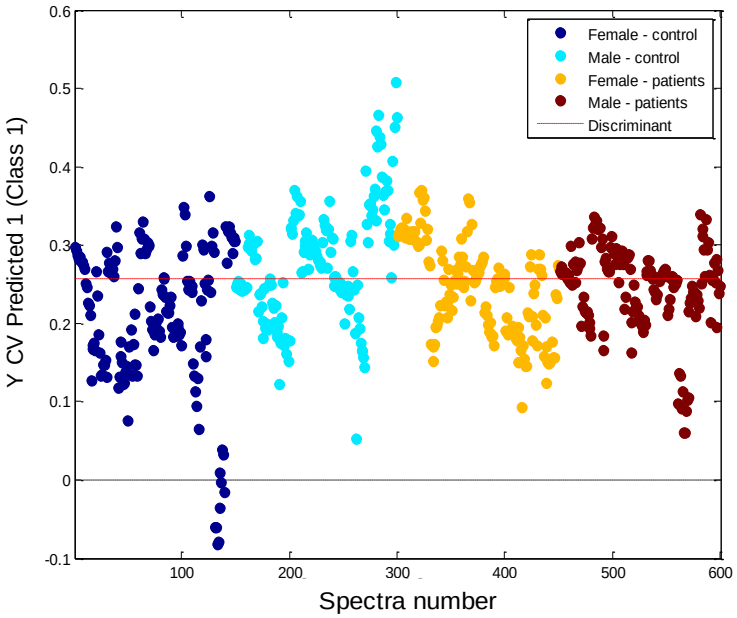

Figure 6.1: Cross validated probability prediction plot showing no discrimination between the female controls, male controls, female patients and male patients.

Table 6-3: **S**ensitivity and specificity from PLSDA classification when differentiating the different genders from group control and patients.

	Female (control)	**Male (control)**	**Female (patients)**	**Male (patients)**
Sensitivity (%)	37	55	56	38
Specificity (%)	44	48	72	69

In terms of ROC curves, the PLSDA results did not show classification based on gender, indicating poor accuracy for all the classifiers (**Figure 6.2**).

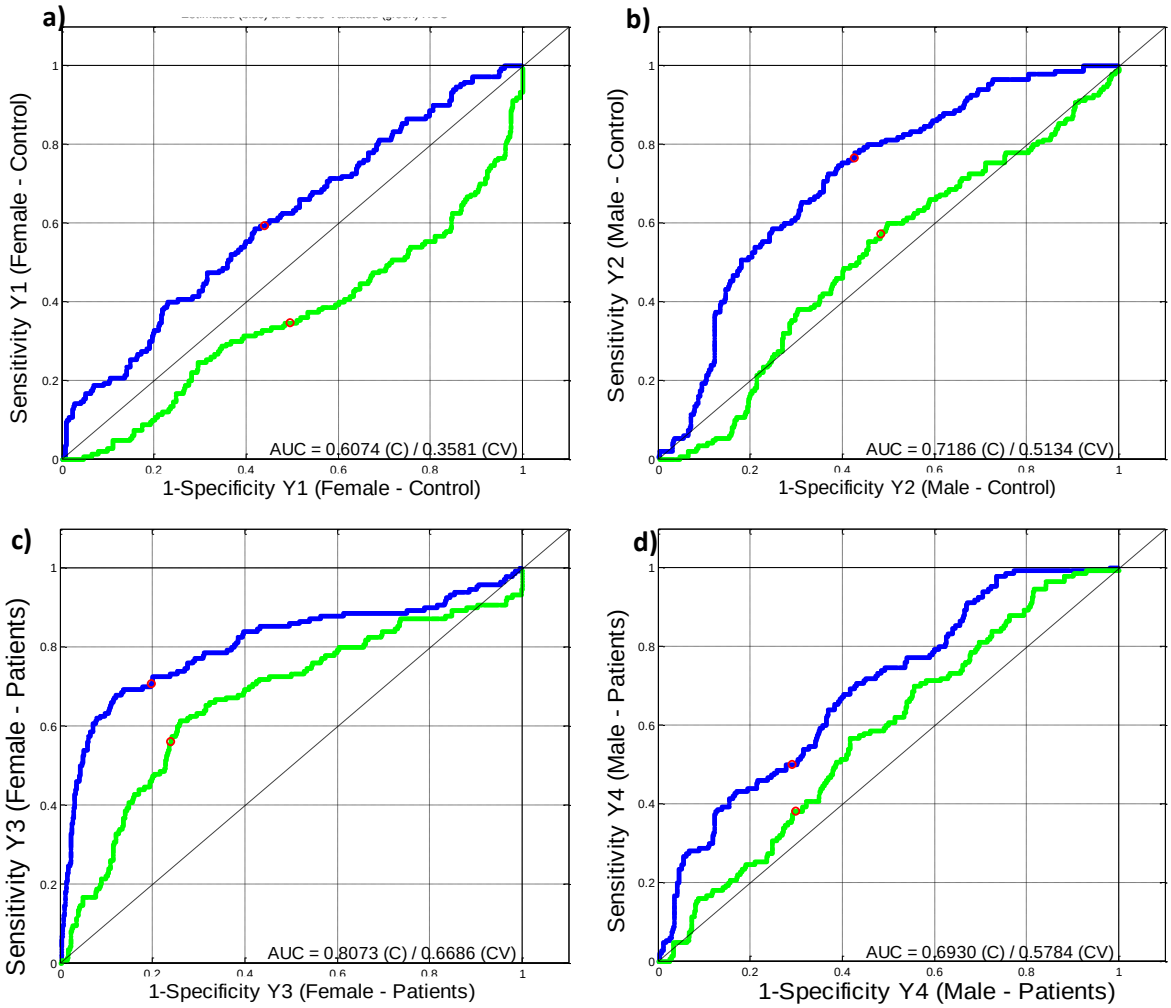

Figure 6.2: ROC curves for (**a**) male controls, (**b**) female controls, (**c**) male patients and (**d**) female patients classification.

To further understand the influence of gender on the whole dataset, the scores of PLSDA latent variables, LV-1 and LV-2, for detection of PMOLs/OSCC (from chapter 5) were plotted (**Figure 6.3a**) and then re-coloured according to the gender profile of each variable (**Figure 6.3b**). This further reveals the lack of influence of the gender on the classification of dysplastic samples.

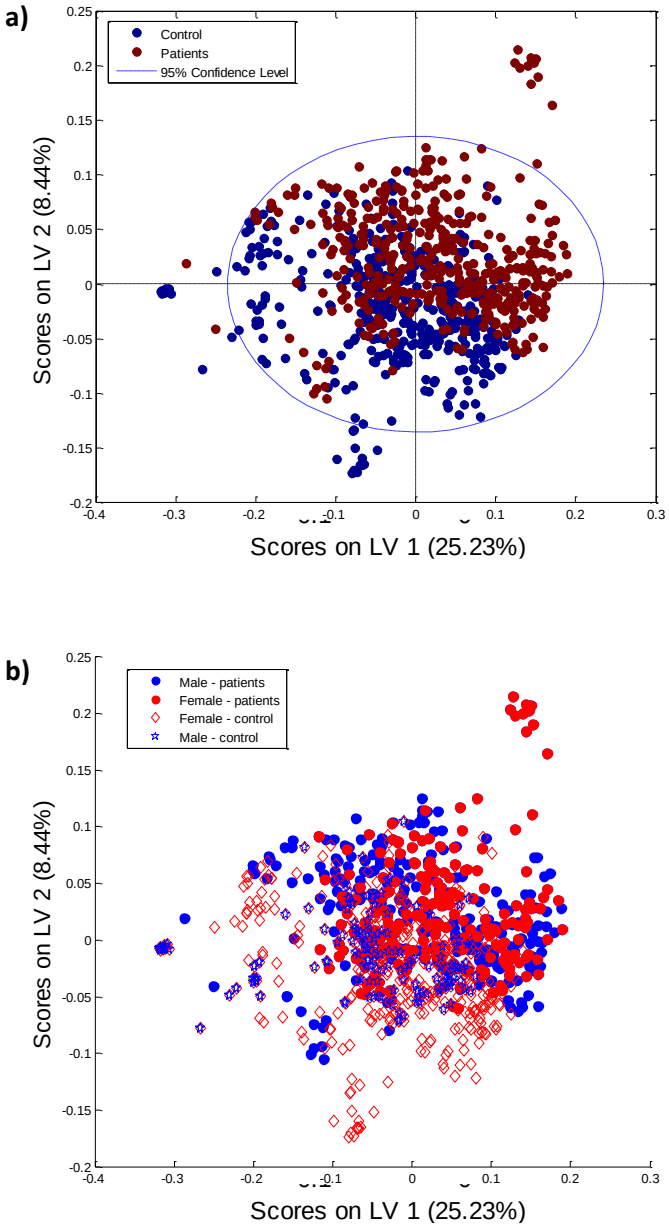

Figure 6.3: Scores of controls and patients on the latent variables from the PLSDA model (**a**) further coloured according to gender (**b**).

6.3.2 Age

Any potential influence of age on the classification was also analysed, as it could be a possible clinical feature with some reasonable impact over the classification. To match with the age average of OSCC incidence and salivary profile changes, a group with five

classes was created to explore possible interferences on the classification: healthy individuals below 30 years of age (n=4), healthy individuals between 30 and 50 years of age (n=4), healthy individuals above 50 years of age (n=4), patients 50 years of age or below (n=4) and patients above 50 years of age (n= 4). These group dimensions were determined by the number of the smallest age group available (4 controls above 50 years of age) and, due to the absence of patients below 30 years of age, the patients were only divided into two groups.

Some differentiation could be noticed through the cross validated probability prediction plot (**Figure 6.4**). When LV-1 was plotted (**Figure 6.5**), the spectral profile responsible for this differentiation was very similar to the one presented in chapter 5 (**Figure 5.5**) which further confirmed that the differentiation could be attributed to the dysplastic profile of these samples and not due to the age. Nevertheless, PLSDA results did not show significant statistical results, as poor sensitivity and specificity was generally obtained for each class (**Table 6-4**).

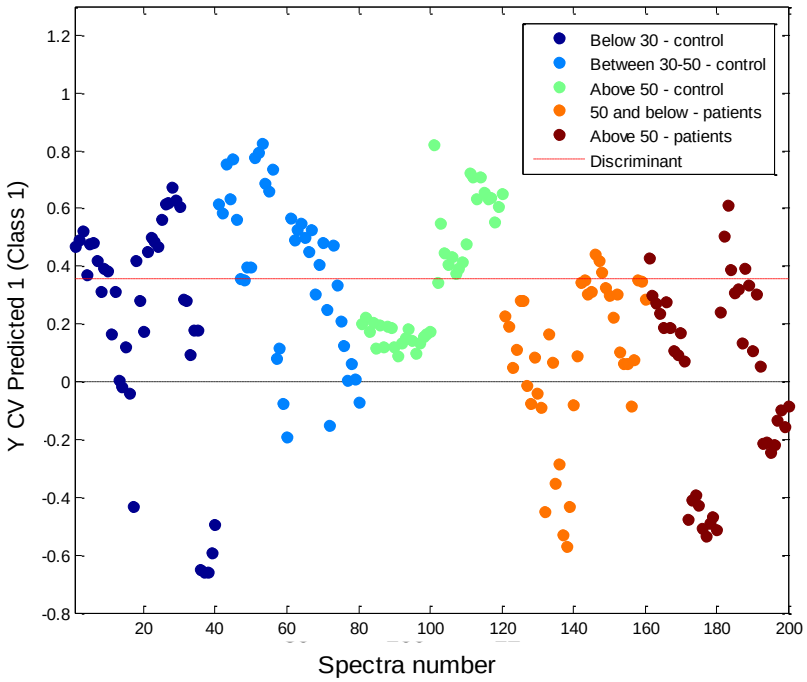

Figure 6.4: Cross validated probability prediction plot showing the discrimination between the different age groups from controls and patients.

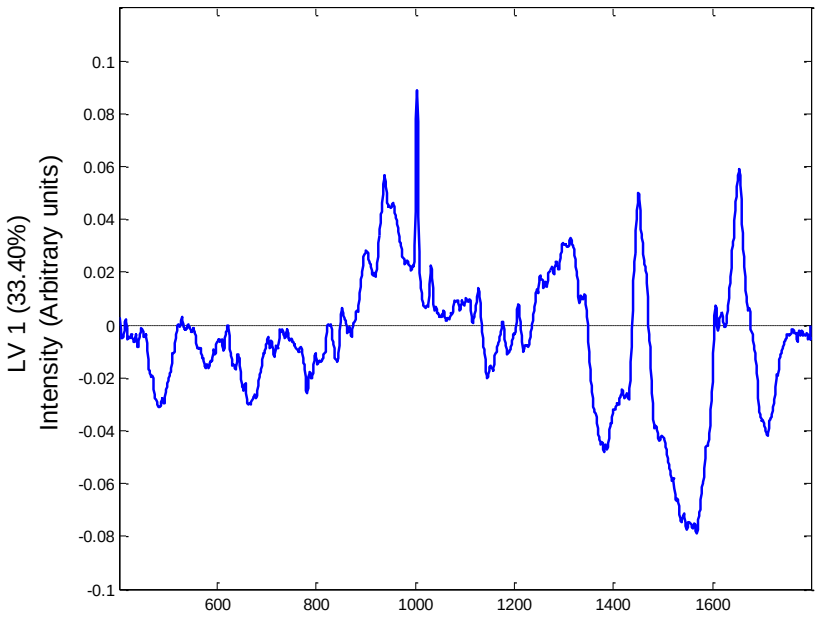

Figure 6.5: LV-1 of PLSDA model which included the different age groups.

Table 6-4: **S**ensitivity and specificity from PLSDA classification when differentiating healthy individuals (control) and patients in the different age groups.

	Above 50yo (control)	**30-50yo (control)**	**Below 30yo (control)**	**50 or below (patients)**	**Above 50 (patients)**
Sensitivity (%)	50	57	3	62	47
Specificity (%)	66	85	58	86	85

Also, the ROC curves (**Figure 6.6**) showed no significant accuracy of the different classifiers: controls below 30 years of age (AUC= 0.5492), controls between 30 and 50 years of age (AUC=0.7173), controls above 50 years of age (AUC=0.2748), patients 50 years of age or below (AUC=0.8523) and patients above 50 years of age (AUC=0.8083). These results seem to reflect the high capability of the analysis in detecting the dysplastic samples rather than the different age groups.

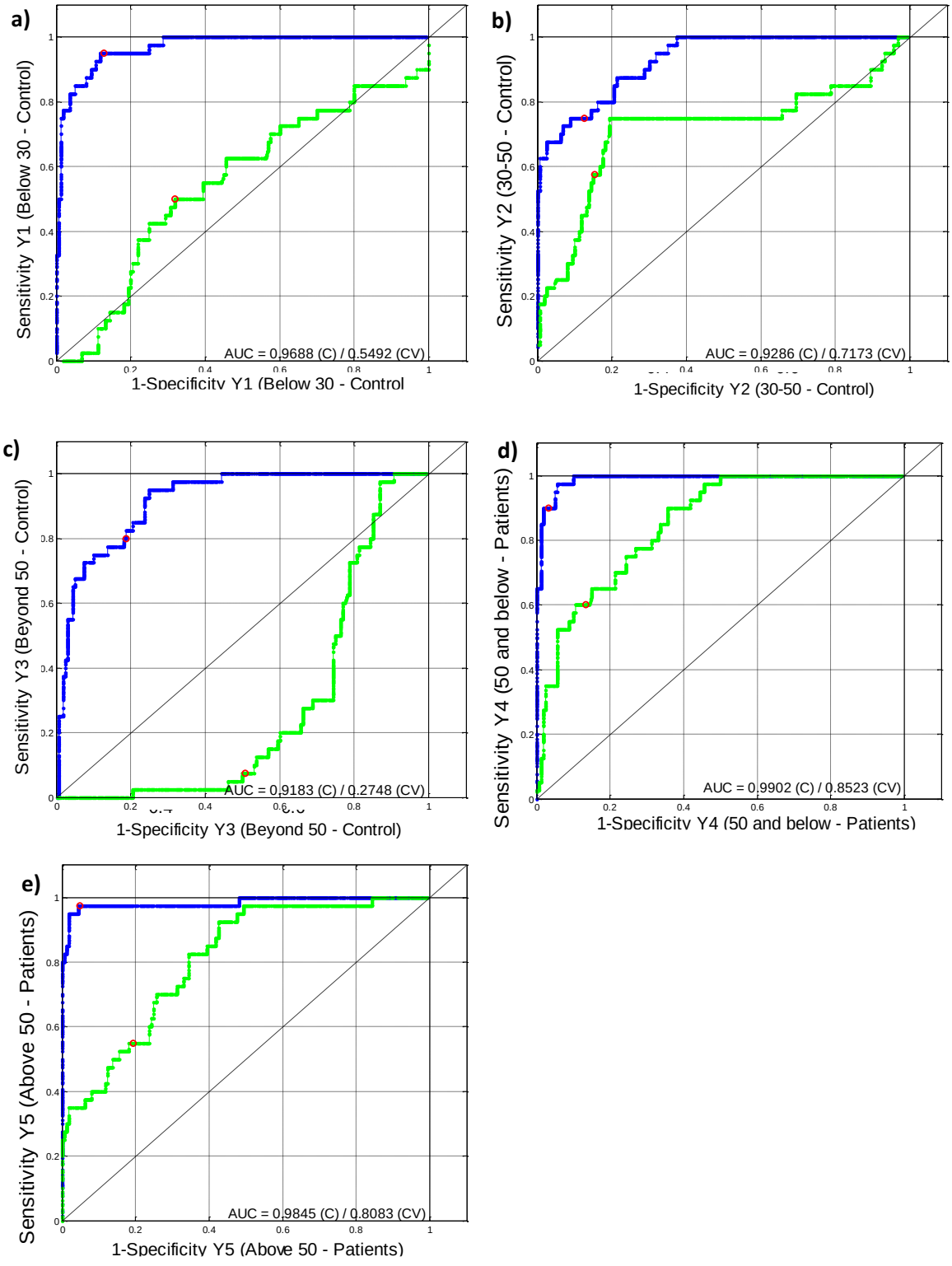

Figure 6.6: ROC curves for the classification of (**a**) individuals below 30 years of age, (**b**) between 30 and 50 years of age and (**c**) above 50 years of age, (**d**) patients at 50 years of age or below and (**e**) patients above 50 years of age.

Furthermore, the scatter plot of the scores of LV-1 and LV-2 based on the PLSDA discrimination of dysplastic samples (**Figure 6.7**), when re-coloured for the different age groups (**Figure 6.7**), did not show a major influence of the age on the analysis.

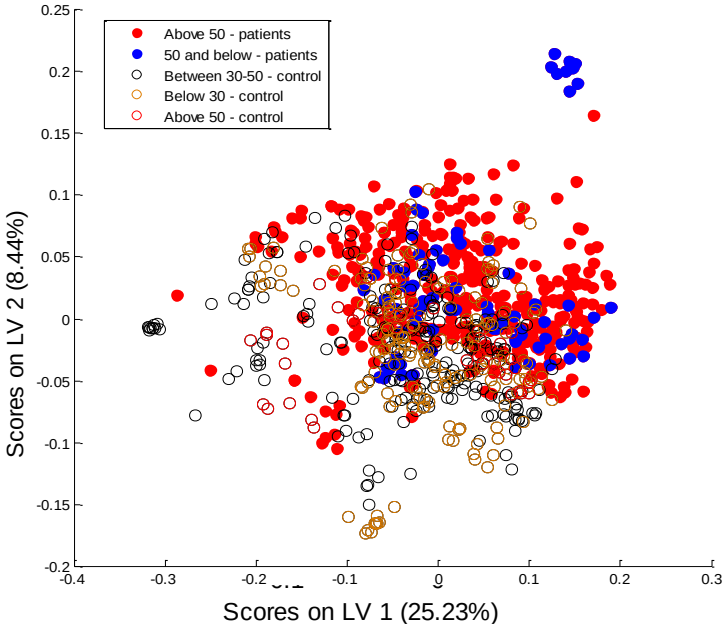

Figure 6.7: Scores of controls and patients on the latent variables from PLSDA model further coloured according to the different groups of age.

6.3.3 Smoking

According to the smoking status of the controls in **Table 6-5**, a PLSDA according to four classes, smoker controls (n=7), non smoker controls (n=7), smoker patients (n=7) and non smoker patients (n=7) was also conducted. The PLSDA results showed no clear classification amongst the different groups, according to the cross validated probability prediction plot (**Figure 6.8**). Also, the sensitivity and specificity of this model was considered poor, albeit with a sensitivity of 66% for non smoker controls (**Table 6-5**).

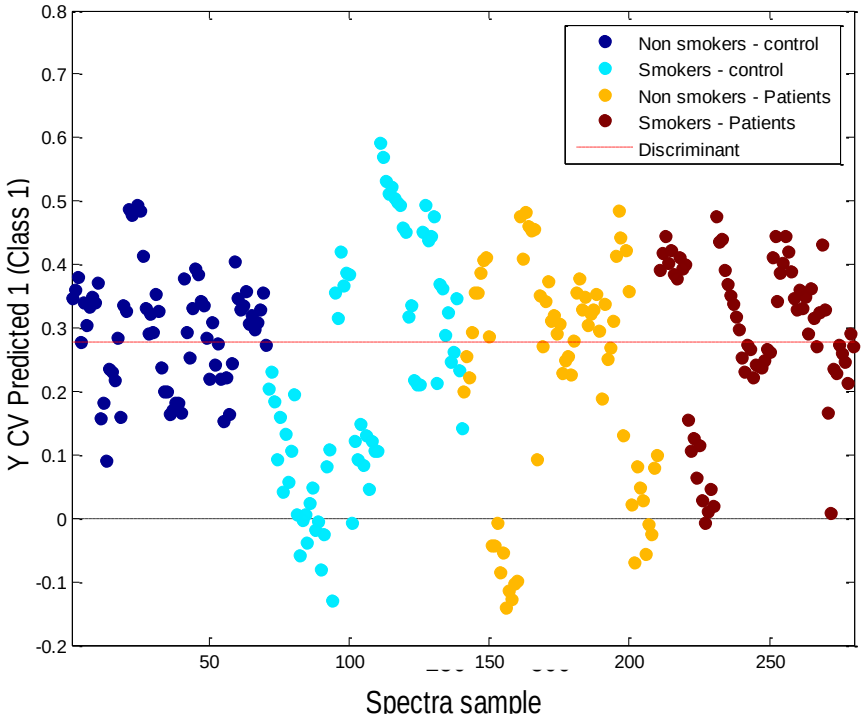

Figure 6.8: Cross validated probability prediction plot showing the discrimination between smokers and non smokers from controls and patients.

Table 6-5: **S**ensitivity and specificity from PLSDA classification when differentiating smoker and non smoker individuals from control and patient group.

	Non smokers (control)	**Smokers (control)**	**Non smokers (control)**	**Smokers (patients)**
Sensitivity (%)	61	54	44	31
Specificity (%)	51	78	74	77

Although, there was no clear classification, it was noticeable that the smoker control and patient groups seemed to exhibit a high degree of misclassification, which could represent a possible influence for the differentiation of smoking and the dysplastic profile of the samples from smoker patients.

For this reason, PLSDA was first performed separately for the controls, to examine the possible cause of this misclassification. The PLSDA results showed low classification sensitivity (68%) and specificity (60%) when differentiating these two categories. Although low, this differentiation could be visualised through the cross validated probability prediction plot (**Figure 6.9a**). The LV-1, responsible for 27.54 % of the variability, indicated that the classification seemed to be mainly associated with peaks at 789 and 1696 cm^{-1} in the positive side (**Figure 6.9a**). Most importantly, the peaks that could be correlated to smoking habit (negative side) could be seen at 1003 (Phenylalanine, C-C skeletal), 1125 (υ (C-C) skeletal of acyl backbone in lipid), 1448 (CH_2CH_3 deformation) and 1659 cm^{-1} (disulfide bonds).

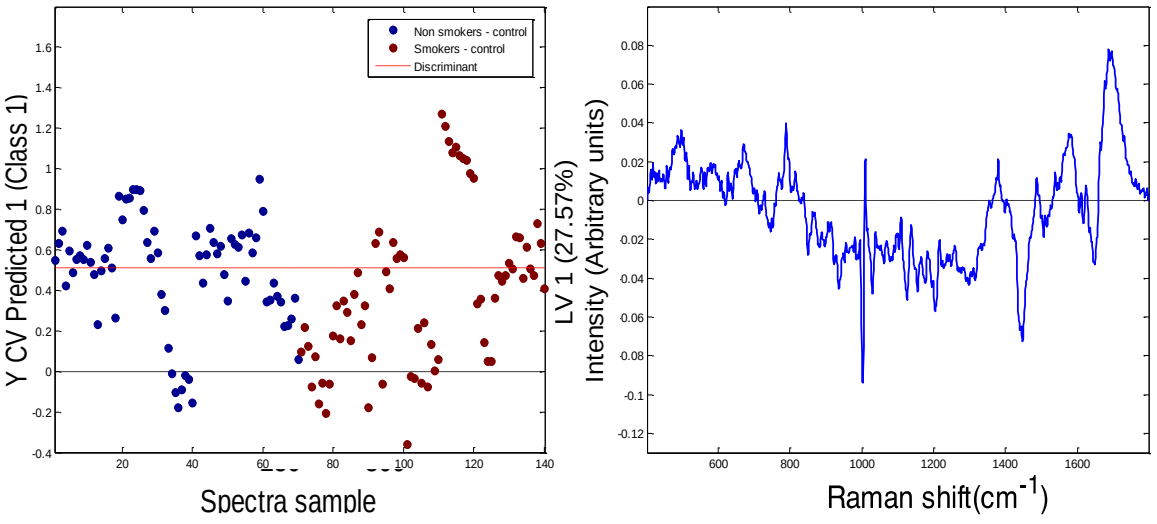

Figure 6.9: Plot of the (**a**) cross validated probability prediction showing the discrimination between non-smokers and smokers and (**b**) PLSDA LV-1.

Furthermore, the ROC curves showed low accuracy (AUC=0.6171) of the classifiers for smokers and non smokers (**Figure 6.10**).

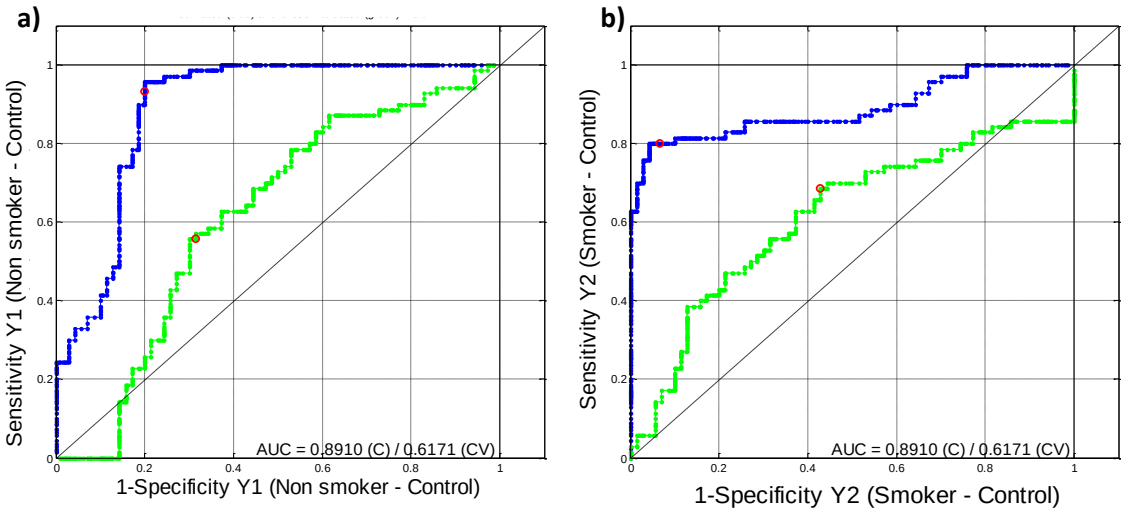

Figure 6.10: ROC curves for saliva samples of controls (**a**) non smokers and (**b**) smokers.

Also, to ensure that smoking was not a habit that could influence the classification in the patient data, a PLSDA of smoking as a clinical factor was also performed using the patient data. Knowing the complexity of the interaction between smoking habits and the salivary profile/state, the analysis of smoking habits for the patient data was performed using different classes: No-smokers (n=12), ex-smokers (n=12) and smokers (n=12) (this could not be performed with the data of controls due to the absence of declared ex-smokers within the healthy volunteers). When analysed by PLSDA, the cross validated probability prediction plot did not show a clear differentiation between the different groups (**Figure 6.11a**). Also, when LV-1 was plotted, the small differences that could be detected by this method showed that the spectral profile was very similar to those cited in the LV-1 for controls (**Figure 6.11b**), with the exception of the peak at 921 cm^{-1} (C-C stretch/Proline). Also, the groups exhibited very poor sensitivity for either of the classes (**Table 6-6**).

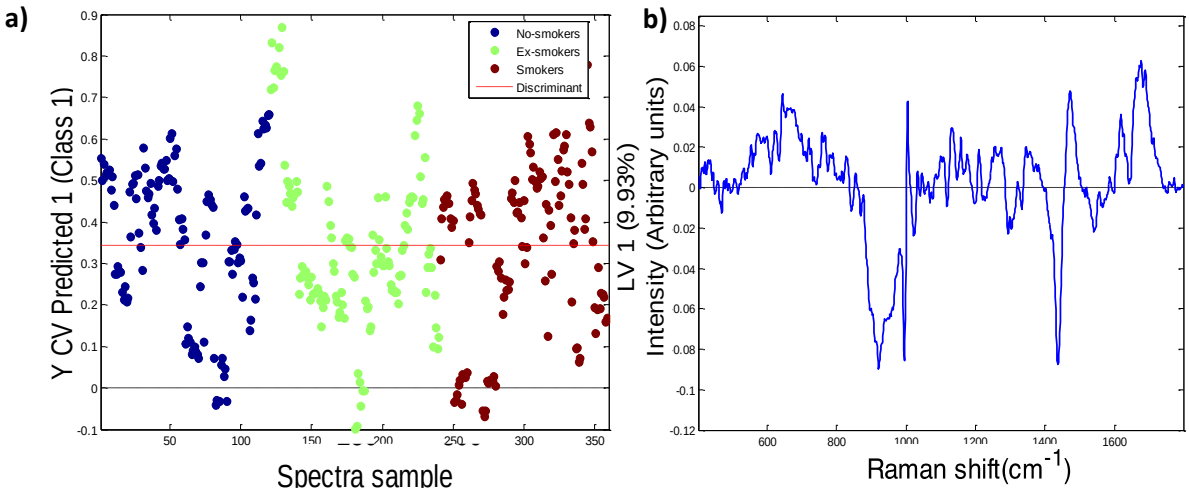

Figure 6.11: Plot of the (**a**) cross validated probability prediction showing the discrimination between non-smokers, ex-smokers and smokers; and (**b**) PLSDA LV-1 from patients' saliva samples.

Table 6-6: **S**ensitivity and specificity from PLSDA classification when differentiating no-smokers, ex-smokers and smokers amongst the patient group.

	Non-smokers	**Ex-smokers**	**Smokers**
Sensitivity (%)	58	56	32
Specificity (%)	52	75	72

In terms of accuracy, the ROC curves, in **Figure 6.12**, provided low values for all classifiers: non-smokers (AUC=0.5631), ex-smokers (AUC=0.6241) and smokers (AUC=0.5979).

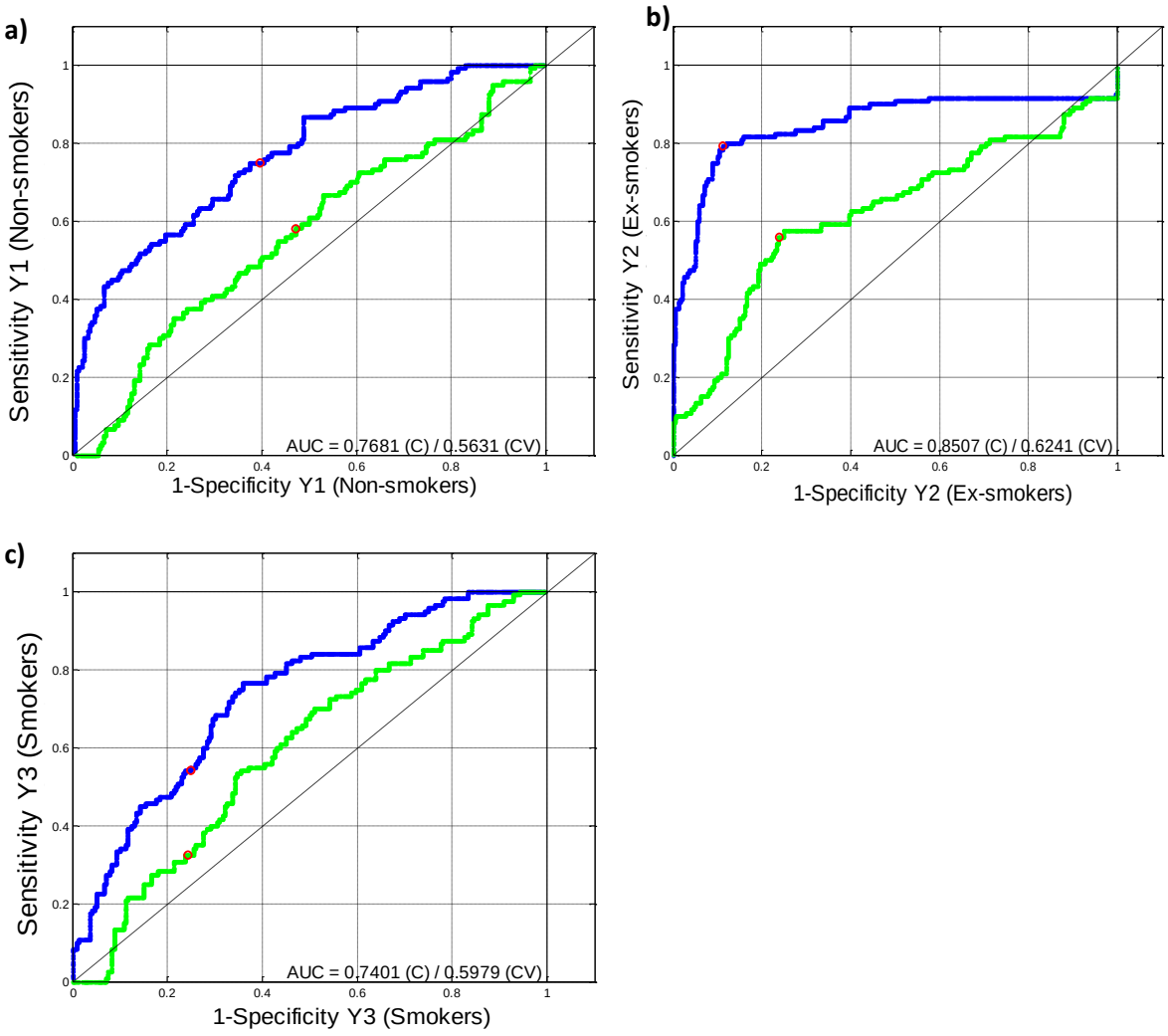

Figure 6.12: ROC curves for the classification of (**a**), no-smokers, (**b**) ex-smokers and (**c**) smokers.

Although the results show no clear influence of smoking on the classification, the LV-1 and LV-2 scores from PLSDA of the controls and patients were also plotted and coloured by smoking status to further understand the source of the variance (**Figure 6.13**). When visualised, the LV-1 and LV-2 scatter plot exhibits a tendency to differentiate patients (independent of smoking status) and smokers (control), from non smokers from the control group. This fact, however, might re-inforce the importance of smoking for the classification of saliva samples.

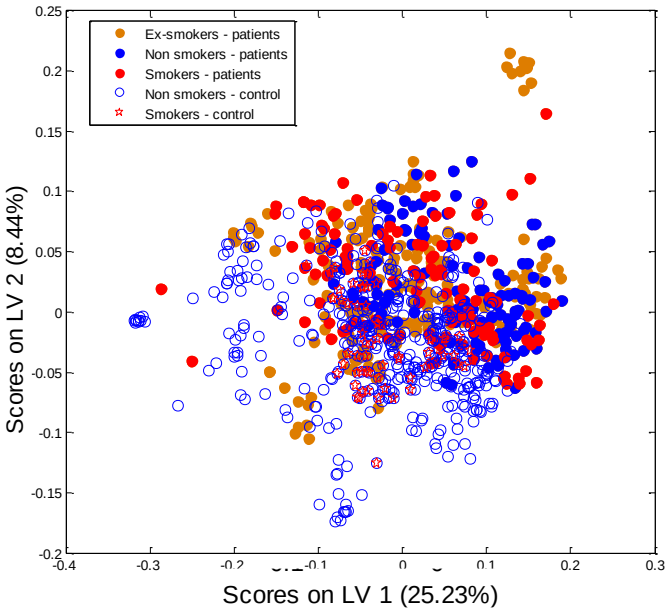

Figure 6.13: Scores of controls and patients on the latent variables from PLSDA model further coloured according to the smoking status.

6.3.4 Alcohol consumption

The alcohol consumption within the control group had a significant range. Simplifying the analysis, as the data numbers were not large, they were organised in four classes: alcohol consuming controls (n=12), non-alcohol consuming controls (n=12), alcohol consuming patients (n=12) and non-alcohol consuming patients (n=12). According to the PLSDA results, no significant discrimination was evident, as sensitivity and specificity were very poor across the different groups (**Table 6-7**), and this was further validated by the cross validated probability prediction plot (**Figure 6.14**). The ROC curves (**Figure 6.15**) further ratified the results, showing a very low accuracy for all classifiers.

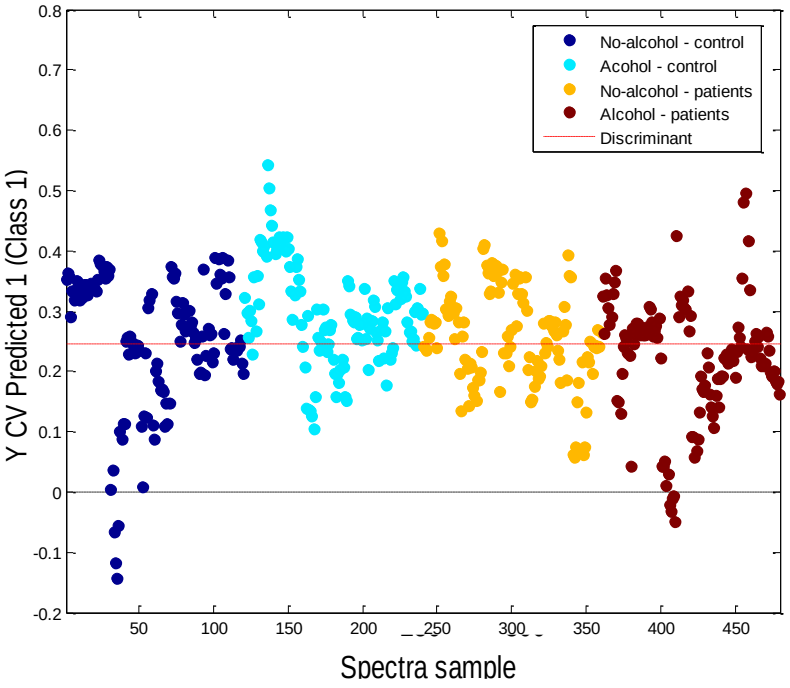

Figure 6.14: Cross validated probability prediction plot showing the discrimination between alcohol and non-alcohol consuming individuals from control groups and patient group.

Table 6-7: **S**ensitivity and specificity from PLSDA classification when differentiating between alcohol and non-alcohol consuming individuals from control groups and patient group.

	No-alcohol consuming (control)	**Alcohol consuming (control)**	**No-alcohol consuming (patients)**	**No-alcohol consuming (patients)**
Sensitivity (%)	64	41	30	50
Specificity (%)	40	51	63	69

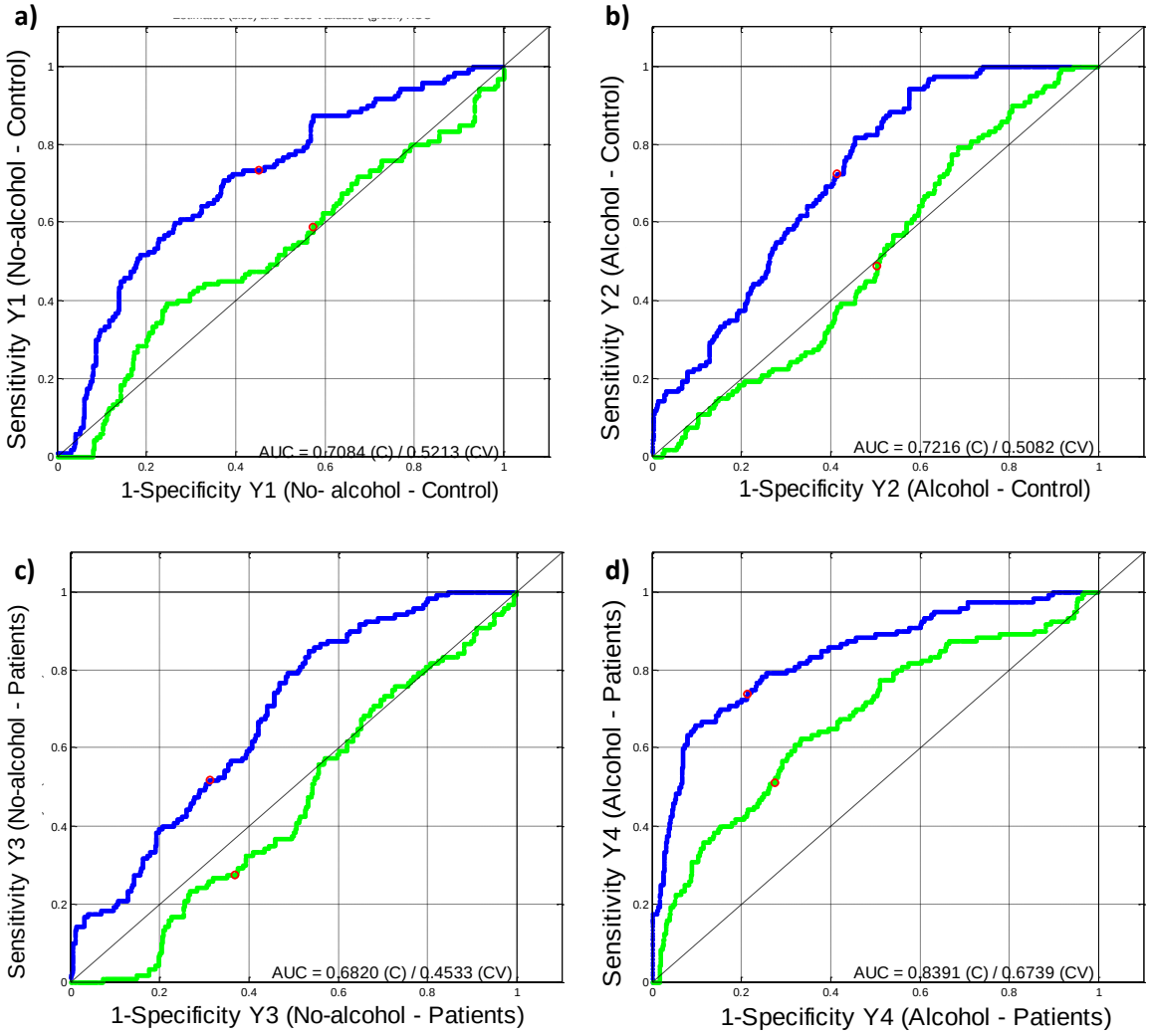

Figure 6.15: ROC curves for the classification of (**a**) alcohol consuming controls, (**b**) no alcohol consuming control, (**c**) alcohol consuming patients and (**d**) no alcohol consuming patients.

The scores of LV-1 and LV-2 from the PLSDA of the whole data involving controls and patients to differentiate dysplastic lesions did not show any influence of alcohol consumption on the classification (**Figure 6.16**).

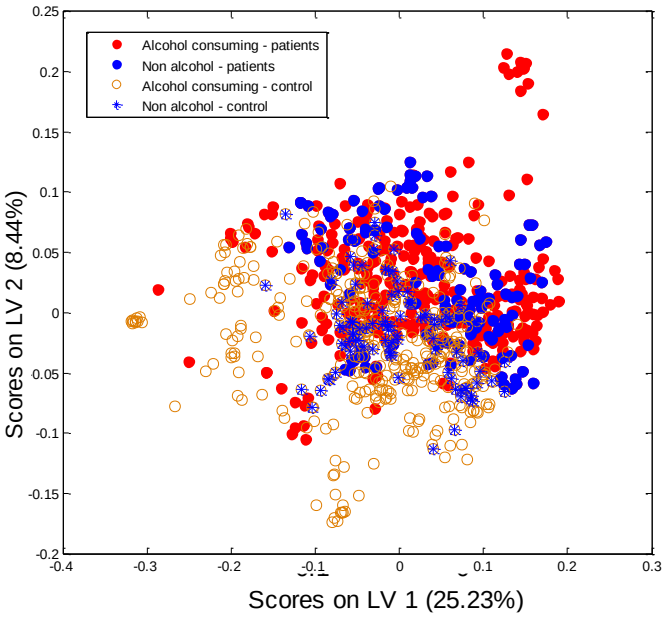

Figure 6.16: Scores of the between alcohol and non-alcohol consuming individuals from control group and patient group on the latent variables from PLSDA model.

6.4 Discussion

The findings of this chapter suggest that no clear influence on classification by PLSDA was evident, based on the following factors: gender, age and alcohol consumption. It is important, however, to observe that the PLSDA for the different age groups could show a tendency of differentiation based on the presence of dysplasia and not due to the age difference, as denoted by the LV-1 (**Figure 6.5**) from this analysis.

The risk of developing oral cancer has been shown to be related to both the intensity and duration of exposure to both alcohol and smoking[8]. The pathogenetic mechanisms behind alcohol-associated carcinogenesis in OSCC remain unclear, as alcohol is not carcinogenic. However, there is increasing evidence that a major part of the tumour-promoting action of alcohol might be mediated via its first, toxic and carcinogenic metabolite acetaldehyde[8].

In vitro studies have repeatedly shown that alcohol enhances the penetration of tobacco associated carcinogens across the oral mucosa[9]. Squier *et al.* showed that alcohol has the capacity to eliminate the lipid component of the barrier present in the oral cavity that surrounds the granules of the epithelial spinous layer, and short-term exposure to 15% alcohol increased the permeability of human ventral tongue mucosa, which could account for the synergic correlation between alcohol and smoking with the development of OSCC[9].

In saliva, salivary microbial production is supposed to be one of the major sources of acetaldehyde from ethanol[8]. This fact could be a biologically plausible mechanism to explain the synergistic and multiplicative manner by which the attributable cancer risks of alcohol and smoking act. However, the results obtained by PLSDA in this chapter were not able to point out any classification over the spectral profile of saliva and alcohol consumption.

It is already known that some acute effects depend on a direct action of ethanol and formation of reactive oxygen species and fatty acid ethyl esters[10]. This fact might be able to explain the absence of any major classification. Also, most of the salivary changes, with significant changes in parotid saliva secretion and its composition (which may perpetuate and compound ethanol-induced injury), can be only associated with chronic alcohol ingestion[11]. This situation could not be seen in the data presented here, however.

From the results obtained in this chapter, it is not apparent that factors other than the degree of dysplasia can influence the Raman classification of saliva samples. Although not statistically significant, smoking habit was seen to slightly impact the classification of data based on the distribution present on the cross validated probability prediction plot (**Figure 6.8**) and the scores of LV-1 and LV-2 plot (**Figure 6.13**). These results, reinforced by the spectral features provided by LV-1 from controls, are consistent with

other Raman studies in which researchers have shown that the saliva from smokers, especially stimulated saliva, not only contains significantly more proteins in oxidised form with increased disulfide bridges, that reduces protection for oral epithelium, but also could present changes in protein (mucin) conformation[12].

It is important to highlight that a lower impact of smoking habits over the model classification was seen when the patient data was analysed by itself. However, the plot of the scores of LV-1 and LV-2 (**Figure 6.13**) based on the classification of controls and dysplastic samples suggest that smoking might influence the classification. This could be attributed to the fact the smoking is an aetiological factor in developing epithelial oral dysplasia, and hence biochemical changes occurring in saliva of smokers could be similar to those patients with these lesions, whether smokers or not [13].

While it has been reported that age related physiological changes can be discriminated with Raman spectroscopy[14], the results obtained in this chapter did not show any statistical differences between the three age groups. This might be explained by the fact that most of the salivary changes in elderly individuals are primarily correlated only with the salivary flow rate[13]. The use of centrifugal filtration might partially even out the concentration of saliva components analysed, once the same amount of sample is used before spectral acquisition.

Other patient factors and clinical features which have not been considered, due to the lack of metadata, can still have some influence on the Raman classification. These would include the presence or absence of HPV and candida status of the donor/patient and the degree of differentiation in OSCC lesions.

Finally, these results suggest that it is very important when analysing saliva samples from individuals with or without oral pathologies to consider them in the context of different

factors and clinical features, highlighting the need for large scale studies with more representative dimensions.

References

1. Feller L, Chandran R, Khammissa RA, Meyerov R, Lemmer J. Alcohol and oral squamous cell carcinoma. SADJ. 2013;68:176-80.

2. Pelucchi C, Gallus S, Garavello W, Bosetti C, La Vecchia C. Cancer risk associated with alcohol and tobacco use: focus on upper aero-digestive tract and liver.Alcohol Res Health. 2006;29:193-8.

3. Marttila E, Uittamo J, Rusanen P, Lindqvist C, Salaspuro M, Rautemaa R. Acetaldehyde production and microbial colonization in oral squamous cell carcinoma and oral lichenoid disease. Oral Surg Oral Med Oral Pathol Oral Radiol. 2013;116:61-8.

4. Mehanna H, Paleri V, West CM, Nutting C. Head and neck cancer part1: epidemiology, presentation, and preservation. Clin Otolaryngol. 2011;36:65-8.

5. Perry BJ, Zammit AP, Lewandowski AW, Bashford JJ, Dragovic AS, Perry EJ, et al. Sites of origin of oral cavity cancer in nonsmokers vs smokers: possible evidence of dental trauma carcinogenesis and its importance compared with human papillomavirus. JAMA Otolaryngol Head Neck Surg. 2015;141:5-11.

6. Schipper RG, Silletti E, Vingerhoeds MH. Saliva as research material: biochemical, physicochemical and practical aspects. Arch Oral Biol 2007;52:1114–35

7. Talari ACS, Movasaghi Z, Rehman S, Rehman IU. Raman spectroscopy of biological tissues. Applied Spectroscopy Reviews, 2015,50(1):493-541.

8. Homann N, Tillonen J, Meurman JH, Rintamäki H, Lindqvist C, Rautio M, Jousimies-Somer H, Salaspuro M. Increased salivary acetaldehyde levels in heavy drinkers and smokers: a microbiological approach to oral cavity cancer. Carcinogenesis. 2000 Apr;21(4):663-8.

9. Squier CA, Cox P, Hall BK. Enhanced penetration of nitrosonornicotine across oral mucosa in the presence of ethanol. J Oral Pathol 1986;15:276–279.

10. Waszkiewicz N, Zalewska A, Szulc A, Kepka A, Konarzewska B, Zalewska-Szajda B, Chojnowska S, Waszkiel D, Zwierz K.Pol Merkur Lekarski. The influence of alcohol on the oral cavity, salivary glands and saliva. Pol Merkur Lekarski. 2011 Jan;30(175):69-74.

11. Dutta SK, Orestes M, Vengulekur S, Kwo P. Ethanol and human saliva: effect of chronic alcoholism on flow rate, composition, and epidermal growth factor. Am J Gastroenterol. 1992 Mar;87(3):350-4.

12. Taniguchi M, Iizuka J, Murata Y, et al. Multimolecular salivary mucin complex is altered in saliva of cigarette smokers: detection of disulfide bridges by Raman spectroscopy. Biomed Res Int. 2013;2013:168765. doi:10.1155/2013/168765

13. Singh SP, Deshmukh A, Chaturvedi P, Murali Krishna C. In vivo Raman spectroscopic identification of premalignant lesions in oral buccal mucosa. J Biomed Opt. 2012 Oct;17(10):105002. doi: 10.1117/1.JBO.17.10.105002.

14. Affoo RH, Foley N, Garrick R, Siqueira WL, Martin RE. Meta-Analysis of Salivary Flow Rates in Young and Older Adults. J Am Geriatr Soc. 2015 Oct;63(10):2142-51. doi: 10.1111/jgs.13652. Epub 2015 Oct 12.

Chapter 7: Conclusions and future work

7.1 Conclusions

The main objective of this thesis was to assess the potential of Raman spectroscopy in detecting oral epithelial dysplasia and OSCC through the analysis of saliva samples. The first two chapters presented an introduction to the thesis; Chapter 1 had a strong emphasis on OSCC, oral dysplasia and saliva, while the chapter 2a placed the emphasis on Raman spectroscopy and its importance in diagnostics, mainly oral cancer diagnosis. Integrating the first two chapters, chapter 2b aimed to clarify the current state-of-art through a systematic review the available and published methodology related to Raman spectral analysis of saliva for oral cancer detection, emphasising instrumental, analytical and sample parameters. The systematic review indicated that the 785 nm laser line was the most applied wavelength and PCA-LDA was the most commonly used method for multivariate analysis. The main salivary components possibly associated with the presence of OSCC were proteins and lipids. The measurement of saliva samples in the liquid physical state, and with no addition of enhancers for SERS, was also highlighted as a better approach. However, in terms of sampling protocols, some issues still needed to be addressed, as no differentiation was generally made between stimulated and non stimulated saliva.

In chapter 3, the aim was to establish the best instrumentation method to be applied to saliva samples, minimising as much as possible the sample preparation steps and, consequently, loss of saliva integrity. Regarding the most suitable wavelength, 532nm as laser line has shown the best results in terms of spectral quality and resolution. Moreover, an inverted geometry associated with a glass bottomed 96 well-plate (no.1 coverslip

thickness) with x60 objective provided a cleaner spectral signal and may be adopted as a high throughput method for use in a clinical application. Also, concentration of the saliva by >75% has been shown to be effective in overcoming the inherent weakness of the spectral signatures of the constituent components of saliva in the liquid form, ratifying the use of centrifugal filtration to concentrate real saliva samples.

Chapter 4 addressed the capability of Raman microspectroscopy to differentiate the saliva based on the collection methodology and intrinsic salivary composition. The Raman profiles from the groups of stimulated saliva and non stimulated saliva showed that, although having differences regarding concentration, both types of saliva collections can be used for diagnosis purposes without major differences. However, the stimulated type can be used as a more efficient technique for sample collection, as the non stimulated method would represent a time consuming procedure to be applied in the clinical environment (45 minutes for non stimulated saliva collection compared to 15 minutes for stimulated saliva collection). Regarding the multivariate analysis, PLSDA could provide a classification of good sensitivity for both types of sample, with the highest sensitivity reached when classifying samples from different donors (88%). The feasibility of Raman microspectroscopy for classification of non stimulated and stimulated samples confirms its capability for detection of biochemical changes that may also be applied to differentiate saliva samples from individuals with oral cancer/potentially malignant lesions and saliva samples from healthy individuals.

In chapter 5, saliva samples from a cohort of patients with OSCC and different grades of dysplasia (mild, moderate and severe) were assessed through Raman spectroscopy and multivariate analysis (PLSDA with LOPOCV). The results demonstrated that dysplastic samples, in general, could be discriminated from control (healthy volunteers saliva samples) with an outstanding accuracy (AUC=0.9444)[1]. However, the results involving

discrimination of the oral epithelial dysplasia saliva samples did not show the same high performance, although better results were obtained for higher grade oral epithelial dysplasia samples and in cases where the matrices had the same dimensions (either artificially increased or paired by decreasing the numbers) before the statistical analysis.

Chapter 6 investigated other factors which could have an influence on saliva samples and, consequently, on the Raman spectral discrimination. The results showed that that no clear classification could be seen based on gender, age, smoking habits and alcohol consumption. However, smoking habits seemed to somehow influence the data, mainly when comparing controls to patients.

7.2 Clinical relevance and other considerations

From a clinical perspective, there is a constant interest in saliva as an alternative diagnostic sample and Raman spectroscopy as diagnostic aid. However, several factors need to be evaluated and further elucidated surrounding both approaches before its clinical application. In salivary analysis as such, a correct standardisation regarding collection, storage and processing is the foundation for a reproducible and faithful technique. Saliva has been successfully applied in other studies to diagnose OSCC/oral potential malignant lesions[2-4]. Keeping the natural physical state of saliva (liquid) is indubitably crucial to preserve possible salivary markers that might be substantial to the detection of oral cancer. In chapter 3, beyond other aspects, the centrifugal filtration can not only preserve the sample in its liquid state but can also represent a cheaper method of "enhancing" the major components of saliva than, for example, nanoparticle enhancers. Also, saliva samples and the Raman technique, when combined, could not only represent a tool for a dental/medical qualified professional but also a screening method that can be

performed by a non dental/medical qualified person, optimising the time of diagnosis and improving the prognosis.

7.3 Future perspectives

Taking into consideration the different approaches related to Raman analysis of saliva samples in the current literature, the methodology proposed by the current study seems to be highly flexible for a future clinical application. However, the number of saliva samples used for these analyses were comprised of 55 healthy controls and 45 patients. Also, in general terms, a limitation of this study was that the controls and patients were not completely matched in terms of age, gender, etc. A more comprehensive study of larger scale[5] may not only result in more effective classifiers (mainly for classification of the different dysplasia grades) but could also better demonstrate the influence of variables such as age, smoking, alcohol consumption, and so on. Also, a better insight could be also obtained from a longitudinal study where dysplastic lesions had transformed into OSCC or regressed to complete absence of dysplasia. As morphology is not a predictor of malignant transformations, Raman spectroscopy could help identifying molecular bonds that are common to several biomolecules through a spectral analysis of the saliva samples in a holistic or more complete way, usually required for the subtle biochemical changes in dysplasia/cancer[6].

In terms of sample preservation, saliva samples have always been a hot topic of discussion in terms of reproducibility. Raman spectroscopy, as mass spectrometry, might need a more tailored methodology for saliva collection and saliva processing. However, the less sample preparation required the higher the chances of a future clinical application of the technique in question. The results have shown a wide variety of instrumentation setups and sample collections. Nevertheless, other factors such as the use of protease inhibitors for saliva conservation and the effects of laser irradiation on sample degradation could

also be important for the reproducibility required before the technique could be accepted as a diagnostic tool[7,8].

Also, the intimate relationship of the salivary glands to the local vascular system network and its reflection in the saliva profile represents an unknown that still has to be better analysed when saliva is used as a diagnostic sample. Defining the properties that are strictly correlated to systemic diseases and those that are strictly correlated to local pathologies is not only essential, but they might represent the missing scientific "breakthrough" for the permanent establishment of saliva as a diagnostic sample.

Finally, it is difficult to compare the studies involving Raman spectroscopy of saliva samples, as the sample collection and preservation, instrumentation, processing of the spectra and data analysis differ between different studies[9]. The disparities in methodologies, unfortunately, widen the steps in bringing Raman spectroscopy closer to a formal clinical application.

However, despite the acknowledged limitations, this current study was successful in establishing new foundations for saliva concentration, Raman spectrum acquisition, processing and Raman data analysis. The standardisation of Raman methodology for saliva analysis represents a reliable and reproducible pathway to be translated into clinics. Also, the advantages associated with the Raman technique, such as its label-free and non-invasive nature; along with the rich biomolecular information of saliva samples suggest great potential for the future of the oral medicine diagnostic field.

References

1. Hajian-Tilaki K. Receiver Operating Characteristic (ROC) Curve Analysis for Medical Diagnostic Test Evaluation. Caspian J Intern Med. 2013;4(2):627–635.

2. Connolly JM, Davies K, Kazakeviciute A, Wheatley AM, Dockery P, Keogh I, Olivo M. Non-invasive and label-free detection of oral squamous cell carcinoma using saliva surface-enhanced Raman spectroscopy and multivariate analysis. Nanomedicine. 2016 Aug;12(6):1593-601. doi: 10.1016/j.nano.2016.02.021. Epub 2016 Mar 23.

3. Rekha P, Aruna P, Brindha E, Koteeswaran D, Baludavid M, Ganesan S. Near-infrared Raman spectroscopic characterization of salivary metabolites in the discrimination of normal from oral premalignant and malignant conditions. J Raman Spectrosc. 2015, 47:763-772.S.

4. Jaychandran S, Meenapriya PK, Ganesan S. Raman Spectroscopic Analysis of Blood, Urine, Saliva and Tissue of Oral Potentially Malignant Disorders and Malignancy-A Diagnostic Study. Int J Oral Craniofac Sci 2016, 2(1): 011-014.

5. Beleites C, Neugebauer U, Bocklitz T, Krafft C, Popp J. Sample Size Planning for Classification Models. Analytica Chimica Acta, 2013,760:25–33.

6. Jermyn M, Desroches J, Aubertin K, St-Arnaud K, Madore WJ, De Montigny E, Guiot MC, Trudel D, Wilson BC, Petrecca K, Leblond F. A review of Raman spectroscopy advances with an emphasis on clinical translation challenges in oncology. Phys Med Biol. 2016 Dec 7;61(23):R370-R400. Epub 2016 Nov 2.

7. Golatowski C, Salazar MG, Dhople VM, Hammer E, Kocher T, Jehmlich N, Völker U. Comparative evaluation of saliva collection methods for proteome analysis. Clin Chim Acta. 2013;18;419:42-6. doi: 10.1016/j.cca.2013.01.013. Epub 2013 Feb

8. Mohamed R, Campbell JL, Cooper-White J, Dimeski G, Punyadeera C. The impact of saliva collection and processing methods on CRP, IgE, and Myoglobin immunoassays. Clin Transl Med. 2012;1(1):19. Published 2012 Sep 5. doi:10.1186/2001-1326-1-19

9. Calado G, Behl I, Daniel A, Byrne HJ, Lyng FM. Raman spectroscopic analysis of saliva for the diagnosis of oral cancer: a systematic review. Translational Biophotonics. Accepted for publication in August/2019.

Appendix I – Participant consent and Ethical approval from DIT (now TU Dublin)

Participant Information Leaflet

(HEALTHY VOLUNTEERS)

Names of researchers:

Prof Fiona Lyng, Dublin Institute of Technology

Mr Genecy Calado, PhD student, Dublin Institute of Technology

Title of study:

"Investigation of saliva samples using Raman spectroscopy"

Introduction

We have a mouth cancer research project which has been funded by Science without Borders and we would be grateful for your assistance.

Mouth cancer ranks as the 15th most common cancer in the world and 10th most frequent in males. It accounts for ~2.1% of total cancer cases worldwide. The 5 year survival rate is approximately 80% for early stage disease but only approximately 20% for late stage disease and patients often present with advanced disease. Early detection of mouth cancer or pre-cancer greatly increases the chances for successful treatment. Bio fluids such as blood, urine, and saliva can provide information about human health and are being widely investigated for clinical diagnosis of various diseases including oral cancers.

The purpose of our study is to investigate whether a novel technology using Raman spectroscopy can identify cancer or pre-cancer in a patient from a sample of their saliva. Raman spectroscopy is a form of laser technology which can produce a unique biochemical fingerprint of a sample when the light is shone on it and analysed. In the future, we would like to apply this technology to saliva samples taken from mouth cancer patients. We would first like to develop the methods using saliva from healthy volunteers.

You have been invited to take part as a healthy volunteer. Our study requires a sample of saliva.

You are completely at liberty to refuse to participate.

What will happen if I take part?

If you decide to take part, after rinsing your mouth with water, you will provide a saliva sample into a plastic container. The sample will frozen at -80^{o}C and will subsequently be analysed using Raman spectroscopy.

The samples and results will be anomymised and coded, so that they will not be identifiable as coming from you. The data will be transferred and stored on a single encrypted computer in the Dublin Institute of Technology. The samples will be destroyed 5 years after completion of the study. This is because Raman technology is relatively new and developing all the time, and we would like the opportunity to take advantage of any new developments in the Raman spectroscopy field in the near future. The data will only be available to the research team and will not be made available to any third parties. It will not be used for any other research other than that for which you have consented.

Possible benefits of the study.

There are no direct benefits to yourself, other than knowing that you have contributed to scientific research on mouth cancer prevention.

Possible risks to participants and after effects

There are no risks or side effects from donating a saliva sample.

What will happen to the results of the study

This project will contribute to a PhD (doctorate) degree and the results of the study will be published in scientific journals and presented at scientific meetings, with due consideration to confidentiality.

Confidentiality of information

Your identity will remain entirely confidential. Your name will not be published and will not be disclosed to anyone outside the study team. Your data and sample will be coded and anonymised and once this has been done, it will be transferred and stored securely on a dedicated, encrypted computer in the Dublin Institute of Technology and thereafter will not be traceable back to yourself.

Voluntary participation

We stress that you are **NOT obliged** to take part. If, after agreeing to assist in our mouth cancer research, you wish to withdraw from the study, all your samples and data will be destroyed.

Permission

Ethical approval has been obtained from Dublin Institute of Technology.

Further information and how to take part

The procedures will be explained to you, any questions that you have answered, and an informed consent form must then be signed by you if you agree to take part in this study.

Contact details of researchers

Prof. Fiona Lyng

Focas Research Institute

Dublin Institute of Technology, Kevin St

Tel 01 4027972

This study is covered by standard institutional indemnity insurance.

Nothing in this document restricts or curtails your rights.

The researchers declare no conflict of interest.

CONSENT FORM

(HEALTHY VOLUNTEERS)

Names of researchers:

Prof Fiona Lyng, Dublin Institute of Technology

Mr Genecy Calado, PhD student, Dublin Institute of Technology

Title of study:

"Investigation of saliva samples using Raman spectroscopy"

***BACKGROUND**:*

Our research involves the use of Raman technology to try to develop a new technique for early detection of mouth cancer and pre-cancer using saliva (see accompanying Patient Information Leaflet). To help us to develop the methods we need to take some saliva samples from healthy volunteers. We are asking your permission for a saliva sample.

Your data will be anonymised, coded, confidential, securely stored and will not be disclosed to third parties.

Voluntary participation

We stress that you are **NOT obliged** to take part. If, after agreeing to assist in our mouth cancer research, you wish to withdraw from the study, all samples and data will be destroyed

DECLARATION:

I have read, or had read to me, this consent form and the accompanying Patient Information Leaflet. I have had the opportunity to ask questions and all my questions have been answered to my satisfaction. I freely and voluntarily agree to be part of this research study, though without prejudice to my legal and ethical rights. I understand I may withdraw from the study at any time. I have received a copy of this agreement.

Participant's Name ……..

Contact Details:……..

……

Participant's Signature:……**Date:……**

Nothing in this document restricts or curtails your rights.

_____

I …….. the Researcher :

I have explained the nature and purpose of this research study, the procedures to be undertaken and any risks that may be involved. I have offered to answer any questions and fully answered such questions. I believe that the participant understands my explanation and has freely given informed consent.

Investigator's Signature:…… Date:……

Appendix II – Participant form from DIT (now TU Dublin)

Participant Form

Raman Micro-spectroscopic study of oral cancer

Name: Ms. Isha Behl & Mr.Genecy Calado

Supervisors: Prof.s Fiona Lyng and Hugh J. Byrne

Volunteer Number: _____

Date of Birth: ___/___/____

Gender: ☐ Male ☐ Female

Ethnicity[1]: ☐ White Irish or other White Background ☐ Black or Black Irish - African or other Black Background ☐ Asian or Asian Irish - Chinese or other Asian Background

Note:

_____

_____

_____

A) HABITS

1) Alcohol consumption:

a) How many units per week:

b) Time of last consumption:

2) Tobacco consumption:

a) Consumption in which form: ☐ Cigarettes ☐ Cigar ☐ Narquile (Shish)

Others: _____

b) How many/much per day:

c) Time of last consumption:

3) Sexual preferences:

a) Sexual Orientation: ☐ Heterosexual ☐ Homosexual ☐ Bisexual

b) Number of partners in last 3 months:

[1] According to Central Statistics Office, Ireland

4) Oral Hygiene:

a) Brushing: ☐ Yes ☐ No

If yes so, how many times per day: Last brushing:

b) Mouthwash: ☐ No ☐ Yes, Name:

If yes so, how many times per day: Last consumption:

e) Flossing: ☐ Yes ☐ No

If yes so, how often: Last flossing:

f) Periodontal disease: ☐ Gingivitis ☐ Periodontitis ☐ Unknown

Others: _____

g) Dry mouth: ☐ Yes ☐ No

If yes, reason: _____

f) How regularly do you see a dentist/oral hygienist?

When last visited:_____

B) MEDICAL CONDITION

1) Any known disease: ☐ No ☐ Yes,

_____ .

2) Medication (last consumption):

3) How do you consider your current state of health?

☐ Excellent

☐ Good

☐ Fair

☐ Poor

Annex I -

Volunteer Number: _____

Date of collection: ___/___/____ Time: _____

PHYSICAL EXAMINATION:

SAMPLE COLLECTION:

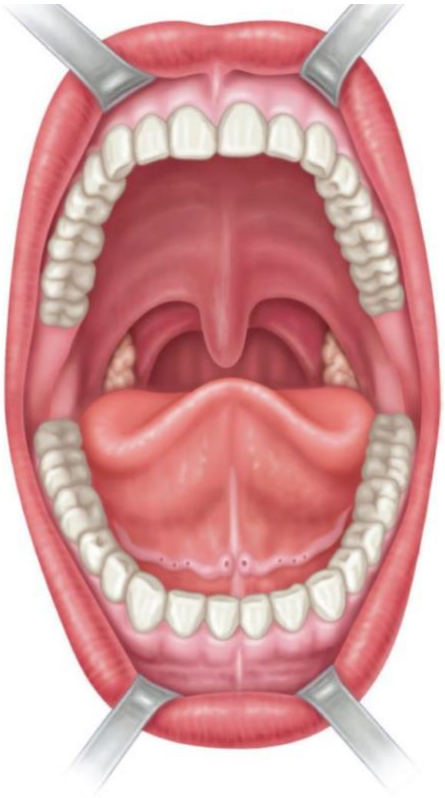

Appendix III – Participant consent and Ethical approval from Dublin Dental University Hospital.

Patient Information Sheet

PATIENTS ATTENDING DYSPLASIA CLINIC

"Identification of high risk-oral precancerous lesions using Raman technology"

Introduction

As academics in Trinity College Dublin, and the Dublin Institute of Technology, we engage in scientific research. One particular area of our interest is mouth cancer and precancer research. We have a mouth cancer research project which has been funded by Science Foundation Ireland and we would be grateful for your assistance.

You are attending the Dysplasia Clinic because you have a white patchin your mouth called a leukoplakia The diagnosis of leukoplakia is made by inspecting the area visually, and if necessary, by taking a sample (a ***biopsy)***, of the tissue and looking at it under a microscope, to confirm the diagnosis. The biopsy test is very good at reaching a diagnosis and telling us if there are any abnormal cells in the sample. Unfortunately, however, at this time, we cannot predict with any certainty which of these leukoplakias will become cancers in the future, although we know that about one in twenty will.

Raman spectroscopy is a new form of laser technology which can produce a unique biological fingerprint (like a bar code in the supermarket) of cells in a biopsy sample when the light is shone on it and analysed. It has already been used on cervical smears (the smear test for cancer of the cervix in women) and can identify high-risk, precancerous cells. We should like to apply this technology to samples of leukoplakias taken from the mouths of our patients, to see if we can identify high-risk, precancerous cells, so that we can provide a treatment aimed at preventing the leukoplakia turning into a mouth cancer.

We ask you to consent to having a "brush biopsy" of the leukoplakia to analyse with the laser technology. This involves scraping the area to remove a superficial layer of cells. In addition, we would like to take a saliva sample as saliva can provide important information about human health and is being researched as an indicator of various diseases including oral diseases.

You are completely at liberty to refuse to participate. Refusal to participate will not affect your treatment, or future management, in any way.

What happens to the tissue I donate to the study?

The brush biopsy cells and the saliva sample will be processed in the laboratory so that the samples can be analysed with the Raman laser. We will also carry out staining (immunocytochemistry) on the brush biopsy cells to look at different proteins. In addition, we will need to record some limited clinical details, after access to your clinical file.

The samples and results, and clinical details will be anonymised and coded, so that they will not be identifiable as coming from you. The data and samples will be transferred and stored in the Dublin Institute of Technology, the data on a single encrypted computer. The code will remain in the Dental Hospital. The samples will be destroyed 5 years after completion of the study. This is because Raman technology is relatively new and developing all the time, and we would like the opportunity to take advantage of any new developments in the Raman laser field in the near future. The data will only be available to the research team and will not be made available to any third parties. Only members of the clinical team, when you attend the clinic in the Dublin Dental University, will be allowed access to your clinical files. The data and samples will not be used for any other research other than that for which you have consented.

Possible benefits of the study.

If we can identify high-risk lesions and treat these lesions early, we may be able to prevent the lesions progressing to cancer. Oral leukoplakias are often quite ***extensive*** and since we cannot predict which one in twenty will become cancers, it is difficult to justify ***extensive*** operations to remove every lesion completely, since this treatment would be unjustified in nineteen out of twenty cases. If this technology proves effective, we can justify more extensive surgical treatment in selected patients, with an aim to prevent these lesions developing into mouth cancer in the future. Mouth cancer is a particularly nasty disease because the treatment for established mouth cancer is an extensive mouth and neck surgical operation, which is both disfiguring and may involve visible scarring and complex reconstructive surgery afterwards.

Possible risks to participants and after effects

There are no more risks than if you were not in the research study. The “brush biopsy” will only cause minimal, if any, discomfort and will leave no scar.

Location of research: Dublin Dental School and Hospital and Dublin Institute of Technology.

What will happen to the results of the study

This project will contribute to a PhD (doctorate) degree and the results of the study will be published in scientific journals, with due consideration to confidentiality.

Confidentiality of information

Your identity will remain entirely confidential. Your name will not be published and will not be disclosed to anyone outside the study team. Your data and sample will be coded and anonymised and once this has been done, it will be transferred and stored securely on a dedicated, encrypted computer in the Dublin Institute of Technology and will not be traceable back to yourself, without the code, which will remain secure in the Dublin Dental University Hospital

Voluntary participation

We stress that you are **NOT obliged** to take part. If, after agreeing to assist in our mouth cancer research, you wish to withdraw from the study, all samples and data will be destroyed.

Permission

Ethical approval has been obtained from the Faculty Research Ethics Group – Faculty of Health Sciences, Trinity College Dublin. Granted October 2016.

Further information and how to take part

The procedures will be explained to you, any questions that you have answered, and an informed consent form must then be signed by you if you agree to take part in this study.

Contact details of researchers

Prof. Stephen Flint and Prof Fiona Lyng

C/O Department of Oral and Maxillofacial Surgery, Oral Medicine and Oral Pathology

Dublin Dental School & Hospital, Lincoln Place, Dublin 2

Tel: 01 6127200.

This study is covered by standard institutional indemnity insurance.

Nothing in this document restricts or curtails your rights.

The researchers declare no conflict of interest

CONSENT FORM

PATIENTS ATTENDING DYSPLASIA CLINIC

Names of researchers:

Prof. Stephen Flint (Dublin Dental University Hospital)

Prof Fiona Lyng (Dublin Institute of Technology)

Title of study:

"Identification of high risk-oral precancerous lesions using Raman technology"

BACKGROUND:

Our research involves the use of sophisticated laser technology to try to identify lesions in the mouth that are high risk for becoming cancer, in order that we can treat these lesions with a view to preventing them becoming cancerous (see accompanying Patient Information Leaflet). We ask permission to take and analyse a "brush biopsy" sample and a saliva sample.

Your data, and any clinical information, will be anonymised, coded, confidential, securely stored and will not be disclosed to third parties.

Voluntary participation

We stress that you are **NOT obliged** to take part. If, after agreeing to assist in our mouth cancer research, you wish to withdraw from the study, all samples and data will be destroyed.

DECLARATION:

I have read, or had read to me, this consent form and the accompanying Patient Information Leaflet. I have had the opportunity to ask questions and all my questions have been answered to my satisfaction. I freely and voluntarily agree to be part of this research study, though without prejudice to my legal and ethical rights. I understand I may withdraw from the study at any time. I have received a copy of this agreement.

Patient's Name ……..

Contact Details:……..

……

Participant's Signature:……**Date:……**

Nothing in this document restricts or curtails your rights.

I …….. the Researcher :

I have explained the nature and purpose of this research study, the procedures to be undertaken and any risks that may be involved. I have offered to answer any questions and fully answered such questions. I believe that the participant understands my explanation and has freely given informed consent.

Investigator's Signature:…… Date:……

Appendix IV – Publications and Conference presentations

Conference Presentations:

2015 - 6th Annual Graduate Research Symposium, Dublin, Ireland (Poster);

2016 - 40th annual symposium of the Microscopy Society of Ireland, Dublin, Ireland (Poster);

2016 - SPEC Conference, Montreal, Canada (Poster);

2016 - Brazilian Society for Oral Pathology and Oral Medicine, Manaus, Brazil (Poster);

2017 - 2017 British Society for Oral Medicine Annual Scientific Meeting, Dublin, Ireland (Poster);

2017 - 40th annual symposium of the Microscopy Society of Ireland (Poster), Dublin, Ireland;

2018 - SPEC, Glasgow, UK (Poster Presentation);

2018 – International Association of Oral Pathologists (IAOP) and American Academy of Oral and Maxillofacial Pathology joint Annual Meeting 2018, Vancouver, canada (Oral presentation);

2018 - International Association for Dental Research/PER General Session – London, England (Oral presentation);

2019 - Microscopy Society of Ireland, Dublin, Ireland (Oral Presentation);

2019- British Society for Oral Medicine Annual Scientific Meeting, Dublin, Ireland, (Poster)*;

2019 – Portuguese Dental Association Conference, Lisbon, Portugal (Oral Presentation);

*RCSI award for best poster presentation

Publications:

- **Published:**

Full-article: Isha Behl, Genecy Calado, Ola Ibrahim, Alison Malkin, Stephen Flint, Hugh J. Byrne and Fiona M. Lyng. Development of methodology for Raman microspectroscopic analysis of oral exfoliated cells. Anal. Methods, 2017;9:937.

Abstract: Genecy Calado, Isha Behl, Ola Ibrahim, Stephen Flint, Hugh J. Byrne and Fiona M. Lyng. DEVELOPMENT OF METHODOLOGIES FOR RAMAN SPECTRAL ANALYSIS OF HUMAN SALIVA FOR DETECTION OF ORAL CANCER. Oral Surgery, Oral Medicine, Oral Pathology, Oral Radiology, and Endodontology 124(2):e142

Abstract: Isha Behl, Genecy Calado, Ola Ibrahim, Alison Malkin, Stephen Flint, Hugh J. Byrne and Fiona M. Lyng. A STUDY OF ORAL EXFOLIATED CELLS USING RAMAN MICROSPECTROSCOPY. Oral Surgery, Oral Medicine, Oral Pathology, Oral Radiology, and Endodontology 124(2):e144 · August 2017

Abstract: Dr. Calado Genecy, Ms. Isha Behi, Dr. Marina Leite Pimentel, Dr. Sheila Galvin, Dr. Stephen Flint, Prof. Hugh J Byrne, Prof. Fiona Lyng, RAMAN SPECTRAL STUDY OF SALIVA: A NEW TOOL FOR DETECTION OF MALIGNANT AND PREMALIGNANT ORAL LESIONS, Oral Surgery, Oral Medicine, Oral Pathology and Oral Radiology. 2019;128;(1):e90.

- Accepted for publication:

Full-article: Calado G, Behl I, Daniel ., Byrne HJ, Lyng. FM. Raman spectroscopic analysis of saliva for the diagnosis of oral cancer: a systematic review. Translational Biophotonics. Accepted for publication in August/2019.

- Submitted publications::

Isha Behl, Genecy Calado, Alison Malkin, Stephen Flint, Sheila Galvin, Claire M. Healy,Marina Leite Pimentel, Hugh J. Byrne, Fiona M. Lyng, “A pilot study for Early detection of potentially malignant oral lesions using minimally invasive oral cytology through Raman microspectroscopy: Assessment of confounding factors”, Oral diseases, 2019, submitted

Amuthachelvi Daniel, Genecy Calado, Isha Behl, Stephen Flint, Sheila Galvin, Claire Healy, Hugh J. Byrne, Fiona M. Lyng, “Comparative study of label-free detection of oral dysplasia by conventional and surface enhanced Raman spectroscopy of whole saliva” SPIE conference proceedings submitted and under review

Genecy Calado, Isha Behl, Hugh J. Byrne, Fiona M. Lyng. Raman spectroscopic characterisation of non stimulated and stimulated human whole saliva: a new methodology. Article submitted in Analyst (September/2019).

Carta de Aprovação

17 December 2019

Genecy Calado
90 Glasnevin Downs, Glasnevin, Dublin 11

Dear Genecy,

Further to the receipt of the report on the examination of your thesis entitled *"Development of Methodologies for Raman Spectral Analysis of Human Saliva for Detection of Oral Cancer"*, we are pleased to inform you that:

"The award of PhD is recommended, subject to the inclusion in the thesis of minor corrections and revisions as specified".

Please find enclosed a copy of the examination report outlining corrections required.

Minor corrections may take up to three months to complete. I would be grateful if you could amend the thesis as specified and return one soft-bound copy of the corrected thesis to the Graduate Research School Office on or before 17th March 2020.

I trust the above meets with your approval, but should you have any queries, please do not hesitate to contact me.

Kind regards,

Shane Byrne
Graduate Research School Office
Technological University Dublin – City Campus
Kevin Street
Dublin 8
T: +353 (0)1 402 7921
E: shane.byrne@tudublin.ie

Cc: Prof. Fiona Lyng, Professor Hugh Byrne, Dr. John Doran, Dr. Tony Betts

Cartão de Embarque

BOARDING PASS

AIR PORTUGAL
A STAR ALLIANCE MEMBER

Nome/*Name* **CALADODEMELO/GENECY**

Bilhete/*Ticket* **0472174151835**

Passageiro Frequente/
Frequent Flyer

KEYCODE: 62682

TP1323	DUBLIN (Terminal 1)				LISBON		
DATE	DEPARTURE	BOARDING	GATE	CLASS	SEAT	BOARDING ZONE	ENTITLED TO
27 Dec 19	11:15	10:45	Check monitors	Y	20D	A	
TP11	LISBON (Terminal 1)				RECIFE		
DATE	DEPARTURE	BOARDING	GATE	CLASS	SEAT	BOARDING ZONE	ENTITLED TO
27 Dec 19	16:40	15:40	Check monitors	Y	15F	B	

Verifique a porta de embarque no aeroporto / *Check gate at the airport*
Porta fecha 30min antes de partida/Gate closes 30min before departure
BOARDING AREA N

Certifique-se de que a sua bagagem de mão está dentro dos limites permitidos/
Please make sure that your hand luggage is within the permitted allowance

Para mais informações consulte flytap.com/*For more information see flytap.com*